APPLICATION OF RAMAN SPECTROSCOPY TO THE DIFFERENTIATION OF LIPSTICKS FOR FORENSIC PURPOSES

A thesis submitted to

the University of Kent at Canterbury

in partial fulfilment of the requirements for the degree of

Doctor of Philosophy

By

Fatma Salahioglu

November 2012

Acknowledgements

I would like to express my thanks to my supervisor, Prof. Michael. J. Went, for all his help, support and guidance throughout my research; to Dr. Matt J. West, for teaching me how to use the spectrometer; to Mr. Ian Ross and Mr. M. J. Cole for their technical support; to Caroline Rolfe, who managed to find a way to obtain a large number of lipsticks and then kindly let me use them for my research after she was done with hers; to the kind lady working at Boots, Canterbury, for supplying the lipstick samples free of charge; and to Katherine Jones for volunteering for the 'cigarette butt' experiments. I would also like to express my thanks to Dr. Stuart Gibson, who has kindly agreed to help me with the chemometrics studies, for writing the MATLAB code required for the analyses and helping out with the technique in general.

Just to start this paragraph differently: I would like to express my sincere gratitude to Trevor Ferris for his help and support during my difficult times, and for being there to pick me up when I had fallen (not literally).

And most importantly, I would like to express my eternal gratitude to Dr. Mark Price, who has been the most helpful person for the majority of my studies. Thank you so much for letting me bother you whenever I had a question or a problem with the spectrometer(s), and thank you for your patience and for helping me out with the countless questions I had for the past two to three years.

Finally, I would like to express my thanks to my parents for their continued support and understanding throughout my studies; I would not have been here otherwise.

As a last minute addition, I would like to send my eternal gratitude to Kumar Gaurav, my eternal love, for his help and support at the very end of my PhD.

Abstract

Raman spectroscopy was applied to the forensic analysis and differentiation of lipstick samples. Spectra were obtained from 73 different lipstick samples. 11% of the samples gave fluorescent spectra. 21.9% gave spectra that were unique to the individual lipstick. The remaining 67.1% could be divided into seven groups, each of which could be differentiated from one another. Identification of the component dye peaks in the lipstick spectra allowed further classification of the samples within each group. A spectral library of lipstick samples was built.

Effects of ageing on the Raman spectra of lipsticks were investigated. The majority of the spectra of deposited lipstick samples remained unchanged over a period of up to two years. In some of the aged lipstick spectra, the (C=C) band at 1655 cm^{-1} and the (=CH) band at 3011 cm^{-1} were found to decrease in intensity and disappear over time.

Trace amounts of lipstick smears deposited on textile fibres, cigarette butts and paper tissues were analysed. Differentiation of lipstick smears could be achieved with little or no interference from the underlying medium. Lipstick smears on glass slides, cigarette butts and tissues could also be analysed and identified in situ through evidence bags.

Use of chemometrics for the characterisation of large numbers of lipstick spectra was explored. Thirty spectra each from ten different lipsticks were analysed by Principal Components Analysis (PCA) and classified using the *K*-Nearest Neighbours (KNN) classifier. Up to 98.7% correct classification was achieved. Spectra from trace amounts of lipstick smears deposited on fibres were also analysed and classified using the same technique. 100% correct classification of these samples was achieved.

This study has demonstrated that Raman spectroscopy is an invaluable tool for discriminating between lipstick samples under a range of forensically relevant situations.

TABLE OF CONTENTS

CHAPTER I

Introduction

Over the past twenty years, advancements in modern technology have replaced the bulky, complicated and expensive Raman spectrometers of the past with faster, highly sensitive and more affordable spectrometers that can be used by both specialists and non-specialists. Due to these advancements, Raman spectroscopy has found application in many fields and its usefulness is becoming widely recognised across a range of disciplines.

Raman spectroscopy is a powerful analytical technique for the non-destructive analysis of trace or bulk amounts of materials. It provides information on chemical structures of substances and gives characteristic spectral patterns which can be used for the identification of unknown substances. It requires minimum to no sample preparation, and it can be used to analyse materials through glass containers, packaging materials and evidence bags [1]. These fundamental properties make it an important tool for the forensic analysis of evidential material.

Evidence can come in all sizes, shapes and forms, and there are a variety of materials that can be encountered as forensic evidence. One of these is cosmetic evidence such as lipstick smears. Lipsticks are easily transferrable and smears of lipstick can be found on a variety of crime scene objects and surfaces, as well as on individuals. It is important to be able to identify and differentiate between lipstick samples as, like other types of evidence, it can help form a link between suspects, victims and crime scenes.

Even though lipstick smears have been recognised as forensic evidence for many years, very little research has been done on the analysis and differentiation of lipsticks using Raman spectroscopy [2, 3]. Therefore the aim of this research is to fill

in this gap in literature and to explore the application of Raman spectroscopy to the analysis and differentiation of lipstick smears as forensic evidence.

Chapter II of this study provides background information on Raman spectroscopy. It gives an introduction to the theory of Raman scattering and provides an overview of the instrumentation, drawbacks of the technique and the methods used to overcome these drawbacks. This chapter also includes a brief overview of the applications of Raman spectroscopy across a range of disciplines, including forensic science.

Chapter III discusses lipsticks as cosmetic evidence. It introduces the historical evolution of lipsticks and discusses its modern day uses. It gives a detailed description of the composition of modern lipsticks, providing fundamental information on the types of chemical bonds that might be expected from their Raman spectra. This chapter also provides a review of previous studies carried out on the forensic analysis of lipsticks. This review also includes the only two studies reported (to the best of the author's knowledge) on the analysis of lipstick smears using Raman spectroscopy.

Chapter IV is the first of the two results chapters which describes the experiments conducted for the analysis and differentiation of lipstick smears on glass slides using Raman spectroscopy. This chapter presents the results of experiments obtained using a *Jobin-Yvon 640* spectrometer, which was the spectrometer used for the majority of this research. The chapter includes classification of lipsticks by their spectra, identification of component peaks and a comprehensive library of 65 lipstick spectra.

Chapter V, the second results chapter, contains the results of experiments conducted using a *Horiba LabRAM-HR* Raman spectrometer, which was purchased during the final quarter of this research. This chapter investigates the effects of ageing on lipstick spectra and explores the application of Raman spectroscopy to the analysis and differentiation of trace amounts of lipstick smears found on media such as textile

fibres, cigarette butts and tissues; and the analysis of these smears through evidence bags. This chapter also explores the application of chemometric methods such as Principal Components Analysis (PCA) to the analysis and characterisation of hundreds of lipstick spectra.

The final chapter, Chapter VI, provides the concluding remarks on this research and summarises the results and findings. A section on further research that can be carried out in this field is also included within this chapter.

The relevant appendices and a CD containing all the individual Raman spectra of samples obtained throughout the research are also supplied.

CHAPTER II

Raman Spectroscopy

2.1. Discovery of the Raman effect

In 1922, the Indian physicist C. V. Raman, who was interested in the theories regarding the wave and quantum natures of light, began a series of experiments in which he paid particular attention to how light is scattered in liquids and crystals. Six years later, in 1928, his experiments finally led to the discovery of what he called a "modified scattered radiation" [4, 5].

Raman and his student, K. S. Krishnan, set up an experiment whereby they observed sunlight, focused by a telescope, as it passed through a variety of liquids and vapours. They used complementary light filters (blue-violet and yellow-green) which, when placed together between the incident light and the sample, blocked the light going through the sample. Having shown that the two complementary filters efficiently blocked out the wavelengths of light coming from the sun, they then moved the sample between the two filters. When they set up this experiment, they realised that the light that was previously blocked by the two filters, could now pass through the sample and the filters, and reach their eyes. The blue-violet filter lets the wavelengths of light responsible for blue-violet colours through, which are then blocked by the yellow-green filter. Therefore the appearance of light at the other end (when the sample was placed in between the two filters) meant that the wavelength of the incident light changed when it interacted with the sample, enabling it to then pass through the yellow-green filter. Raman examined sixty different liquids this way and found out that this effect was observed in all of them, with varying degrees. He also noticed that this effect was quite weak, and determined that this was a genuine scattering effect of light rather than fluorescence, which is a much stronger effect [4, 6].

2.2. Theory and principles of Raman spectroscopy

(The following discussion is based on the references [1, 7-10])

There are many ways in which light can interact with a molecule. It can be absorbed by the molecule when the incident photon's energy matches the gap between the ground and an excited state of the molecule, and the molecule goes into a higher energy excited state. This is the basis for absorption spectroscopy. Light can also pass through the molecule without any interactions; or it can be "scattered", which involves a change in the direction of the incident light.

During the scattering process, photons interact with a molecule, distorting the electron cloud around the nuclei, causing the molecule to form a higher energy 'complex' state. This virtual state is unstable and very short-lived, so the photon is very quickly re-radiated (i.e. scattered) to bring the energy of the molecule to a stable state. There are two types of scattering: Rayleigh and Raman scattering, both named after the scientists who discovered them. In Rayleigh scattering, when the photon polarises the electron cloud around the nuclei, the molecule goes into the higher energy virtual state. At this point the electronic configuration is distorted, however there is not enough time for the nuclei to move and adjust to this configuration. Therefore as the electron cloud relaxes, the photon is released as elastically scattered radiation with no appreciable change in its energy. The majority of photons are scattered this way.

Raman scattering occurs for about one in every $10^6 - 10^8$ photons and thus is a much rarer event. With Raman scattering, as the electron cloud is polarised by the incident photon, the nuclei start to move as well. The molecule forms a 'complex' in the higher energy virtual state, just like in Rayleigh scattering. However since the nuclei are much heavier than electrons, their movement causes an energy transfer to take place between the photon and the molecule. The photon is inelastically scattered with an energy different by one vibrational unit as the molecule drops back down to a different vibrational state than its initial state. Depending on the initial vibrational

state of the molecule, two types of Raman scattering can occur. At room temperature, most of the molecules are in a low energy, ground vibrational state; so interaction with a photon causes absorption of the energy of the photon by the molecule, promoting it to a higher energy vibrational state. The photon is then scattered with a lower energy than the incident photon. This is called Stokes scattering. Conversely, due to thermal energy in the surroundings, there may be some molecules that are already in an excited (higher energy) vibrational state. Therefore there will be a transfer of energy from the molecule to the photon as the molecule drops down to a lower energy vibrational state, and the photon is scattered with a higher energy than the incident photon. This is referred to as anti-Stokes scattering (**Fig. 2.1**).

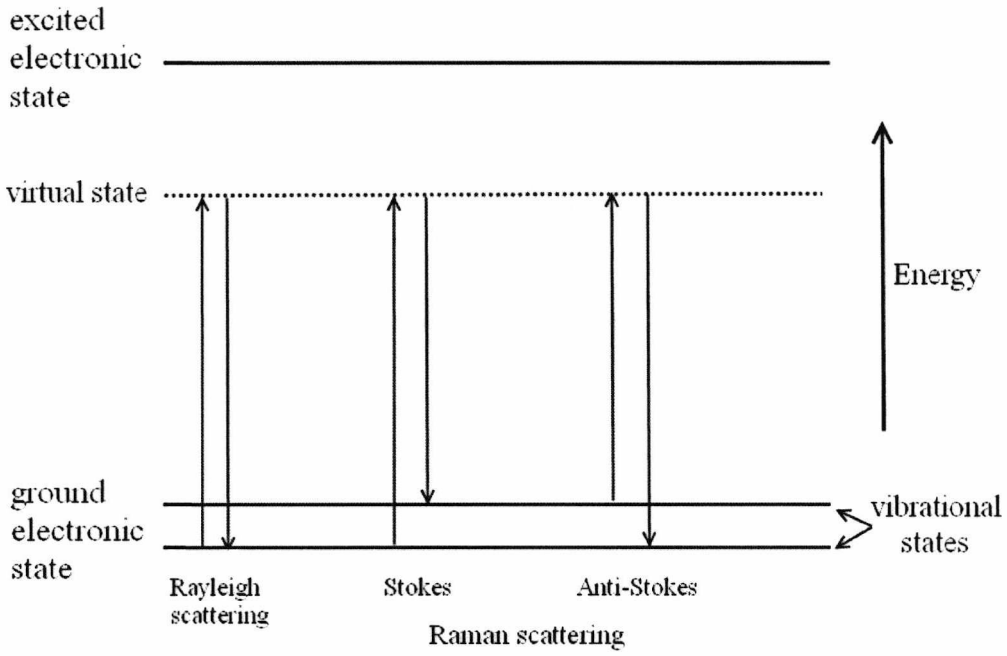

Figure 2.1. Diagram showing Rayleigh and Raman scattering processes.

The ratio of Stokes to anti-Stokes scattering is dependent on the number of molecules in ground and excited states, which is governed by the Boltzmann distribution given by [1, 7]:

$$\frac{N_n}{N_m} = exp\left[\frac{-(E_n - E_m)}{kT}\right]$$

where N_n is the number of molecules in the excited vibrational energy level (n), N_m is the number of molecules in the ground vibrational energy level (m), $(E_n - E_m)$ is the difference in energy between the vibrational levels, k is the Boltzmann constant (1.38×10^{-23} JK^{-1}), and T is the temperature (K).

In Raman spectroscopy, it is these changes in the energy of the scattered photon that are detected and analysed. A monochromatic light source (i.e. a laser) is used to irradiate the sample and the differences in the energy (or the 'shifts' from the energy of the incident photons) are recorded and presented in terms of Raman bands or peaks in a spectrum, where each peak represents a shift from the incident light energy. These peaks are positioned at particular wavenumbers (cm^{-1}) along the x-axis depending on the amount of the shift, with the intensity of scattering along the y-axis.

The bonds between atoms vibrate at characteristic frequencies allowing the identification of groups by interpretation of the Raman spectrum. Vibrations between lighter atoms give rise to peaks in the higher frequency region, such as the C-H vibrations at around 3000 cm^{-1}. Likewise, heavier atoms have lower vibration frequencies, such as the C-I vibrations at less than 500 cm^{-1}. The strength of the bond also helps determine the frequency of vibration: the stronger a bond is, the higher the frequency will be. These are generally governed by the Hooke's law which is given as:

$$v = \frac{1}{2\pi c}\sqrt{\frac{K}{\mu}}$$

where v is the frequency, c is the velocity of light, K is the force constant of the bond (which is a measure of its strength), and μ is the effective mass of the system.

Although the Stokes shifts are negative shifts (due to a loss of energy of the incident light), by convention they are assigned as positive shifts and the peaks appear on the positive side of the x-axis.

The intensity of the Raman peaks is governed by the change in polarisability (α) of the molecules, which is the tendency of the electron cloud around the molecules to be distorted by an external electric field, such as that of the incident light. Raman scattering is a result of the dipole moment induced in the molecule by the oscillating electric field of the incident light. This induced dipole (or polarisation) is given by the equation:

$$\mu = \alpha E$$

where μ is the dipole moment created in the molecule, α is the polarisability of the molecule, and E is the incident electric field (of the photon). Vibrations are 'Raman active' (i.e. they give effective Raman scattering) if the polarisability changes during the vibration and this is known as the "basic selection rule". Symmetric vibrations cause the greatest change in polarisability; therefore these vibrations have the strongest Raman bands. This is contrary to infrared spectroscopy, where the strongest absorption bands are caused by a change in dipole; hence asymmetric vibrations are stronger in IR spectra (**Fig. 2.2**). Another selection rule called the mutual exclusion rule, which only applies to molecules with a centre of symmetry (such as ethyne), states that a vibration can either be Raman or IR active, but not both.

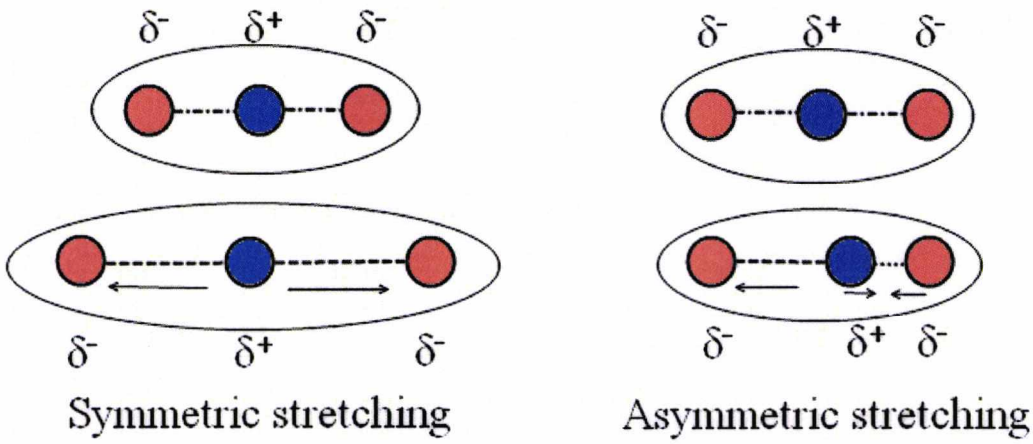

Figure 2.2. Electron cloud model of a CO_2 molecule showing symmetric and asymmetric stretching vibrations. There is a change in the polarisability of the electron cloud during the symmetric stretch, so this is the Raman active vibration of the molecule. In contrast, there is no change in polarisability during the asymmetric stretch, but there is a change in the dipole, which makes the vibration IR active.

Raman and infrared spectroscopies are complementary to each other: a vibration that is Raman active may be infrared inactive, and vice versa. For this reason both spectroscopies are frequently used together for the identification of compounds. For example, analysis of an ester would reveal that the C=O stretches are more intense in IR spectra due to a change in dipole, and weak in Raman; whereas the C=C stretches are more intense in Raman spectra due to a change in polarisability, but weak in IR because there is no change in dipole. Therefore interpreting both Raman and IR spectra of a compound could help identify the compound more readily than just using one type of spectra.

2.3. Instrumentation

(The following discussion is based on the references [1, 7-10])

Since Raman scattering is a shift from the energy (or frequency) of an excitation source, a light source of a known, single frequency (i.e. monochromatic) is required in order to be able to measure these shifts accurately. For this purpose, lasers are

exclusively used as excitation sources in Raman spectrometers. There are a variety of lasers of different wavelengths, or tuneable lasers with adjustable wavelengths, available for modern Raman spectrometers.

The intensity of Raman scattering depends not only on the polarisability of molecules in a sample, but also on the frequency and power of the laser used. The Raman intensity increases by the fourth power of the frequency of the laser; therefore using higher frequency (lower wavelength) lasers could help improve the Raman signal intensities. Ar^+ ion lasers operating at wavelengths of 488.8 nm and 514.5 nm are examples of such lasers with high energies. Even though they have the capability to produce intense Raman signals, they can also cause degradation of the sample by photodecomposition or overheating. Helium-neon lasers operating at a wavelength of 632.8 nm have lower energies, but still have the potential to cause photodegradation. These visible lasers also induce strong fluorescence when used for the analysis of coloured or biological samples. Lasers working in the near-infrared region, such as neodymium-doped yttrium aluminum garnet (Nd^{+3}:YAG) operating at 1064 nm, can get round this problem. However, the fourth power of the frequency factor means that the Raman intensity will be much reduced; therefore longer accumulation times are required to obtain an acceptable signal-to-noise ratio.

The laser (regardless of wavelength) is focused onto the sample via a microscope that is integrated into the majority of spectrometers. Coupling the spectrometer to a microscope allows extremely small amounts of materials to be analysed. The light scattered by the sample is then collected at either 90° or 180° (reflection) angles. In the former collection system, the scattered light is collected at 90° to the incident beam by placing a lens in a suitable position. In the latter, the scattered light is collected back through the lens it was delivered from (**Fig. 2.3**).

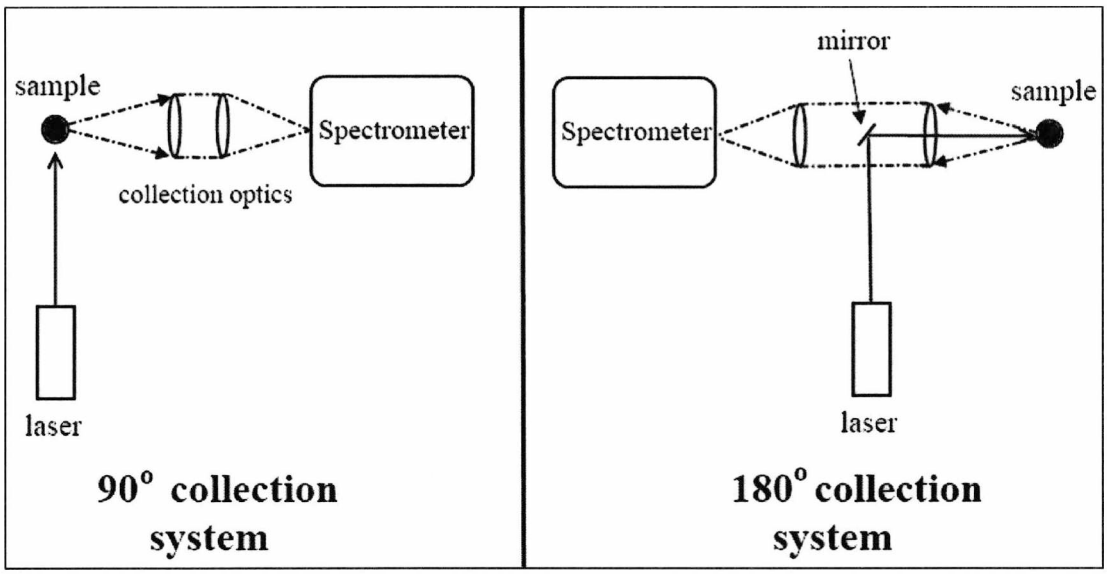

Figure 2.3. A simplified diagram showing the 90° and 180° collection systems.

The majority of the scattered photons are a result of Rayleigh scattering with no change in their energies, with a very small proportion being the Raman scattered light of interest. To filter out the Rayleigh scattered photons, as well as any stray light produced upon light dispersion on the spectrometer gratings, laser rejection filters such as notch or edge filters are used. These filters are designed to absorb the light within about 200 cm^{-1} of the excitation frequency. Depending on the quality of the filter, it can be possible to make measurements closer to the excitation line.

The collected Raman scattered light is then focused onto a diffraction grating which separates the light into its constituent frequencies. The separated light is focused onto a detector such as a charge coupled device (CCD), which is the most widely used detector in modern Raman spectrometers. A CCD is composed of an array of pixels positioned on a silicon chip, each of which can be addressed. The separated frequencies of shifted light are detected and stored on these pixels, and the output is used to construct a spectrum. Since the Raman effect is very weak, increasing the accumulation time increases the Raman signal integrated on these pixels, which in turn increases the signal intensity of the output. The signals collected from the detector are then readout by a computer, where spectral software packages, such as Labspec or OMNIC, are used to present the data in terms of Raman spectra.

Conventionally, only the Stokes spectra are presented and anti-Stokes spectra omitted. **Figure 2.4** gives a schematic of the main components of a Raman spectrometer and **Fig. 2.5** shows an example spectrum.

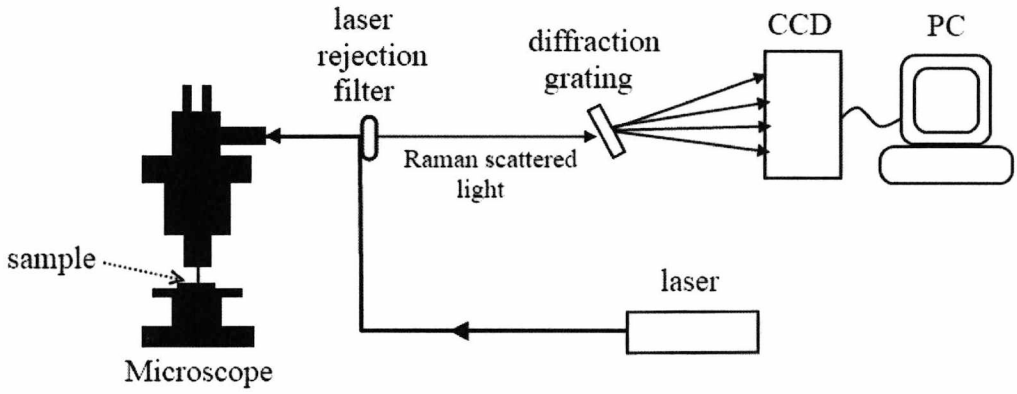

Figure 2.4. A simplified diagram of the main components of a Raman spectrometer.

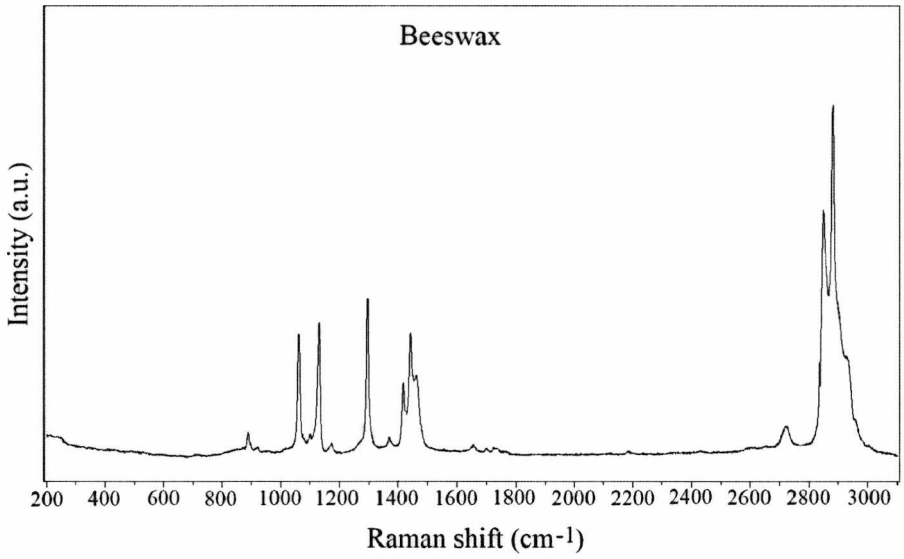

Figure 2.5. Raman spectrum of beeswax, a major component of lipsticks.

In order to ensure a spectrometer is working correctly and consistently, it is calibrated by checking that the wavenumber (cm^{-1}) positions along the x-axis are correct compared to standard calibration samples. These samples include materials such as silicon, which has a strong band at 520.6 cm^{-1}; diamond, with a band at 1364 cm^{-1}; and barium sulphate with a strong band at 988 cm^{-1}. Ideally, the spectrometer should be calibrated at least daily before starting analyses.

The majority of Raman spectrometers are coupled to microscopes for the analysis of samples. However, they can also be coupled to fibre optic cables with probe heads that enable in situ analysis of materials in inaccessible areas, or of materials that cannot be sampled from and/or are too big to fit under a microscope, such as paintings and archaeological artefacts. Portable and handheld Raman spectrometers have also been developed, increasing the flexibility of Raman spectroscopy and the range of materials that can be analysed, irrespective of size, shape and location [11, 12].

With the technological advancements in microscopy that started in the 1990s, confocal Raman imaging has become an important technique for enabling the analysis of materials at different depths of focus. Confocal microscopes have an additional aperture that limits the sampling depth by rejecting the light collected from out-of-focus regions of the sample, before the light enters the spectrometer; so that only the in-focus region is being analysed. Confocality becomes vital, for example, when examining polymers formed of two or more layers; or analysing trace amounts of materials found on different surfaces, where no interference from the surface material is desired.

Another advancement in Raman spectroscopy is Raman mapping. This technique utilises a motorised microscope stage that can move the stage in the XYZ axes and record spectra at predetermined points on the area to be mapped. Mapping is very useful for analysing materials and their distribution in a heterogeneous sample; such as studying the distribution of drugs in tablets by mapping the surface. This can be used in quality control when checking the formulation of tablets. It can also be used in forensics to help determine counterfeit drugs because the distribution of components in a tablet is more difficult to counterfeit than the formulation itself.

2.4. Fluorescence

(The following discussion is based on the references [1, 7-10])

A common problem encountered in Raman spectroscopy is fluorescence interference. Fluorescence occurs when the exciting radiation has sufficient energy to excite the molecule to a higher energy electronic state. The molecule then relaxes to a lower energy electronic state, emitting a photon with less energy than the incident photon during the process (**Fig. 2.6**).

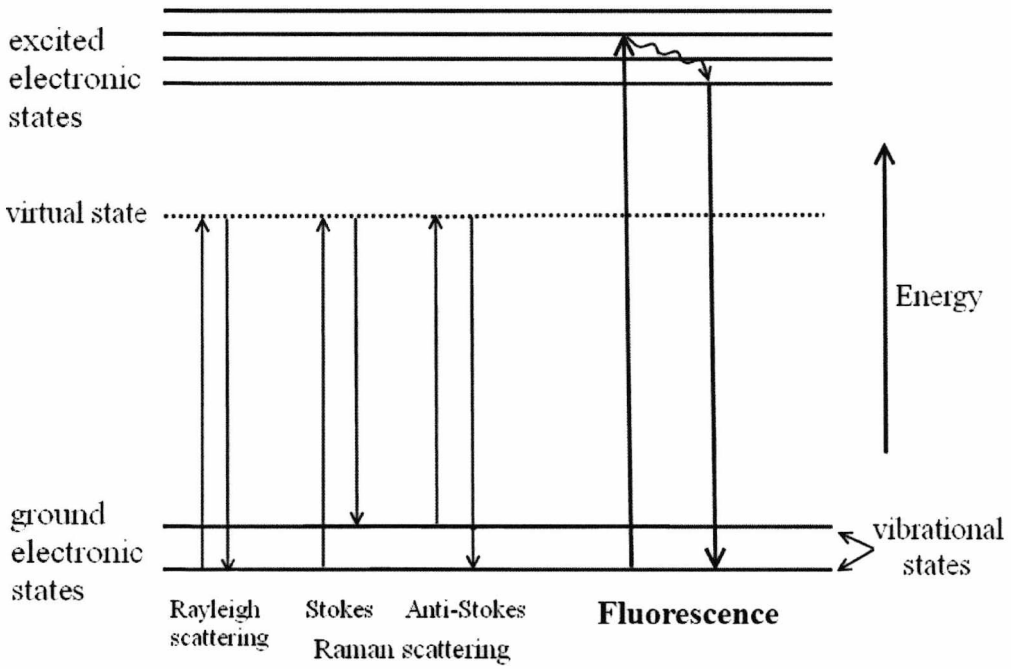

Figure 2.6. Diagram showing the process of fluorescence emission in comparison to scattering.

Unlike Raman scattering, fluorescence is an emission process. It is a very strong effect and even the fluorescence from trace amounts of impurities in a sample can be enough to obscure the weak Raman signals of the sample. Fluorescence is evident by a very broad, intense band covering a wide range of wavenumbers (**Fig. 2.7**).

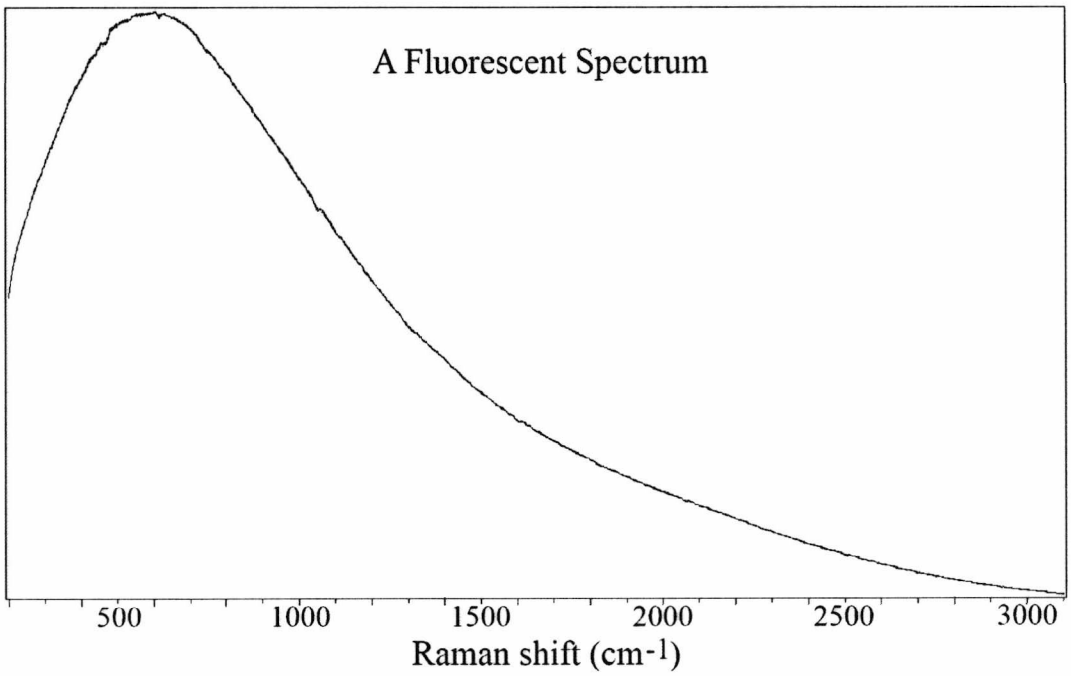

Figure 2.7. Raman spectrum of a lipstick showing fluorescence which obscured any Raman peaks.

Fluorescence usually occurs with coloured samples, or with coloured impurities in samples, especially when excited using a visible wavelength excitation source. It can be avoided by purifying the samples, or using confocal microscopy to avoid analysing the impurity [1]. However, this is not possible in cases where the actual sample itself is causing the fluorescence. Nevertheless, many studies in overcoming fluorescence observed in Raman spectroscopy have led to the discovery of various methods for quenching fluorescence and improving Raman signals of the analysed sample.

2.4.1. Changing the excitation wavelength

Since fluorescence occurs when the excitation source has enough energy to cause electronic transitions within the sample, selecting an excitation wavelength that has a lower energy than any electronic transitions in the sample can avoid the problem. For this purpose, lasers with longer wavelengths (i.e. lower energies) such as those operating in the near-infrared region are preferred [13, 14]. However it must also be

borne in mind that the Raman signal intensity is dependent on the fourth power of frequency, hence it drops with decreasing frequency. Therefore, if the sample is already a weak Raman scatterer, using other methods for reducing fluorescence would be more desirable.

2.4.2. Resonance Raman Spectroscopy

The resonance Raman effect is observed when the exciting frequency is approximately equal to the energy required for the lowest allowed electronic transition in the molecule. At this point, the intensities of the Raman bands associated with symmetric vibrations are strongly coupled to the electronic excited state, and an enhancement by a factor of up to 10^6 can be seen in these bands.

To obtain resonance Raman scattering, a laser frequency is chosen that is close to the energy of an electronic transition in the analysed sample. Tuneable lasers are preferred, since the laser frequency can be adjusted to match (or get as close as possible to) the energy gap between the ground and excited electronic states.

A disadvantage of resonance Raman scattering is the possibility that, when the excitation frequency is equal to the energy required for an electronic transition, absorption of the photon by the sample might occur, causing sample decomposition or fluorescence. The difference between resonance Raman scattering and fluorescence is the time it takes for the molecule to return to the lower electronic state: scattering relaxation is significantly faster than fluorescence. Therefore the nuclei do not have time to reach equilibrium in the excited electronic state; whereas with fluorescence, the nuclei absorb and relax into an excited electronic state, before emitting a photon to return to the ground electronic state (**Fig. 2.8**).

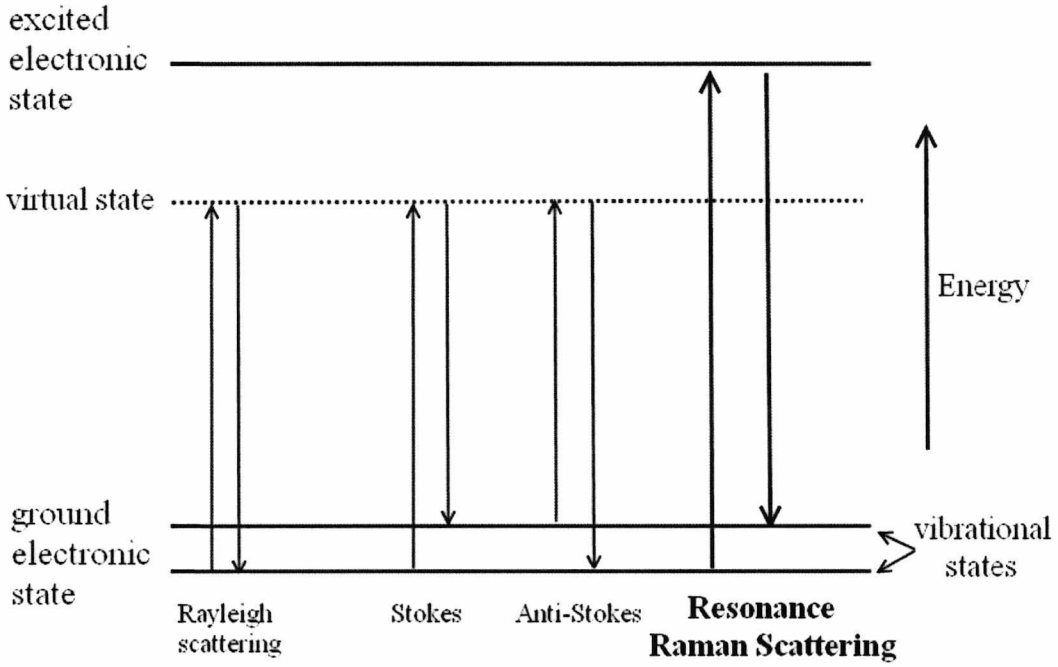

Figure 2.8. Diagram showing the resonance Raman scattering process in comparison to normal Raman scattering. The difference between resonance Raman scattering and fluorescence can be seen in that the photon is quickly re-radiated before the nuclei reaches equilibrium in the electronic state with resonance Raman scattering, unlike fluorescence which is explained in **Fig. 2.6**.

Apart from fluorescence, absorption of the photon by the sample can also cause sample decomposition, which can be observed in a coloured sample as a change in colour or the production of a black (burnt) spot.

Another disadvantage of resonance Raman spectroscopy is that only bands corresponding to a certain class of molecules (such as porphyrin rings found in enzymes, phthalocyanine pigments and polyacetylenes that have allowed electronic transitions in the visible range of the electromagnetic spectrum) are enhanced this way. In some cases, where the sample is a mixture of different classes of molecules, the obtained Raman spectrum may not be a good representation of the sample as a whole. However this technique is potentially extremely useful for detecting minute quantities of a specific substance.

2.4.3. Surface Enhanced (Resonance) Raman Spectroscopy (SER(R)S)

Another effective way of quenching fluorescence is the use of surface enhancement. This is achieved when the analyte molecule is adsorbed onto a SERS active roughened metal surface, which is excited using the excitation laser. For a surface to be SERS active, the metal needs to be inert enough not to form oxides in the presence of oxygen, as this alters the nature of the surface. It also needs to favour scattering over absorption and the analyte needs to be effectively adsorbed onto its surface. Silver and gold are found to be two of the most suitable metals for use with SERS [15].

There are two theories behind how enhancement is achieved through SERS: the electromagnetic enhancement theory and chemical (or charge transfer) enhancement theory.

When a light beam interacts with the electrons found on the surfaces of metals, the electrons begin to oscillate as a group across the surface. These oscillations are called surface plasmons. On a smooth metal surface, these plasmons oscillate along the plane of the surface, which can cause absorption of light but no scattering. In order to get scattering, there has to be oscillations perpendicular to the surface of the metal, which is achieved by 'roughening' the metal surface.

According to the electromagnetic enhancement theory, an interaction occurs between the analyte and the surface plasmons when the analyte is adsorbed onto, or is in close proximity to, the metal surface. The electrons in the analyte interact with the freely moving electrons at the surface of the metal, which increases the polarisation of the molecule. Since Raman scattering is based on the polarisability of molecules, enhanced scattering is achieved.

The chemical enhancement theory on the other hand states that the analyte chemically bonds to the surface, which creates new electronic states in the molecule. This causes an increase in the polarisability of the molecules and the excitation occurs through transfer of electrons from the metal to the molecule and back to the metal during the Raman scattering process.

SERS can give a signal enhancement of up to 10^6 compared to normal Raman scattering. It is found that the plasmons found in silver and gold oscillate at frequencies in the visible and NIR region, and therefore are the most preferred metals for use with most Raman spectroscopy systems.

When applying SERS to samples with resonant molecules (i.e. chromophores), the signal intensity is enhanced even further due to the resonance Raman scattering effect as well as the surface enhancement. This Surface Enhanced Resonance Raman Spectroscopy (SERRS) can give considerable increase in enhancement, even rivalling or surpassing fluorescence. For this to happen, the chromophore needs to be adsorbed onto the metal surface for SERS; and the energy of the excitation laser needs to get very close, or be equal, to the energy gap between the electronic transition states of the chromophore for the resonance effect.

SER(R)S has many applications across a variety of disciplines. It has been especially useful in the analysis of dyes that are mostly fluorescent when analysed with normal Raman spectroscopy. SER(R)S has been used for the analysis and identification of a variety of dyes found in archaeological and historical textiles, in paintings and other works of art [16-21]; as well as those used in modern applications [15, 22-24]. Dyes are frequently used to colour a large number of materials such as food, drinks, cosmetics, inks and fibres. Identification of these dyes can be helpful in forensic investigations where the origin of a dyed compound needs to be established. There have been studies on the analysis and identification of dyes of forensic interest [25-27], including synthetic dyes found in ballpoint pen inks [28]. SERRS has also been

successfully applied to the detection of explosives [29-31] and differentiation of lipsticks for forensic purposes [2].

Other uses of SERRS include biological applications such as medical diagnostics and biological imaging [32], detection of DNA sequences [33], and analysis of biologically active compounds [34].

SER(R)S has been used and evaluated not only as a qualitative technique, but also as a quantitative analytical tool [35]. Owing to the sensitivity of the technique, even single molecule detection can be achieved [36].

There have been many studies on improving SER(R)S methods, including finding suitable substrates as metal surfaces or developing a new method to use the existing substrates more efficiently [37, 38]. A comprehensive review of SERS and its applications has been published by Sharma *et al* [39], and forensic applications of SERS are described by White [40].

Despite its advantages and successful application in many areas, SER(R)S has disadvantages. It is very difficult to interpret SER(R)S spectra. New peaks might appear due to resonance enhancement that are normally absent from normal Raman spectra. Some of the peaks that are strong in normal Raman spectra can appear as very weak peaks, or be completely absent from SER(R)S spectra. Orientation of the sample molecules with the SERS surface can cause selective enhancement of certain peaks and when the resonance Raman effect is in action as well as surface enhancement, further selective enhancement of peaks can make the spectrum look completely different than its normal Raman spectrum [21]. This means that standard spectral libraries of materials cannot be used for the identification of unknown samples.

Even though Raman and IR vibrations and bands are dictated by selection rules such as the 'mutual exclusion rule', which states that no vibration can be both Raman and IR active for a centrosymmetric molecule; adsorption of those molecules on a SERS surface can break that centre of symmetry, changing the rule and causing some IR active bands to appear in the SER(R)S spectrum.

These differences in the spectra can make identification of unknown compounds difficult when comparing their spectra to those found in literature since the intensity of peaks depend largely on the experimental conditions and setups, such as the frequency of the laser used for resonance Raman spectroscopy, or the type of metal substrate used for SERS.

2.4.4. Subtracted Shifted Raman Spectroscopy

One of the methods used for dealing with fluorescence includes recording spectra of the same sample using slightly different excitation frequencies (different by approximately 10 cm^{-1} relative to one another), and subtracting the two spectra acquired to obtain a derivative-shaped spectrum. Fluorescence is a very broad feature and such a small difference in the excitation wavelength does not change the position of the band. Thus subtraction of the two spectra eliminates the fluorescence band, leaving behind the slightly shifted Raman signals with positive and negative intensities where the subtraction has occurred. The spectrum is then reconstructed using mathematical functions to obtain a conventional Raman spectrum. This technique of eliminating fluorescence is called Shifted Excitation Raman Difference Spectroscopy (SERDS) [41-44]. Because it is based on shifting the excitation frequency by a small amount, it requires a tuneable laser source with nearly identical laser power output at the two excitation frequencies to generate equal amounts of fluorescence; which may not always be feasible.

Another technique based on the same principle of shifting the Raman bands and subtracting spectra to remove fluorescence involves shifting of the diffraction grating instead of the laser frequency, which can be readily done using the existing equipment in Raman spectrometers. This method was first suggested by Mosier-Boss *et al* in 1995 [45], and later was realised to be a more powerful technique than it was originally thought. It involves recording a Raman spectrum of the sample at the normal calibrated position and then manually moving the spectrometer grating from the initial calibrated position by approximately 1-3 nm (which corresponds to a shift of about 22 cm^{-1} on the spectrum) to record another spectrum at this shifted position [46]. The two spectra are then subtracted and the difference spectrum is mathematically reconstructed through a curve-fitting process to obtain a conventional Raman spectrum with eliminated fluorescence. This method is termed Subtracted Shifted Raman Spectroscopy (SSRS) and has been successfully applied to the analysis of a variety of materials including dyes and pigments used in ancient artefacts [47-50].

2.4.5. Photobleaching

Photobleaching is a simple way of reducing fluorescence in samples [51]. It involves irradiation of the sample with laser light for a period of several minutes up to several hours before acquiring a spectrum, during which time photodecomposition is induced and the fluorescent molecules degrade, which subsequently reduces the fluorescence.

This has been found to be a simple yet effective method for reducing fluorescence in some cases. However, irradiation of samples for extended periods of time has been found to cause physical and chemical changes in compounds other than the chromophores in the sample. This means that this method cannot be used when analysing fragile, irreplaceable materials such as historic textiles or forensic evidence materials [51-53].

2.4.6. Baseline correction

Baseline correction involves manipulation of the spectra to remove the underlying sloping fluorescent baseline. Software packages such as OMNIC, Labspec or Matlab can be used to correct the baseline so that it appears flat at near zero intensity units. It can be done automatically by choosing a baseline fitting algorithm (such as a linear or polynomial fit to the data); or it can be done manually by selecting baseline points to be corrected along the spectrum. This is a simple method of removing the fluorescent baseline to produce a better looking spectrum. However, there is the possibility that it can accidentally remove some weak features that are a part of the sample's Raman spectrum, rather than fluorescence, especially when automatic baseline correction functions are used. Manual baseline correction can provide supervised baseline correction, but it involves human opinion as to where the baseline should be and which features should be counted as peaks. Therefore, there are always uncertainties involved with the use of such methods, and the possibility of unintentionally corrupting the original data.

A number of algorithms have been developed to improve upon existing baseline correction methods, such as the "intelligent background-correction algorithm" for highly fluorescent Raman spectra developed by Zhang *et al.* This involves peak detection and width estimation for a more reliable and valid baseline correction [54].

2.4.7. Anti-Stokes Raman Scattering

Fluorescence and Stokes Raman scattering result in a decrease in the frequency of the re-radiated radiation compared to the incident laser beam, since energy from the incident beam is transferred to the molecules in both cases. Therefore they should be plotted on the negative side of the x-axis (but are conventionally presented on the positive side). Anti-Stokes Raman scattering on the other hand results in an increase in the frequency of the re-radiated photons as energy transfers from the molecules to

the scattered beam. This means that measuring the anti-Stokes scattering should result in a Raman spectrum free of fluorescence. Even though anti-Stokes scattering is less frequent, hence much weaker, than Stokes scattering, methods have been developed to solve this problem. The most widely used method is Coherent Anti-Stokes Raman Scattering (CARS) which involves irradiation of the sample using multiple excitation sources to produce strong anti-Stokes Raman scattering [1, 55-57].

2.4.8. Other methods

Other methods for dealing with fluorescence include rejection of the fluorescent light using Fourier filtering methods [45]; use of mathematical functions and algorithms [58, 59]; increasing the temperature of the sample [60]; and use of optical gates or shutters that take advantage of the time difference between the Raman scattering event and fluorescence emission in order to reject fluorescence [61-63].

2.5. Applications of Raman Spectroscopy

Raman spectroscopy is a non-destructive spectroscopic method that can be used to obtain information on the chemical bonding and the crystalline structure of substances, as well as to identify unknown substances by looking at their characteristic spectral patterns. It requires minimum or no sample preparation, and can analyse solids, liquids or gases in bulk, or microscopic amounts. It can also analyse materials in aqueous solutions, through glass containers and packaging materials [1].

These abilities therefore make it an ideal tool for the analysis of a variety of materials related to a broad range of disciplines, and the range of applications is

continuously growing. The following sections give a brief overview of the applications of Raman spectroscopy across multiple disciplines.

Das *et al* and Kiefer provide extensive reviews of Raman spectroscopy and its applications [64-67].

2.5.1. Biology and biomedical sciences

The non-invasive nature and the wealth of information Raman spectroscopy provides on molecules, and their structures, has enabled the technique to be used for the analysis of biological and biochemical molecules without the need for stains or markers. Especially when dealing with biological material, which is made up of mostly water, Raman spectroscopy has a great advantage over other analytical techniques due to water being a weak Raman scatterer.

Raman spectroscopy (and resonance Raman spectroscopy) has been successfully applied to the analysis of a variety of biological macromolecules. These include the investigation of interactions between proteins and their conformational structures [68, 69]; the structures of nucleic acids [70]; analysis of enzymes and their mechanisms [71]; determination of the oxygenation state of haemoglobin in blood [72]; detection of metabolic activity of mitochondria in living cells [73]; and detection of hormones, such as the thyroid-stimulating hormone [74]. It has been used to investigate the physical properties of human nails and effects of nail hydration on the protein structure [75]. It has also been used in quality assessment of meat and fish by looking at the changes that occur in proteins, as well as lipids, during deterioration [76].

Raman spectroscopy can analyse materials in microscopic amounts, and this property makes it a useful analytical tool in microbiology. It has been used to detect

and analyse microorganisms such as bacteria found in spoiled food [77], or viruses [78, 79]. It is also recognised as a powerful tool that can detect chemical and biological agents used in biological warfare, such as bacterial spores [80].

Additionally, it has been found to be a great tool in medical diagnostics and has been applied to the detection of malignant tumours, such as tumours found in the mucosal tissues of the colon [81], breast tissues [82, 83], cervical tissue [84], kidneys [85], and skin [86]. Raman spectroscopy successfully discriminated the malignant cells from the normal cells, and it is believed to be a potentially powerful technique for early detection of cancer.

Other medical applications include the analysis of brain tissue for Parkinson's disease [87]; diagnosis of atherosclerosis in human arteries [88]; detection of silicone in the lymph node tissues of patients with ruptured breast implants [89]; analysis of the arterial wall for chemical decomposition that can help identify rupture-prone plaques before the onset of symptoms [90]; and monitoring the oxygenation of tissues which could be helpful in the diagnosis of clinical shock [91].

It is also used in detection of toxins and biochemical changes in cells, which provides a potential method for monitoring pharmaceuticals and their interactions with cells, as well as monitoring the growth of engineered tissues [92].

Pappas *et al* provides an overview of bioanalytical applications of Raman spectroscopy [93].

2.5.2. Pharmaceuticals and pharmacology

Raman spectroscopy is a very useful tool in qualitative and quantitative analysis of drugs, characterisation of drug formulations and identification of pharmaceutical tablets. Studies on qualitative [94] and quantitative [95, 96] analysis of pharmaceutical tablets has shown the potential of this technique in the pharmaceutical industry. It has been used as a technique for quality control in tablet manufacturing due to the information it provides on tablet composition and uniformity [97]; as well as a tool to monitor processes during formulations of topical gels and emulsions [98].

Raman spectroscopy can identify the formulation of drugs by observing the characteristic frequencies of molecules, as well as their distribution in the tablet via Raman mapping. It can also analyse materials through different types of packaging. These properties make it an especially valuable tool for the detection of counterfeit drugs even through packaging materials [99, 100].

It is also able to detect the interaction of drug molecules with the target cells or other biomolecules such as nucleic acids [101]; and has been used for studying the binding of anti-cancer drugs [102, 103].

A summary of pharmaceutical applications of Raman spectroscopy is given by Fini [104].

2.5.3. Materials science

Raman spectroscopy is a versatile spectroscopic tool and is readily applicable to any materials system. It is used to study lattice vibrations and structures of glasses [105], amorphous solids [106] and crystals [107-109]. It is an indispensable technique for

the analysis and characterisation of a variety of materials including minerals [110, 111], ceramics [112] and cement [113]. In addition, it is used to examine the composition, phase structure and crystallisation behaviour of polymers [114-117].

It is applied to the field of electronics to investigate semiconductors [118] and superconductors [119, 120], as well as the sizes and forms of their crystals, their dopant levels, and presence of stress or strain, and is also used to monitor the carbon coating on computer hard disks [121].

Raman spectroscopy is a valuable tool for the analysis of environmental contaminants such as perchlorate found in water [122], nitrate and nitrite found during waste water treatment processes [123], or uranium found in environmental samples [124]. It is also used for the detection of biological threat organisms in the presence of complex environmental backgrounds [125].

2.5.4. Art and archaeology

Raman spectroscopy is one of the preferred techniques for the analysis of objects of art and archaeology. Because it requires no sample preparation it can analyse samples in situ using fibre optic probes; it is non-destructive and non-invasive; and it gives substantial chemical information about the samples.

Many studies have been done on the detection and discrimination of historical dyes and pigments used in works of art [21, 126-128], found in fabrics and textile fibres [16, 129, 130], and those used in maps [131] and ancient manuscripts [132-134]. Pigments found in wall paintings [135-137], portrait miniatures [138], pottery artefacts [139-141], frescoes [142, 143], prehistoric rock art [144, 145], and polychrome stone statues [146] have also been analysed and characterised using Raman spectroscopy.

Pigment analysis is important in art and archaeology because it allows the artefacts to be dated and authenticated [147]. A large number of studies have been carried out on the characterisation of pigments and dyes found in historic and modern works of art. Several libraries of Raman spectra exist for historic [148, 149] and modern [150, 151] pigments, including natural pigments found in ochres and iron-containing ores [152] and those found in artists' materials and other works of art [153-155]. There are also several on-line databases of natural and synthetic dyes and pigments available [156].

Organic materials found in historical and archaeological objects can also be classified using Raman spectroscopy. These include natural resins [157], glues, gums, oils and other organic media used in ancient varnishes [158]. Raman spectroscopy can also be used to determine the maturation process and age of fossil resins [159].

Other organic compounds that are analysed and identified using Raman spectroscopy include human skeletal remains [160], and the heme-containing compounds and haemoglobin breakdown products found in dinosaur bones [161].

A review of Raman spectroscopy and its applications in art and archaeology are given by Vandenabeele *et al* and Smith *et al* [156, 162, 163].

2.5.5. Nanotechnology

Raman spectroscopy is a useful analytical tool for the characterisation of nanomaterials such as nanosensors, nanotubes and nanowires due to its ability to analyse materials that are microscopic in size. Such applications include characterisation of nano-structured carbon materials [164-168] and quantitative analysis of nanomaterials [169].

2.5.6. Forensic applications

As mentioned before, Raman spectroscopy is non-destructive; it does not require sample preparation; it can be used with minute amounts of sample; it can analyse samples found in aqueous solutions and/or in glass containers [1] and through hinge lifters and evidence bags [170-172]. These aspects of Raman spectroscopy make it especially suitable for use in forensic analysis of trace evidence.

Identification and establishment of the source of trace evidence in forensic science is an important task. Raman spectroscopy has been applied to the analysis and characterisation of a variety of materials encountered as forensic evidence. One example of which is paint evidence. Paint traces can be found in the form of chipped paint coat fragments, droplets or smears. Establishing the source of paint samples can help form a link between victims, suspects and crime scenes (for example, hit and run victims and vehicles). A variety of studies done on the analysis and characterisation of paint as evidence using Raman spectroscopy includes discrimination of automotive paint flakes [173-176], household paint and spray paint samples [53, 177].

Inks are another type of forensic evidence that is frequently encountered. Raman spectroscopy has been applied to the discrimination of dyes found in pen inks [28]; ink entries found on suspected forged documents [178, 179]; and inks found on printed documents [180, 181]. Stability of SERRS colloids applied to biro inks on suspect documents has also been investigated and it was found that good SERRS spectra can be obtained from the same sample even a few years after the application of the colloid [182].

Fibres, being one of the most common forms of trace evidence, have also been analysed using Raman spectroscopy. Many studies involved the analysis of the dye components found in fibres as a way of differentiating between fibres [174, 183-186]

and the characterisation of fibres by their polymer type [187]. It was also found that Raman spectroscopy could detect dyes in fibres with concentrations as low as 0.005% [188].

Drugs of abuse can be encountered as evidence on clothing of suspects or in the fingerprints of persons who have handled illicit drugs. Raman spectroscopy has been found to be a valuable technique in the detection of drugs of abuse at border controls [189], on clothing materials [190], and in fingerprints [191]. It has also been shown to be effective in the detection of drug particles on fibres, or in fingerprints, after recovery with adhesive lifters, and through evidence bags [170-172].

Explosive materials can also be efficiently detected and identified using Raman spectroscopy, as has been demonstrated by studies on the detection of explosives on clothing [192, 193] and liquid explosives in bottles [194]. It is a useful tool in real-time detection of explosive materials for environmental and security purposes [195, 196] and fibre optic probes can be utilised for remote detection of such materials [197].

It is also used for the identification and characterisation of gunpowders [198], and trace evidence materials on a discharged lead bullet to determine its origin or the intermediary objects of its trajectory [199].

Another application of Raman spectroscopy in forensic science includes identification of bodily fluid traces [200] such as sweat [201], semen [202], vaginal fluid [203], blood [204, 205], or mixtures of bodily fluids such as semen and blood mixtures [206]. Raman spectroscopy has an advantage over other techniques in this field due to its non-destructive nature: analysis of these materials does not prohibit subsequent DNA analysis unlike many of the other techniques [207].

Raman spectroscopy can be combined with other techniques for a more in depth analysis of forensic evidence, such as X-ray fluorescence spectroscopy for the analysis of inks, paint chips, fibres and plastics [208] and scanning electron microscopy (SEM) for the analysis of paint chips and explosives [209].

Another type of evidence that can be encountered in a forensic investigation is cosmetic evidence. Cosmetic evidence can be found in the form of smears, powders, or chipped fragments that originate from a variety of cosmetic products such as lipstick, foundation, nail polish or eye shadow. Establishing the source of the cosmetic evidence can help create a link between a cosmetic-wearing victim and a suspect, as well as a cosmetic-wearing suspect and a crime scene.

Raman spectroscopy has been successfully applied to the analysis and discrimination of some of these cosmetic evidence materials. For example, glitter, a component of decorative and cosmetic products, has been analysed and differentiated using Raman spectroscopy [210]. Lipstick, one of the most commonly used cosmetic products, has also been recognised as forensic evidence and some studies have been done on the analysis and discrimination of lipsticks using Raman spectroscopy [2, 3].

2.6. Summary

For many years since its discovery, Raman spectroscopy was generally being used only by experts in academic or industrial research laboratories. The instrumentation was complicated, bulky and expensive; and it suffered a major drawback: fluorescence. However, over the past decade, development of cheap, powerful lasers, improved optical configurations, highly sensitive charge-coupled device (CCD) detectors and effective Rayleigh rejection filters enabled Raman spectrometers to be used in several fields. The spectrometers became smaller, more sensitive and more affordable, and started being regularly used not only by experts, but also by non-specialists [1, 163].

Modern Raman spectroscopy is a powerful technique and its usefulness is becoming widely recognised across several disciplines. Its non-destructive nature and the wealth of information it provides on trace amounts of samples make it an especially valuable tool in forensic science. Therefore this research investigates the application of Raman spectroscopy to the analysis and differentiation of lipstick smears as forensic evidence.

CHAPTER III

Lipstick as Cosmetic Evidence

3.1. Lipstick through the Ages

Even before the beginning of written history, humans were interested in using some form of 'paint' to decorate their bodies. This practice of painting parts of the body has been around for thousands of years, but when prehistoric men first decided to colour their bodies, it was not for the same reason as modern civilisations do today.

Not being the strongest, or the most aggressive, of creatures that inhabited the Earth in ancient times, prehistoric man had to learn to use his only other weapon, his intellect, to invent his own tools for protection and hunting. Aside from creating tools and weapons using wood and stone, he also discovered the staining properties of the natural materials around him and started using them for painting his body in order to blend in with the environment. The more he experimented with different colours, the more he learned how to use them in different situations. Soon, these paint materials were being used not only for camouflage, but also for scaring the opponent away in case of an aggressive confrontation [211].

As prehistoric man became more civilised, he started using paint not only for survival, but also for other reasons. He discovered new uses for those primitive paints, including their use in rituals for spiritual practice, and later on in a more social context that has persisted throughout the ages until the modern day: for the creation of 'beauty' [211].

Since humans discovered that they could change their appearances to look more attractive to potential mates by using natural dyes and pigments, use of these natural paint materials for aesthetic purposes started to become more and more widely

practised. While many recipes and concoctions must have been used for making up a variety of cosmetic products in different shapes and forms, the earliest evidence of cosmetics use in ancient history did not emerge until 1920, when Sir Leonard Woolley excavated a 5000-year-old Sumerian tomb in the 'Royal Cemetery' of the city of Ur near Babylon, revealing a variety of cosmetic cases that were buried with their owners, including the first "lipstick" in history [212-214].

It was not only Sumerian royalty however who desired to paint their faces to achieve beauty. An ancient Egyptian scroll portraying a woman painting her lips while holding a mirror showed that this cosmetic practice was popular amongst other ancient civilisations as well [214]. Whereas the Sumerian royalty, such as Queen Schub-ad of Ur, preferred crushed red rocks to decorate her lips; the aristocratic Egyptian women used a mixture of red ochre (iron ore) with fat or oil, as well as crushed flower petals and spices to give their lip-paints a pleasant scent [211]. Over the years, experimenting with different ingredients, the Egyptians found out that mixing their pigments with resin or gum would give a more lasting finish [212], whereas using crushed carmine beetles mixed with ant eggs as the base resulted in a deeper red colour [215]. They would put these into plant stems and apply it on their lips, even going so far as adding slimy ointments for a glossy effect. Blue-black, red and orange lip-paints were the most popular among Egyptians and it was not only the women of Egypt, but the men as well, who used these techniques to paint their lips [213].

Unlike the Egyptian women, who used to paint their faces freely, the Grecian women in the fourth century B.C. had little independence and wore no make-up. When they wanted to enhance their looks, they would only use cheek and lip paint made by mixing vermillion, also known as mercuric sulphide, with vegetable substances such as seaweed and mulberry. On the other hand, another class of Greek women, namely the prostitutes, were able to use as much of this make-up as they desired [211, 212, 214].

Ancient Romans also enjoyed painting their lips, and they used iron ores and sediments from red wine together with a potentially poisonous reddish-purple plant dye called fucus. Palestinian women of the second century A.D. opted for bolder colours, such as bright orange and purple, and adjusted their recipes accordingly [213, 214].

During the medieval period, women preferred rose-coloured lips and cheeks, and created their own recipes using ingredients such as crushed red roots mixed with sheep fat; or alternatively, if they did not use (or could not afford) any make-up they would bite their lips and pinch their cheeks to give them some colour [212, 213].

During this period, the English were not accustomed to using cosmetics to enhance their beauty. It was Queen Elizabeth I herself who made cosmetics popular in England and brought about the "Golden Age" of lipstick, making crimson-stained lips fashionable. She would prepare her lipstick herself using a mixture of cochineal (a scaly insect from which the red dye carmine is derived), egg white, fig milk, as well as the most widely used ingredient nowadays – beeswax. It is also believed that the first 'lip pencil' emerged during this period. This pencil would be made by mixing ground 'plaster of Paris' (also known as gypsum plaster) with a colouring ingredient, which was then rolled into a pencil shape and dried in the sun. As international trade spread, more ingredients for cosmetics such as saffron flowers, henna, gum Arabic and exotic dyes and spices began to flow into the country from different places including Baghdad, Marseilles, Italy and Cyprus [211, 214, 215].

Towards the end of the seventeenth century, cosmetics were being heavily used, especially by actors and actresses for theatrical performances. 'Lip rouge' was particularly fashionable during the Baroque period, not only for women, but also for the respectable male members of the society [211, 213].

During the eighteenth century a number of recipes for lip paints appeared. Many of these recipes included hog's lard, butter or beeswax as the base; and cochineal, sandalwood, safflower, raisins, alkanet root or roses as the colouring agents. Whereas the more daring women followed a variety of recipes published in books, or suggested by the well-known people of the time, some women coloured their lips just by washing them with brandy, or by rubbing 'Spanish Papers' (papers thickened with carmine dye) on their lips. In 1724 an act was passed in England to regulate the materials used in cosmetics since some of them were potentially dangerous (such as vermillion – mercuric sulphide). In spite of this, some women continued to use traditional harsh recipes to achieve the look they desired. At approximately the same time in America, colonial men, as well as women, would paint their lips. Amongst them, the Virginians were the ones who coloured their lips the most. They would use Spanish Papers, as well as Bavarian Red Liquor, rubbed on their lips or drank, and lemons to be sucked on throughout the day for redder lips. The Puritan settlers however would frown upon the practice of 'rouging the lips' and the Puritan women who really wanted to colour their lips would rub red ribbons onto their lips in secret [211-214].

The nineteenth century was the time cosmetics became safer to use, when the harmful blends of the previous century were replaced with those made from herbs, flowers, vegetable fats and oils. Standards of hygiene improved and cleanliness became one of the most important virtues. Cosmetics were still being used liberally by women in England; however, this changed dramatically when Queen Victoria ascended the throne in 1837. She publicly declared that make-up was "impolite", and the image of the 'ideal woman' began to change from having an artificially enhanced face, to having a more natural beauty. Women would still use face powder and rouge for the cheeks, but so sparingly that it would barely be noticeable; and the use of any lip colouring was considered to be "undesirable and vulgar". Slightly tinted lip salves could still be used with the excuse of moistening chapped lips, but lip paints were considered to be the most indecent of all make-up. Women did not completely stay away from lip paints however, as recipes were being shared and new concoctions being made and traded secretly behind closed doors. On the other hand, actresses

(and actors) were still able to wear as much make-up as they desired, but it still was not acceptable to do so in public [211-213].

Towards the end of the nineteenth century, the tolerance towards the use of cosmetics to enhance beauty increased, and women began applying make-up more liberally than previously. In 1880 the French cosmetics company, Guerlain, manufactured the first commercial 'lip-stick' made of pomade of grapefruit, butter and wax, wrapped in silk paper in stick form; and therefore lipstick once again became one of the most popular form of cosmetic products [211, 213].

The lipsticks produced by Guerlain, however, were not mass produced and were only available to aristocratic clients. Lip paints and salves were still being home-made until 1915 when the designer Maurice Levy from the Scovil Manufacturing Company in Connecticut, America, took Guerlain's invention further and mass produced the first modern lipstick in metal tubes [211, 213, 214].

In the early 1900s, theatre and films had a great impact on everyday make-up. Women, especially young women, began to use bright coloured lipsticks and lipstick became the most favourite cosmetic product. New metal containers where lipstick can twist up out of the tube were produced and applying make-up in public became a normal thing to do. These lipsticks were uncomfortable to wear though, as they were made of a soap base which made the lipstick thick and matte. Due to the increasing popularity of this particular cosmetic product, companies all over the world started doing more research on ways of improving the lipstick. They started using new ingredients such as Spanish alkanet root and red lithol salts, which are sulfonated azo pigments [216], as well as chemically extracted carmine dyes as colouring ingredients; and spermaceti (wax derived from the head of the sperm whales [217]), beeswax and lanolin (wax extracted from the wool of sheep) as the oily base material. Permanent long-lasting lipsticks that became coloured upon reacting with the skin were also introduced in the 1920s [211-213, 215].

In 1930s the image of beauty advertised in magazines and films made women more aware of their looks, and they started spending more time and money achieving the beauty they desired. Cosmetics manufacturers started mass producing a variety of new products, such as Elizabeth Arden who introduced a wide range of lipstick shades to match one's clothes; Helena Rubinstein who used sun protectants in her lipsticks; the Hollywood cosmetician Max Factor, who introduced a large variety of bright lipstick colours using his experience in film make-up; and the French company Lancôme who produced lipsticks with a shiny finish. As the cosmetics industry expanded, the United States Food and Drug Administration (FDA) passed the Federal Food, Drug, and Cosmetic Act in 1938 in order to regulate the use of ingredients in cosmetics for safety and quality of products [211, 213, 214].

During World War II, lipstick production suffered when key components such as castor oil, petroleum and metal were required for the war effort. Metal cases had to be replaced with plastic and paper. Magazines asked women to use their lipsticks sparingly and advised them to melt down scraps of lipstick from old tubes to create a new one; or recommended use of beetroot juice to tint the lips [212-214].

After the war, lipstick manufacture made a comeback. The dark, vivid colours were replaced by paler shades, including white and silver. Manufacturers all over the world started using titanium dioxide to achieve these paler shades, as well as fish scales for a frosted, shimmery effect [211, 212, 214].

In the 1970s legislation was adopted globally to make sure all cosmetic products were tested, and seen fit for purpose, before going on to the market. Concerns over the use of synthetic colours, fragrances and additives in cosmetics caused a rise in the number of manufacturers that used natural or 'organic' ingredients such as fruit acids, aloe vera, essential oils and mineral pigments. This was the time when manufacturers such as Yves Saint Laurent introduced lipsticks labelled with numbers instead of names to mark their colour. Towards the 1990s, almost all colours and shades of lipsticks were already being produced, so the cosmetics companies started

focusing on products that provided protection from sun damage, fought signs of aging, improved skin tone and provided long lasting colour [212, 213].

3.2. Lipsticks Today

For the past few decades, the manufacture of cosmetic products, and the ingredients used, have been regulated by a variety of authorities such as the Food and Drug Administration (FDA) in the United States; the European Commission in the European Union; and the Ministry of Health, Labour and Welfare in Japan [218]. Because the manufacturers have to follow the regulations put forward by these authorities, the individuality of lipsticks that used to be made up at home, or by a local chemist, to suit the individual's taste in previous centuries is now gone. This means that, even though the exact chemical composition of lipsticks differs between manufacturers, the majority of the composition is very similar regardless of the manufacturer.

Having gone through many changes over the centuries the recipe for lipstick now contains none of the harmful, or potentially poisonous, substances of the previous centuries. Modern lipsticks are now carefully formulated to provide uniform colour coverage and protection for the lips without the disturbing odour of the waxes and the toxicity and irritancy of harmful compounds; while being stable under ordinary changes in temperature and moisture [215].

All of the ingredients listed below were obtained from the manufacturers' website, their catalogues that have a complete list of ingredients at the brands' own stands in shops, or on the individual lipsticks themselves [219, 220]. Even though the manufacturers have a list of ingredients on each product, when it comes to dyes and pigments the ingredients are listed after stating "May or may not contain", and the manufacturers are reluctant in revealing the formula for their products when

contacted personally; therefore it is not possible to give a definite list of ingredients for each lipstick.

Typically a lipstick is composed mostly of a 'base' material which is a mix of waxes and emollients. Waxes are mixtures of C25–C35 alkanes, esters, long-chain alcohols and aldehydes; and they usually form about 8-18% of the lipstick (by weight) depending on the type of lipstick (matte, glossy etc.). Wax is what keeps the lipstick in 'stick' form. The waxes that are commonly used in the manufacture of lipsticks are plant derived candelilla and carnauba waxes; beeswax and lanolin that originate from animals; ozokerite which is a wax-like mineral that occurs naturally; paraffin and microcrystalline waxes which are obtained from petroleum; and synthetic hydrocarbon wax derived from various oils [213, 214, 217, 218, 221].

Emollients are the other major class of compounds (besides waxes) that form a lipstick's base. These are composed of non-volatile oils and oily compounds that are added to lipsticks to improve the texture and ease of application, to help pigment dispersion, and to give the lipstick soothing and moisturising properties, as well as its shine. Typically emollients form about 40-70% (by weight) of the lipstick. The emollients commonly used to soften the wax base are oils such as castor (ricinus communis) oil, jojoba (simmondsia chinensis) oil, coconut (cocos nucifera) oil, sunflower (helianthus annuus) seed oil, soybean (glycine soja) oil, mineral oil (paraffinum liquidum), silicon oils and hydrogenated vegetable oils. Esters, especially fatty acid esters, are also widely used in lipsticks for their emollient properties i.e. they improve the texture of the lipstick, reduce the 'stickiness' and have skin conditioning properties. Most commonly used esters are ethylhexyl hydroxystearate, cetyl lactate, glyceryl caprylate, PPG-3 benzyl ether myristate, ethylhexyl palmitate, isopropyl isostearate, hydrogenated castor oil dimer dilinoleate, isopropyl titanium triisostearate, trimethylolpropane triisostearate, isodecyl neopentanoate, bis-diglyceryl polyacyladipate-2, diethylhexyl adipate, triisodecyl trimellitate, C12-15 alkyl benzoate, diisosteryl dimer dilinoleate, neopentyl glycol diethylhexanoate, octyldodecyl lanolate, octyldodecyl neopentanoate, myristyl lactate, and myristyl myristate [213, 215, 217, 218, 221].

Other compounds used as emollients include polymers such as hydrogenated polyisobutene, polyester-4, dimethicone/bis-isobutyl PPG-20 crosspolymer and castor oil/IPDI copolymer; alcohols such as caprylyl glycol and cetyl alcohol; polysaccharides such as hydrolyzed glycosaminoglycans and sodium hyaluronate; glycerin; lauroyl lysine; fatty acids found in rice (oryza sativa) extract; caprylic/capric/lauric triglyceride for its role in pigment dispersion; as well as oils and butters such as camomile oil (chamomilla recutita), pot marigold (calendula officinalis) oil, aloe vera (aloe barbadensis) leaf extract, argan (argania spinosa) oil, Brazil nut (bertholletia excels) seed oil, evening primrose (oenothera biennis) oil, cocoa (theobroma cacao) seed butter, shea (butyrospermum parkii) butter, meadowfoam (limnanthes alba) seed oil and sweet almond (prunus amygdalus dulcis) oil for their soothing and skin conditioning properties. Vitamin E and its derivatives (tocopherol, tocopheryl acetate, and tocopheryl nicotinate) are often added for their antioxidant and skin conditioning properties. All these fatty compounds are an important link between waxes and oils as they play a vital role in the homogeneity and texture of lipsticks, and they improve the longevity of the film of colour applied on lips. [217, 218].

The main purpose of a lipstick is to give lips colour, and this is achieved by finely dispersing colouring agents in the wax/oil base of the lipstick. There are many different types and colours of colourants used, and to classify these, codes have been assigned by regulatory authorities in different countries. In the EU, the substances certified for use as colouring agents in cosmetics are listed by their Colour Index (C.I.) numbers, which is a code assigned by the Society of Dyers and Colourists (SDC) together with the American Association of Textile Chemists and Colourists (AATCC). In the US, the colourants that are not certified by the Food and Drug Administration (FDA) are listed by their Colour Index (C.I.) numbers; whereas those that are certified are assigned a code by the FDA consisting of prefixes FD&C or D&C, if the colourant is authorised for use in food (F), drugs (D) or cosmetics (C); followed by its colour and a number (for example, D&C Red No. 7) [218].

The colouring agents used in lipsticks are divided into two groups: dyes and pigments. Dyes are organic materials and are soluble in water or in oil. Since water soluble dyes can be dissolved and washed away naturally by saliva, they have to be made water-insoluble before they can be used in lipsticks. This is done by combining the organic dye with metal oxides, such as aluminium hydroxide, to form an insoluble precipitate which is then dispersed in the wax/oil base of the lipstick. A dye processed in this way is called a "lake" and the resulting water-insoluble dye becomes the "(metal) lake" of the original water-soluble dye [215, 218].

The majority of the organic dyes used in cosmetics are divided into seven classes depending on their chemical structures: azo (**Fig.3.1**), triarylmethane (**Fig.3.2**), anthraquinone (**Fig.3.3**), xanthene (**Fig.3.4**), phthalocyanine (**Fig.3.5**), indigoid (**Fig.3.6**), and quinoline (**Fig.3.7**) dyes. [221].

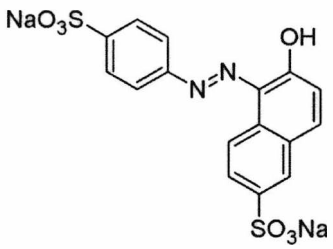

Figure 3.1. An azo dye, FD&C Yellow No.6

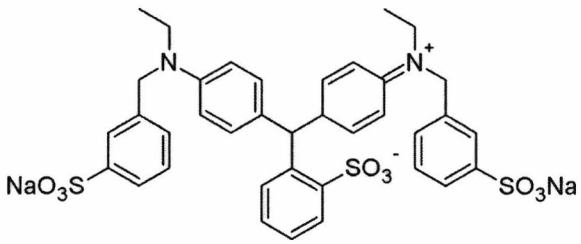

Figure 3.2. A triarylmethane dye, FD&C Blue No.1

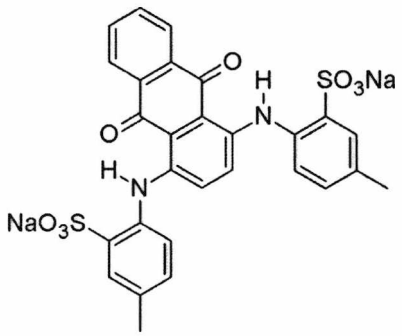

Figure 3.3. An anthraquinone dye, D&C Green No.5

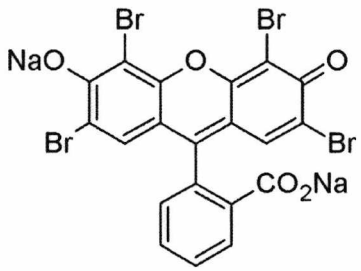

Figure 3.4. A xanthene dye, D&C Red No.22

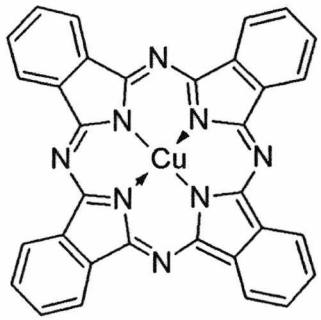

Figure 3.5. A phthalocyanine dye, Phthalocyanine Blue

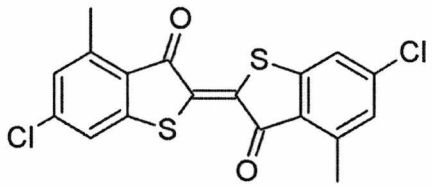

Figure 3.6. An indigoid dye, D&C Red No.30

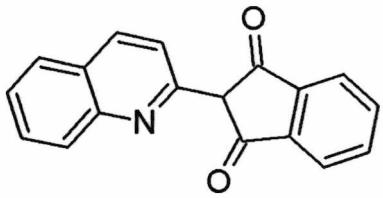

Figure 3.7. A quinoline dye, D&C Yellow No.11

Dyes that are commonly used in the manufacture of lipsticks are as follows:

Azo dyes: FD&C Red No. 40 (allura red, C.I. 16035), FD&C Yellow No. 5 Aluminium lake (tartrazine, C.I. 19140), FD&C Yellow No. 6 Aluminium lake (Sunset yellow, C.I. 15895), D&C Red No. 6 Aluminium and Barium lakes (C.I. 15850), D&C Red No. 7 Aluminium and Calcium lakes (C.I. 15850), D&C Red No. 33 Aluminium lake (C.I. 17200), D&C Red No. 36 (C.I. 12085)

Triarylmethane dyes: FD&C Blue No. 1 Aluminium lake (C.I. 42090)

Anthraquinone dyes: D&C Green No. 5 (C.I. 61570)

Xanthene dyes: D&C Red No. 22 (Eosin Y, C.I. 45380), D&C Red No. 27 Aluminium lake (C.I. 45410), D&C Red No. 28 (C.I. 45410), D&C Red No. 21 Aluminium lake (C.I. 45380), D&C Orange No. 5 (C.I. 45370)

Indigoid dyes: D&C Red No. 30 (C.I. 73360)

Quinoline dyes: D&C Yellow No. 10 (C.I. 47005)

Another type of dye commonly used in the manufacture of lipsticks includes the natural dye, carmine (C.I. 75470).

Pigments on the other hand are insoluble, inorganic substances, that are ground and finely dispersed in the oil base of the lipstick, which has an affinity with the pigments used to ensure an even dispersion of colour. When used, pigments remain as crystals or particles in the oil base of the lipstick and stick to the surface of the skin, rather than being absorbed by the skin like the dyes in long-lasting lipsticks. Most commonly used pigments include iron oxides (C.I. 77491, 77492, 77499); manganese violet, $MnNH_4P_2O$ (C.I. 77742); silica; tin oxide (C.I. 778161); titanium dioxide, also known as Pigment White 6 (C.I. 77891); zinc oxide (C.I. 77947); talc, which is hydrated magnesium silicate (C.I. 77718); and aluminium powder, also called Pigmental Metal 1 (C.I. 77000). Sometimes pearlescent pigments such as fine-grained mica (muscovite, potassium aluminium silicate dihydrate; C.I.77019) and bismuth oxychloride (C.I. 77163) are added for a shimmery effect due to their high refractive indices. Mica coated with titanium dioxide or iron oxides is also used to give a certain coloured shine, which is determined by the thickness of the metal oxide layer. This happens by interference of light due to the metal oxide coating which causes some wavelengths to be reflected and others transmitted. As the thickness of the layer increases, the reflection goes from silver to yellow, red, blue and green. [217, 218, 221].

The concentration of dyes and pigments in lipsticks can vary from 0.5% to 15% (by weight) depending on the type of lipstick (light/dark lipstick or a lip-gloss) [218, 221, 222].

Due to a variety of ingredients having differing miscibilities, it is important to make sure that the final product is homogenous. This is achieved by using emulsifiers. Emulsifiers are amphiphilic compounds that decrease the surface tension between immiscible compounds permitting them to spread out easily. They interact with both hydrophilic and lipophilic phases in an emulsion, keeping the two phases together.

This helps form stable emulsions and results in improved consistency of the final product. Compounds that are commonly used as emulsifiers in lipsticks are: acetylated lanolin, C10-30 cholesterol/lanosterol esters, octyldodecanol, sorbitan sesquioleate, hexyl laurate, polyglyceryl-3 diisostearate, polyglyceryl-2 triisostearate, polyglyceryl-4 isostearate, hydrogenated palm kernel glycerides, cetyl PEG/PPG 10/1 dimethicone, epoxy resin, isopropyl lanolate, pentaerythrityl tetracaprylate/tetracaprate, ethylene/propylene/styrene copolymer, butylene/ethylene/ styrene copolymer, vinylpyrrolidone/hexadecene copolymer, pentaerythrityl tetraethylhexanoate and pentaerythrityl tetraisostearate. Compounds that are used for their emulsion stabilising properties are dimethyl silylate, C30-50 alcohols, polyethylene and cetyl alcohols [217, 221].

To help shape the lipstick and improve its flexibility, compounds known as plasticisers are used. These include epoxy resin, phthalates, polybutene, propylene carbonate and sucrose acetate isobutyrate. Thickeners are also used to add body to lipsticks and these include compounds like C10-18 triglycerides, calcium aluminium borosilicate, trihydroxystearin, nylon-12, polyethylene terephthalate and styrene/acrylates copolymer [217].

It is important for the lipstick to stay well-preserved and stable over time. To prevent the fatty compounds (especially the animal derived ones) from spoiling, preservatives and antioxidants such as pentaerythrityl tetra-di-t-butyl hydroxyhydrocinnamate, BHA (butylated hydroxyanisole), BHT (butylated hydroxytoluene), ascorbyl palmitate, propyl gallate, disteardimonium hectorite, trioctyldodecyl citrate (citric acid), vitamin E (tocopherol) and its derivative, tocopheryl acetate, are used. It is very common to use preservatives such as sorbic acid, phenoxyethanol, methylparaben, sodium methylparaben and propylparaben due to their anti-microbial properties. It is also important to preserve the moisture in the lipstick to prevent it from drying out over time. To achieve this, compounds called humectants that help retain the moisture content of materials are used. Most commonly used humectants are butylene glycol, glycerin, diglycerin and sorbic acid [217].

Since lipsticks are composed mostly of waxes and oils, they tend to be unpleasant to smell and taste; therefore to make them pleasant to use, and thus more appealing to the consumers, manufacturers add perfumes and flavourings to mask the fatty odour of the ingredients. These vary greatly depending on the 'scent' or 'taste' desired, but they generally include natural compounds such as vanilla extract, citronellol, rosa gallica flower extract, geraniol, hexyl cinnamal, linalool, magnolia acuminata flower extract and black lovage (olus) herb extract; and synthetic compounds such as cinnamyl alcohol, alpha-isomethyl ionone, hydroxycitronellal, isononyl isononanoate and limonene. Some manufacturers also choose to improve their lipsticks by adding UV sunscreens such as ethylhexyl methoxycinnamate and salicylates [217].

The colour of a lipstick is not the only variable; there are many options available as to what kind of lipstick might be used depending on the look desired. One might opt for a basic, dark coloured, non-shiny lipstick; or a glossier, lighter coloured one; or maybe a long-lasting, indelible lipstick that stays on for a very long time.

To achieve this, the manufacturers have created different 'types' of lipsticks with different properties by varying the ratio of the ingredients, mainly that of the waxes and emollients. For example *matte* lipsticks are opaque, strong-coloured lipsticks that have a wax content that is heavier than the emollient content; therefore they do not shine as much. *Creme* lipsticks on the other hand have more emollients added for a smooth and moisturising feel, and they have slightly more shine than the matte lipsticks. *Shimmer* lipsticks have a balanced content of wax and emollients, and their extra sparkle comes from reflective ingredients such as mica, coated mica or silica particles. *Sheer* lipsticks in the other hand are more translucent; they look more natural and lighter in colour with a slight shine, which is obtained by mixing a medium amount of wax with a lot of emollients. *Stains* are lipsticks similar to sheer lipsticks in composition, but they differ in that they contain dyes that have staining properties where the dye reacts with the surface of the skin to stay on for longer than any other dye. These lipsticks still have light and natural-looking colours compared to other types of lipsticks. There are also *long-lasting* lipsticks that are high in

pigment concentration and have high molecular weight dimethicones or cyclomethicones that form water resistant films on the skin to improve the staying power of the lipstick. These are more long-wearing than the matte lipsticks [213, 214, 221].

Another type of lip product is *lip-gloss*. These are made with softer waxes and contain more emollients than other lipsticks, giving them a lot of shine. Because they tend to be softer and more fluid, they come in pots rather than in stick form. The last type of lip product is *lip liners* or *lip crayons*. These come in pencil form and contain more waxes and less emollients than other lipsticks. They are also quite dense in colour.

Lipsticks form a significant fraction of the cosmetic inventory used by people in the world. Usually perceived as a symbol of femininity, lipsticks are mainly used by women, starting in their preteen years and carrying on for many years throughout their lives. Lipsticks provide a range of colours and shades for the lips, as well as moisturisation and protection from the harmful UV rays of the sun. They are easy to apply and carry, and there are even lipsticks that make lips plumper. They come in various sizes and shapes, the most common being the 0.5-inch diameter 'bullet' form in metal (or plastic) cases [218, 222].

The application of lipstick is considered to be an important part of a woman's daily routine. Studies have shown that wearing lipstick makes women feel 'presentable', 'comfortable', 'confident', and 'feel good about themselves'; and that the majority of lipstick users wear lipstick on most days of the week, re-applying it three to four times a day, purchasing four or more lipsticks per year [213, 223].

Lip-cosmetics and lip-products are not used exclusively by women. Certain lip-products, such as colourless lip treatment balms, are not gender specific and can also be used by men as well as children [222].

3.3. Lipsticks in Forensic Science

Being such a significant part of (predominantly) women's daily lives, it is common to come across lipstick smears and lipstick stains almost anywhere at any given time. Being sticky, waxy and oily substances, lipsticks are easily transferrable on contact with an object or another person. This means that, for example, lipstick smears can be encountered at crime scenes during forensic investigations on surfaces such as cups, drinking glasses, cigarette butts, tissues, garments; or on other persons and/or their clothing. Therefore, as with other types of forensic evidence, lipstick smears can provide a link between the victim, suspect and the crime scene. For example, if found on a suspect's clothing it can form a link between the victim and the suspect; if found at a crime scene where a lipstick-wearing suspect has been, then it can place the suspect at the scene; likewise, if found at a location where a victim has been, then it can provide a link between the victim and the location.

There are many cases where lipstick smears have been recovered and analysed as evidential material in forensic investigations. They appear in legal cases as early as 1933, such as in the case of *State v. Johnson* [224] mentioned in law journals in 1935 [225, 226], where the defendant was convicted of murder with the help of microscopic and chemical examination of scrapings from underneath his fingernails, which were revealed to be particles of lipstick similar to the one worn by the victim at time of her death. Similarly, lipstick smears can also appear in other types of cases, such as adultery, where the husband's handkerchief or clothes are stained with lipstick smears [227].

Lipsticks and lipstick smears can also be found in unexpected contexts in crimes and crime scenes: for example, as a message written in lipstick by the killer on the wall as in the case of the "Lipstick Killer" [228]; or on the lips of male robbers who used cosmetics to disguise their appearance and robbed banks in the United States in two different instances, one in Oklahoma City [229] and the other in Houston [230].

Considering the possibility of encountering lipstick smears in a number of different forensic situations, it is important to be able to analyse and distinguish between different lipstick smears. Just like other forms of evidence such as fibres, where one can identify what type of textile material the fibre came from (cotton, wool, nylon, polyester etc.) or compare and match a sample found at a crime scene to that from a suspect's clothing; it might also be possible to analyse and identify the brand, if not the individual lipstick, or to compare a smear found at a scene with either a suspect sample, or a database of known samples to search for a match; thereby eliminating samples that do not match, narrowing down the number of potential matches, or even finding a match which might then assist the investigation.

The importance of lipstick smears as forensic evidence has been recognised for many years, and there have been numerous studies using different analytical techniques on the analysis and discrimination of lipstick smears. Since lipstick smears may be recovered in trace amounts, it is important to try to analyse them, ideally, using non-destructive methods. Many authors have recognised the destructive nature of some of the most widely used analytical techniques (such as high-performance liquid chromatography), and initially used non-destructive methods such as visual colour comparison, as a first step in the characterisation and discrimination of lipsticks, before moving on to more powerful, yet destructive, techniques.

For example, Russell *et al* characterised 304 different lipsticks, first by visually grouping them by their colour in daylight, and further categorising them using a reflecting polarised light microscope. The lipsticks that were visually indistinguishable were then analysed with thin layer chromatography (TLC) using the dye components extracted from lipsticks that were smeared on paper. In addition to TLC, gas chromatography (GC) was used to analyse lipsticks dissolved in chloroform. Small amounts of lipstick (about 10 μg) were used and it was found that discrimination was possible, especially when analysed in conjunction with GC [231].

Andrasko also analysed 117 different lipsticks by (again) first visually comparing their colours and then using a combination of different techniques to achieve discrimination. After the initial colour comparison, X-ray analysis was carried out to differentiate between lipsticks by looking at their elemental composition. TLC was used to differentiate between the lipsticks that had similar elemental compositions, by extracting the dyes found in these lipsticks. High-performance liquid chromatography (HPLC) was found to be useful in distinguishing between the samples that could not be differentiated using previous methods. The mentioned techniques were used on pure lipstick samples as well as lipstick stains deposited on paper and coloured fabric. All of the 117 lipstick samples could be distinguished from each other when the combination of all these analytical techniques was used [232].

One other study on lipsticks, carried out by Reuland, looked at the discrimination of lipsticks using HPLC, by comparing not only the dyes but also the other components of lipsticks, using trace amounts of smears. In this study, twelve different lipsticks were analysed. Lipstick smears on inert materials, such as glass drinking cups and facial tissues, and smears on materials containing extractable chemical compounds, such as cigarette butts and laundered shirts, were analysed and characterised. The lipsticks were found to give sufficiently characteristic chromatograms and differentiation could be achieved between the smears found on inert materials, whereas differentiation between smears on other materials was more complicated due to interference from background peaks [233].

Another study on differentiation of lipsticks, carried out by Ehara *et al*, involved analysis of 174 lipsticks from Japanese manufacturers by initial observation of their colour under white light, and subsequent observation of their fluorescence under light at three different wavelengths (350, 445 and 515 nm). Purge-and-trap gas chromatography (P&T-GC) was employed as another analytical technique for the discrimination of lipsticks and lipstick smears on wool, cigarette butts and filter paper (which is commonly used in collection of evidence). Peaks that were characteristic of each manufacturer were observed and nearly all of the studied

lipsticks could be distinguished by combination of visual comparison and P&T-GC. Therefore it was concluded that this method was suitable for forensic identification of trace amounts of lipsticks [234].

Lucas *et al* analysed lipstick stains found on cigarette butts and clothing, initially by visible absorption spectrophotometry. The samples that could not be differentiated this way went through an extraction process that extracted the bromo acid dyes found in lipsticks, and the extracted dyes were analysed by paper chromatography. The combination of the two techniques were found to be more discriminative than other techniques such as visual comparison under white or ultraviolet light, or colour reactions with acids [235].

In a study done by Choudhry, thirty lipstick-stained lip impressions on white sheets of paper were analysed using microspectrophotometry and minute differences in their colours were studied to determine whether they could be differentiated in this way. Additionally, scanning electron microscopy combined with energy-dispersive X-ray spectroscopy (SEM-EDX) was used as another method for differentiating between the samples by measuring their elemental composition and observing differences in their relative ratios. Backscattered electron imaging was found to be more useful than secondary electron imaging, and all of the samples could be differentiated from each other using both techniques [236].

Another study, reported by Keagy, involved analysis of cosmetic smudges, such as lipstick stains, using GC-MS. Castor oil found in lipsticks was identified after a derivatisation process called transesterification, which breaks apart the triglyceride molecules in castor oil, and methyl esters of the fatty acids are formed. These esters are then detected by GC-MS. This procedure was applied in four cases and proved to yield good results [237].

Misra *et al* employed neutron activation analysis with γ-ray spectrometry to analyse and differentiate between 31 lipstick samples (Indian and 'foreign') by measuring and comparing the concentrations of trace elements found in those lipsticks. The bromine concentration enabled identification of the Indian brands; and the relative concentrations of caesium, antimony and scandium allowed differentiation between the Indian and 'foreign' lipsticks. Therefore it was determined that the lipsticks could be differentiated on the basis of their trace element concentration and profile [238].

Another study, done by Abraham *et al*, demonstrated the potential of X-ray diffractometry (XRD) for the analysis of trace evidence materials such as lipsticks. For the purpose of this study, six different lipsticks were smeared on glass slides and analysed using an X-ray diffractometer. It was found that the lipsticks produced XRD patterns that were characteristic of each sample and it was therefore concluded that XRD is a useful non-destructive technique for analysing evidence materials and individual XRD patterns could be used as a "signature" of the material analysed when comparing samples [239].

In a brief study Desiderio *et al* explored the use of micellar electrokinetic capillary chromatography (MEKC) to demonstrate its applicability to forensic analysis of lipsticks. Lipstick blotted on a paper handkerchief was analysed using MEKC to determine its dye composition. The method was found to be sensitive enough to determine the dyes even with minute amounts (a few μg) of lipstick [240].

As mentioned before it is highly desirable – from a forensic perspective – that the evidence material is analysed and identified using non-destructive techniques to preserve the integrity of the sample. Whereas non-destructive methods such as microscopy, microspectrophotometry, visual colour comparison and observation of fluorescence under different wavelengths of light allow for samples to be categorised to a certain degree, these techniques do not allow the analyst to chemically identify and categorise the sample. To achieve a better level of identification more complex techniques, such as chromatography, are required. Even though these techniques are

very powerful and give abundant information on physical and chemical structures of analysed compounds, the majority of them (HPLC, GC, TLC, etc.) require sample handling and (ultimately destructive) extraction processes in order to be able to analyse the sample, which interferes with the integrity of the sample, and the sample is used up during the analytical process.

This is undesirable in instances where the evidential material is recovered in trace, rather than bulk amounts. In these cases, the forensic analyst only has a limited number of attempts at analysing and identifying the evidence. Therefore, what becomes extremely useful in such circumstances is an analytical technique that gives as much information about the sample as possible while being non-destructive at the same time. Raman spectroscopy, being such a technique, can identify unknown substances by looking at their characteristic spectral patterns. It can be used for the in situ analysis of samples with little or no sample preparation, and it can analyse materials through glass containers or plastic evidence bags [1, 171].

Despite all the advantages of Raman spectroscopy, there have been surprisingly few studies on the analysis and differentiation of lipsticks using this technique. One such study was carried out by Rodger *et al*, which explored the potential of Raman spectroscopy for the in-situ analysis and discrimination of lipsticks. The study included the analysis of six commercial lipsticks smeared on glass microscope slides and cotton samples, using a 514.5 nm (green) laser source and employing the method of surface enhanced resonance Raman spectroscopy (SERS – described in **Chapter 2**). The surfaces of the samples were treated with surfactants and colloids to suppress the fluorescence and enhance the Raman signals from the lipstick samples. Each sample gave characteristic spectra and could readily be differentiated from each other, both on glass and on cotton surfaces. This demonstrated the potential of Raman spectroscopy for forensic analysis of lipsticks [2].

Another study followed a different approach in dealing with the analysis and differentiation of spectra. In this study, Goodacre *et al* used chemometric methods to

reduce the dimensionality of data obtained from four different lipsticks using dispersive Raman spectroscopy. They applied three different techniques:

1) Self organising feature maps (SOMs), which is a computational pattern recognition technique;
2) Principal component analysis (PCA), which is a technique that creates a new set of variables called principal components (PCs) from the original data, where the first few PCs account for the most of the variation in the original data and can be easily plotted so that the 'clusters' that form can be visualised (a similar analysis was performed during this research, and is described in **Chapter 5**);
3) Hierarchical cluster analysis (HCA) which measures the distances between the plotted PCs to construct a dendrogram.

All of these analyses gave the same results and a non-invasive, non-destructive differentiation of lipsticks was achieved [3].

3.4. Summary

As demonstrated by these previous studies, Raman spectroscopy has great potential for the non-destructive analysis of lipsticks. Raman spectroscopy was not widely used in forensic analyses more than a decade ago due to the lower sensitivity of the detectors, bulky spectrometers and high costs. However, modern spectrometers are a lot more sensitive. They can analyse wavelength regions closer to the laser excitation frequency, they are able to utilise a variety of different laser frequencies and powers, and there are many portable spectrometers that can be used for the in situ analysis of evidence. These advancements in Raman technology have given forensic science a powerful tool for the non-destructive analysis of evidential materials.

This research aims to further explore the potential of this tool as a forensic analytical technique, by applying it to the analysis and differentiation of lipsticks as cosmetic evidence. The goals are to build a comprehensive library of lipstick spectra that

could be useful in searching for a match to a particular lipstick, while also exploring some forensically relevant situations, such as the effects of ageing on the smear sample and the effect of the underlying medium the lipstick is deposited on.

CHAPTER IV

Differentiation of Lipsticks Using Raman Spectroscopy

4.1. Introduction

In forensic science, it is common practice to analyse a piece of evidential material to determine its origin, or to find out the similarities and/or differences between one material and another, suspected to be from the same origin, in order to establish a link between the evidence, people and crime scenes.

The main purpose of this study is to explore the potential of Raman spectroscopy in the differentiation of lipsticks of different colours and shades from a variety of brands. This part of the study looks at the individual spectra obtained from sample lipsticks in order to establish the differences and similarities between lipsticks by visual inspection of spectra, in order to determine whether each lipstick gives a unique spectrum that can be used as a "signature" for that lipstick; or whether there are any correlations between colours and/or brands.

Initially, as a feasibility study, several spectra were obtained from seven test lipstick samples to assess whether they gave acceptable Raman spectra that could be used to differentiate between the samples. Five of the lipsticks gave spectra with a fluorescent baseline, however many peaks could still be observed. One of the lipsticks gave a very fluorescent spectrum with no peaks, and one produced a spectrum with a non-fluorescent, flat baseline and strong intensity peaks (see **Fig. 4.1** to **4.4**).

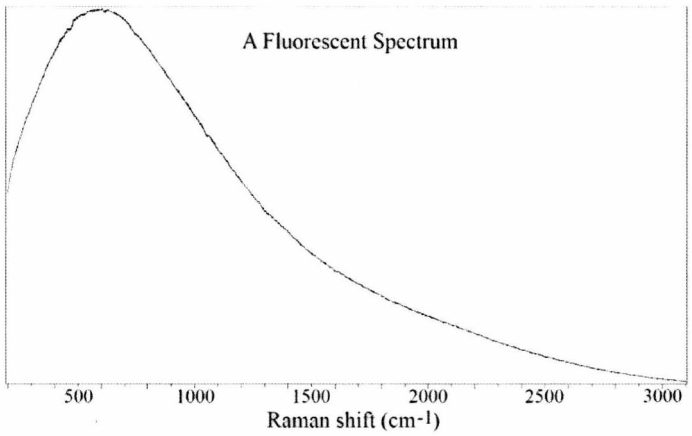

Figure 4.1. An example of a fluorescent lipstick spectrum where there are no visible peaks.

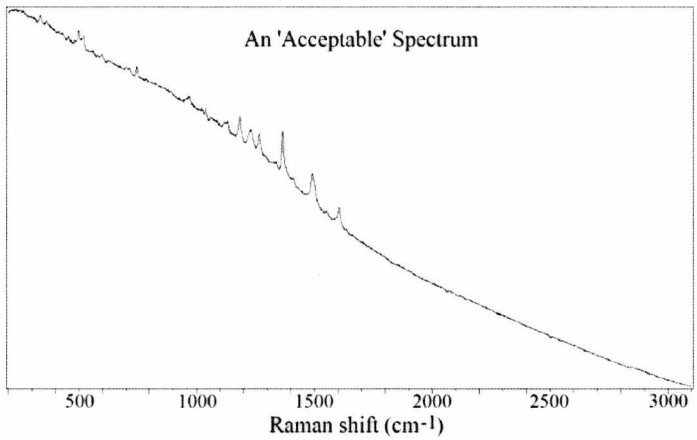

Figure 4.3. An example of an 'acceptable' lipstick spectrum with a fluorescent baseline and discernible peaks.

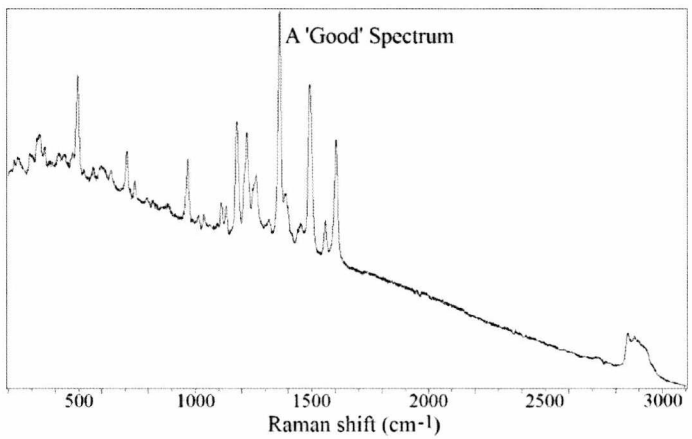

Figure 4.2. An example of a 'good' lipstick spectrum with a fluorescent baseline, but more intense peaks.

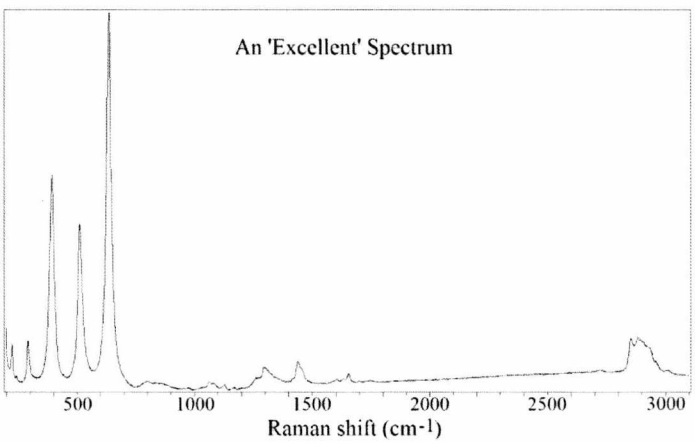

Figure 4.4. An example of an 'excellent' spectrum with an almost flat baseline and intense peaks.

Following these initial results it was determined that Raman spectroscopy could be used to obtain spectra from lipstick samples in order to determine the feasibility of the technique in discrimination of a large number of lipsticks.

4.2. Methods and materials

The experiments described in this chapter were carried out using a *Jobin-Yvon 640* micro-Raman spectrometer (**Fig. 4.5**) utilising a Uniphase (model 1145) helium-neon laser operating at a wavelength of 632.8 nm. It incorporated a liquid-nitrogen cooled charge coupled device (CCD) detector, and a diffraction grating of 1200 gr/mm (grooves per millimetre) with a slit width of 50 μm, giving the spectrometer a spectral resolution of 2 cm^{-1}. The laser had a fixed output of 35 mW and the laser power at the sample was 4 mW. A ×100 objective lens was used to give a beam diameter of approximately 1 μm. The spectrometer was calibrated before each session against the silicon line standard at 520.6 cm^{-1} (**Fig. 4.6**).

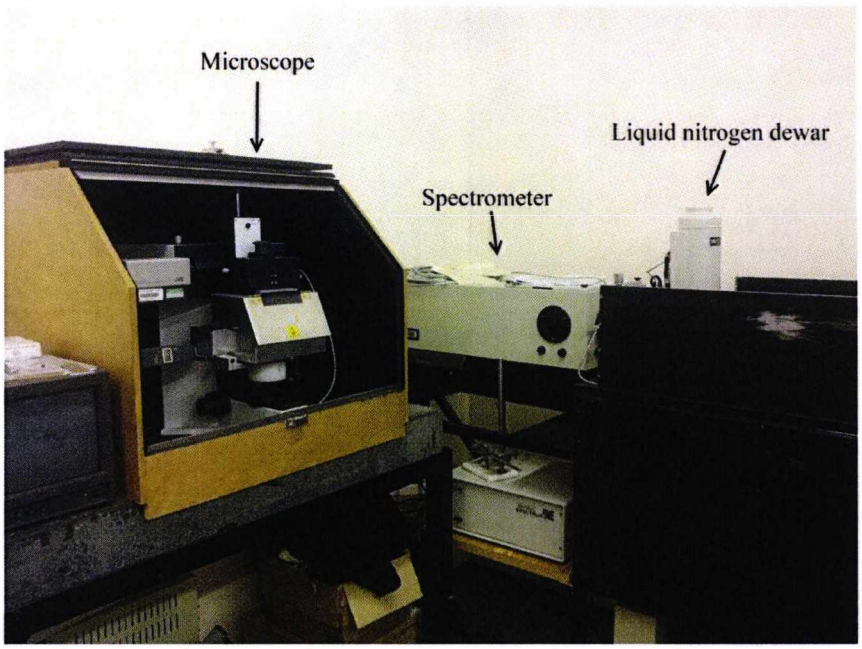

Figure 4.5. The Jobin-Yvon 640 Raman spectrometer used in this study

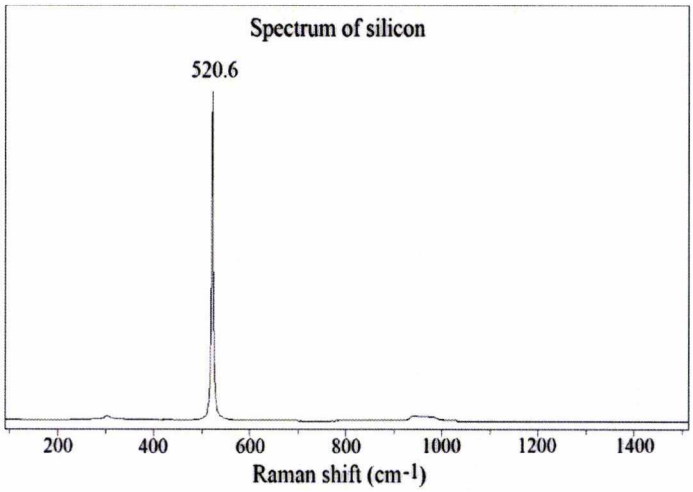

Figure 4.6. A spectrum showing the silicon peak at 520.6 cm^{-1} against which the spectrometer was calibrated.

Each lipstick was smeared onto a glass microscope slide (BDH Super Premium low iron, clear glass slides) and analysed under a ×100 objective lens. Whilst some lipsticks appeared homogeneous (**Fig. 4.7**), others appeared heterogeneous with fragments of materials dispersed within the granular matrix of the lipstick (**Fig. 4.8**).

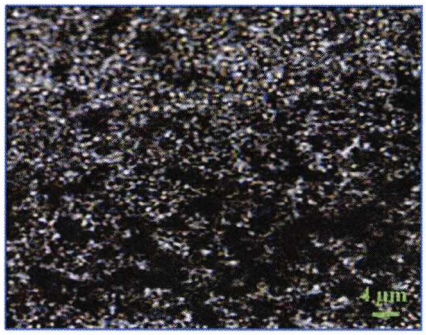

Figure 4.7. Image of a homogeneous-looking lipstick smear as observed under a ×100 objective lens

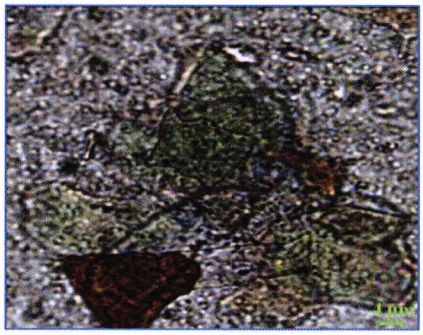

Figure 4.8. Image of a heterogeneous-looking lipstick smear as observed under a ×100 objective lens.

Five spectra were obtained from different parts of each sample (both from the matrix and any other particles within the matrix) to ensure that the spectra obtained were not dependent on the part of the lipstick smear from which they were sampled. An example of five spectra obtained from the lipstick Revlon 035, a heterogeneous-looking lipstick, is given in **Figure 4.9**, and shows that even though some lipsticks appear heterogeneous, the spectra taken from any part of the lipstick are the same.

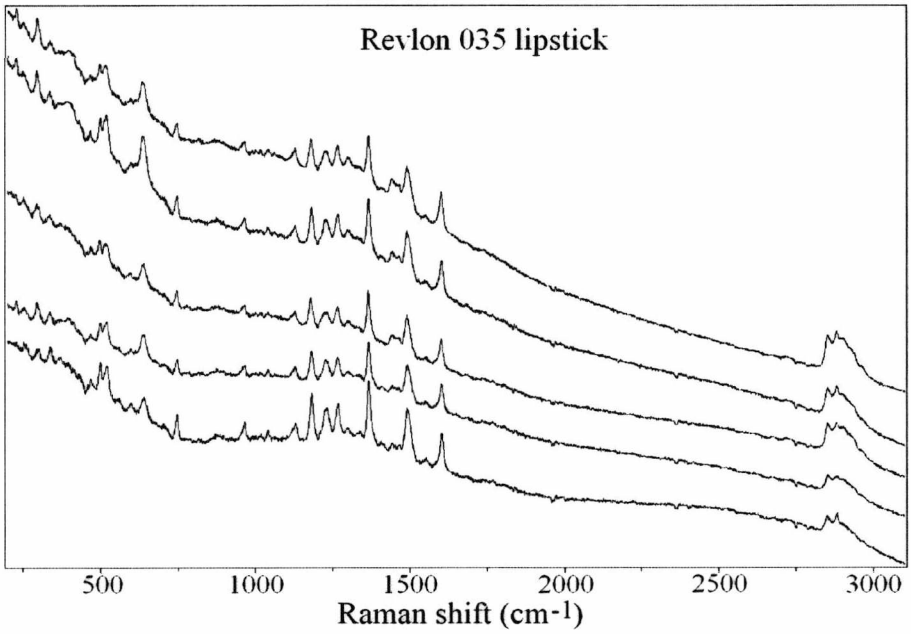

Figure 4.9. Five different spectra obtained from five different positions on a smear of Revlon 035 lipstick.

It was established that the majority of the peaks were found within the spectral range of 200 - 1800 cm^{-1} with a gap composed of no peaks up to 2700 cm^{-1}; and then another set of peaks within the range of 2700 - 3050 cm^{-1} in some lipsticks. Therefore the spectral range to be scanned was selected to be between 200 cm^{-1} (the spectrometer minimum) and 3100 cm^{-1}.

For this part of the study, a total of 73 lipsticks from twelve different brands were analysed. **Table A1** in **Appendix I** lists the lipstick brand, type, colour (as on the label) and the perceived colour (under white light).

Out of the 73 lipsticks: Almay 36, Bourjois (No's. 15, 16, 32, 54), L'Oreal (No's. 164, 243, 524, 900), Revlon (No's. 07, 46, 455, 675), Elizabeth Arden 17, Maybelline 18, Max Factor (No's. 30 and 210) and La Femme 29 were purchased online at www.cosmetics4less.net;

Barry M (No's. 52, 53, 54, 62, 101, 113, 117, 121, 136, 140, 141, 144, 145, 146), Prestige (CL93A, CL78A, PL28A, PL38A, PL49A), Revlon (No's. 004, 005, 006,

008, 009, 020, 025, 030, 035, 045, 075, 080, 090, 095, 103, 353, 359, 371, 430, 450, 663, 750), and UNE lipsticks (L02, L05, L07, L09, S03, S05, S07, S08, S12, S15, S17, S19) were obtained from the local Boots store in Canterbury, Kent; and Coty Mainz 070 and L'Oreal 345 were obtained from friends.

In order to obtain a good signal-to-noise ratio for each lipstick, a variety of different accumulation times and number of accumulations were tried to determine the optimal acquisition parameters to use for each lipstick. To obtain peaks with higher intensity, longer accumulation times were used. To improve the baseline by averaging out the background noise, a larger accumulation number was used. The more fluorescent samples required shorter accumulation times, whereas the lipsticks with weaker signals and no fluorescence required longer count times. The variations in these parameters only served to improve the signal-to-noise ratio and did not have an effect on the positions or the relative intensities of the peaks. **Table 4.1** lists the parameters used for each lipstick analysed in this study.

Table 4.1. A table listing the Raman acquisition parameters used for each lipstick. Those denoted as "fluorescent" are lipsticks that gave very fluorescent spectra with no discernible peaks regardless of the parameters used.

	RAMAN ACQUISITION PARAMETERS	
LIPSTICK	Accumulation Time (s)	Accumulation Number
Almay	2	40
Barry M 52	1	70
Barry M 53	2	70
Barry M 54	0.5	100
Barry M 62	1	70
Barry M 101	2	60
Barry M 113	2	70
Barry M 117	2	70
Barry M 121	1	70
Barry M 136	3	70
Barry M 140	4	60
Barry M 141	fluorescent	
Barry M 144	fluorescent	
Barry M 145	1	100
Barry M 146	0.5	100

Bourjois 15	2	40
Bourjois 16	2	40
Bourjois 32	2	40
Bourjois 54	2	40
Coty Mainz 070	0.5	100
Elizabeth Arden 17	fluorescent	
La Femme 29	2	40
L'Oreal 164	0.5	100
L'Oreal 243	fluorescent	
L'Oreal 345	2	40
L'Oreal 524	0.5	100
L'Oreal 900	0.5	100
Max Factor 210	fluorescent	
Max Factor 30	fluorescent	
Maybelline 18	fluorescent	
Prestige CL-78A	2	40
Prestige PL-28A	0.5	100
Prestige PL-38A	0.5	100
Prestige PL-49A	0.5	100
Prestige CL-93A	0.5	100
Revlon 004	2	40
Revlon 005	2	50
Revlon 006	0.5	100
Revlon 07	2	50
Revlon 008	3	50
Revlon 009	2	50
Revlon 020	3	30
Revlon 025	2	70
Revlon 030	1	70
Revlon 035	2	70
Revlon 045	1	40
Revlon 46	2	40
Revlon 075	1	40
Revlon 080	2	70
Revlon 090	1	70
Revlon 095	0.5	100
Revlon 103	3	50
Revlon 353	4	50
Revlon 359	2	70
Revlon 371	3	60
Revlon 430	0.5	100
Revlon 450	1	70
Revlon 455	4	50
Revlon 663	fluorescent	
Revlon 675	1.5	50

Revlon 750	1	70
UNE L02	4	30
UNE L05	5	25
UNE L07	4	30
UNE L09	4	30
UNE S03	4	30
UNE S05	4	30
UNE S07	4	30
UNE S08	5	20
UNE S12	4	30
UNE S15	5	25
UNE S17	4	30
UNE S19	5	30

In order to be able to identify individual peaks, or groups of peaks, in a lipstick's spectrum, some of the common ingredients used in the manufacture of lipsticks were obtained and analysed. These included beeswax, castor oil, carnauba wax, FD&C Yellow No. 6 Aluminium lake (Sunset Yellow, C.I. 15985) dye, and titanium (IV) oxide (both rutile and anatase form) which were purchased from Sigma-Aldrich; FD&C Yellow No. 5 Aluminium lake (tartrazine, C.I. 19140) dye, carminic acid (carmine, C.I. 75470), D&C Red No. 28 (C.I. 45410) and FD&C Blue No. 1 (erioglaucine disodium salt, C.I. 42090) dye that were purchased from Acros Organics; and iron oxide (Fe_3O_4) which was obtained from Fisons Scientific Apparatus Ltd. The results of these experiments are presented later in the chapter.

The spectra obtained were exported to OMNIC 7.3 and Labspec version 5 for spectral processing, analysis, comparison and presentation.

4.3. Fluorescence

A problem often encountered in Raman spectroscopy is fluorescence interference which washes out spectral information, and the lipstick samples were not exempt from this problem. The majority of the lipsticks analysed had fluorescent baselines as mentioned before, some being so intensely fluorescent that any of the relatively

weak Raman signals that might have been present were obscured by the intense, broad fluorescence band.

In the literature, there are numerous ways described of dealing with fluorescence, and in an attempt to reduce the fluorescence encountered and to improve the Raman signal intensity of peaks, some of these methods were tested.

4.3.1. Surface-Enhanced Raman Spectroscopy

Following the study on discrimination of lipsticks by Rodger *et al* [2], which used surface-enhanced resonance Raman spectroscopy, a similar experiment was carried out to assess whether surface enhancement could quench the fluorescence encountered with the studied samples. It should be noted that the study by Rodger *et al* employed resonance Raman scattering with an argon laser operating at 514.5 nm; however this study utilised a helium-neon laser operating at 632.8 nm and no discernible resonance effect was observed.

For the SERS experiment, a lipstick sample, known to have a fluorescent baseline but with evident Raman peaks, was smeared on to a clean, glass microscope slide and was treated with the surfactant poly-L-lysine. A gold colloid solution was added to the treated surface and left to dry out naturally. Surface-enhanced Raman spectra were then obtained from the sample.

Figure 4.10 shows a spectrum of Coty Silksticks "Perfect Red" (not listed in **Table 4.1**) lipstick with and without surface-enhancement. Even though surface-enhancement quenched the fluorescence by about 3000 intensity units (a.u.), there was no significant enhancement in the intensity of the peaks themselves.

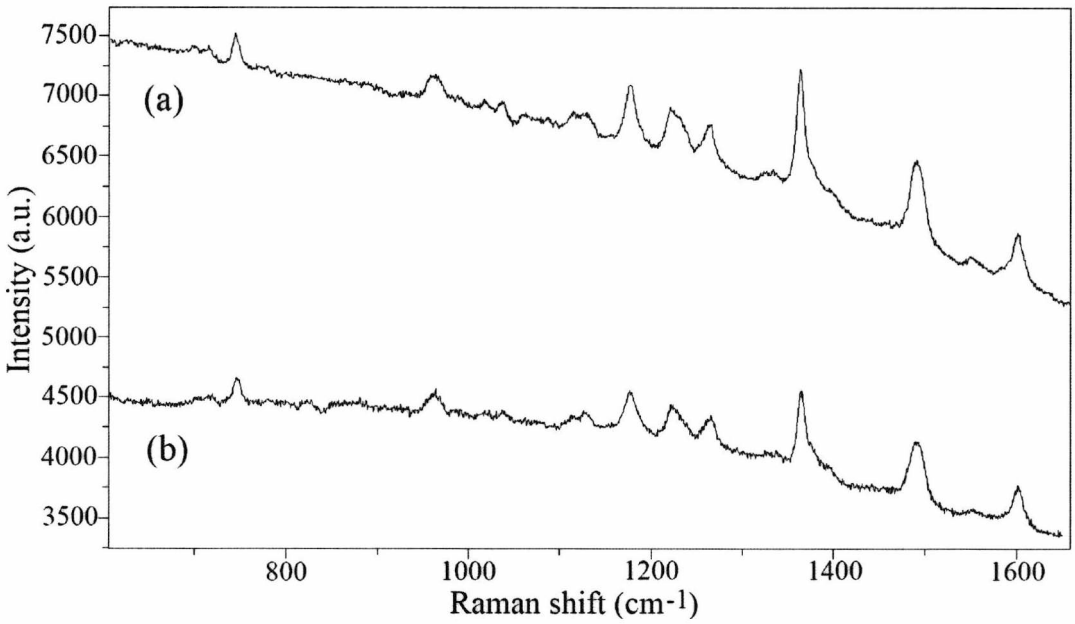

Figure 4.10. (a) Normal Raman spectrum of the lipstick "Perfect red"
(b) SERS spectrum of the lipstick "Perfect Red"

For this reason, it was decided that surface enhancement would not be effective for the purposes of this study, and the rest of the study was pursued without using SERS. This also presented the advantages of no sample preparation, minimised risk of contamination and preservation of the integrity of the sample, all of which are important factors in forensic evidence analysis.

4.3.2. Photobleaching

A simpler method of reducing fluorescence in samples is photobleaching which involves irradiation of the sample with laser light for an extended length of time (minutes up to hours) which induces photodecomposition of the fluorescent molecules, and a subsequent reduction in the fluorescent background [51].

To test if photobleaching would be effective, a lipstick sample that gave a spectrum with a fluorescent baseline as well as discernible peaks, and a lipstick sample that gave a very fluorescent spectrum with no discernible peaks were chosen. Both

lipsticks were smeared on glass microscope slides and they were analysed after being exposed to the laser light for varying lengths of time.

Figure 4.11 shows the spectra for Rimmel London 080, a lipstick with a fluorescent baseline and discernible peaks, before and after photo-bleaching. Even though this procedure reduced the intensity of the fluorescent baseline, there was no visible improvement in the signal intensities of the peaks.

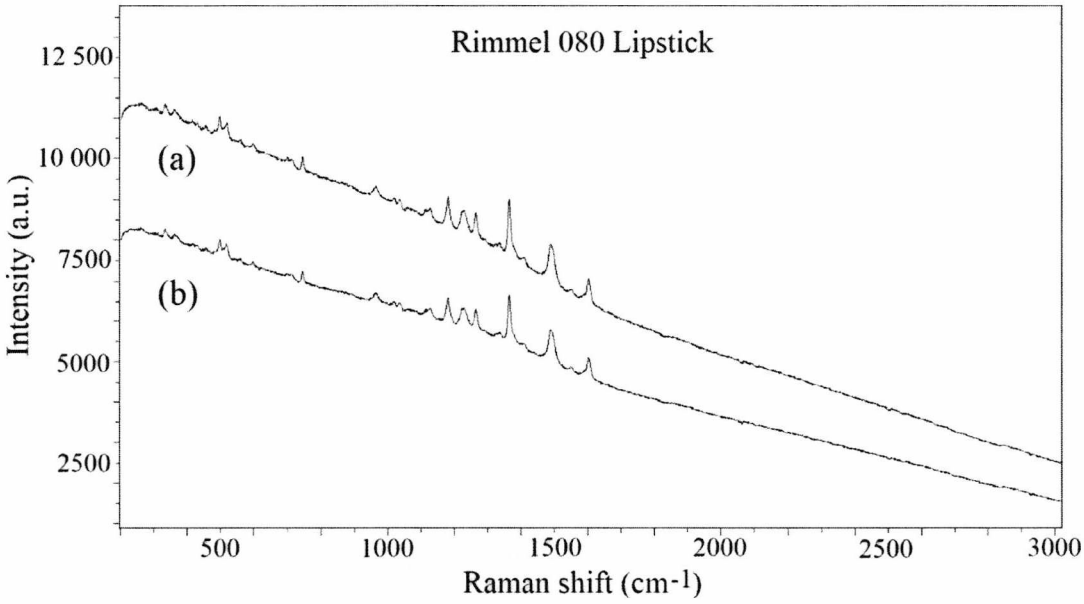

Figure 4.11. (a) Spectrum of Rimmel 080 lipstick before photo-bleaching
(b) Spectrum of Rimmel 080 after being exposed to the laser for 50 minutes

Figure 4.12 shows the spectra for Max Factor 210, a very fluorescent lipstick with no discernible peaks, before and after photo-bleaching. The intensity of the fluorescence was reduced; however, there were still no visible peaks even after three hours of photo-bleaching with the laser at full power on the sample.

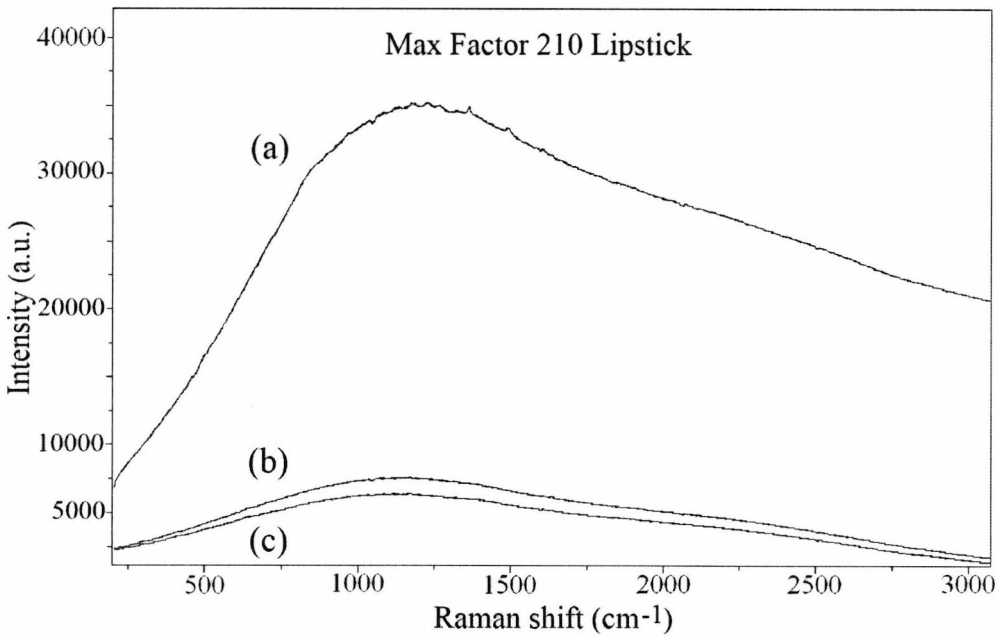

Figure 4.12. (a) Spectrum of Max Factor 210 lipstick before photo-bleaching
(b) Spectrum of Max Factor 210 after being exposed to the laser for 1 hour
(c) Spectrum of Max Factor 210 after being exposed to the laser for 3 hours

Even though the method of photo-bleaching is effective and useful in dealing with fluorescence in some cases, it was found to be ineffective in this study.

Following these results, it was concluded that the spectra obtained (apart from the very fluorescent ones) would still be good enough to be used as they were without using any fluorescence reduction methods, and conventional Raman spectroscopy was employed for the analysis and discrimination of 73 lipsticks.

4.4. Results and discussion

The spectra for the 73 lipsticks were initially analysed by visual inspection to determine the presence/absence of peaks and their positions. This resulted in lipsticks being categorised by their spectral similarities and differences, and an initial

level of discrimination was achieved. In order to be able to identify the peaks, some compounds found in lipsticks were also analysed and their spectra compared to those of the lipsticks. The spectra were then inspected in more detail, determining the peak positions (cm^{-1}), relative signal intensities and the identity (if known) of the peaks to achieve a better level of discrimination, and to build a comprehensive library of lipstick spectra.

4.4.1. Visual examination and categorisation of spectra

Examination of spectra showed that the peak positions for each spectrum taken from different parts of the same lipstick were within ± 4 cm^{-1} of each other; however, there was variability in the absolute intensities of the peaks. These variations, however, were not significant and the relative intensities (in terms of the strength of the peak relative to the other peaks in the spectrum) remained similar. To average out these small differences the spectra were averaged using the statistical analysis function within the OMNIC version 7.3 software. This function averages the y-axis (intensity) values for each wavenumber given to produce a single, averaged spectrum from the number of spectra selected (i.e. it makes no attempt to average peaks together; it is merely a simple arithmetic mean of the intensity versus Raman shift data). Individual spectra, as well as their average spectrum, are supplied on the CD accompanying this thesis.

Visual examination of each spectrum revealed that some of the lipstick samples gave very similar spectra that could not be easily differentiated from each other, and hence could be grouped together; whereas some of them were different from all the other lipsticks and could easily be differentiated. This method of categorisation resulted in a total of nine groups being formed. Each of the numbered groups contained lipsticks that gave very similar spectra irrespective of brand or colour. Whereas those *within* the same group could not be discriminated from each other, discrimination could be achieved *between* the different groups. The highly fluorescent lipsticks were placed in Group F (where 'F' stands for 'fluorescent'), and those with a 'unique' spectrum that

could readily be discriminated from each other and the other lipsticks were put in Group U (where 'U' stands for 'unique') (see **Table 4.2**).

Table 4.2. Lipsticks grouped by their discrimination using Raman spectroscopy. "Group F" consists of lipsticks that were too fluorescent, and "Group U" consists of lipsticks that are unique and can be readily discriminated from other lipsticks.

Group	Brand	Colour #	Main Colour	Shade/Comment
1	Almay	36	Red	
1	Barry M	145	Pink	Dark
1	Barry M	121	Red	
1	Bourjois	15	Pink	
1	Bourjois	16	Red	
1	Bourjois	54	Red	
1	Bourjois	32	Red	Dark
1	L'Oreal	900	Brown	Pink
1	L'Oreal	164	Red	Light
1	Prestige	CL93A	Pink	Very dark
1	Revlon	006	Red	Dark
1	Revlon	030	Pink	Very dark
1	Revlon	090	Red	
1	Revlon	675	Red	
1	Revlon	095	Red	Very dark
1	Revlon	009	Red	Matt, brown
2	L'Oreal	345	Brown	Red, shimmery
2	Revlon	371	Brown	Peach
2	Revlon	430	Pink	Dark, shimmery
2	Revlon	045	Brown	Dark pink
2	Revlon	46	Brown	
2	Revlon	080	Red	Bright
3	Barry M	146	Pink	
4	Barry M	53	Orange	Peach
4	Revlon	004	Pink	Dark, peach
4	Revlon	005	Peach	Red
4	Revlon	025	Pink	
4	Revlon	035	Brown	
4	Revlon	450	Pink	Shimmery
4	Revlon	750	Red	Orange
5	Barry M	52	Pink	
5	Barry M	62	Pink	

6	Barry M	140	Pink	Shimmery
6	Barry M	113	Pink	Shimmery, light
6	Revlon	455	Pink	Shimmery
7	Coty Mainz	070	Brown	
7	Revlon	353	Brown	Shimmery, light
7	UNE	L02	Brown	
7	UNE	L05	Brown	
7	UNE	L07	Brown	
7	UNE	L09	Brown	
7	UNE	S03	Brown	
7	UNE	S05	Brown	
7	UNE	S07	Brown	
7	UNE	S08	Brown	
7	UNE	S12	Brown	
7	UNE	S15	Brown	
7	UNE	S17	Brown	
7	UNE	S19	Brown	
F	Barry M	144	Pink	Very dark
F	Barry M	141	Burgundy	
F	Elizabeth Arden	17	Brown	Pink
F	L'Oreal	243	Brown	Light, pink
F	Max factor	30	Brown	Lip-gloss, pink
F	Max factor	210	Brown	
F	Maybelline	18	Burgundy	
F	Revlon	663	Violet	Very dark
U	Barry M	54	Orange	Peach
U	Barry M	101	Flesh	
U	Barry M	117	Orange	
U	Barry M	136	Brown	Light, shimmery
U	L'Oreal	524	Brown	
U	La Femme	29	Brown	Pink
U	Prestige	CL78A	Brown	light
U	Prestige	PL28A	Orange	Peach
U	Prestige	PL38A	Brown	Very light
U	Prestige	PL49A	Brown	Pink
U	Revlon	008	Brown	
U	Revlon	359	Brown	
U	Revlon	07	Brown	
U	Revlon	075	Peach	
U	Revlon	020	Pink	Shimmery
U	Revlon	103	Brown	Shimmery

Group 1 Lipsticks:

A total of sixteen lipsticks from six different brands were placed in this group. The majority of these lipsticks were red in colour, with the rest being pink or brown. **Figure 4.13** shows an example spectrum of a Group 1 lipstick.

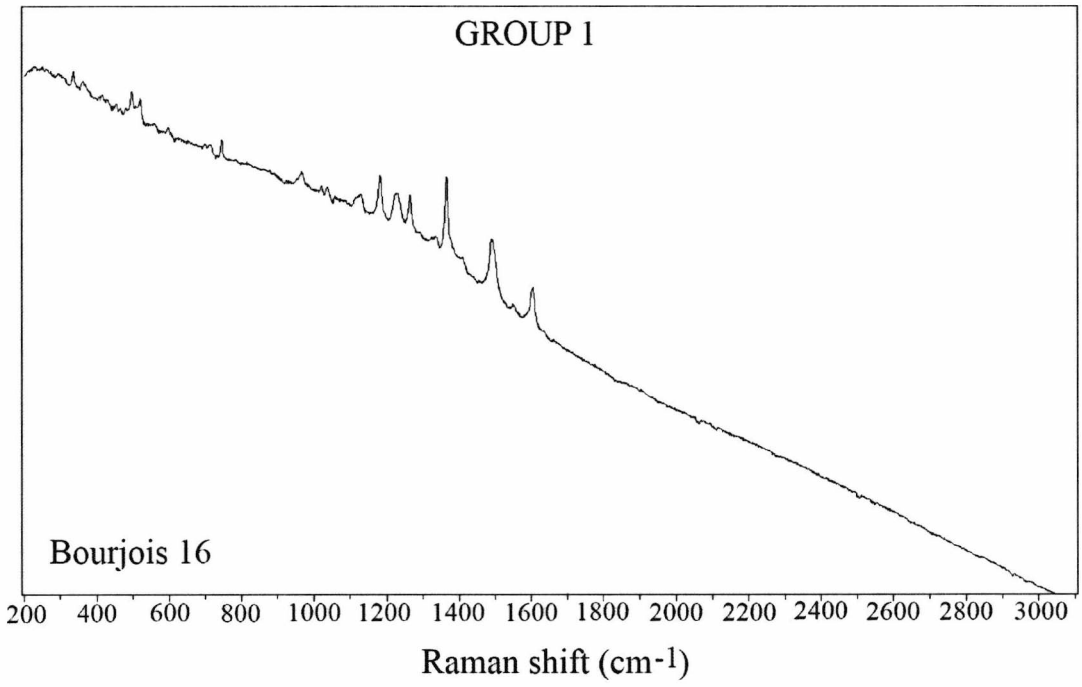

Figure 4.13. Spectrum of Bourjois 16, a Group 1 lipstick.

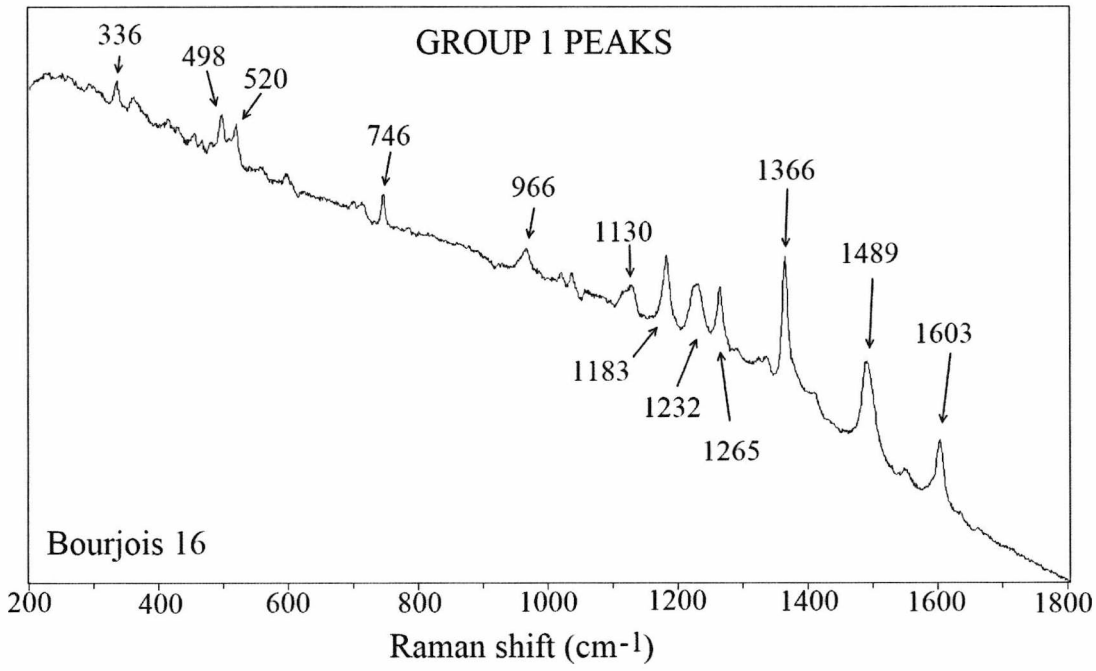

Figure 4.14. Expanded spectrum of Bourjois 16 showing the main peaks of a typical Group 1 lipstick.

Lipsticks in Group 1 all had the same main peaks at: 336 cm^{-1}; the double peak group at 498 and 520 cm^{-1}; 746 cm^{-1}; 966 cm^{-1}; the broad peak (potentially overlapping) at 1130 cm^{-1}; the group of three peaks at 1183, 1232 and 1265 cm^{-1}; and another group of three at 1366, 1489, and 1603 cm^{-1}. Even though the analysed range expands up to 3100 cm^{-1}, there were no visible peaks after 1700 cm^{-1} (**Fig. 4.14**).

Group 2 Lipsticks:

A total of six lipsticks from two different brands and of a variety of colours were placed in Group 2. The lipsticks in this group all had the same main peaks as those in Group 1, as well as the group of overlapping peaks between 2800 and 3000 cm^{-1} which formed the only means of discrimination between Group 1 and Group 2 (**Fig. 4.15**).

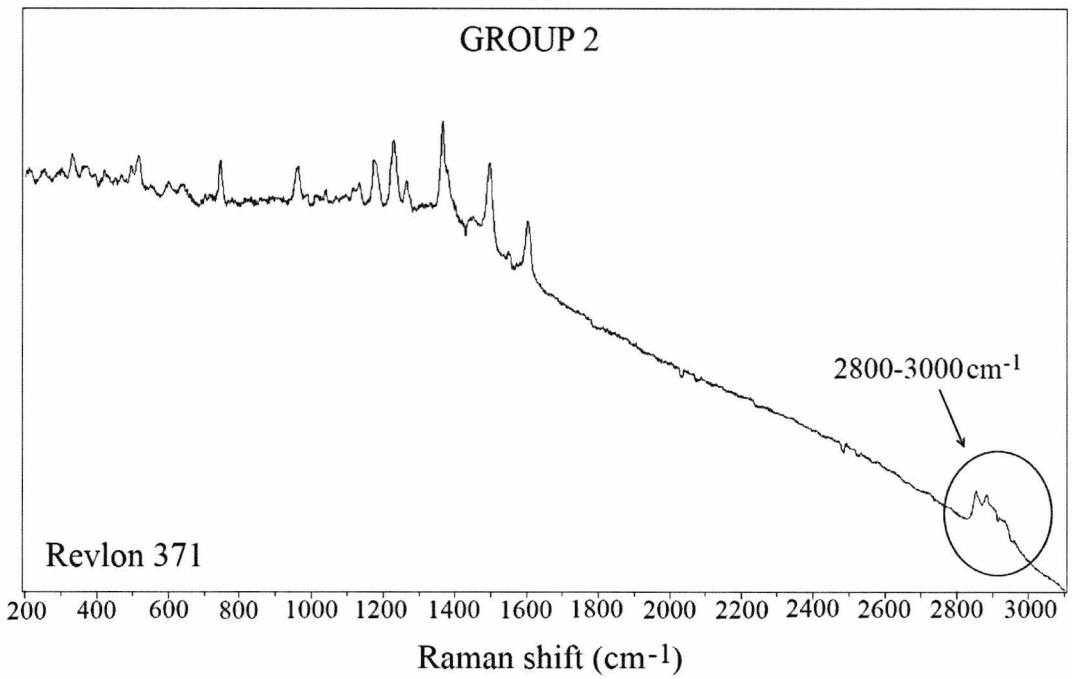

Figure 4.15. Spectrum of Revlon 371, a Group 2 lipstick, showing the extra group of peaks, which is the only difference between Groups 1 and 2.

Group 3 Lipsticks:

Only one of the lipsticks was placed in Group 3. This lipstick contained all the main peaks found in Group 1 lipsticks, as well as an extra peak at 638 cm^{-1}. Also, it did not have the peak group between 2800 and 3000 cm^{-1} that Group 2 lipsticks showed (**Fig. 4.16**). Even though being the only lipstick in the group makes this lipstick unique, it was placed in this group because it only differed from Groups 1, 2 and 4 by either the presence of the peak at 638 cm^{-1}, or the absence of the peak group between 2800 and 3000 cm^{-1}. Even though the peak at 638 cm^{-1} is one of the peaks of titanium dioxide in anatase form (discussed later in the chapter), this peak was not attributed to anatase since the rest of the peak positions and intensities did not match the peaks in the lipstick spectrum.

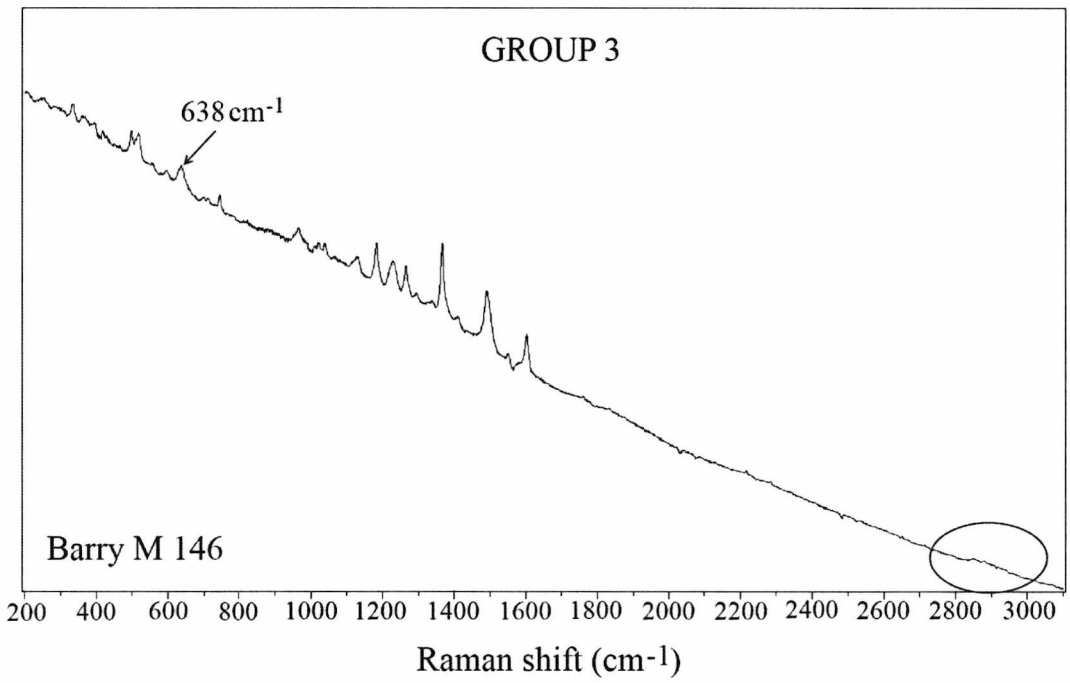

Figure 4.16. Spectrum of Barry M 146, the Group 3 lipstick, showing the differences from Groups 1 and 2.

Group 4 Lipsticks:

A total of seven lipsticks from two different brands and of a variety of colours were placed in Group 4. Lipsticks in this group had the same main peaks as Group 3, as well as the peak group at the end of the spectrum at around 2800 - 3000 cm^{-1} (**Fig. 4.17**). The peak at 638 cm^{-1} was determined to belong to the anatase form of titanium dioxide (as discussed later in the chapter).

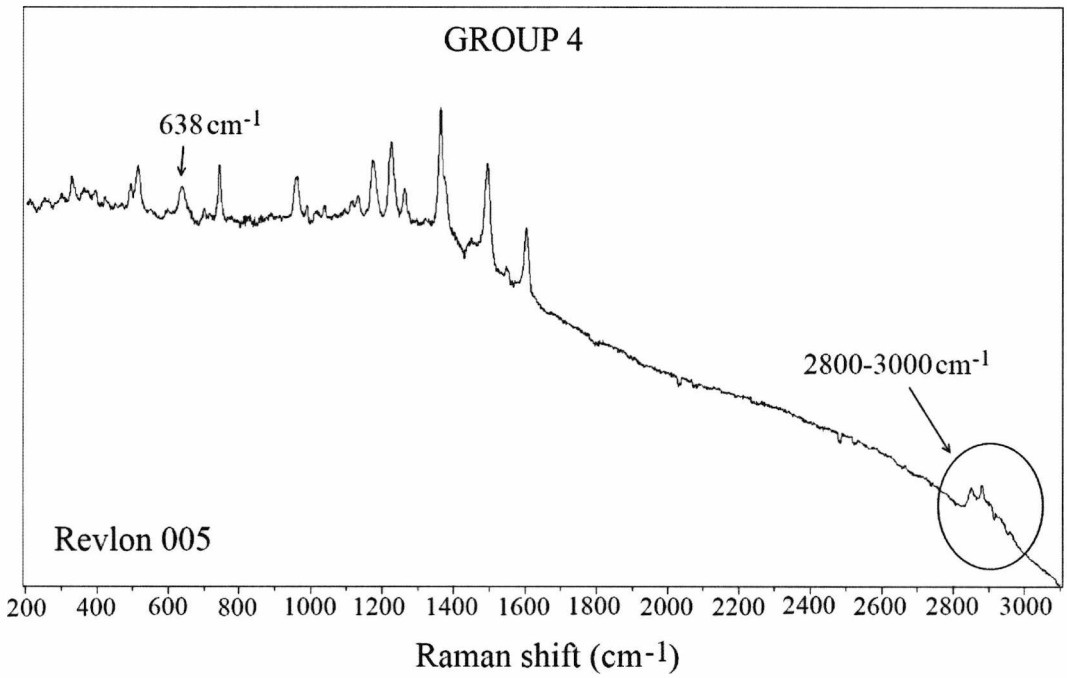

Figure 4.17. Spectrum of Revlon 005, a Group 4 lipstick, which differs from Group 3 by the presence of the peak group between 2800-3000cm^{-1} as shown.

Group 5 Lipsticks:

Only two lipsticks that were very similar in colour (pink) and both belonging to the brand Barry M were placed in this group. The spectra of this group had completely different main peaks to those in the previous groups and could be readily discriminated from the lipsticks in other groups (**Fig. 4.18**). These main peaks were: three strong peaks at 395, 514 and 638 cm^{-1}; and the weaker peaks at 1296, 1341, 1496 and 1623 cm^{-1}; as well as the peak group clustered around 2800-3000 cm^{-1}.

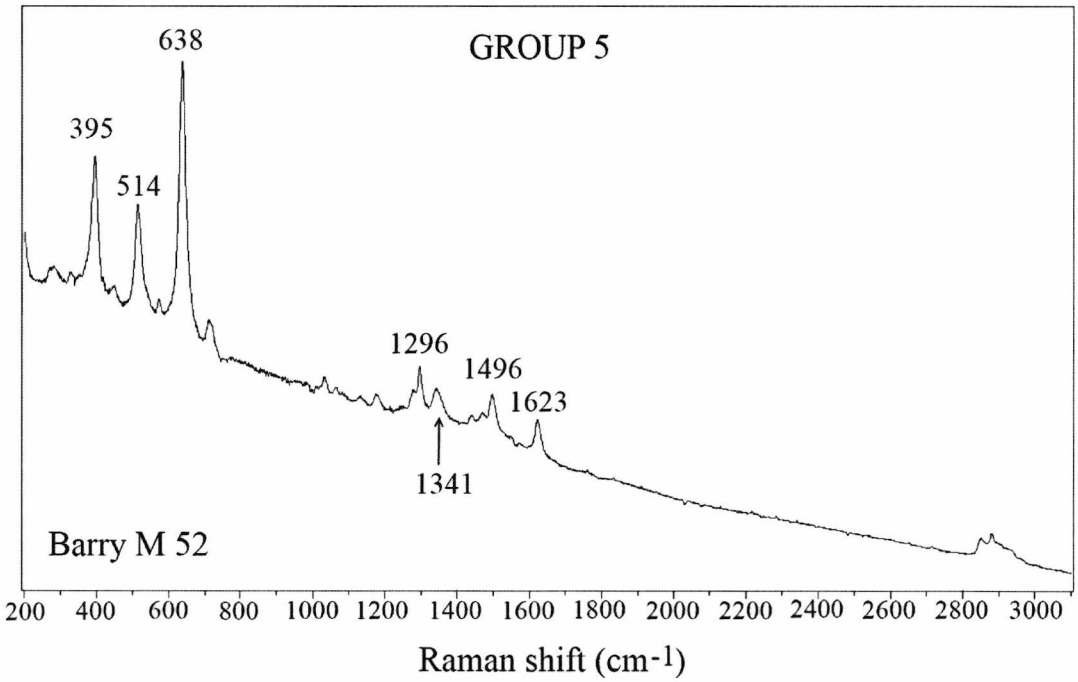

Figure 4.18. Spectrum of Barry M 52, a Group 5 lipstick, which comprises of peaks that differ from the other groups as shown.

Group 6 Lipsticks:

Three of the 73 lipsticks, also pink in colour, were placed in this group. Their spectra differed largely from those in Groups 1, 2, 3 and 4; and although the three strong peaks at 395, 514 and 638 cm^{-1} that feature in Group 5 lipsticks were the same, clear differences could be seen in the rest of the spectrum (**Fig. 4.19**).

Group 7 Lipsticks:

Fourteen lipsticks, which contained all of the UNE brand lipsticks, were placed in this group. The lipsticks were all brown in colour and had peaks that largely differed from all the other groups. The main peaks were at: 227 cm^{-1}; the double peak at 397 and 411 cm^{-1}; 515 cm^{-1}; 638 cm^{-1}; the broad peak at 1309 cm^{-1} and a peak with a shoulder at 1441 cm^{-1}; as well as the peak group at the high wavenumber end of the spectrum (**Fig. 4.20**).

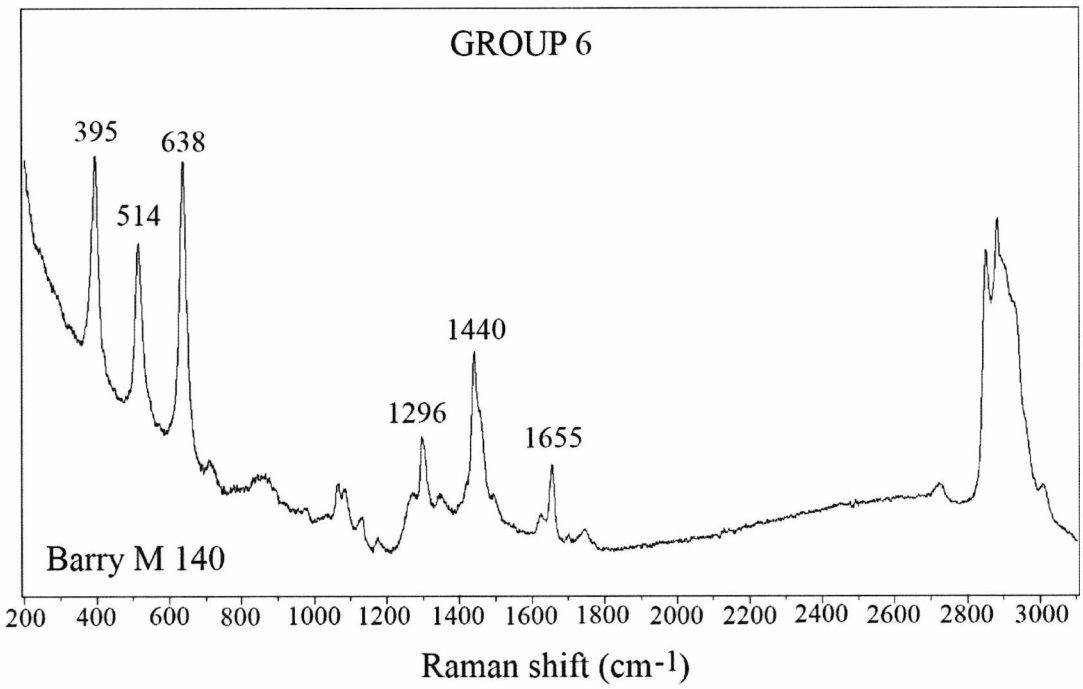

Figure 4.19. Spectrum of Barry M 140, a Group 6 lipstick, showing the main peaks half of which are different from the spectra in Group 5.

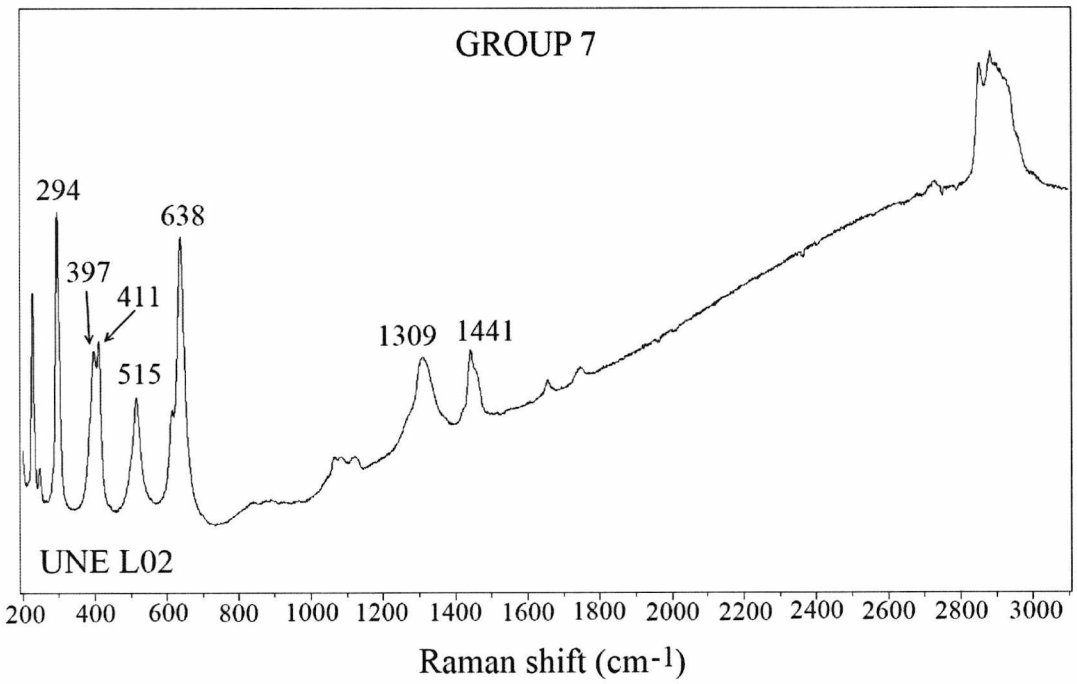

Figure 4.20. Spectrum of UNE L02, a Group 7 lipstick, showing the main peaks.

Group F Lipsticks:

Eight out of the analysed 73 lipstick samples had very fluorescent spectra that could not be used to compare the peak positions with other spectra. Therefore, they were placed in the 'fluorescent group'. This group contained lipsticks from six different brands and of a variety of colours, so no correspondence to the brand or colour could be found (**Fig. 4.21**).

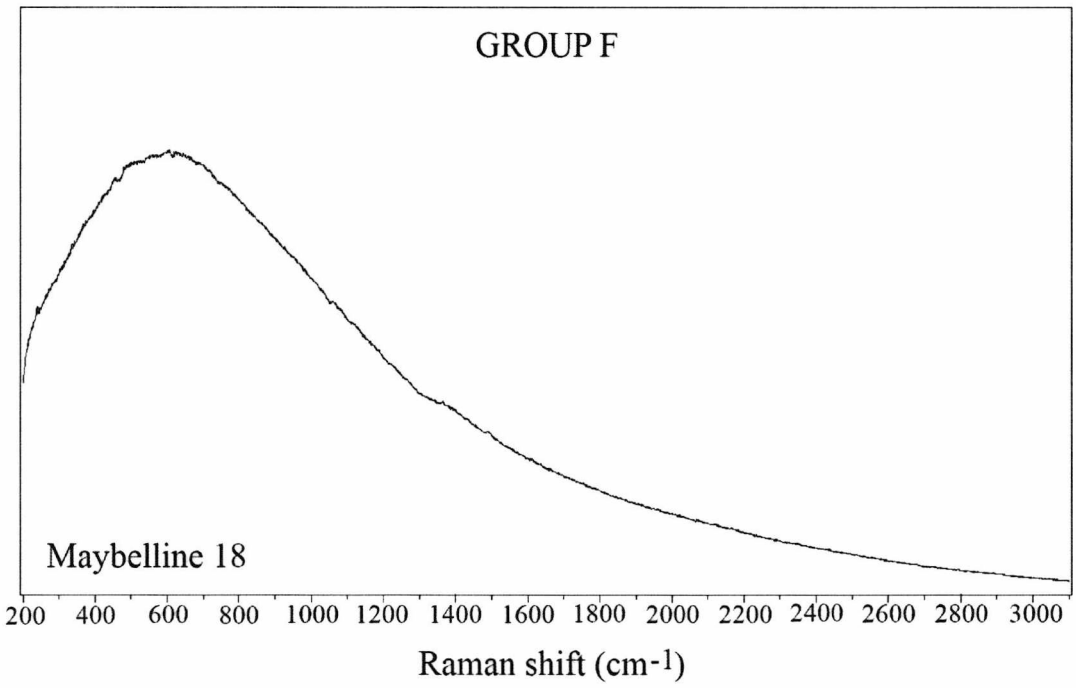

Figure 4.21. Spectrum of Maybelline 18, a typical Group F lipstick.

Group U Lipsticks:

Sixteen of the studied 73 lipsticks produced spectra that could readily be discriminated from each other as well as from the other groups. Some of the spectra from these lipsticks differed largely from each other and other groups despite having some common peaks as shown in **Figure 4.22.**

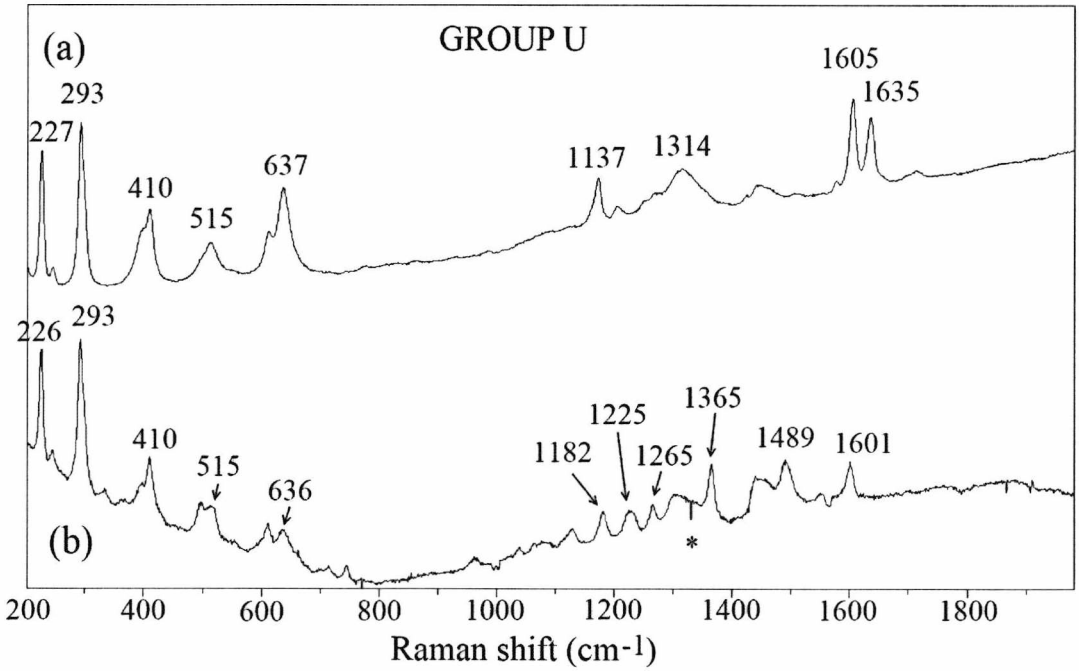

Figure 4.22. (a) Spectrum of Revlon 07 and **(b)** Spectrum of Revlon 103, both of which are spectra that can easily be discriminated from other lipsticks and groups. (*The sharp 'dips' as seen on the spectrum of Revlon 103 are due to a technical problem with the detector and are not due to the lipstick sample)

Some of the spectra in Group U showed similarities to other groups, but clear differences could also be seen (common peaks marked with * in **Fig. 4.23**). Two spectra in particular from Group U appeared largely similar and the only difference was absence of some peaks from one of the spectra (as circled in **Fig. 4.23**). These small differences were reproducible with each spectrum taken.

The averaged spectrum of each Group U lipstick is attached in **Appendix II**. Individual spectral files are also supplied on the accompanying CD.

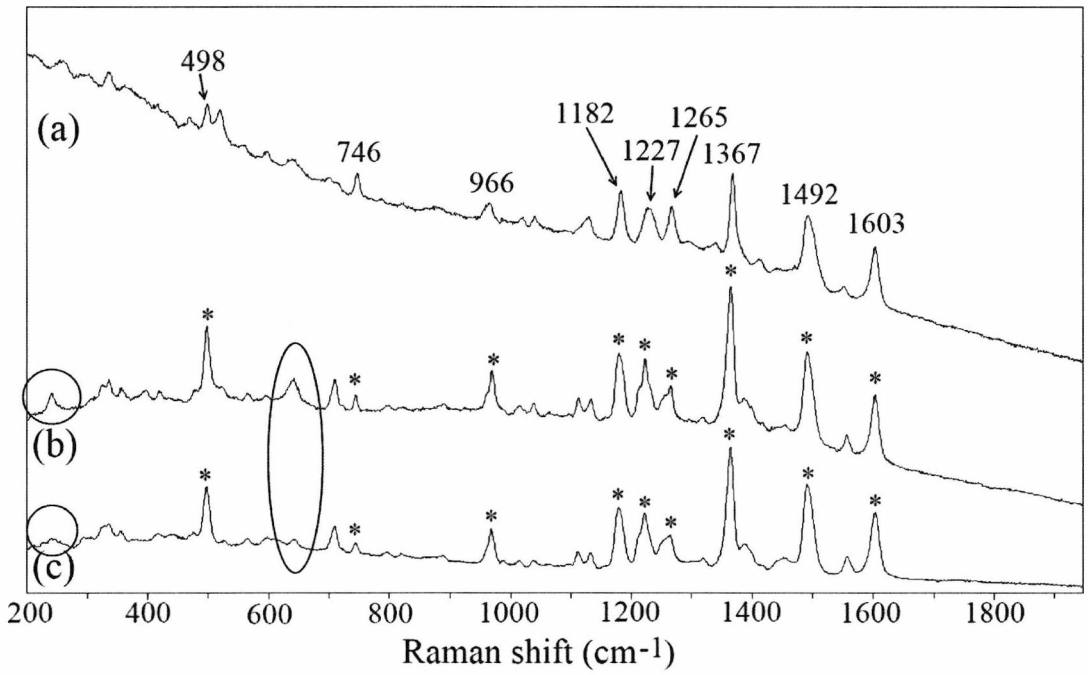

Figure 4.23. (a) Spectrum of Revlon 46, a Group 2 lipstick **(b)** Spectrum of Prestige PL-28A, a Group U lipstick **(c)** Spectrum of La Femme 29, a Group U lipstick. The majority of peaks are common to both group's lipsticks; however some differences can be seen. Even though the two Group U lipsticks look very similar to each other, differences are observed in two places as circled.

The results showed that 21.9% of the analysed lipsticks had characteristic spectra that could be used to identify the individual lipstick. Whereas 11% of the lipsticks were too fluorescent to obtain meaningful spectra from; the remaining 67.1% could be divided into seven groups which all had spectra characteristic to that group. Each of these groups could be differentiated from one another. However, no differentiation could be achieved for the lipsticks within the same group.

Group 1 was composed of mainly red lipsticks which might suggest that the main peaks appearing in this group could be due to the red dyes and/or pigments used in the manufacture of red lipsticks. In the same way, Groups 5 and 6 were composed of pink lipsticks, and their spectra also have some common peaks, that were also different from Group 1's peaks. Group 7 was composed of lipsticks that were all brown and the spectra of these lipsticks had some common peaks with Groups 5 and

6, as well as different, characteristic peaks which might occur due to the brown dyes or pigments used.

On the other hand, the rest of the other groups were composed of lipsticks with a variety of colours, so no association with colour could be established.

Four out of the five Prestige lipsticks were placed in Group U, which suggests that the majority of the spectra obtained from Prestige lipsticks are characteristic of the individual lipstick. All of the UNE lipsticks were in Group 7, which demonstrates that the brand UNE has the least level of discrimination in terms of Raman spectra of the lipsticks. On the other hand, Barry M and Revlon lipsticks were distributed among the groups, and both brands had a number of lipsticks in Group U; which shows that both brands have lipsticks that give spectra characteristic to the lipstick; and some level of discrimination can also be achieved with the rest of their lipsticks, giving a good level of discrimination with these two brands.

Considering that the spectra of most lipsticks had common peaks which allowed for the lipsticks to be classified into groups, identifying these peaks could help with understanding which components gave rise to those peaks, and why some lipsticks with completely different colours sometimes fall into the same group. The next part of the chapter discusses the identification of some of the peaks found in lipstick spectra.

4.4.2. Identification of peaks

Since the majority of modern lipsticks are made up of very similar compounds, the fact that their Raman spectra are also very similar is unsurprising. It is important to be able to discriminate between spectra by comparing the presence/absence of peaks.

However, it is advantageous to also know the constituents within the lipstick that give rise to these peaks.

Lipsticks are composed of many compounds in order to be stable and firm, yet soft enough to leave a film of colour on the lips when applied. To achieve this, a complex mixture of waxes and oils are used as the base of the lipstick, as well as emulsifiers to keep these compounds together in a single consistency. In order to get the colour required, a number of dyes and pigments, as well as sheen-producing compounds like pearlescents, are used. To prevent this mixture of compounds from deteriorating, a variety of preservatives and antioxidants are added. Finally, to mask the unpleasant odour of this mixture, perfumes and flavourings are used.

When examining the spectrum of a lipstick, it can be seen that the complexity of its ingredient mix is reflected in the spectrum. The spectrum of a lipstick contains a large number of peaks, sometimes overlapping, and sometimes obscured by fluorescence.

One way to identify a compound by Raman spectroscopy is to compare the positions of peaks to those that are known to arise from certain chemical bonds. Published tables and charts give the characteristic Raman frequencies of a wide variety of bonds and functional groups [10, 241]. This method works best when the compound being analysed is simple and a pure substance. Attempting to identify each peak in a lipstick spectrum this way is time consuming and inefficient. Even if the peaks are identified, it may not be possible to tell which compound gave rise to those peaks when there are so many compounds with similar properties that could also give peaks in the same region.

Another way of identifying the components is to compare the spectra of lipsticks to the spectra of the constituent compounds such as beeswax, titanium (IV) oxide, or a

variety of dyes. This is much more feasible for lipstick spectra and is the method employed in this study.

For this purpose, some of the main compounds as well as dyes and pigments, used in the manufacture of lipsticks were obtained and analysed. These were beeswax, castor oil, carnauba wax, FD&C Yellow No. 6 Aluminium lake (C.I. 15985) dye, FD&C Yellow No. 5 Aluminium lake (C.I. 19140) dye, FD&C Blue No. 1 (C.I. 42090) dye, carmine (C.I. 75470), D&C Red No. 28 (C.I. 45410) dye, titanium (IV) oxide (rutile and anatase), and iron oxide (Fe_3O_4).

Out of these, castor oil, iron oxide (Fe_3O_4), carmine, FD&C Blue No. 1 and FD&C Yellow No. 6 Aluminium lake dye produced very fluorescent spectra with no discernible peaks (**Fig. 4.24**).

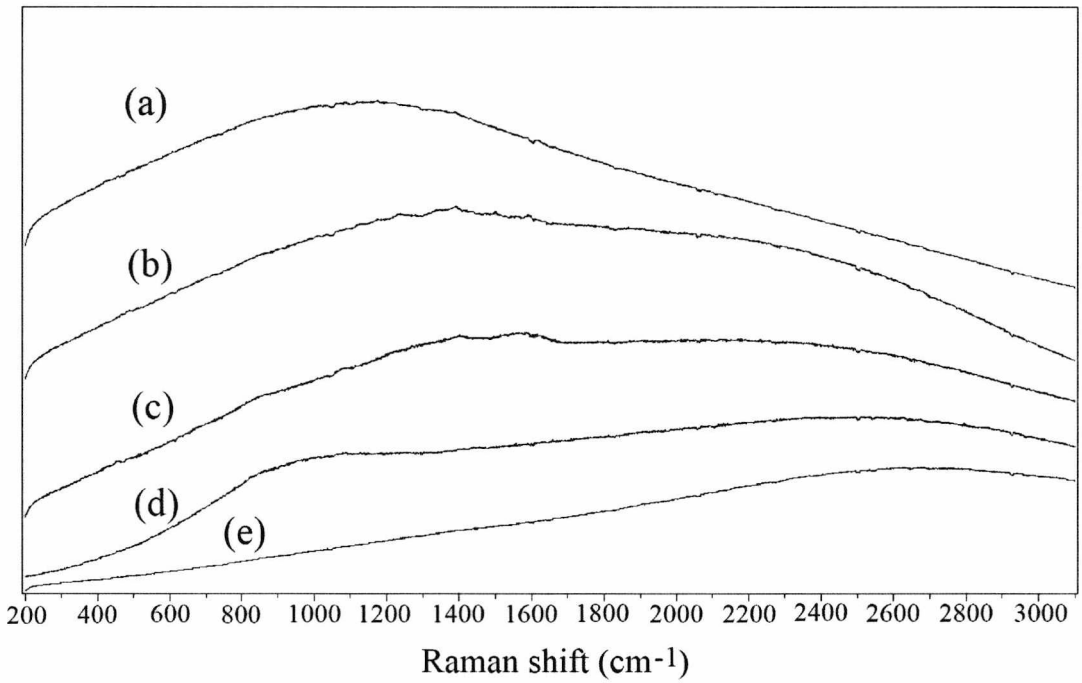

Figure 4.24. Spectrum of **(a)** FD&C Blue No. 1 **(b)** FD&C Yellow No. 6 Aluminium lake **(c)** Carmine **(d)** Castor oil **(e)** Iron oxide

Carnauba wax also produced a very fluorescent spectrum. However, some peaks were visible between 2840 - 2890 cm^{-1} (**Fig. 4.25**). Carnauba wax has an average chain length of 50 carbon atoms. The majority of its composition is taken up by aliphatic and aromatic esters, with the rest being formed of hydrocarbons, fatty acids, alcohols and some inorganic residues [242]. The region where peaks were observed with this compound (around 2840 - 2890 cm^{-1}) is the region where the C-H stretches of many compounds appear in Raman spectra [241]. Therefore, the peaks in this region can be identified as arising from C-H bond vibrations.

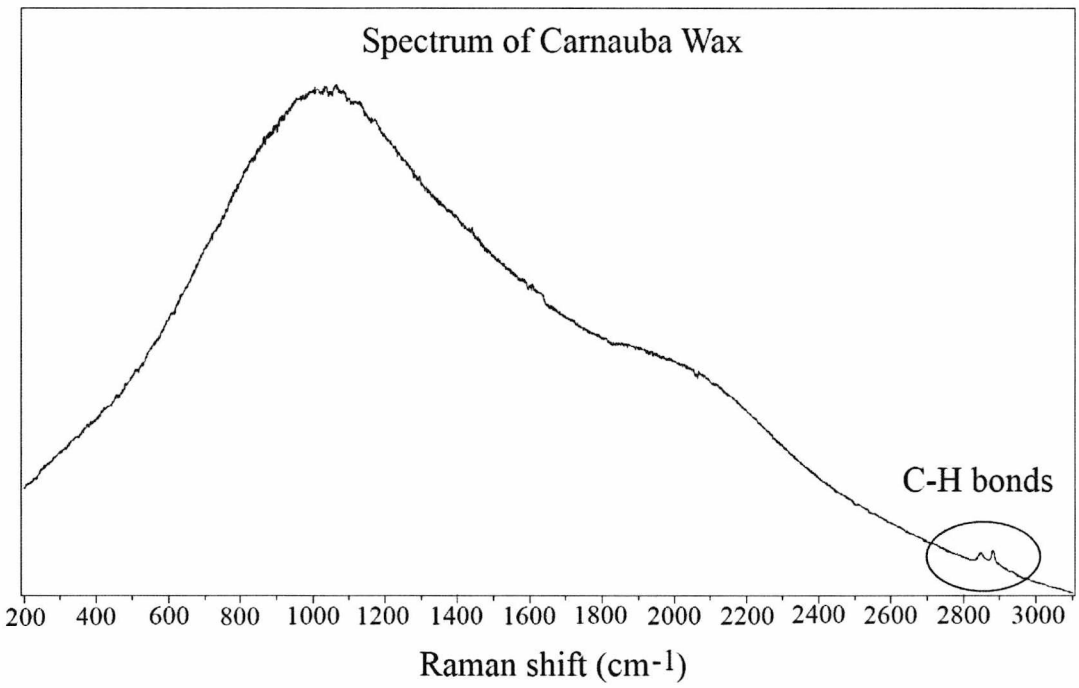

Figure 4.25. Spectrum of carnauba wax. Even though the spectrum is fluorescent, the peaks arising from C-H bond vibrations are still visible.

The dye D&C Red No. 28 also had a fluorescent spectrum. However, some peaks were visible. The predominant peaks were at 644, 720, 1275, 1295, 1349, 1470, 1502 and 1620 cm^{-1}. These peaks matched with those in the spectra of Barry M 52, Barry M 62, and (potentially) Revlon 455 lipsticks (**Fig. 4.26**).

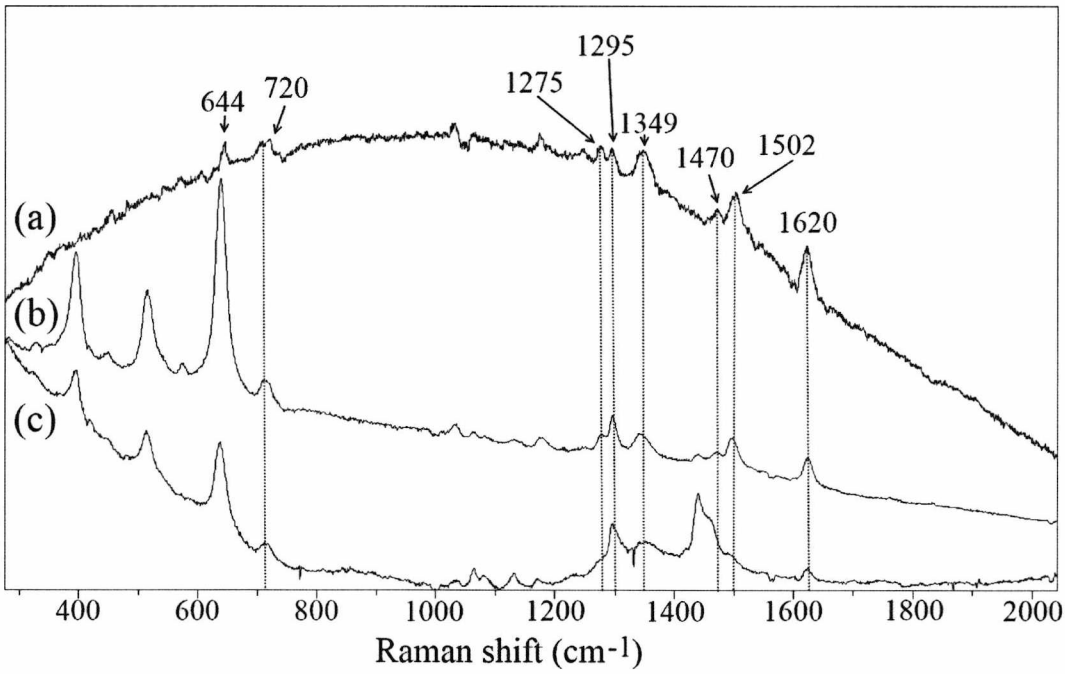

Figure 4.26. (a) Spectrum of the dye D&C Red No. 28 **(b)** Spectrum of Barry M 52, which is also the same as Barry M 62 **(c)** Spectrum of Revlon 455

As can be seen from the figure, the peaks from the dye, especially those at 720, 1349, 1502 and 1620 cm^{-1}, match those from the lipsticks; whereas the peaks at 1275 and 1470 cm^{-1} are probably obscured by the more intense peaks in Revlon 455. The peak at 644 cm^{-1} seems to be obscured by a much stronger peak nearby in both cases; and the peak at 1295 cm^{-1} seems to be relatively stronger in the lipstick spectra, which might be due to another compound with a stronger peak in the same position. In general, there is a good match between the dye and the lipsticks in terms of the positions and relative intensities of the peaks, which suggests the potential presence of this dye, or another dye of the same class (xanthene dyes) with peaks in similar positions.

Another dye listed as one of the ingredients of lipsticks, FD&C Yellow No. 5 Aluminium lake, produced an excellent spectrum with strong peaks. However, careful examination of the positions and relative intensities of the peaks revealed that the spectrum did not match with any of the peaks in the lipstick spectra (**Fig. 4.27**).

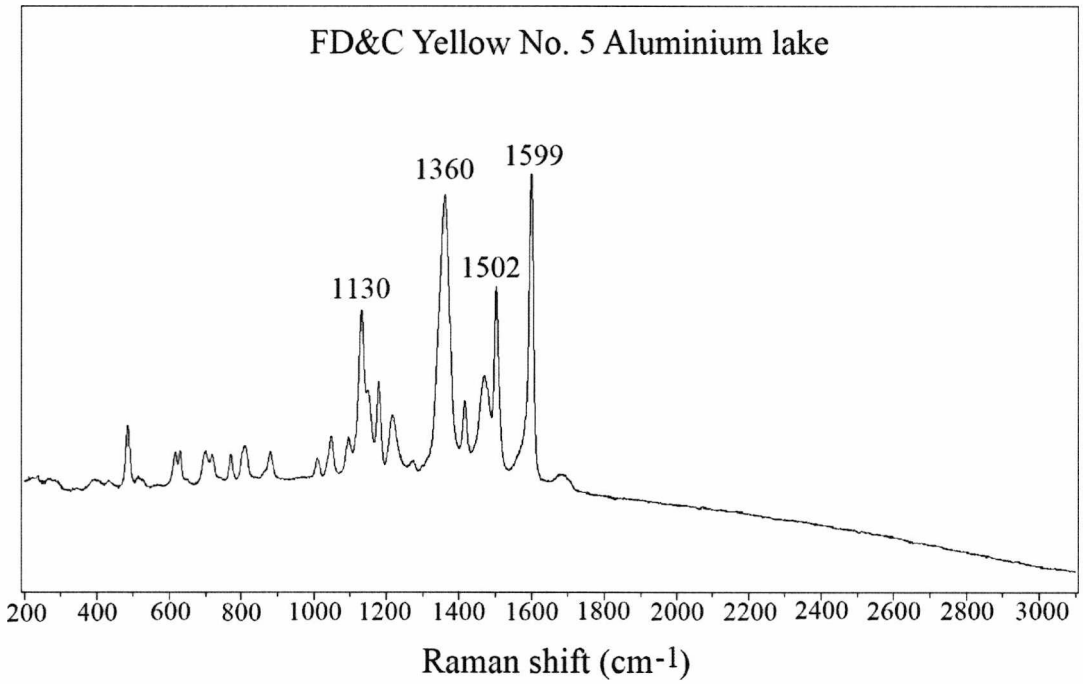

Figure 4.27. Raman spectrum of the dye FD&C Yellow No. 5 Aluminium lake

The analysis of beeswax yielded a non-fluorescent spectrum with many strong peaks, several of which matched the peaks observed in some lipstick spectra. Beeswax is composed of monoesters, diesters, triesters, hydroxyl monoesters, hydroxyl polyesters, free acids, acid monoesters, acid polyesters, hydrocarbons, alcohols and unknown impurities [243]. The average chain length is 40 carbon atoms and, as with the spectrum of carnauba wax, the spectrum of beeswax also contains the peak group at the high frequency end that is the result of C-H bond stretching vibrations. The main peaks of the beeswax spectrum were at 1062, 1130, 1295, 1419, 1441, 1462, 2848 and 2882 cm^{-1} (**Fig. 4.28**).

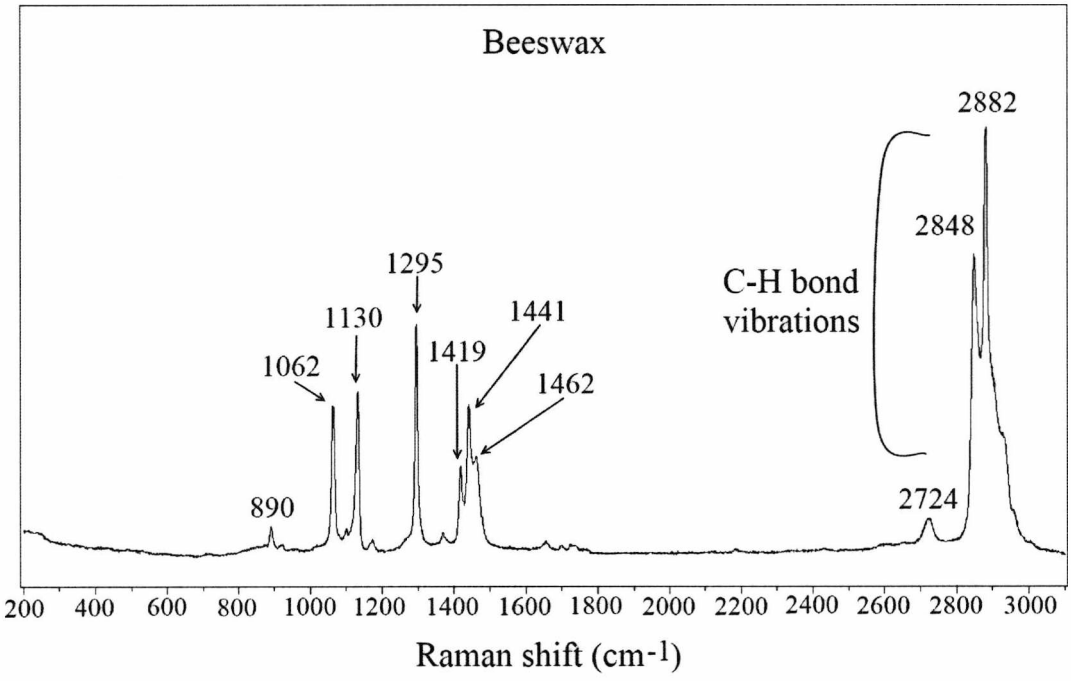

Figure 4.28. Raman spectrum of beeswax.

It was determined that the weak, broad peak at 2724 cm^{-1} arose from the O-H stretches of carboxylic acids (COOH), which are commonly found between 2500 and 3300 cm^{-1} as broad and weak peaks in Raman spectra [241].

Even though the majority of the beeswax peaks match those seen in some lipstick spectra, the relative intensities of some peaks do not match due to peaks from other compounds obscuring or overlapping with the beeswax peaks. For example, the peak at 1441 cm^{-1} appears to be stronger in the lipstick spectrum than it is in the beeswax spectrum (relative to the other peaks) (**Fig. 4.29**) which could be due to another compound in the lipstick that gives a more intense peak in the same position. Due to the number and complexity of compounds found in lipsticks, it is difficult to pinpoint individual peaks as definitely belonging to a certain compound.

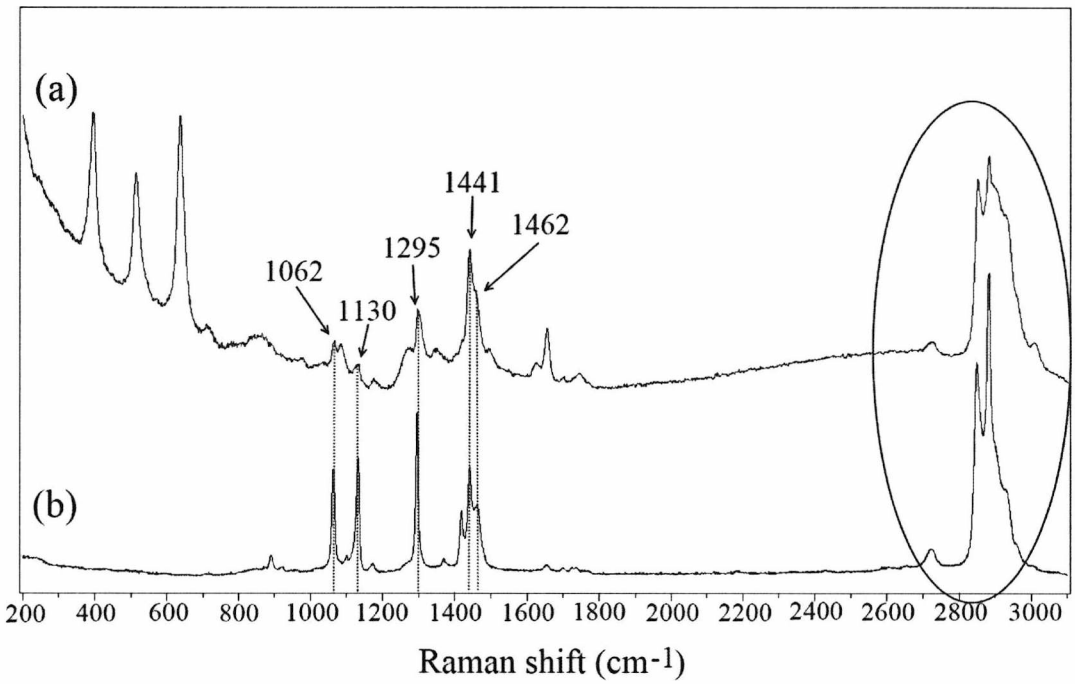

Figure 4.29. (a) Spectrum of Barry M 140 lipstick **(b)** Spectrum of beeswax. The main peaks in the beeswax spectrum match those in the lipstick spectrum.

The analysis of titanium dioxide, both in anatase and rutile form, helped identify some of the peaks that appear in the majority of lipstick spectra (**Fig. 4.30**).

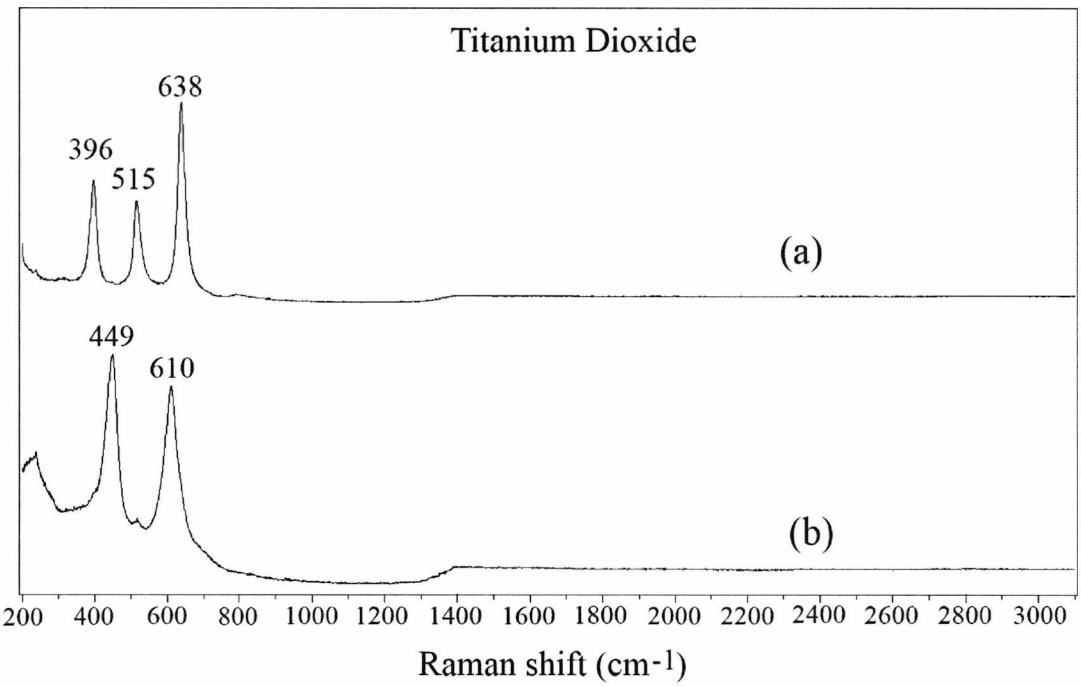

Figure 4.30. (a) Spectrum of the anatase form of titanium dioxide **(b)** Spectrum of the rutile form.

Whereas most of the lipsticks seemed to contain the anatase form of titanium dioxide, a few of them also exhibited rutile peaks. In most cases, the rutile peaks were either quite weak or not present at all. However, in the case of Barry M 136 and UNE L05, rutile peaks appeared stronger in some of the spectra (**Fig. 4.31** and **Fig. 4.32**).

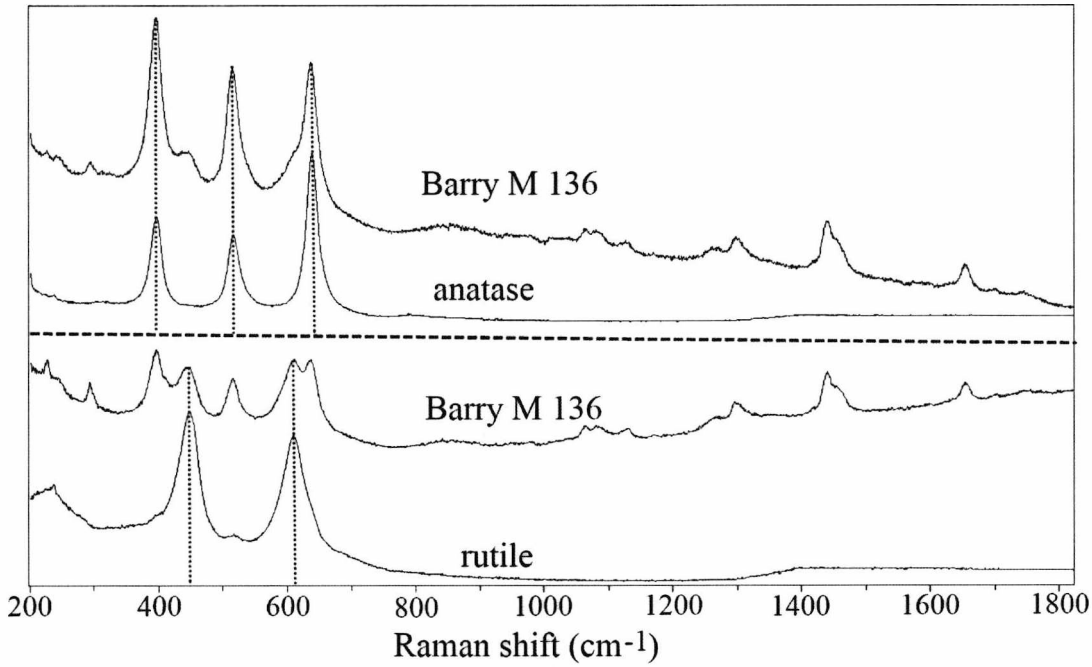

Figure 4.31. A figure showing two different spectra obtained from two different positions on a Barry M 136 smear, where (top) the anatase peaks are dominant; and (bottom) the rutile peaks are more intense, changing the appearance of the lipstick spectrum.

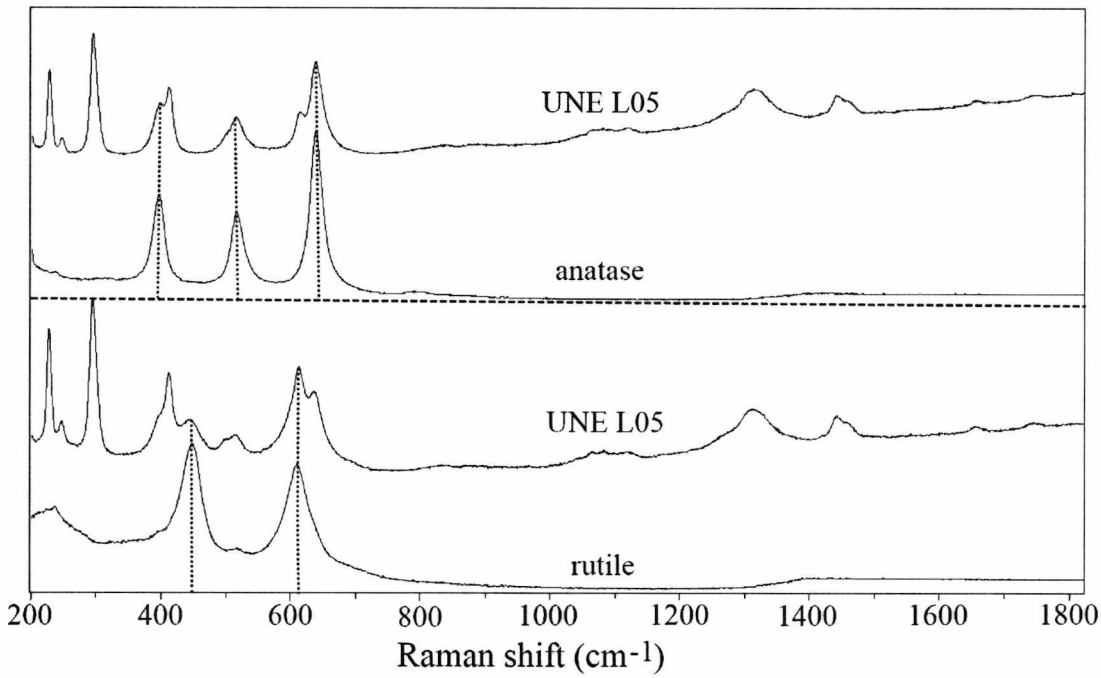

Figure 4.32. A figure showing two different spectra obtained from two different positions on an UNE L05 smear, highlighting the differences that can occur due to anatase and rutile peaks.

These two cases were the only ones out of the analysed lipsticks where each five of the lipstick spectra (per lipstick) did not resemble each other closely. Therefore it is important, when comparing spectra, to bear in mind that on occasion the rutile peaks can appear as strong as the anatase peaks, changing the overall appearance of the spectrum; however, these peaks belong to different forms of the same compound. The manufacturers do not specify which form of titanium dioxide is used in their products, so it is not possible to make the deduction that only some of the lipsticks contain rutile, and that it is an individual characteristic of that lipstick. It is therefore recommended to record at least five different spectra per lipstick sample to ensure the reproducibility of peaks and their relative intensities. This is the reason the lipstick spectra presented here are averaged (unless specified otherwise) in order to account for these occasional 'differences'.

Raman spectroscopy has been used for the analysis and discrimination of a variety of natural and synthetic dyes and pigments, and several papers report libraries of

spectra for these compounds. These include libraries for historic pigments [148, 149], modern pigments [150, 151], natural pigments found in ochres and iron-containing ores [152], and numerous pigments found in artists' materials and works of art [153-155]. There are also several on-line databases, some of which are also mentioned in the references above. These include:

1. The database formed as part of the ColoRaman project which contains spectra of 99 pigments used in art (http://oldweb.ct.infn.it/~archeo/);
2. The e-VISART database which contains spectra from archaeological and artists' materials (http://www.ehu.es/udps/database/ database.html);
3. The database of natural and synthetic pigments compiled by Bell *et al* at the University College London (http://www.chem.ucl.ac.uk/resources/raman/ index.html), which also gives the option of downloading the spectra;
4. A spectral database system (SDBS) for a variety of organic compounds (http://riodb01.ibase.aist.go.jp/sdbs/cgi-bin/direct_frame_top.cgi);
5. A spectral library set up by The Infrared and Raman Users Group (IRUG) which contains over 1250 spectra of oils, waxes, resins, dyes, pigments, proteins, gums, and minerals (http://www.irug.org/ed2k/search.asp);
6. A database put together for a project of the Royal Institute for Cultural Heritage (KIK/IRPA) for the analytical study of 20^{th} century paint (http://modern.kikirpa.be), which also has downloadable spectra.

An extensive review by Vandenabeele *et al* investigates the application of Raman spectroscopy to the analysis of pigments in archaeological and art objects such as medieval books, paintings, minerals, rock paintings etc.; and provides an overview of published and on-line spectral libraries [156].

A thorough search of these libraries and databases helped identify some of the peaks that arose due to dyes commonly used in the manufacture of lipsticks. One of the most useful databases for this was that of the Royal Institute for Cultural Heritage (KIK/IRPA, http://modern.kikirpa.be). The spectra found in this database were recorded using a 785 nm laser excitation wavelength and the availability of spectra for download made it easier to compare spectra. Even though the excitation wavelength was different from the one used for this research, the positions of the

peaks should not differ, because the Raman effect is a shift in energy from the incident laser line and each peak represents the amount of this shift (in wavenumbers, cm^{-1}). Therefore, no matter which excitation wavelength is used, the energy difference between the incident and scattered light should be the same.

Presented in **Fig. 4.33** are the spectra for the dyes D&C Red No. 6 Barium lake and D&C Red No. 7 Calcium lake, both of which are frequently used in lipsticks (obtained from the KIK/IRPA spectral database). Both of these dyes belong to the same chemical class of azo dyes. Therefore, they have very similar chemical structures (**Fig. 4.34**) [218]. The small differences in the positions of the peaks probably arise from the different metals used in producing the lake.

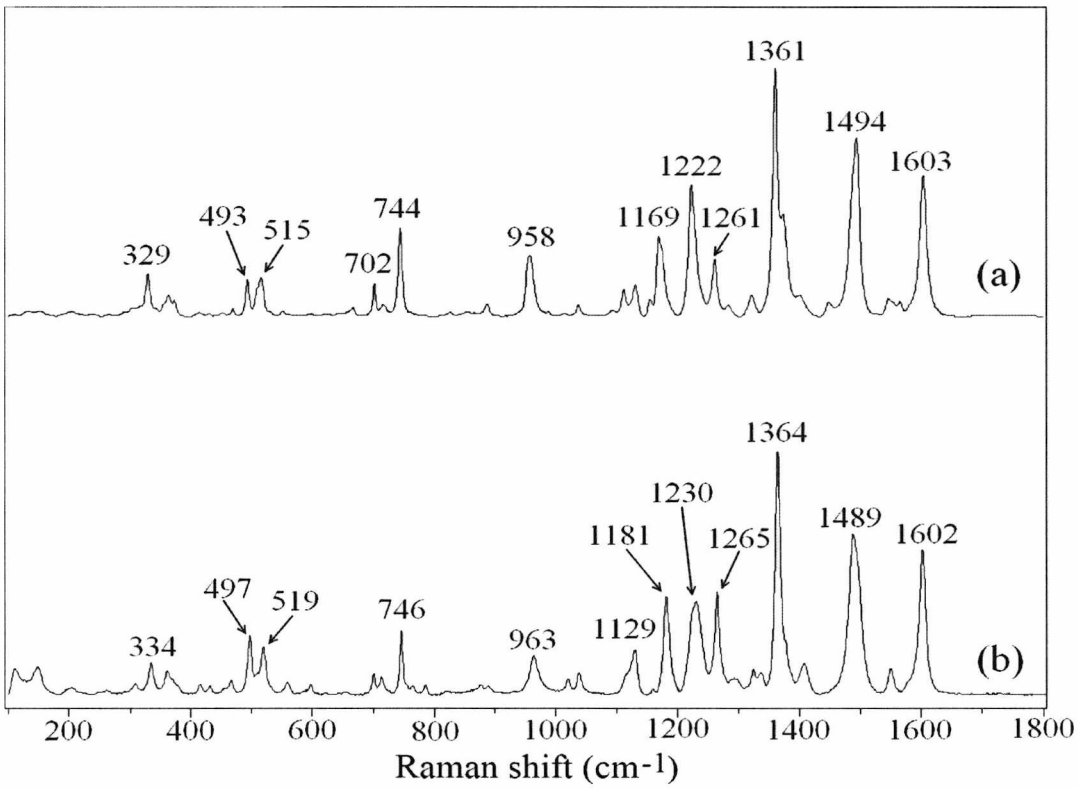

Figure 4.33. (a) Raman spectrum of D&C Red No. 6 Barium lake **(b)** Raman spectrum of D&C Red No. 7 Calcium lake. Spectra are obtained from the KIK/IRPA spectral database. The only difference between the two dyes is the metal used: barium for No. 6 and calcium for No. 7.

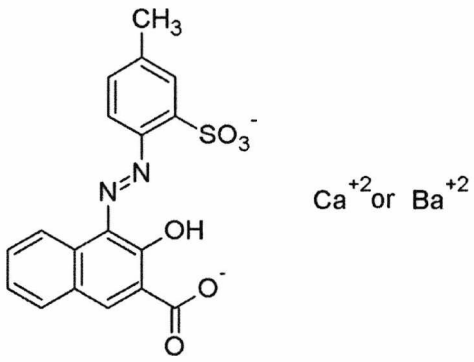

Figure 4.34. The chemical structure of D&C Red No. 6 and 7 dyes. Barium is the metal used in D&C Red No. 6 lake, and calcium is used in D&C Red No. 7 lake.

The main peaks for D&C Red No. 6 Barium lake are: 329, 493, 515, 744, 958, 1169, 1222, 1261, 1361, 1494 and 1603 cm^{-1}. Those for D&C Red No. 7 Calcium lake are: 334, 497, 519, 746, 963, 1129, 1181, 1230, 1265, 1364, 1489, and 1602 cm^{-1}. The positions and relative intensities of these peaks match with those of the lipsticks in Groups 1, 2, 3, and 4, suggesting that the similarities between groups 1, 2, 3 and 4 probably arise because of the same type of dye being used.

Figure 4.35 shows the comparison between the spectrum of D&C Red No. 7 Calcium lake and the spectrum of Almay 36, a Group 1 lipstick. The main peaks, as well as the weaker peaks, match very well in terms of peak positions and relative intensities, showing that the majority of the peaks seen in the lipstick spectrum are due to the dye. This suggests that Raman signals from the dye might be enhanced by resonance Raman scattering since the concentration of dyes in lipsticks is small (0.5% up to 15%) [218, 221, 222].

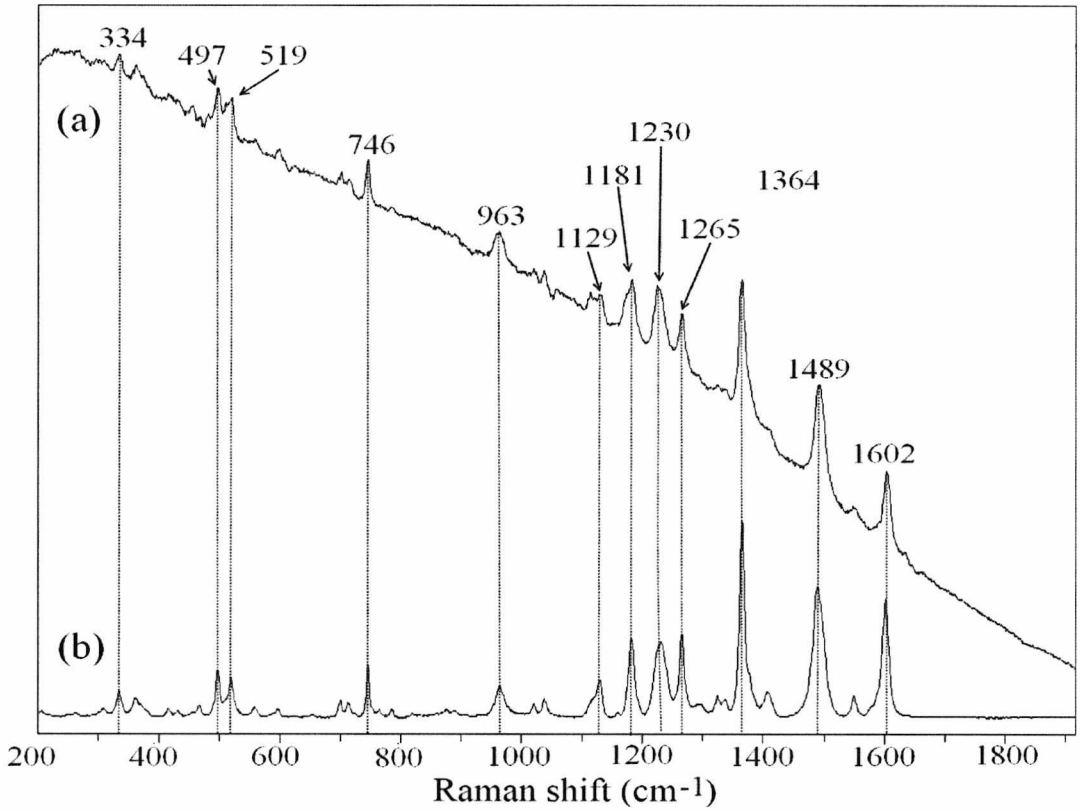

Figure 4.35. (a) Spectrum of Almay 36, a Group 1 lipstick **(b)** Spectrum of D&C Red No. 7 Calcium lake.

Even though the peak positions of each lipstick within a group matched within a few wavenumbers, there were some lipsticks that showed reproducible differences in terms of their peak positions. Examination of the spectra of the two red dyes mentioned showed that these differences were due to a different dye of the same chemical class being present in the lipstick. This enabled the lipsticks within a group to be classified further by determining the dye responsible for the peaks in the lipstick spectrum.

Out of the 16 Group 1 lipsticks:

- 14 of them were identified as having D&C Red No. 7 Calcium lake present [Almay 36, Barry M 145, Bourjois (15, 16, 32, 54), L'Oreal (164, 900), Prestige CL-93A, Revlon (006, 009, 030, 095, 675)]

- The peaks of Barry M 121 and Revlon 090 did not exactly match the peaks of any of the dyes available, even though they looked very similar to those of the two red dyes.

Out of the six Group 2 lipsticks:

- Four of them [L'Oreal 345, Revlon (46, 045, 430)] were identified as containing the dye D&C Red No. 7 Calcium lake.
- Revlon 080 contained D&C Red No. 6 Barium lake
- Revlon 371 did not exactly match the peaks of any dye available.

The only Group 3 lipstick, Barry M 146, contained the dye D&C Red No. 7 Calcium lake. Out of the seven Group 4 lipsticks:

- Barry M 53, Revlon 005 and Revlon 750 contained D&C Red No. 6 Barium lake
- Revlon lipsticks 004, 025, 035, and 450 contained D&C Red No. 7 Calcium lake

These two red dyes did not show up in the spectra of any Group 5, 6 or 7 lipsticks. Two of the Group U lipsticks (L'Oreal 524 and Prestige PL-49A) were identified as containing D&C Red No. 7 Calcium lake. A diagram showing the overall level of classification of lipsticks and the formation of sub-groups due to the dyes is given in **Fig. 4.36**.

Figure 4.36. A diagram showing the further classification of lipsticks by their component dyes (if known).

Further discrimination can also be obtained when the intensities of the C-H peaks relative to the intensities of the dye peaks are compared. Such analysis can be carried out for the lipsticks that have C-H peaks with differing intensities relative to the rest of the peaks in their spectra. If the ratio of the dye peak intensity to the C-H peak intensity is observed to be consistent for the spectra of the same lipstick, statistical analysis can be carried out to compare the variability in the mean ratios of the lipsticks within the group. If this variability between lipsticks is large enough, then further categorisation between the lipsticks of the same group can be achieved.

Groups 1-4 had characteristic spectra that visually differed from each other by the presence/absence of either the peak at 638 cm^{-1} or the C-H peak group between 2800 and 3000 cm^{-1}. Out of these groups, only Groups 2 and 4 displayed the C-H peaks. Therefore the statistical analysis was carried for the lipsticks in Groups 2 and 4. The intensity of the C-H peak at around 2850 cm^{-1} was compared to that of the highest peak in the spectrum (the dye peak observed at around 1360 cm^{-1}) for each lipstick spectrum. The observed ratios of the dye peak intensity to the C-H peak intensity did not differ from their mean (per lipstick) by more than 2 standard deviations (at the confidence interval level of approximately 95%). Therefore it was concluded that the relative peak intensities were consistent per lipstick. These ratios were then used to compare lipsticks within the group.

To carry out the statistical analysis, the Analysis of Variance (ANOVA) technique was used. ANOVA is a hypothesis-testing technique that examines the variances of samples to test the equality of the means of two or more groups of samples. This technique helps determine whether the differences between the peak intensity ratios in lipsticks are due to random errors or whether they are systematic differences that arise due to, for example, peaks arising from different compounds, giving rise to differing relative intensities.

For the lipsticks in Group 2, differences in the mean ratios were observed at 5% significance level which resulted in further discrimination between the lipsticks in this group. The resultant sub-groups formed were:

- Sub-group A: L'Oreal 345 and Revlon 371
- Sub-group B: Revlon 045, 46 and 430
- Sub-group C: Revlon 080

Further discrimination could also be achieved for the lipsticks in Group 4 and the observed sub-groups matched the grouping obtained due to their component dyes (**Fig. 4.36**). These were:

- Sub-group A: Barry M 53, Revlon 005 and Revlon 750
- Sub-group B: Revlon 004, 025, 035 and 450

The results demonstrated that a better level of discrimination can be obtained by identifying the compounds, especially dyes, found in lipsticks, as well as by comparing the relative intensities of peaks arising from different compounds (such as the dye peaks versus the C-H peaks arising due to the oily/waxy composition).

The next part of the chapter describes a more detailed analysis of spectra, including the compilation of a library of lipstick spectra composed of averaged peak positions, standard deviation calculated for each peak position, relative intensities of peaks and the identity of the peaks if known (i.e. which compound it originates from).

4.4.3. A comprehensive library of 65 lipstick spectra

Each lipstick spectrum was analysed to find out the peak positions and relative intensities of the peaks. For this purpose OMNIC 7.3 software was used to measure the peak positions in units of wavenumbers (cm^{-1}). For symmetrical features, the position of the peak was determined to be at the mid-point of the peak as measured at half its maximum intensity. For broad and asymmetric peaks, the assigned

wavenumber was taken to be at the maximum intensity of the peak. The criterion for a feature to be considered as a 'peak' was for the height of the peak to be greater than three times the noise level. To measure the peak height and the noise level, the "Peak Height Tool" function found in OMNIC software was used. This tool measures the height of a peak by taking into consideration the shape and the position of the baseline. It calculates the distance between the selected *peak position* (positioned at the top of the peak) and the two *baseline connection points* which can be adjusted to fit either side of the peak along the baseline (**Fig. 4.37**).

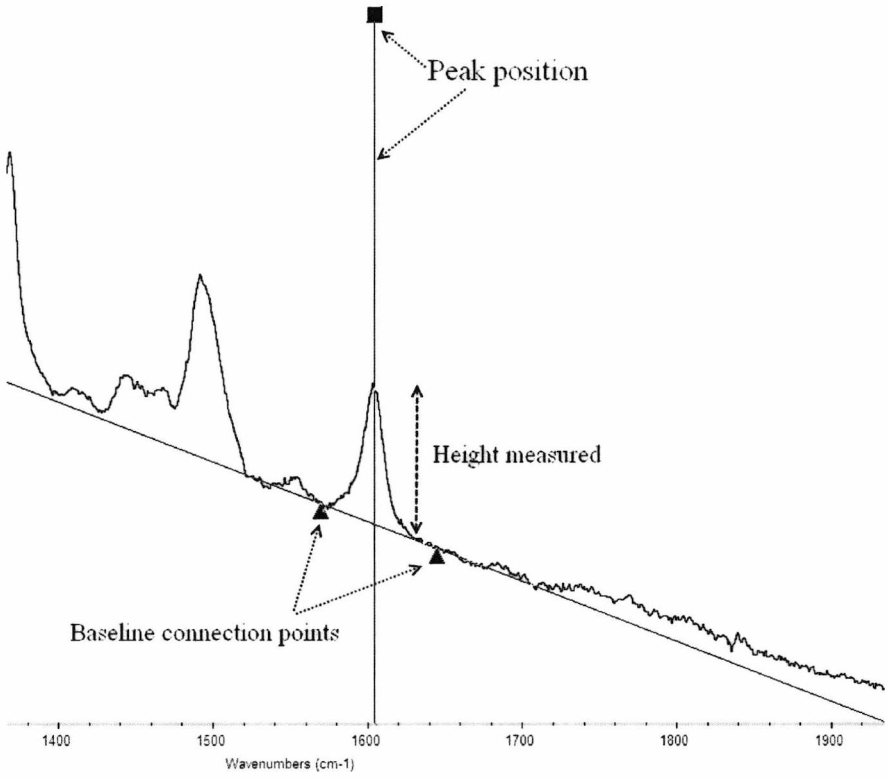

Figure 4.37. Diagram showing the use of 'Peak Height Tool' in OMNIC 7.3 software. The *peak position* and *baseline connection points* can manually be adjusted to define the peak height to be measured.

The same tool was used to measure the height of the noise along the baseline at ten different points, and the average was taken. This was then multiplied by three, and the resulting value was taken as the minimum height for a feature to be considered as a real peak and not a noise deviation.

The values for peak positions for each spectrum were tabulated, and the average peak positions, as well as the standard deviation for each position, were calculated. Standard deviation is a measure of how far a datum (in this case, peak position) is from the average of a given distribution, and it gives a metric on how much the wavenumbers for each peak varies from the average. The formula for standard deviation is given by [244]:

$$s = \sqrt{\sum (x_i - \bar{x})^2/(n-1)}$$

where s is the standard deviation; x_i is the peak position; $\bar{x}$ is the mean of the peak positions; and n is the number of measurements (i.e. the total number of spectra per lipstick).

The relative intensities of peaks (in qualitative terms of 'strong', 'medium', 'weak' etc.) were also determined, as well as any distinguishing features of the peaks (such as 'shoulder', 'broad', or 'overlapping'). **Figure 4.38** shows an example spectrum with labelled peaks to demonstrate how the intensities of peaks were determined; and **Figure 4.39** shows examples for a 'broad' peak, a 'shoulder', and 'overlapping' peaks.

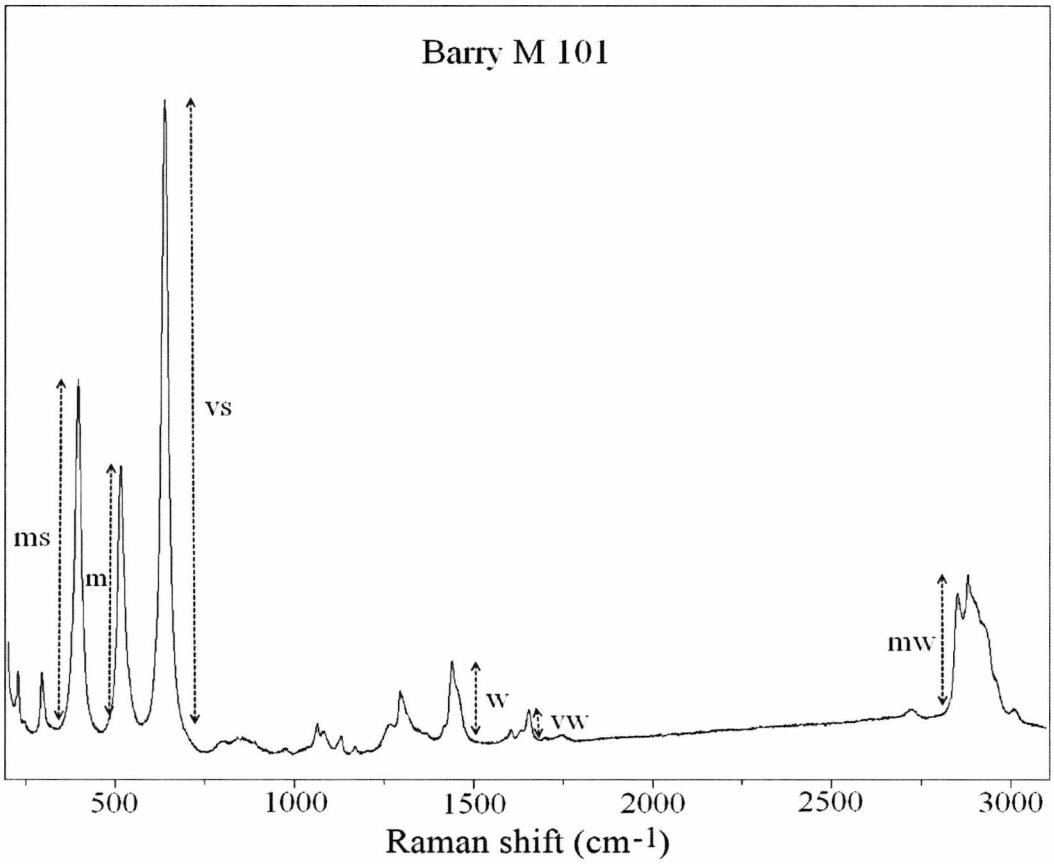

Figure 4.38. An example spectrum showing the relative intensities of peaks, where **vs**: very strong, **ms**: medium-strong, **m**: medium, **mw**: medium-weak, **w**: weak, **vw**: very weak

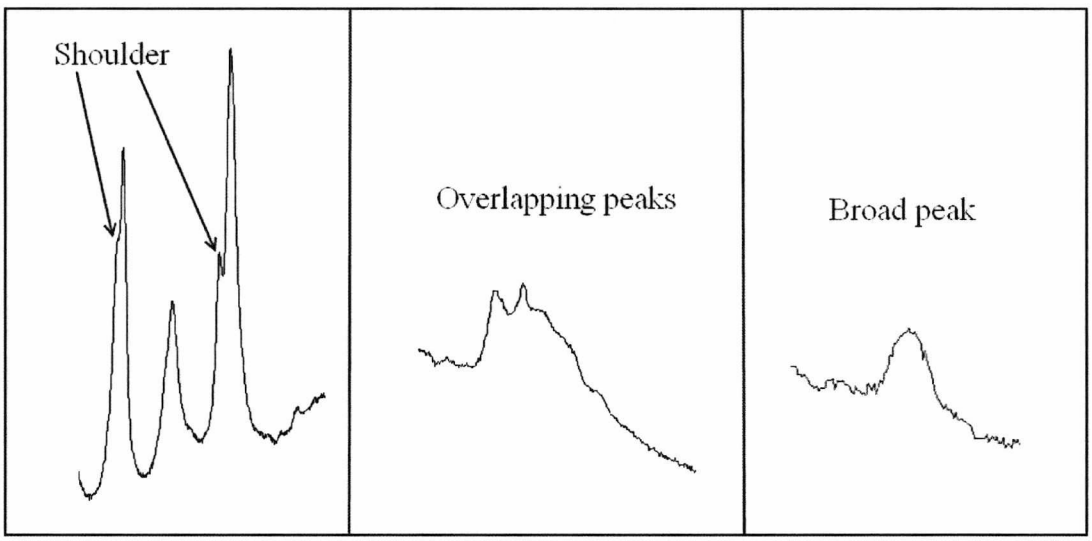

Figure 4.39. A diagram showing examples of 'shoulders', 'overlapping' peaks and 'broad' peaks.

The 'overlapping' peaks were frequently found between 2800 and 3000 cm^{-1} which were attributed to the C-H bond stretching vibrations. It was more difficult to measure the position of these peaks; therefore the positions of the protruding peaks were measured (see **Fig. 4.39**, middle diagram) and recorded. In each case where these peaks were present, the range was always between 2800 and 3000 cm^{-1}.

In some cases, the 'very weak' peaks did not fulfil the criterion for the peak height for each spectrum of the same lipstick. In these cases, if the peak was present for the majority of the spectra (for the same lipstick), it was included in the average; if not, it was discarded from the average. The Group F lipsticks were excluded from this part of the study due to no peaks being present in their spectra. The complete tables are supplied on the accompanying CD.

Following are the tabulated results (**Table 4.3**) for each lipstick where the averaged peak positions, relative peak intensities, standard deviation and the compound that the peak originates from are given. Even though the deviation from the average is very small for the majority of peaks (approximately 1 cm^{-1} or less), the standard deviations for broad and weaker peaks are greater. This is due to the variations in the measured peak positions because of the widths of those peaks being greater. Note that a standard deviation of zero is quoted where the peak positions for each spectrum per lipstick were identical.

Table 4.3. Tables giving average peak positions (cm^{-1}), signal strengths, standard deviation and peak identities where; **vw**: very weak, **w**: weak, **mw**: medium-weak, **m**: medium, **ms**: medium-strong, **s**: strong, **vs**: very strong, **br**: broad, **sh**: shoulder, **ov**: overlapping; and **A**: anatase, **R**: rutile, **BW**: beeswax.

Almay 36			
Average Peak Position	**Raman Signal Strength**	**Standard Deviation**	**Peak ID**
335.2	vw	0.548	D&C Red No.7 Ca lake
362.8	br, vw	0.402	D&C Red No.7 Ca lake
415.6	vw	0.000	D&C Red No.7 Ca lake
430.4	vw	0.531	D&C Red No.7 Ca lake
455.1	vw	0.672	
465.7	vw	0.000	D&C Red No.7 Ca lake
480.6	sh, vw	0.894	
497.4	vw	1.041	D&C Red No.7 Ca lake
517.8	vw	1.518	D&C Red No.7 Ca lake
597.4	br, vw	1.464	D&C Red No.7 Ca lake
701.6	vw	0.548	D&C Red No.7 Ca lake
715.8	br, vw	0.844	D&C Red No.7 Ca lake
745.4	vw	0.000	D&C Red No.7 Ca lake
961.1	br, vw	0.402	D&C Red No.7 Ca lake
1020.2	vw	0.000	D&C Red No.7 Ca lake
1037.5	vw	0.672	D&C Red No.7 Ca lake
1114.7	vw	0.000	D&C Red No.7 Ca lake
1130.1	vw	1.344	D&C Red No.7 Ca lake
1172.1	sh, br, vw	0.894	
1182.7	br, w	0.850	D&C Red No.7 Ca lake
1224.4	br, w	0.447	
1232.5	sh, w	1.416	D&C Red No.7 Ca lake
1265.5	vw	0.493	D&C Red No.7 Ca lake
1324.5	br, vw	0.548	D&C Red No.7 Ca lake
1336.6	br, vw	1.069	D&C Red No.7 Ca lake
1364.2	mw	0.447	D&C Red No.7 Ca lake
1409.3	br, vw	0.850	D&C Red No.7 Ca lake
1492.6	w	0.672	D&C Red No.7 Ca lake
1550.7	br, vw	1.416	D&C Red No.7 Ca lake
1603.7	w	0.447	D&C Red No.7 Ca lake
1634.6	br, vw	0.450	

Barry M 52			
Average Peak Position	**Raman Signal Strength**	**Standard Deviation**	**Peak ID**
281.7	vw, br	1.076	
328.8	vw	1.164	
395.1	mw	0.434	A
449.9	vw	0.548	
514.1	mw	0.433	A
572.3	vw	0.503	
639.2	ms	0.773	A
713.4	vw	1.971	
1031.9	vw	1.741	BW, D&C Red No.28
1175.1	vw	1.886	D&C Red No.28
1277.8	sh, vw	0.910	
1296.5	w	0.912	BW, D&C Red No.28
1342.0	br, vw	0.792	
1440.4	vw	0.462	BW
1470.6	vw	1.699	D&C Red No.28
1496.7	w	1.510	
1622.8	vw	0.953	D&C Red No.28
2851.2	ov, br, w	0.000	C-H
2881.4	ov, br, w	0.794	C-H

Barry M 53			
Average Peak Position	**Raman Signal Strength**	**Standard Deviation**	**Peak ID**
330.9	vw	0.447	D&C Red No. 6 Ba lake
395.0	w	0.844	A
494.1	sh,vw	1.105	D&C Red No. 6 Ba lake
514.5	w	0.548	A, D&C Red No. 6 Ba lake
637.9	w	1.464	A
743.6	vw	0.447	D&C Red No. 6 Ba lake
958.4	vw	1.646	D&C Red No. 6 Ba lake
1130.3	vw	0.789	D&C Red No. 6 Ba lake
1171.3	w	0.402	D&C Red No. 6 Ba lake
1224.4	w	0.447	D&C Red No. 6 Ba lake
1261.4	vw	1.041	D&C Red No. 6 Ba lake
1363.4	mw	0.000	D&C Red No. 6 Ba lake
1377.0	sh, w	1.361	D&C Red No. 6 Ba lake
1445.2	sh, br, vw	2.669	D&C Red No. 6 Ba lake
1494.6	mw	0.000	D&C Red No. 6 Ba lake
1549.7	br, vw	0.447	D&C Red No. 6 Ba lake
1603.1	w	0.850	D&C Red No. 6 Ba lake
2851.6	ov, br, w	0.894	C-H
2883.1	ov, br, w	0.000	C-H

Barry M 54			
Average Peak Position	**Raman Signal Strength**	**Standard Deviation**	**Peak ID**
396.1	m	0.447	A
515.5	mw	0.548	A
637.6	ms	1.055	A
1127.4	vw	1.055	
1177.3	vw	1.689	
1228.0	vw	0.493	
1498.6	vw	1.027	
1598.5	w	0.837	
2851.2	ov, br, vw	0.672	C-H
2881.1	ov, br, vw	0.000	C-H

Barry M 62			
Average Peak Position	**Raman Signal Strength**	**Standard Deviation**	**Peak ID**
281.6	br, vw	0.776	
395.3	m	0.672	A
449.3	vw	0.000	
514.5	mw	0.548	A
571.9	vw	0.902	
638.5	ms	0.447	A
711.2	vw	0.548	
1033.7	vw	0.000	BW, D&C Red No.28
1174.2	br, vw	1.838	D&C Red No.28
1280.5	sh, vw	1.379	
1295.5	w	1.092	BW, D&C Red No.28
1342.8	br, vw	1.471	
1440.8	vw	1.440	BW
1468.5	vw	1.950	D&C Red No.28
1498.8	w	0.850	
1622.6	vw	1.095	D&C Red No.28
2851.4	br, ov, vw	0.801	C-H
2882.7	br, ov, vw	0.548	C-H

Barry M 101			
Average Peak Position	**Raman Signal Strength**	**Standard Deviation**	**Peak ID**
226.8	w	0.447	
293.5	w	0.548	
395.7	ms	0.548	A
514.9	m	0.000	A
637.4	vs	0.000	A
1062.8	vw	1.055	BW
1080.3	vw	1.290	

1130.1	vw	0.000	BW
1169.3	vw	0.844	
1266.0	sh, vw	1.534	
1296.1	w	0.447	BW
1440.2	w	0.548	BW
1456.0	sh, vw	1.184	
1606.0	vw	0.894	
1633.0	sh, vw	1.451	
1655.4	vw	0.837	BW
2724.1	br, vw	1.258	O-H (COOH)
2851.6	ov, br, mw	0.548	C-H
2883.1	ov, br, mw	0.000	C-H
3011.1	br, vw	0.837	O-H (COOH)

Barry M 113			
Average Peak Position	**Raman Signal Strength**	**Standard Deviation**	**Peak ID**
396.7	mw	1.312	A
514.9	mw	0.707	A
638.5	m	0.447	A
1063.1	w	0.493	BW
1080.3	sh, vw	1.748	
1131.0	vw	0.672	BW
1170.8	vw	0.402	
1266.2	br sh, vw	0.447	
1296.7	mw	0.447	BW
1441.7	m	1.041	BW
1457.0	sh, mw	0.672	
1494.8	vw	1.055	
1607.0	vw	0.894	
1632.2	vw	1.254	
1655.8	w	1.588	
2722.0	br, vw	0.950	O-H (COOH)
2849.7	ov, br, s	0.850	C-H
2882.5	ov, br, s	0.548	C-H
3009.4	br, vw	0.950	O-H (COOH)

Barry M 117			
Average Peak Position	**Raman Signal Strength**	**Standard Deviation**	**Peak ID**
395.1	w	0.789	A
514.3	w	0.548	A
637.6	mw	0.789	A
1064.9	vw	0.548	BW
1125.8	vw	1.464	BW
1179.6	vw	0.844	

1228.2	vw	0.789	
1296.7	vw	0.837	BW
1334.9	vw	0.894	
1389.5	vw	0.950	
1440.6	vw	0.000	BW
1476.6	ov, br, vw	0.856	
1500.9	vw	0.894	
1597.7	w	0.000	
1656.0	vw	0.548	
2851.0	ov, br, w	0.402	C-H
2881.9	ov, br, w	0.837	C-H

Barry M 121			
Average Peak Position	**Raman Signal Strength**	**Standard Deviation**	**Peak ID**
251.9	br, vw	1.055	
331.7	vw	0.707	
363.9	br, vw	0.850	
421.8	br, vw	2.023	
495.4	vw	1.216	
516.7	vw	1.258	
596.3	vw	1.451	
744.4	vw	1.000	
961.0	br, vw	1.297	
1019.2	vw	1.184	
1040.0	vw	0.548	
1113.3	vw	0.548	
1130.6	vw	0.493	
1177.5	w	2.300	
1225.1	w	0.493	
1263.7	w	0.850	
1363.4	mw	0.707	
1493.2	mw	0.894	
1603.9	w	0.856	

Barry M 136			
Average Peak Position	**Raman Signal Strength**	**Standard Deviation**	**Peak ID**
226.6	vw	0.818	
293.5	vw	1.110	
395.7	m	0.548	A
446.9	sh, br, w	1.655	R
514.5	m	0.894	A
610.1	sh, mw	0.577	R
635.8	m	1.110	A
1063.5	vw	1.534	BW

1080.7	vw	0.500	
1126.4	vw	1.262	BW
1267.2	sh, br, vw	1.750	
1296.9	w	1.000	BW
1440.0	mw	1.297	BW
1455.8	sh, w	1.952	
1654.3	w	1.297	
2723.3	br, vw	0.500	O-H (COOH)
2852.0	ov, br, m	1.069	C-H
2882.1	ov, br, m	1.000	C-H
3009.1	br, vw	0.577	O-H (COOH)

Barry M 140			
Average Peak Position	**Raman Signal Strength**	**Standard Deviation**	**Peak ID**
396.3	m	0.707	A
514.7	m	0.837	A
638.1	ms	0.789	A
714.8	vw	0.577	
860.8	br, vw	1.445	
1064.3	w	1.588	BW
1084.4	w	1.451	
1130.5	vw	1.431	BW
1176.7	vw	0.520	
1266.4	sh, vw	1.484	
1299.4	w	1.474	BW
1441.0	mw	0.850	BW
1456.8	sh, mw	1.069	BW
1495.1	sh, br, vw	1.863	
1625.7	sh, br, vw	1.518	
1656.0	w	0.548	
1745.5	br, vw	1.877	
2724.6	br, vw	0.844	O-H (COOH)
2852.0	br, ov, ms	0.837	C-H
2883.3	br, ov, ms	0.789	C-H
3009.4	br, vw	0.950	O-H (COOH)

Barry M 145			
Average Peak Position	**Raman Signal Strength**	**Standard Deviation**	**Peak ID**
335.6	vw	0.000	D&C Red No.7 Ca lake
366.0	br, vw	0.894	D&C Red No.7 Ca lake
498.9	vw	0.894	D&C Red No.7 Ca lake
518.8	vw	1.184	D&C Red No.7 Ca lake
597.7	vw	1.041	
638.7	br, vw	0.548	

746.9	vw	0.548	D&C Red No.7 Ca lake
965.2	br, vw	0.000	D&C Red No.7 Ca lake
1022.1	vw	0.000	D&C Red No.7 Ca lake
1040.4	vw	0.000	D&C Red No.7 Ca lake
1129.1	br, vw	1.326	D&C Red No.7 Ca lake
1183.5	w	0.856	D&C Red No.7 Ca lake
1229.8	br, w	1.286	D&C Red No.7 Ca lake
1266.2	w	0.447	D&C Red No.7 Ca lake
1365.6	mw	0.402	D&C Red No.7 Ca lake
1411.0	br, vw	0.844	D&C Red No.7 Ca lake
1492.4	mw	0.402	D&C Red No.7 Ca lake
1604.5	w	0.672	D&C Red No.7 Ca lake

Barry M 146			
Average Peak Position	**Raman Signal Strength**	**Standard Deviation**	**Peak ID**
335.2	vw	0.894	D&C Red No.7 Ca lake
363.1	br, vw	0.493	D&C Red No.7 Ca lake
394.6	br, vw	0.402	
498.3	vw	0.447	D&C Red No.7 Ca lake
519.0	vw	0.402	D&C Red No.7 Ca lake
597.3	vw	0.850	
639.3	br, vw	0.000	
745.6	vw	0.402	D&C Red No.7 Ca lake
963.7	br, vw	0.493	D&C Red No.7 Ca lake
1021.1	vw	1.534	D&C Red No.7 Ca lake
1038.5	vw	0.672	D&C Red No.7 Ca lake
1130.1	br, vw	1.646	D&C Red No.7 Ca lake
1182.4	vw	0.402	D&C Red No.7 Ca lake
1227.9	br, vw	0.850	D&C Red No.7 Ca lake
1264.9	vw	0.801	D&C Red No.7 Ca lake
1294.2	vw	0.447	
1366.9	w	0.548	D&C Red No.7 Ca lake
1410.8	br, vw	1.258	D&C Red No.7 Ca lake
1489.7	w	0.000	D&C Red No.7 Ca lake
1549.9	br, vw	0.894	D&C Red No.7 Ca lake
1603.5	vw	0.000	D&C Red No.7 Ca lake

Bourjois 15			
Average Peak Position	**Raman Signal Strength**	**Standard Deviation**	**Peak ID**
336.2	vw	0.424	D&C Red No.7 Ca lake
362.6	br, vw	0.000	D&C Red No.7 Ca lake
455.1	vw	0.000	
498.1	vw	0.590	D&C Red No.7 Ca lake
520.1	br, vw	0.548	D&C Red No.7 Ca lake

598.2	br, vw	1.097	D&C Red No.7 Ca lake
746.2	vw	0.179	D&C Red No.7 Ca lake
965.2	br, vw	0.816	D&C Red No.7 Ca lake
1021.8	vw	0.577	D&C Red No.7 Ca lake
1037.2	vw	0.695	D&C Red No.7 Ca lake
1114.0	sh, br, vw	2.602	D&C Red No.7 Ca lake
1129.1	br, vw	0.776	D&C Red No.7 Ca lake
1182.4	w	0.402	D&C Red No.7 Ca lake
1228.2	br, w	0.402	D&C Red No.7 Ca lake
1265.5	w	0.464	D&C Red No.7 Ca lake
1366.1	mw	0.447	D&C Red No.7 Ca lake
1490.2	w	0.743	D&C Red No.7 Ca lake
1603.5	w	0.000	D&C Red No.7 Ca lake

Bourjois 16			
Average Peak Position	**Raman Signal Strength**	**Standard Deviation**	**Peak ID**
336.1	vw	0.455	D&C Red No.7 Ca lake
361.8	br, vw	1.502	D&C Red No.7 Ca lake
429.7	vw	0.520	D&C Red No.7 Ca lake
455.6	br, vw	0.950	
466.4	vw	1.155	
497.7	vw	0.756	D&C Red No.7 Ca lake
519.9	vw	0.826	D&C Red No.7 Ca lake
597.3	br, vw	1.092	D&C Red No.7 Ca lake
713.3	br, vw	0.906	D&C Red No.7 Ca lake
746.3	vw	0.881	D&C Red No.7 Ca lake
965.4	br, vw	1.055	D&C Red No.7 Ca lake
1020.0	vw	0.500	D&C Red No.7 Ca lake
1037.7	vw	0.737	D&C Red No.7 Ca lake
1113.7	sh, br, vw	1.000	D&C Red No.7 Ca lake
1128.2	br, vw	0.881	D&C Red No.7 Ca lake
1182.7	w	0.840	D&C Red No.7 Ca lake
1228.4	br, w	0.000	D&C Red No.7 Ca lake
1265.2	w	0.699	D&C Red No.7 Ca lake
1337.6	br, vw	0.844	D&C Red No.7 Ca lake
1365.9	mw	0.862	D&C Red No.7 Ca lake
1410.0	br, vw	0.957	D&C Red No.7 Ca lake
1490.7	mw	1.184	D&C Red No.7 Ca lake
1550.2	br, vw	1.155	D&C Red No.7 Ca lake
1603.5	w	0.000	D&C Red No.7 Ca lake

Bourjois 32			
Average Peak Position	**Raman Signal Strength**	**Standard Deviation**	**Peak ID**
336.2	vw	0.397	D&C Red No.7 Ca lake

362.3	br, vw	0.937	D&C Red No.7 Ca lake
430.7	vw	0.577	D&C Red No.7 Ca lake
455.3	vw	0.358	
482.5	vw	1.097	
498.3	vw	0.447	D&C Red No.7 Ca lake
519.8	vw	0.957	D&C Red No.7 Ca lake
598.3	br, vw	1.253	D&C Red No.7 Ca lake
700.5	vw	1.253	D&C Red No.7 Ca lake
714.3	vw	1.630	D&C Red No.7 Ca lake
746.5	vw	1.027	D&C Red No.7 Ca lake
966.0	br, vw	0.801	D&C Red No.7 Ca lake
1020.6	vw	0.493	D&C Red No.7 Ca lake
1037.5	vw	0.776	D&C Red No.7 Ca lake
1114.0	sh, br, vw	0.957	D&C Red No.7 Ca lake
1129.3	br, vw	1.262	D&C Red No.7 Ca lake
1183.1	w	0.672	D&C Red No.7 Ca lake
1228.3	br, w	1.258	D&C Red No.7 Ca lake
1265.3	w	0.402	D&C Red No.7 Ca lake
1324.9	sh, br, vw	0.000	D&C Red No.7 Ca lake
1337.9	br, vw	1.000	D&C Red No.7 Ca lake
1366.1	mw	0.447	D&C Red No.7 Ca lake
1410.5	br, vw	0.500	D&C Red No.7 Ca lake
1490.3	br, mw	0.548	D&C Red No.7 Ca lake
1550.5	br, vw	1.155	D&C Red No.7 Ca lake
1603.5	w	0.000	D&C Red No.7 Ca lake

Bourjois 54			
Average Peak Position	**Raman Signal Strength**	**Standard Deviation**	**Peak ID**
335.4	vw	0.492	D&C Red No.7 Ca lake
363.1	br, vw	0.520	D&C Red No.7 Ca lake
497.7	vw	1.041	D&C Red No.7 Ca lake
519.7	vw	0.950	D&C Red No.7 Ca lake
597.4	vw	0.520	D&C Red No.7 Ca lake
746.3	vw	0.672	D&C Red No.7 Ca lake
965.2	br, vw	0.707	D&C Red No.7 Ca lake
1020.7	vw	0.950	D&C Red No.7 Ca lake
1037.8	vw	0.914	D&C Red No.7 Ca lake
1114.1	sh, br, vw	0.894	D&C Red No.7 Ca lake
1130.1	br, vw	1.344	D&C Red No.7 Ca lake
1182.9	w	0.402	D&C Red No.7 Ca lake
1228.0	br, w	1.092	D&C Red No.7 Ca lake
1265.6	w	0.493	D&C Red No.7 Ca lake
1336.9	br, vw	0.577	D&C Red No.7 Ca lake
1365.8	w	1.092	D&C Red No.7 Ca lake
1410.9	br, vw	0.450	D&C Red No.7 Ca lake

1490.5	br, w	0.837	D&C Red No.7 Ca lake
1603.5	w	0.000	D&C Red No.7 Ca lake

Coty Mainz 070			
Average Peak Position	**Raman Signal Strength**	**Standard Deviation**	**Peak ID**
227.6	s	0.000	
241.8	mw	0.906	
293.6	s	0.577	
397.8	sh, mw	0.520	A
411.0	m	0.906	
514.2	br, mw	0.500	A
611.3	sh, mw	0.776	
637.1	m	0.914	A
1311.1	br, mw	1.450	
1446.2	br, mw	0.500	
2852.2	ov, br, m	0.000	C-H

La Femme 29			
Average Peak Position	**Raman Signal Strength**	**Standard Deviation**	**Peak ID**
226.9	sh, vw	0.577	
243.8	br, vw	0.447	
296.1	br, vw	1.900	
329.8	w	0.950	
356.0	vw	1.744	
416.5	vw	0.672	
439.9	vw	0.837	
475.2	sh, vw	1.069	
497.3	m	0.402	
525.7	vw	1.095	
565.0	vw	1.379	
602.1	sh, br, vw	3.619	
642.5	vw	1.290	
708.7	w	0.000	
743.6	vw	0.801	
796.3	vw	0.826	
819.9	br, vw	1.155	
887.7	br, vw	1.297	
968.1	mw	0.000	
1014.9	vw	0.520	
1037.5	vw	0.672	
1112.1	vw	0.844	
1132.2	vw	0.447	
1179.3	m	0.950	
1213.4	sh, mw	0.548	

1221.9	m	0.789	
1252.0	sh, mw	0.850	
1261.0	mw	1.739	
1316.6	vw	1.431	
1363.6	s	0.801	
1386.0	sh, w	0.548	
1449.4	sh, br, vw	1.446	
1490.9	ms	0.447	
1556.5	vw	0.789	
1603.3	m	0.402	
2850.7	ov, br, w	0.850	C-H
2881.5	ov, br, w	0.548	C-H

L'Oreal 164			
Average Peak Position	**Raman Signal Strength**	**Standard Deviation**	**Peak ID**
336.1	vw	0.493	D&C Red No.7 Ca lake
365.1	vw	1.992	D&C Red No.7 Ca lake
498.1	vw	0.850	D&C Red No.7 Ca lake
520.5	vw	0.447	D&C Red No.7 Ca lake
558.3	vw	1.000	D&C Red No.7 Ca lake
598.1	vw	1.445	D&C Red No.7 Ca lake
700.0	vw	0.950	D&C Red No.7 Ca lake
714.5	vw	1.367	D&C Red No.7 Ca lake
746.5	vw	0.447	D&C Red No.7 Ca lake
965.0	br, vw	1.270	D&C Red No.7 Ca lake
1021.4	vw	1.226	D&C Red No.7 Ca lake
1037.7	vw	0.801	D&C Red No.7 Ca lake
1117.1	sh, br, vw	1.240	D&C Red No.7 Ca lake
1129.1	br, vw	0.950	D&C Red No.7 Ca lake
1182.7	w	1.092	D&C Red No.7 Ca lake
1228.6	br, w	1.281	D&C Red No.7 Ca lake
1266.2	w	0.447	D&C Red No.7 Ca lake
1336.4	br, vw	0.776	D&C Red No.7 Ca lake
1366.1	mw	0.402	D&C Red No.7 Ca lake
1409.5	br, vw	0.500	D&C Red No.7 Ca lake
1490.9	mw	0.447	D&C Red No.7 Ca lake
1550.0	br, vw	1.000	D&C Red No.7 Ca lake
1602.7	w	1.041	D&C Red No.7 Ca lake

L'Oreal 345			
Average Peak Position	**Raman Signal Strength**	**Standard Deviation**	**Peak ID**
335.4	vw	0.447	D&C Red No.7 Ca lake
361.0	vw	1.484	D&C Red No.7 Ca lake
415.4	vw	0.447	D&C Red No.7 Ca lake

467.7	vw	0.672	D&C Red No.7 Ca lake
497.0	vw	0.850	D&C Red No.7 Ca lake
520.7	vw	0.707	D&C Red No.7 Ca lake
557.7	vw	0.856	D&C Red No.7 Ca lake
596.5	vw	0.548	D&C Red No.7 Ca lake
698.8	vw	0.577	D&C Red No.7 Ca lake
713.3	vw	0.906	D&C Red No.7 Ca lake
746.1	vw	0.402	D&C Red No.7 Ca lake
965.6	br, vw	0.894	D&C Red No.7 Ca lake
1019.0	vw	0.837	D&C Red No.7 Ca lake
1039.6	vw	0.801	D&C Red No.7 Ca lake
1117.1	sh, br, vw	0.950	D&C Red No.7 Ca lake
1129.5	br, vw	0.856	D&C Red No.7 Ca lake
1182.7	w	1.092	D&C Red No.7 Ca lake
1227.5	br, w	0.672	D&C Red No.7 Ca lake
1265.8	w	0.789	D&C Red No.7 Ca lake
1339.6	br, vw	0.577	D&C Red No.7 Ca lake
1366.9	mw	0.548	D&C Red No.7 Ca lake
1411.1	br, vw	0.950	D&C Red No.7 Ca lake
1491.8	mw	1.041	D&C Red No.7 Ca lake
1551.3	br, vw	1.446	D&C Red No.7 Ca lake
1603.5	w	0.672	D&C Red No.7 Ca lake
2851.6	ov, br, vw	0.856	C-H
2882.1	ov, br, vw	0.707	C-H

L'Oreal 524			
Average Peak Position	**Raman Signal Strength**	**Standard Deviation**	**Peak ID**
227.4	vw	0.447	
294.1	vw	0.000	
300.1	sh, vw	1.254	
336.0	vw	0.950	D&C Red No.7 Ca lake
498.5	vw	1.184	D&C Red No.7 Ca lake
518.8	br, vw	1.184	D&C Red No.7 Ca lake
638.1	br, vw	0.402	
746.7	vw	0.856	D&C Red No.7 Ca lake
968.6	br, vw	1.253	D&C Red No.7 Ca lake
1130.8	vw	0.789	D&C Red No.7 Ca lake
1182.7	br, vw	0.493	D&C Red No.7 Ca lake
1227.3	br, vw	1.564	D&C Red No.7 Ca lake
1266.0	vw	0.950	D&C Red No.7 Ca lake
1366.1	w	0.402	D&C Red No.7 Ca lake
1490.9	br, w	1.270	D&C Red No.7 Ca lake
1603.3	vw	1.055	D&C Red No.7 Ca lake

L'Oreal 900			
Average Peak Position	Raman Signal Strength	Standard Deviation	Peak ID
336.0	vw	0.550	D&C Red No.7 Ca lake
497.3	vw	0.789	D&C Red No.7 Ca lake
519.7	vw	0.950	D&C Red No.7 Ca lake
746.5	vw	1.027	D&C Red No.7 Ca lake
965.2	br, vw	0.816	D&C Red No.7 Ca lake
1037.2	vw	1.097	D&C Red No.7 Ca lake
1113.7	sh, br, vw	1.414	D&C Red No.7 Ca lake
1128.9	br, vw	1.055	D&C Red No.7 Ca lake
1182.9	w	0.753	D&C Red No.7 Ca lake
1228.0	br, w	0.493	D&C Red No.7 Ca lake
1266.0	w	0.000	D&C Red No.7 Ca lake
1365.9	mw	0.493	D&C Red No.7 Ca lake
1489.7	br, w	0.950	D&C Red No.7 Ca lake
1603.5	vw	0.000	D&C Red No.7 Ca lake

Prestige CL-78A			
Average Peak Position	Raman Signal Strength	Standard Deviation	Peak ID
225.9	mw	0.914	
242.3	w	0.500	
292.9	mw	1.212	
396.8	mw	0.577	A
513.5	mw	1.240	A
637.4	s	1.097	A
1305.9	br, w	1.097	
1366.3	vw	0.000	
1446.9	br, vw	0.520	
2854.1	ov, br, mw	0.000	C-H

Prestige CL-93A			
Average Peak Position	Raman Signal Strength	Standard Deviation	Peak ID
336.0	vw	0.950	D&C Red No.7 Ca lake
363.1	br, vw	0.520	D&C Red No.7 Ca lake
498.3	vw	0.957	D&C Red No.7 Ca lake
509.8	sh, vw	0.914	
519.8	vw	1.367	D&C Red No.7 Ca lake
699.7	vw	0.577	D&C Red No.7 Ca lake
713.2	vw	0.520	D&C Red No.7 Ca lake
746.1	vw	0.450	D&C Red No.7 Ca lake
965.0	br, vw	0.957	D&C Red No.7 Ca lake
1021.9	vw	0.500	D&C Red No.7 Ca lake
1038.7	vw	0.450	D&C Red No.7 Ca lake

1114.7	sh, br, vw	1.367	D&C Red No.7 Ca lake
1127.7	br, vw	0.577	D&C Red No.7 Ca lake
1182.9	w	0.450	D&C Red No.7 Ca lake
1228.7	br, w	1.801	D&C Red No.7 Ca lake
1265.3	w	0.450	D&C Red No.7 Ca lake
1294.5	br, vw	1.253	D&C Red No.7 Ca lake
1337.4	br, vw	1.155	D&C Red No.7 Ca lake
1367.1	mw	0.500	D&C Red No.7 Ca lake
1490.0	w	0.500	D&C Red No.7 Ca lake
1603.5	w	0.776	D&C Red No.7 Ca lake

Prestige PL-28A			
Average Peak Position	**Raman Signal Strength**	**Standard Deviation**	**Peak ID**
241.1	w	0.000	
324.7	sh, w	1.445	
336.1	w	0.520	
356.5	vw	1.226	
396.8	br, vw	0.577	
419.5	vw	1.097	
477.3	sh, vw	1.155	
497.3	m	0.450	
522.4	sh, br, vw	0.450	
563.9	vw	0.500	
596.2	vw	0.577	
639.5	br, w	1.212	
708.7	w	0.000	
743.7	vw	0.500	
796.3	br, vw	0.500	
960.4	sh, w	0.000	
969.1	w	0.000	
1014.9	vw	0.520	
1038.7	vw	0.450	
1112.7	vw	0.776	
1133.9	vw	0.000	
1180.0	mw	0.906	
1213.0	sh, w	0.816	
1222.9	mw	0.500	
1253.5	sh, w	1.367	
1264.9	w	0.500	
1317.9	br, vw	0.957	
1364.7	ms	0.500	
1386.1	sh, w	0.577	
1491.7	m	0.000	
1556.8	vw	0.520	
1603.8	mw	0.500	

2851.2	ov, br, vw	0.000	C-H
2882.6	ov, br, vw	0.707	C-H

Prestige PL-38A			
Average Peak Position	**Raman Signal Strength**	**Standard Deviation**	**Peak ID**
241.1	w	0.000	
294.6	vw	0.707	
396.1	br, w	1.845	A
514.9	br, vw	1.367	A
638.1	br, w	0.906	A
1061.6	vw	0.950	
1129.2	vw	1.344	
1295.7	br, vw	1.626	
1440.1	w	0.577	
1459.9	sh, br, vw	1.367	
2851.7	ov, br, mw	0.707	C-H
2882.1	ov, br, mw	0.000	C-H

Prestige PL-49A			
Average Peak Position	**Raman Signal Strength**	**Standard Deviation**	**Peak ID**
227.6	vw	0.776	
241.8	vw	0.906	
293.6	vw	1.000	
336.5	vw	0.000	D&C Red No.7 Ca lake
364.0	vw	0.950	D&C Red No.7 Ca lake
396.1	vw	1.212	A
498.5	vw	1.000	D&C Red No.7 Ca lake
519.5	br, vw	0.402	A, D&C Red No.7 Ca lake
635.9	br, vw	0.950	A
745.7	vw	0.844	D&C Red No.7 Ca lake
964.6	br, vw	0.548	D&C Red No.7 Ca lake
1021.1	vw	1.361	D&C Red No.7 Ca lake
1039.3	vw	1.041	D&C Red No.7 Ca lake
1128.7	sh, br, vw	1.092	D&C Red No.7 Ca lake
1182.9	w	0.402	D&C Red No.7 Ca lake
1228.6	br, w	0.801	D&C Red No.7 Ca lake
1265.8	w	0.402	D&C Red No.7 Ca lake
1366.9	mw	0.548	D&C Red No.7 Ca lake
1489.9	w	0.447	D&C Red No.7 Ca lake
1550.8	vw	1.155	D&C Red No.7 Ca lake
1602.9	vw	0.844	D&C Red No.7 Ca lake
2852.5	ov, br, vw	1.155	C-H

Revlon 004			
Average Peak Position	**Raman Signal Strength**	**Standard Deviation**	**Peak ID**
335.4	vw	1.069	D&C Red No.7 Ca lake
395.0	vw	1.471	A
498.3	vw	1.750	D&C Red No.7 Ca lake
517.4	vw	1.896	A, D&C Red No.7 Ca lake
637.0	br, vw	1.477	A
745.2	vw	1.069	D&C Red No.7 Ca lake
962.9	br, vw	1.297	D&C Red No.7 Ca lake
1038.3	vw	1.224	D&C Red No.7 Ca lake
1129.9	br, vw	2.182	D&C Red No.7 Ca lake
1182.1	vw	1.361	D&C Red No.7 Ca lake
1228.8	br, vw	1.110	D&C Red No.7 Ca lake
1265.6	vw	0.493	D&C Red No.7 Ca lake
1295.2	vw	0.906	
1367.1	w	0.801	D&C Red No.7 Ca lake
1491.3	w	1.471	D&C Red No.7 Ca lake
1602.0	vw	0.850	D&C Red No.7 Ca lake
2850.4	ov, br, vw	1.258	C-H
2882.3	ov, br, w	1.095	C-H

Revlon 005			
Average Peak Position	**Raman Signal Strength**	**Standard Deviation**	**Peak ID**
330.3	vw	0.850	D&C Red No.6 Ba lake
365.1	br, vw	1.473	D&C Red No.6 Ba lake
396.1	vw	0.500	A
423.9	vw	1.097	
494.1	vw	0.548	D&C Red No.6 Ba lake
515.3	w	0.548	A, D&C Red No.6 Ba lake
639.3	br, vw	0.707	A
744.0	w	0.894	D&C Red No.6 Ba lake
959.4	w	1.184	D&C Red No.6 Ba lake
1038.5	vw	0.000	D&C Red No.6 Ba lake
1114.0	vw	1.473	D&C Red No.6 Ba lake
1130.4	vw	0.844	D&C Red No.6 Ba lake
1172.9	w	1.312	D&C Red No.6 Ba lake
1224.2	w	0.548	D&C Red No.6 Ba lake
1233.3	sh, vw	0.045	
1261.8	vw	1.075	D&C Red No.6 Ba lake
1363.8	mw	0.548	D&C Red No.6 Ba lake
1374.2	sh, w	1.069	D&C Red No.6 Ba lake
1493.2	mw	0.548	D&C Red No.6 Ba lake
1547.9	vw	0.577	D&C Red No.6 Ba lake
1603.7	w	0.447	D&C Red No.6 Ba lake

2851.4	ov, br, vw	1.446	C-H
2882.1	ov, br, vw	0.816	C-H

Revlon 006			
Average Peak Position	**Raman Signal Strength**	**Standard Deviation**	**Peak ID**
252.4	br, vw	1.254	
293.9	br, vw	1.262	
336.5	vw	0.000	D&C Red No.7 Ca lake
362.7	br, vw	1.258	D&C Red No.7 Ca lake
420.6	br, vw	1.095	
498.5	vw	0.000	D&C Red No.7 Ca lake
518.7	vw	0.950	D&C Red No.7 Ca lake
561.2	vw	0.950	D&C Red No.7 Ca lake
598.0	vw	0.801	D&C Red No.7 Ca lake
700.0	vw	0.000	D&C Red No.7 Ca lake
714.7	vw	0.447	D&C Red No.7 Ca lake
745.8	vw	0.493	D&C Red No.7 Ca lake
963.7	br, vw	1.092	D&C Red No.7 Ca lake
1021.9	vw	0.447	D&C Red No.7 Ca lake
1038.5	vw	0.045	D&C Red No.7 Ca lake
1129.5	br, vw	0.856	D&C Red No.7 Ca lake
1182.6	w	0.493	D&C Red No.7 Ca lake
1227.5	w	1.184	D&C Red No.7 Ca lake
1265.5	w	0.493	D&C Red No.7 Ca lake
1339.3	br, vw	0.000	D&C Red No.7 Ca lake
1367.1	mw	0.447	D&C Red No.7 Ca lake
1412.6	br, vw	0.000	D&C Red No.7 Ca lake
1491.1	mw	0.548	D&C Red No.7 Ca lake
1551.8	br, vw	0.844	D&C Red No.7 Ca lake
1602.0	w	0.850	D&C Red No.7 Ca lake

Revlon 07			
Average Peak Position	**Raman Signal Strength**	**Standard Deviation**	**Peak ID**
227.0	ms	0.850	
246.3	sh, vw	0.493	
293.5	s	0.894	
397.8	sh, mw	0.493	A
410.4	m	1.110	
501.2	sh, w	0.447	
513.7	w	1.739	A
613.3	sh, mw	0.950	
637.4	m	1.184	A
1172.7	mw	0.837	
1204.9	vw	1.105	

1250.8	sh, br, vw	1.095	
1267.4	sh, br, w	1.464	
1314.9	br, mw	1.290	
1424.9	sh, vw	0.789	
1447.9	br, w	1.593	
1577.3	sh, vw	1.583	
1605.4	m	0.672	
1635.9	mw	0.548	
1713.7	br, vw	0.500	
2853.0	br, ov, w	1.443	C-H
2880.7	br, ov, w	2.023	C-H

Revlon 008			
Average Peak Position	**Raman Signal Strength**	**Standard Deviation**	**Peak ID**
227.6	m	0.000	
247.4	sh, vw	0.548	
294.5	m	0.894	
397.9	sh, w	1.471	A
411.7	mw	0.950	
501.2	sh, vw	1.270	
513.9	br, w	1.379	A
613.3	sh, w	1.184	
638.7	mw	0.856	A
746.7	vw	1.075	
1318.5	br, w	0.850	
1454.1	br, ov, vw	0.672	
1599.7	vw	0.776	
2852.6	br, ov, vw	1.885	C-H
2882.7	br, ov, vw	0.894	C-H

Revlon 009			
Average Peak Position	**Raman Signal Strength**	**Standard Deviation**	**Peak ID**
251.1	vw	0.894	
293.9	vw	0.837	
336.3	vw	0.402	D&C Red No.7 Ca lake
497.9	vw	0.894	D&C Red No.7 Ca lake
518.8	vw	0.950	D&C Red No.7 Ca lake
597.8	vw	0.000	D&C Red No.7 Ca lake
638.3	br, vw	0.950	
745.6	vw	0.402	D&C Red No.7 Ca lake
964.4	br, vw	0.447	D&C Red No.7 Ca lake
1022.3	vw	0.447	D&C Red No.7 Ca lake
1038.3	vw	0.447	D&C Red No.7 Ca lake
1129.1	br, vw	0.672	D&C Red No.7 Ca lake

1182.9	vw	0.402	D&C Red No.7 Ca lake
1227.7	br, vw	0.402	D&C Red No.7 Ca lake
1265.6	vw	0.493	D&C Red No.7 Ca lake
1366.7	w	0.548	D&C Red No.7 Ca lake
1490.9	w	1.095	D&C Red No.7 Ca lake
1601.6	vw	1.184	D&C Red No.7 Ca lake

Revlon 020			
Average Peak Position	**Raman Signal Strength**	**Standard Deviation**	**Peak ID**
334.2	vw	0.548	
364.1	sh, vw	0.548	
394.4	br, w	0.000	A
496.8	sh, vw	0.402	
517.0	w	0.801	A
637.0	w	0.856	A
745.4	vw	0.000	
961.7	br, vw	1.297	
1038.5	vw	0.000	
1062.2	vw	0.856	BW
1118.9	sh, vw	0.548	
1130.5	br, vw	0.493	BW
1181.2	w	1.000	
1226.3	w	1.095	
1264.9	w	0.447	
1297.1	vw	0.837	BW
1305.4	sh, vw	0.801	
1365.9	mw	0.522	
1441.5	w	0.000	BW
1460.2	sh, vw	0.548	BW
1490.9	mw	1.055	
1603.1	w	0.493	
2850.5	ov, br, mw	0.402	C-H
2881.1	ov, br, mw	0.000	C-H

Revlon 025			
Average Peak Position	**Raman Signal Strength**	**Standard Deviation**	**Peak ID**
254.6	br, vw	0.672	
334.6	vw	0.045	D&C Red No.7 Ca lake
369.5	br, vw	1.262	
396.3	br, vw	0.000	A
468.4	vw	0.906	D&C Red No.7 Ca lake
498.5	w	0.000	D&C Red No.7 Ca lake
519.5	w	0.789	A, D&C Red No.7 Ca lake
597.8	vw	0.950	D&C Red No.7 Ca lake

638.3	br, vw	0.950	A
747.1	vw	0.447	D&C Red No.7 Ca lake
963.8	br, vw	0.493	D&C Red No.7 Ca lake
1019.0	vw	0.500	D&C Red No.7 Ca lake
1040.4	vw	0.000	D&C Red No.7 Ca lake
1119.5	sh, vw	0.000	D&C Red No.7 Ca lake
1130.1	br, vw	0.000	BW, D&C Red No.7 Ca lake
1182.9	w	0.402	D&C Red No.7 Ca lake
1226.5	br, w	1.000	D&C Red No.7 Ca lake
1234.2	sh, vw	0.672	
1266.2	w	0.447	D&C Red No.7 Ca lake
1296.9	vw	0.707	BW
1367.3	mw	0.000	D&C Red No.7 Ca lake
1410.4	br, vw	0.486	D&C Red No.7 Ca lake
1441.5	br, vw	0.000	BW
1467.6	br, vw	0.045	
1491.1	mw	0.548	D&C Red No.7 Ca lake
1551.5	vw	0.000	D&C Red No.7 Ca lake
1604.1	w	0.548	D&C Red No.7 Ca lake
2851.4	br, ov, vw	0.801	C-H
2882.3	br, ov, vw	0.447	C-H

Revlon 030			
Average Peak Position	**Raman Signal Strength**	**Standard Deviation**	**Peak ID**
255.4	br, vw	1.258	
298.9	br, vw	0.000	
335.2	vw	0.856	D&C Red No.7 Ca lake
370.3	vw	0.000	
468.4	vw	0.789	D&C Red No.7 Ca lake
498.5	vw	1.184	D&C Red No.7 Ca lake
519.4	vw	0.844	D&C Red No.7 Ca lake
558.5	vw	1.219	D&C Red No.7 Ca lake
596.3	br, vw	0.894	D&C Red No.7 Ca lake
638.9	br, vw	0.548	
746.5	vw	1.027	D&C Red No.7 Ca lake
964.4	br, vw	1.069	D&C Red No.7 Ca lake
1018.7	vw	1.253	D&C Red No.7 Ca lake
1040.4	vw	0.000	D&C Red No.7 Ca lake
1118.7	sh, vw	1.270	D&C Red No.7 Ca lake
1130.3	vw	1.055	D&C Red No.7 Ca lake
1182.2	w	1.361	D&C Red No.7 Ca lake
1226.9	br, w	1.464	D&C Red No.7 Ca lake
1266.0	w	0.950	D&C Red No.7 Ca lake
1296.4	br, vw	0.577	BW
1366.7	mw	1.075	D&C Red No.7 Ca lake

1410.9	br, vw	1.212	D&C Red No.7 Ca lake
1467.6	sh, vw	0.000	
1491.5	mw	0.801	D&C Red No.7 Ca lake
1552.0	br, vw	0.950	D&C Red No.7 Ca lake
1603.5	w	1.143	D&C Red No.7 Ca lake

Revlon 035			
Average Peak Position	**Raman Signal Strength**	**Standard Deviation**	**Peak ID**
251.9	br, vw	1.055	
295.1	vw	0.000	
335.0	vw	0.850	D&C Red No.7 Ca lake
395.7	br, vw	1.097	A
498.9	vw	1.297	D&C Red No.7 Ca lake
518.6	vw	0.447	A, D&C Red No.7 Ca lake
597.1	sh, vw	0.450	D&C Red No.7 Ca lake
638.1	w	1.254	A
746.7	vw	1.075	D&C Red No.7 Ca lake
964.4	br, vw	0.801	D&C Red No.7 Ca lake
1130.1	br, vw	0.000	D&C Red No.7 Ca lake
1181.8	w	1.593	D&C Red No.7 Ca lake
1228.8	br, w	0.894	D&C Red No.7 Ca lake
1266.4	w	0.548	D&C Red No.7 Ca lake
1300.4	br, sh, vw	1.593	
1367.3	mw	0.000	D&C Red No.7 Ca lake
1443.5	br, sh, vw	0.000	
1465.9	br, sh, vw	1.445	
1490.9	mw	0.447	D&C Red No.7 Ca lake
1603.2	w	1.252	D&C Red No.7 Ca lake
2852.2	br, ov, w	1.000	C-H
2882.7	br, ov, w	0.548	C-H

Revlon 045			
Average Peak Position	**Raman Signal Strength**	**Standard Deviation**	**Peak ID**
255.9	br, vw	1.290	
335.6	vw	0.950	D&C Red No.7 Ca lake
468.8	vw	0.801	D&C Red No.7 Ca lake
498.7	vw	0.447	D&C Red No.7 Ca lake
518.8	vw	0.950	D&C Red No.7 Ca lake
557.1	vw	1.212	D&C Red No.7 Ca lake
596.7	vw	0.801	D&C Red No.7 Ca lake
640.1	br, vw	1.041	
745.6	vw	0.402	D&C Red No.7 Ca lake
964.0	br, vw	0.789	D&C Red No.7 Ca lake
1018.7	vw	1.000	D&C Red No.7 Ca lake

1040.0	vw	0.850	D&C Red No.7 Ca lake
1127.8	br, vw	0.548	D&C Red No.7 Ca lake
1182.5	w	0.844	D&C Red No.7 Ca lake
1227.5	br, w	0.672	D&C Red No.7 Ca lake
1265.6	w	0.493	D&C Red No.7 Ca lake
1338.0	vw	1.097	D&C Red No.7 Ca lake
1367.3	mw	0.000	D&C Red No.7 Ca lake
1411.4	vw	0.402	D&C Red No.7 Ca lake
1491.5	mw	1.041	D&C Red No.7 Ca lake
1551.1	vw	0.548	D&C Red No.7 Ca lake
1603.1	w	0.493	D&C Red No.7 Ca lake
2850.7	br, ov, vw	0.493	C-H
2880.6	br, ov, vw	0.493	C-H

Revlon 46			
Average Peak Position	**Raman Signal Strength**	**Standard Deviation**	**Peak ID**
257.3	br, vw	0.447	
335.2	vw	0.856	D&C Red No.7 Ca lake
467.9	vw	1.055	D&C Red No.7 Ca lake
498.3	vw	0.447	D&C Red No.7 Ca lake
519.3	vw	0.850	D&C Red No.7 Ca lake
596.9	vw	0.000	D&C Red No.7 Ca lake
640.5	br, vw	0.906	
701.8	br, vw	0.500	D&C Red No.7 Ca lake
746.7	vw	0.548	D&C Red No.7 Ca lake
964.4	br, vw	0.801	D&C Red No.7 Ca lake
1020.0	vw	0.500	D&C Red No.7 Ca lake
1040.2	vw	0.447	D&C Red No.7 Ca lake
1129.3	br, vw	0.801	D&C Red No.7 Ca lake
1182.6	w	0.493	D&C Red No.7 Ca lake
1227.7	br, w	0.402	D&C Red No.7 Ca lake
1266.0	w	0.950	D&C Red No.7 Ca lake
1339.8	br, vw	0.577	D&C Red No.7 Ca lake
1367.3	mw	0.000	D&C Red No.7 Ca lake
1410.7	br, vw	0.776	D&C Red No.7 Ca lake
1492.2	mw	0.493	D&C Red No.7 Ca lake
1551.8	br, vw	0.844	D&C Red No.7 Ca lake
1603.3	w	0.402	D&C Red No.7 Ca lake
2851.2	br, ov, vw	0.950	C-H
2881.3	br, ov, vw	0.801	C-H

Revlon 075			
Average Peak Position	**Raman Signal Strength**	**Standard Deviation**	**Peak ID**
227.1	vw	0.577	
295.3	vw	0.789	
334.2	vw	0.548	
395.3	w	0.950	A
412.1	sh, vw	0.856	
498.9	sh, vw	0.548	
517.6	w	0.447	A
597.4	sh, vw	0.950	
637.6	mw	0.402	A
745.9	vw	1.092	
964.0	br, vw	0.789	
1039.7	vw	0.577	
1128.7	br, vw	1.092	
1181.6	w	0.894	
1229.0	br, w	1.105	
1265.8	w	0.789	
1366.9	mw	0.548	
1491.3	mw	0.856	
1550.9	vw	0.548	
1602.8	w	0.402	
2851.6	br, ov, vw	1.110	C-H
2881.5	br, ov, w	0.548	C-H

Revlon 080			
Average Peak Position	**Raman Signal Strength**	**Standard Deviation**	**Peak ID**
250.9	br, vw	1.416	
293.3	br, vw	1.069	
329.4	vw	0.856	D&C Red No.6 Ba lake
362.4	br, vw	0.801	D&C Red No.6 Ba lake
469.6	vw	0.672	
494.3	vw	0.856	D&C Red No.6 Ba lake
515.9	vw	0.000	D&C Red No.6 Ba lake
596.1	br, vw	1.416	
702.0	br, vw	0.672	D&C Red No.6 Ba lake
744.0	w	0.850	D&C Red No.6 Ba lake
887.1	vw	0.000	D&C Red No.6 Ba lake
959.0	w	0.548	D&C Red No.6 Ba lake
1015.0	vw	0.844	D&C Red No.6 Ba lake
1038.5	vw	0.000	D&C Red No.6 Ba lake
1111.6	vw	0.801	D&C Red No.6 Ba lake
1130.5	vw	1.092	D&C Red No.6 Ba lake
1155.7	sh, vw	1.092	D&C Red No.6 Ba lake

1171.7	w	0.447	D&C Red No.6 Ba lake
1223.6	w	0.000	D&C Red No.6 Ba lake
1260.7	w	0.850	D&C Red No.6 Ba lake
1322.9	br, vw	0.000	D&C Red No.6 Ba lake
1363.6	mw	0.447	D&C Red No.6 Ba lake
1376.0	sh, w	0.000	D&C Red No.6 Ba lake
1450.2	br, vw	0.000	D&C Red No.6 Ba lake
1468.9	br, vw	0.856	
1494.2	mw	0.856	D&C Red No.6 Ba lake
1554.5	br, vw	0.447	
1604.7	w	0.402	D&C Red No.6 Ba lake
2850.8	br, ov, vw	1.092	C-H
2881.7	br, ov, vw	0.850	C-H

Revlon 090			
Average Peak Position	**Raman Signal Strength**	**Standard Deviation**	**Peak ID**
251.9	br, vw	1.659	
294.6	br, vw	1.000	
332.1	vw	0.894	
366.9	br, vw	1.253	
468.3	vw	1.097	
495.8	vw	0.447	
519.6	vw	1.041	
595.9	br, vw	0.000	
745.0	vw	0.548	
961.9	br, vw	0.894	
1017.0	vw	0.914	
1040.0	vw	0.850	
1113.4	sh, br, vw	1.450	
1129.9	br, vw	0.447	
1179.6	w	0.844	
1224.8	w	0.789	
1265.1	w	1.184	
1365.6	mw	0.402	
1468.8	sh, vw	0.914	
1492.1	mw	0.493	
1552.0	br, vw	0.950	
1603.0	w	0.493	

Revlon 095			
Average Peak Position	**Raman Signal Strength**	**Standard Deviation**	**Peak ID**
226.8	vw	0.837	
252.1	br, vw	0.493	
292.9	vw	0.402	

334.6	vw	0.707	D&C Red No.7 Ca lake
365.8	br, vw	0.894	D&C Red No.7 Ca lake
414.4	vw	1.254	D&C Red No.7 Ca lake
468.0	vw	0.513	D&C Red No.7 Ca lake
498.5	vw	0.000	D&C Red No.7 Ca lake
519.2	vw	0.493	D&C Red No.7 Ca lake
597.3	vw	0.493	D&C Red No.7 Ca lake
746.5	vw	0.447	D&C Red No.7 Ca lake
964.2	br, vw	0.672	D&C Red No.7 Ca lake
1018.6	vw	1.484	D&C Red No.7 Ca lake
1040.6	vw	0.447	D&C Red No.7 Ca lake
1117.3	sh, vw	0.402	D&C Red No.7 Ca lake
1129.9	br, vw	0.447	D&C Red No.7 Ca lake
1183.1	w	0.000	D&C Red No.7 Ca lake
1227.8	br, w	1.297	D&C Red No.7 Ca lake
1266.2	w	0.447	D&C Red No.7 Ca lake
1367.3	mw	0.000	D&C Red No.7 Ca lake
1468.9	br, vw	0.856	
1491.3	mw	0.856	D&C Red No.7 Ca lake
1551.3	br, vw	0.447	D&C Red No.7 Ca lake
1602.8	w	0.402	D&C Red No.7 Ca lake

Revlon 103			
Average Peak Position	**Raman Signal Strength**	**Standard Deviation**	**Peak ID**
226.4	ms	0.447	
245.5	vw	1.097	
292.9	ms	0.402	
396.3	sh, w	1.000	A
410.6	mw	0.447	
497.9	w	0.548	
515.1	w	1.095	A
612.1	w	0.447	
637.4	w	2.589	A
745.1	vw	0.577	
1129.2	br, vw	1.097	
1182.2	w	0.672	
1228.2	br, w	0.789	
1266.0	w	0.776	
1306.7	br, w	1.258	
1365.4	mw	0.000	
1449.4	br, w	1.592	
1491.5	mw	1.069	
1601.6	w	0.000	
2852.6	br, ov, m	1.312	C-H
2882.9	br, ov, m	1.069	C-H

Revlon 353			
Average Peak Position	**Raman Signal Strength**	**Standard Deviation**	**Peak ID**
227.6	s	0.000	
246.6	vw	0.789	
293.9	s	0.837	
398.2	sh, w	0.776	A
411.0	m	0.402	
498.7	sh, w	1.461	
514.9	br, w	1.000	A
612.7	mw	0.548	
639.7	mw	1.105	A
718.8	br, vw	1.092	
1063.9	sh, br, vw	1.110	
1079.4	sh, br, vw	1.092	
1131.0	vw	0.950	
1309.0	br, mw	0.850	
1440.6	mw	0.672	
1457.2	sh, mw	0.789	
2721.1	br, vw	1.534	
2852.6	ov, br, ms	0.548	C-H
2882.9	ov, br, ms	0.447	C-H

Revlon 359			
Average Peak Position	**Raman Signal Strength**	**Standard Deviation**	**Peak ID**
226.7	s	0.045	
245.7	vw	1.041	
293.1	s	0.000	
398.0	sh, mw	1.254	A
410.4	m	0.548	
494.9	sh, w	0.789	
514.5	mw	0.894	A
613.1	sh, mw	0.801	A
637.6	m	1.055	
742.9	vw	0.850	
958.1	vw	0.844	
1129.1	vw	1.184	
1173.7	w	1.601	
1224.9	w	0.844	
1263.5	sh, vw	1.471	
1314.1	sh, br, w	0.447	
1362.1	mw	1.110	
1440.8	sh, br, w	0.402	
1495.4	mw	1.258	

1600.3	mw	0.844	
2851.4	ov, br, m	1.069	C-H
2882.7	ov, br, m	0.548	C-H

Revlon 371			
Average Peak Position	**Raman Signal Strength**	**Standard Deviation**	**Peak ID**
331.7	vw	0.707	
370.9	br, vw	1.473	
421.7	vw	0.520	
495.8	vw	1.534	
517.0	w	1.258	
600.5	br, vw	2.268	
640.9	br, vw	0.520	
746.3	w	0.950	
960.6	w	1.254	
989.3	sh, vw	0.000	
1038.7	vw	0.906	
1115.2	vw	0.520	
1132.0	vw	1.000	
1175.6	w	1.270	
1227.5	mw	0.000	
1264.5	vw	1.312	
1365.2	mw	1.069	
1378.1	sh, w	1.095	
1495.5	mw	1.791	
1602.4	mw	1.592	
2853.6	ov, br, vw	0.850	C-H
2883.1	ov, br, vw	1.184	C-H

Revlon 430			
Average Peak Position	**Raman Signal Strength**	**Standard Deviation**	**Peak ID**
253.8	br, vw	0.837	
335.8	vw	0.789	D&C Red No.7 Ca lake
362.6	br, vw	0.000	D&C Red No.7 Ca lake
421.2	br, vw	1.262	
498.5	vw	0.000	D&C Red No.7 Ca lake
519.5	vw	0.789	D&C Red No.7 Ca lake
598.2	vw	0.548	D&C Red No.7 Ca lake
639.3	br, vw	0.000	
700.3	vw	0.500	D&C Red No.7 Ca lake
713.9	vw	0.548	D&C Red No.7 Ca lake
745.9	vw	0.493	D&C Red No.7 Ca lake
963.1	br, vw	0.801	D&C Red No.7 Ca lake
1021.3	vw	1.041	D&C Red No.7 Ca lake

1038.9	vw	0.493	D&C Red No.7 Ca lake
1130.7	br, vw	0.844	D&C Red No.7 Ca lake
1182.7	w	0.493	D&C Red No.7 Ca lake
1227.9	br, w	0.850	D&C Red No.7 Ca lake
1266.0	w	0.000	D&C Red No.7 Ca lake
1296.2	br, vw	0.500	
1338.6	br, vw	0.402	D&C Red No.7 Ca lake
1367.1	mw	0.447	D&C Red No.7 Ca lake
1492.6	mw	0.000	D&C Red No.7 Ca lake
1552.4	br, vw	0.000	D&C Red No.7 Ca lake
1602.4	w	1.041	D&C Red No.7 Ca lake
2851.6	ov, br, vw	1.638	C-H
2881.9	ov, br, vw	0.837	C-H

Revlon 450			
Average Peak Position	**Raman Signal Strength**	**Standard Deviation**	**Peak ID**
251.7	br, vw	1.367	
335.2	vw	0.548	D&C Red No.7 Ca lake
364.3	sh, br, vw	1.041	D&C Red No.7 Ca lake
395.3	vw	0.950	A
498.1	sh, vw	0.548	D&C Red No.7 Ca lake
517.2	w	1.110	A, D&C Red No.7 Ca lake
597.6	sh, vw	0.906	D&C Red No.7 Ca lake
638.3	br, w	0.950	A
701.0	vw	1.000	D&C Red No.7 Ca lake
714.3	vw	1.212	D&C Red No.7 Ca lake
745.6	vw	0.402	D&C Red No.7 Ca lake
962.5	br, vw	0.447	D&C Red No.7 Ca lake
1021.5	vw	0.856	D&C Red No.7 Ca lake
1038.3	vw	0.801	D&C Red No.7 Ca lake
1130.3	br, vw	1.055	D&C Red No.7 Ca lake
1181.6	w	1.312	D&C Red No.7 Ca lake
1226.7	br, w	0.837	D&C Red No.7 Ca lake
1265.3	w	0.402	D&C Red No.7 Ca lake
1365.8	mw	0.493	D&C Red No.7 Ca lake
1492.4	mw	0.402	D&C Red No.7 Ca lake
1550.0	br, vw	0.577	D&C Red No.7 Ca lake
1602.4	w	1.041	D&C Red No.7 Ca lake
2852.0	ov, br, vw	1.270	C-H
2882.5	ov, br, vw	0.548	C-H

Revlon 455			
Average Peak Position	**Raman Signal Strength**	**Standard Deviation**	**Peak ID**
396.3	w	1.000	A
514.3	w	0.548	A
637.6	mw	1.254	A
717.4	br, vw	1.689	
1063.3	vw	0.789	BW
1081.1	vw	1.966	
1131.0	vw	0.950	BW
1169.3	vw	0.520	
1296.7	w	1.027	BW, D&C Red No.28
1351.1	br, vw	1.416	D&C Red No.28
1439.2	mw	1.105	BW
1458.3	sh, w	1.075	
1624.1	vw	1.471	D&C Red No.28
2720.6	br, vw	1.684	
2851.0	ov, br, m	0.402	C-H
2881.9	ov, br, m	0.447	C-H

Revlon 675			
Average Peak Position	**Raman Signal Strength**	**Standard Deviation**	**Peak ID**
251.3	br, vw	0.548	
335.6	vw	0.672	D&C Red No.7 Ca lake
363.0	br, vw	0.850	D&C Red No.7 Ca lake
422.0	br, vw	1.290	
498.1	vw	0.548	D&C Red No.7 Ca lake
519.2	vw	0.850	D&C Red No.7 Ca lake
598.2	vw	0.548	D&C Red No.7 Ca lake
636.6	br, vw	0.837	
701.0	vw	0.000	D&C Red No.7 Ca lake
713.9	vw	0.894	D&C Red No.7 Ca lake
745.6	vw	0.402	D&C Red No.7 Ca lake
963.3	br, vw	0.000	D&C Red No.7 Ca lake
1021.3	vw	1.041	D&C Red No.7 Ca lake
1037.9	vw	0.817	D&C Red No.7 Ca lake
1129.7	br, vw	0.548	D&C Red No.7 Ca lake
1182.6	w	0.493	D&C Red No.7 Ca lake
1228.0	br, w	0.493	D&C Red No.7 Ca lake
1265.3	w	0.402	D&C Red No.7 Ca lake
1291.5	br, vw	0.850	
1338.2	br, vw	1.258	D&C Red No.7 Ca lake
1366.7	mw	0.548	D&C Red No.7 Ca lake
1409.5	br, vw	1.095	D&C Red No.7 Ca lake
1490.5	mw	1.095	D&C Red No.7 Ca lake

1551.6	vw	1.258	D&C Red No.7 Ca lake
1602.0	w	0.850	D&C Red No.7 Ca lake

Revlon 750			
Average Peak Position	**Raman Signal Strength**	**Standard Deviation**	**Peak ID**
330.3	vw	0.850	D&C Red No.6 Ba lake
364.7	br, vw	1.445	D&C Red No.6 Ba lake
395.0	vw	0.844	A
493.7	vw	0.707	D&C Red No.6 Ba lake
514.9	vw	1.000	A, D&C Red No.6 Ba lake
639.3	br, vw	1.344	A
701.3	vw	0.957	D&C Red No.6 Ba lake
743.6	vw	0.447	D&C Red No.6 Ba lake
957.9	vw	0.850	D&C Red No.6 Ba lake
1037.8	vw	0.914	D&C Red No.6 Ba lake
1112.7	vw	0.672	D&C Red No.6 Ba lake
1130.7	vw	0.844	D&C Red No.6 Ba lake
1172.7	w	0.837	D&C Red No.6 Ba lake
1224.2	w	0.856	D&C Red No.6 Ba lake
1260.7	vw	0.850	D&C Red No.6 Ba lake
1363.2	mw	0.402	D&C Red No.6 Ba lake
1375.4	sh, w	1.312	D&C Red No.6 Ba lake
1447.3	br, vw	0.950	D&C Red No.6 Ba lake
1494.2	mw	0.894	D&C Red No.6 Ba lake
1548.6	vw	0.776	D&C Red No.6 Ba lake
1603.3	w	1.055	D&C Red No.6 Ba lake
2851.6	ov, br, vw	0.894	C-H
2882.5	ov, br, vw	0.856	C-H

UNE L02			
Average Peak Position	**Raman Signal Strength**	**Standard Deviation**	**Peak ID**
227.6	m	0.000	
246.8	vw	0.000	
294.9	ms	0.447	
396.9	sh, m	0.548	A
410.8	m	1.184	
498.5	sh, mw	0.000	
515.7	mw	0.447	A
614.0	sh, mw	0.789	
638.5	ms	0.801	A
1063.5	ov, br, vw	0.950	
1080.9	ov, br, vw	1.900	
1120.8	ov, br, vw	1.290	
1269.5	br, sh, vw	1.635	

1310.2	br, w	2.090	
1441.5	w	0.000	
1458.5	sh, w	1.260	
1655.6	br, vw	0.707	
1747.0	br, vw	1.095	
2728.4	br, vw	1.105	O-H (COOH)
2852.8	ov, br, mw	1.290	C-H
2882.9	ov, br, mw	1.041	C-H

UNE L05			
Average Peak Position	**Raman Signal Strength**	**Standard Deviation**	**Peak ID**
227.8	ms	0.402	
246.8	vw	0.000	
294.9	s	0.447	
398.2	sh, mw	0.976	A
412.3	m	0.548	
446.0	sh, vw	0.636	R
500.2	sh, w	0.789	
514.5	w	0.894	A
613.9	sh, mw	1.290	R
638.1	ms	0.789	A
1063.7	ov, br, vw	1.564	
1082.1	ov, br, vw	1.440	
1118.9	ov, br, vw	1.635	
1271.2	br, sh, w	1.290	
1312.9	br, mw	1.474	
1440.9	w	1.290	
1459.1	sh, w	1.216	
1656.4	vw	1.041	
1745.8	br, vw	2.109	
2728.2	br, vw	1.075	O-H (COOH)
2853.4	ov, br, mw	0.789	C-H
2883.5	ov, br, mw	1.092	C-H

UNE L07			
Average Peak Position	**Raman Signal Strength**	**Standard Deviation**	**Peak ID**
226.4	ms	0.447	
245.3	vw	1.062	
293.1	s	0.000	
397.1	sh, m	1.262	A
410.0	m	0.447	
499.5	sh, w	0.950	
513.2	mw	0.416	A
612.3	sh, mw	0.707	

636.4	ms	0.707	A
1064.3	br, ov, vw	1.212	
1081.7	br, ov, vw	1.981	
1119.0	br, ov, vw	2.002	
1270.1	sh, br, vw	1.416	
1311.6	br, mw	3.143	
1440.0	w	1.105	
1456.7	sh, w	1.226	
1655.1	vw	1.253	
1746.5	br, vw	1.981	
2853.4	ov, br, mw	0.402	C-H

UNE L09			
Average Peak Position	**Raman Signal Strength**	**Standard Deviation**	**Peak ID**
226.6	ms	0.000	
245.7	vw	0.447	
293.3	s	0.447	
395.9	sh, w	0.894	A
411.4	m	0.844	
499.1	sh, vw	1.290	
512.6	sh, vw	1.290	A
612.5	mw	0.447	
637.6	w	0.789	A
1063.4	ov, br, vw	1.699	
1080.5	ov, br, vw	1.286	
1119.9	ov, br, vw	1.626	
1277.4	sh, br, vw	1.270	
1311.6	br, w	0.789	
1440.6	w	0.950	
1453.7	sh, vw	1.638	
1655.4	vw	1.416	
1745.8	br, vw	0.520	
2728.1	br, vw	0.500	O-H (COOH)
2852.2	ov, br, mw	0.707	C-H

UNE S03			
Average Peak Position	**Raman Signal Strength**	**Standard Deviation**	**Peak ID**
227.4	mw	0.447	
246.6	vw	0.402	
294.1	mw	0.000	
397.3	sh, w	0.672	A
411.0	mw	0.814	
500.5	sh, vw	0.883	
513.9	w	0.950	A

612.7	sh, w	0.894	
638.3	mw	0.672	A
1063.1	ov, br, vw	0.493	
1083.0	ov, br, vw	1.041	
1122.6	ov, br, vw	0.789	
1275.7	sh, br,, vw	0.675	
1306.7	br, w	1.843	
1441.9	w	0.894	
1457.5	sh, w	1.431	
1744.3	br, vw	1.184	
2727.3	br, vw	0.493	O-H (COOH)
2852.6	ov, br, mw	0.548	C-H
2881.7	ov, br, mw	0.894	C-H

UNE S05			
Average Peak Position	**Raman Signal Strength**	**Standard Deviation**	**Peak ID**
226.6	m	0.000	
245.9	vw	0.672	
293.3	ms	0.447	
397.5	sh, mw	0.789	A
410.2	m	0.548	
499.3	sh, w	1.262	
512.6	w	0.856	A
612.7	sh, w	0.548	
637.9	m	0.850	A
1064.1	ov, br, vw	0.548	
1079.4	ov, br, vw	1.431	
1119.1	ov, br, vw	1.110	
1277.8	sh, br, vw	1.095	
1309.4	br, mw	1.817	
1441.1	mw	0.850	
1457.6	sh, w	0.844	
1741.6	br, vw	0.837	
2726.1	br, vw	1.095	O-H (COOH)
2852.2	ov, br, m	0.707	C-H
2882.7	ov, br, m	0.856	C-H

UNE S07			
Average Peak Position	**Raman Signal Strength**	**Standard Deviation**	**Peak ID**
227.2	ms	0.894	
246.1	vw	1.558	
293.9	s	1.055	
396.7	sh, mw	0.548	A
411.0	m	1.838	

500.0	sh, br, w	1.626	
513.5	w	1.092	A
612.3	sh, mw	1.184	
638.1	mw	1.055	A
1064.3	ov, br, vw	0.500	
1081.9	ov, br, vw	1.367	
1123.6	ov, br, vw	0.914	
1274.7	sh, br, vw	1.344	
1307.3	br, mw	1.859	
1441.5	w	0.776	
1457.2	sh, br, vw	0.906	
1743.1	br, vw	0.906	
2728.1	br, vw	0.500	O-H (COOH)
2853.0	ov, br, mw	0.801	C-H
2882.6	ov, br, mw	0.950	C-H

UNE S08			
Average Peak Position	**Raman Signal Strength**	**Standard Deviation**	**Peak ID**
227.6	vw	0.000	
247.2	vw	1.110	
294.3	w	0.447	
412.1	br, vw	0.548	
613.3	br, vw	0.950	
638.6	br, vw	0.577	
1310.2	br, vw	1.583	
1442.1	br, vw	0.548	
1458.7	br, vw	1.534	
2851.0	ov, br, vw	0.789	C-H
2881.7	ov, br, vw	0.548	C-H

UNE S12			
Average Peak Position	**Raman Signal Strength**	**Standard Deviation**	**Peak ID**
226.8	m	0.447	
245.9	vw	0.950	
293.1	ms	0.000	
394.9	sh, mw	1.092	A
410.4	mw	0.856	
498.3	sh, br, w	1.859	
513.9	w	0.950	A
611.9	sh, w	1.105	
637.4	mw	1.534	A
1062.2	ov, br, vw	0.850	
1079.7	ov, br, vw	1.440	
1121.2	ov, br, vw	1.952	

1277.8	sh, br, vw	1.270	
1310.0	br, mw	1.748	
1440.4	mw	1.258	
1457.9	sh, w	1.143	
1743.1	br, vw	0.814	
2727.1	br, vw	1.440	O-H (COOH)
2851.8	ov, br, m	0.894	C-H
2881.3	ov, br, m	0.447	C-H

UNE S15			
Average Peak Position	**Raman Signal Strength**	**Standard Deviation**	**Peak ID**
227.2	vw	0.548	
247.0	vw	0.801	
294.7	w	0.548	
395.5	sh, br, w	1.742	A
411.4	w	0.844	
501.1	sh, br, vw	0.577	
513.8	br, vw	1.592	A
613.1	sh, vw	0.447	
638.1	w	0.789	A
1063.9	ov, br, vw	0.856	
1080.1	ov, br, vw	1.742	
1121.7	ov, br, vw	1.155	
1270.7	sh, br, vw	0.801	
1306.3	br, vw	1.254	
1441.5	br, w	1.184	
1458.9	sh, br, vw	1.925	
1744.3	br, vw	1.000	
2728.2	br, vw	1.260	O-H (COOH)
2851.8	ov, br, mw	1.590	C-H
2881.3	ov, br, mw	0.447	C-H

UNE S17			
Average Peak Position	**Raman Signal Strength**	**Standard Deviation**	**Peak ID**
226.6	mw	0.000	
245.3	vw	0.850	
293.1	m	0.000	
394.9	sh, w	1.896	A
410.4	mw	0.548	
499.5	sh, br, w	0.776	
512.2	w	0.837	A
612.7	sh, w	1.342	
638.3	mw	0.672	A
1062.0	ov, br, vw	0.856	

1080.3	ov, br, vw	1.764	
1121.6	ov, br, vw	1.583	
1272.8	sh, br, vw	0.707	
1305.8	br, mw	1.588	
1440.7	mw	1.041	
1455.6	sh, mw	0.894	
1743.7	br, vw	0.548	
2726.9	br, vw	0.672	O-H (COOH)
2852.6	ov, br, m	0.548	C-H
2882.3	ov, br, m	0.837	C-H

UNE S19			
Average Peak Position	**Raman Signal Strength**	**Standard Deviation**	**Peak ID**
226.6	mw	0.707	
244.7	vw	0.450	
293.3	mw	1.069	
392.2	sh, br, vw	0.789	A
411.3	w	1.092	
498.5	sh, br, vw	1.000	
513.0	sh, br, vw	1.674	A
610.8	vw	1.092	
637.6	vw	1.254	A
1063.2	ov, br, vw	1.097	
1078.3	ov, br, vw	0.577	
1275.5	sh, br, vw	1.969	
1309.2	br, vw	2.921	
1439.8	vw	0.447	
1457.2	sh, br, vw	0.402	
2851.8	ov, br, w	0.856	C-H
2881.1	ov, br, w	0.000	C-H

As seen from the data presented, the majority of the lipstick spectra are dominated by the red dyes found in most lipsticks, with some of them only displaying the dye peaks in their spectra. Red dyes and pigments are known to fluoresce [16, 21], especially when analysed using a visible excitation wavelength, such as the 632.8 nm laser used in this study. Considering the total concentration of dyes and pigments in lipsticks is no more than 15% (by weight) [218, 221, 222], it is possible that the signals from the dyes are being enhanced due to a resonance effect. The Raman signals from other compounds making up the rest of the lipstick could be obscured

by the compounds that are fluorescent under visible excitation frequencies, such as carnauba wax.

Besides the peaks that come from dyes, titanium dioxide peaks are also commonly encountered in lipstick spectra, anatase being the most common form observed. Unsurprisingly, the C-H stretching vibration bands at around 2800-3000 cm^{-1} are frequently present in most lipsticks, which originate from the abundant C-H bonds found in the majority of lipstick ingredients. These peaks are very weak, or completely absent, in some of the lipstick spectra; however, this does not mean that such compounds are absent from the lipstick's composition; only that any Raman signal arising from such a compound is below the detection limit or the signal is being obscured by a dominant fluorescent background. For this reason, care must be taken when making comparisons between lipsticks that show C-H peaks and those that do not.

It was shown that Raman spectroscopy can be used to analyse and differentiate between lipsticks without having to use complicated techniques such as SERS. Visual inspection of spectra can help categorise different lipsticks into a number of groups that can be differentiated from each other, and can even identify some individual lipsticks. Because lipsticks are made up of a large number of components, it is very difficult to assign individual peaks in a lipstick spectrum. However, by analysing those individual components, it becomes possible to assign some peaks that arise due to those compounds. This has been shown to be very important in differentiating between lipsticks that have extremely similar spectra, such as in the case of those containing the two red dyes, D&C Red No. 6 Barium lake or D&C Red No. 7 Calcium lake. Because these dyes belong to the same chemical class of dyes (azo dyes), their chemical structures are very similar, giving rise to peaks at approximately the same positions in the spectra. However, the subtle differences in terms of peak positions and shapes of some of the peaks make it possible to differentiate between these two dyes. In the case of the lipsticks in Groups 1, 2, 3 and 4, identification of these dyes in each lipstick helped further differentiate

between the lipsticks within the same group, increasing the overall level of successful discrimination achieved between lipsticks.

4.5. Summary

The work presented here has demonstrated the viability of using Raman spectroscopy for the analysis and differentiation of lipsticks. It has been demonstrated that visual inspection of spectra can help categorise lipsticks by their spectrum, and identification of the component dye peaks can further classify lipsticks within each group. Further discrimination between lipsticks with similar spectra can also be obtained by comparing the relative intensities of peaks arising from different compounds in a spectrum. Therefore, it has been shown that a good level of discrimination can be achieved between lipsticks of a variety of colours and brands using Raman spectroscopy. Additionally, a comprehensive library of lipstick spectra has been presented, which has the potential to help with the identification and classification of unknown lipstick spectra, and/or the identification of component peaks in a lipstick spectrum.

Some of the results from this chapter have recently been published in Salahioglu *et al* [245].

CHAPTER V

Differentiation of Lipsticks Deposited on Different Surfaces, Effects of Ageing, and Chemometrics

5.1. Introduction

There are many circumstances that surround forensic evidence, and the analysis of evidence is not always as simple as analysing pure samples under laboratory conditions. Evidential material can be found in many different surroundings from wet and muddy places, to hot and dry environments. The material can be a mixture of several compounds. It can undergo variations of the temperature and moisture of its immediate surroundings; and days or even years can pass before it is recovered. It can be found on different types of surfaces or materials. All of these conditions can affect the results of forensic analysis. Therefore it is important to understand what sorts of environmental conditions could cause a change in the evidential material recovered, and to investigate how these conditions would affect the analytical results for the correct identification of evidence.

Modern Raman spectrometers are equipped with many tools that enable a better analysis of materials, such as confocal microscopes for the analysis of materials at different depths of focus, and automated mapping stages for analysing the distribution of compounds in a given sample. Such spectrometers are much more advanced, powerful and sensitive than the one described in **Chapter IV** of this study. Due to the improved sensitivity of the detectors, a good signal-to-noise ratio can be obtained from samples without the need for long accumulation times. This decreases the overall analysis time as well as the laser exposure time for the sample, which in turn minimises the risk of photodegradation. Better laser rejection filters enable the analysis of the spectral region closer to the excitation line. Higher resolution diffraction gratings can provide better resolved spectra which can separate out overlapping peaks in a complex mixture. Different excitations wavelengths can

be used to analyse samples that are fluorescent when analysed with other excitation sources.

A new Raman spectrometer was purchased towards the end of this study (a *LabRAM-HR*) and therefore it became possible to examine the effects of depositing lipstick smears on different surfaces, and analysing samples which were previously fluorescent under the old, single laser system.

In this chapter the detection, and differentiation, of trace amounts of lipstick smears deposited on textile fibres, cigarette butts and tissues; as well as the analysis of smears on these materials through evidence bags are described. The study also includes investigation of the effects of time on the lipstick spectra, and a preliminary investigation into the use of different excitation wavelengths for the analysis of fluorescent samples.

Due to the improved sensitivity of the *LabRAM-HR* spectrometer, it was possible to obtain a large number of good quality spectra in a relatively short amount of time. A need then arose for a technique that would allow the analysis of large amounts of data quickly and efficiently – such as chemometrics. Therefore this chapter also describes the application of chemometrics to the classification and discrimination of lipstick samples.

Due to time constraints, some of these investigations were designed to be brief explorations rather than detailed, in-depth analyses. More research needs to be done which would involve the analysis of a larger number of lipsticks and investigation of more environmental conditions, such as the effects of temperature and humidity on the spectra of lipsticks.

5.2. Methods and materials

The experiments in this part of the study were carried out using a *Horiba LabRAM-HR* Raman spectrometer (**Fig. 5.1**) utilising three different lasers operating at wavelengths of 472.96, 632.80 and 784.15 nm (Note that these wavelengths will be referred to as 473, 633 and 784 nm respectively throughout the chapter for convenience). The spectrometer incorporated a Peltier cooled charge coupled device (CCD) detector which operated at -70 °C. High quality edge filters were used that enabled the analysis of the region closer to the excitation line (down to 90 cm^{-1} in the case of the 633 nm red laser).

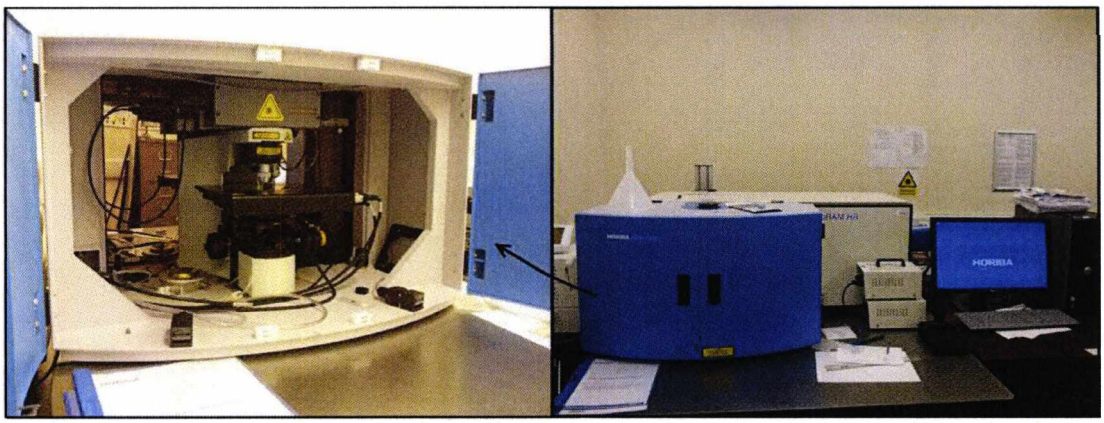

Figure 5.1. *Horiba LabRAM-HR* Raman spectrometer.

The laser power at the sample was 15 mW with the 633 nm laser and 30 mW with the 473 nm laser. Even though Raman spectroscopy is a 'non-destructive' technique, such powerful lasers focused onto the sample can increase the chance of causing decomposition of the sample during the analysis. Decomposition was observed with some of the lipstick smears; therefore, neutral density filters were used to decrease the laser intensity at the sample. There were six filters available: "D0.3" filter blocked 50% of the laser intensity; "D0.6" filter blocked 75%; "D1" filter blocked 90%; "D2" filter blocked 99%; "D3" filter blocked 99.9%; and "D4" filter blocked 99.99% of the laser intensity at the sample. Depending on the experiment, different filters were used to ensure the samples did not degrade during analyses.

A ×50 objective lens was used giving a beam diameter of approximately 2 μm on the sample. The spectrometer was calibrated at the start of each session against the silicon line at 520.6 cm^{-1}.

There were two diffraction gratings available: a 600 gr/mm and an 1800 gr/mm giving spectral resolutions of 2 cm^{-1} and 0.5 cm^{-1} respectively. The slit width was kept constant at 100 μm. The diameter of the confocal aperture ("hole size") was adjusted depending on the experiment. A smaller hole size meant sampling of a thinner layer whereas a larger hole sampled a deeper area of the sample. Depending on the experiment, different diffraction gratings and hole sizes were used.

At least five spectra were obtained from different parts of each sample analysed. The parameters used for each experiment are given in the respective sections.

5.3. Comparison between the two spectrometers

It is especially important in forensic science that the results of analyses do not change when different instrumentation is used. This provides flexibility over the range of instrumentation that can be used while still obtaining accurate and reproducible results.

In order to ensure that the spectra obtained were independent of the instrument used, a spectrum of the same lipstick obtained using both spectrometers were compared (**Fig. 5.2**).

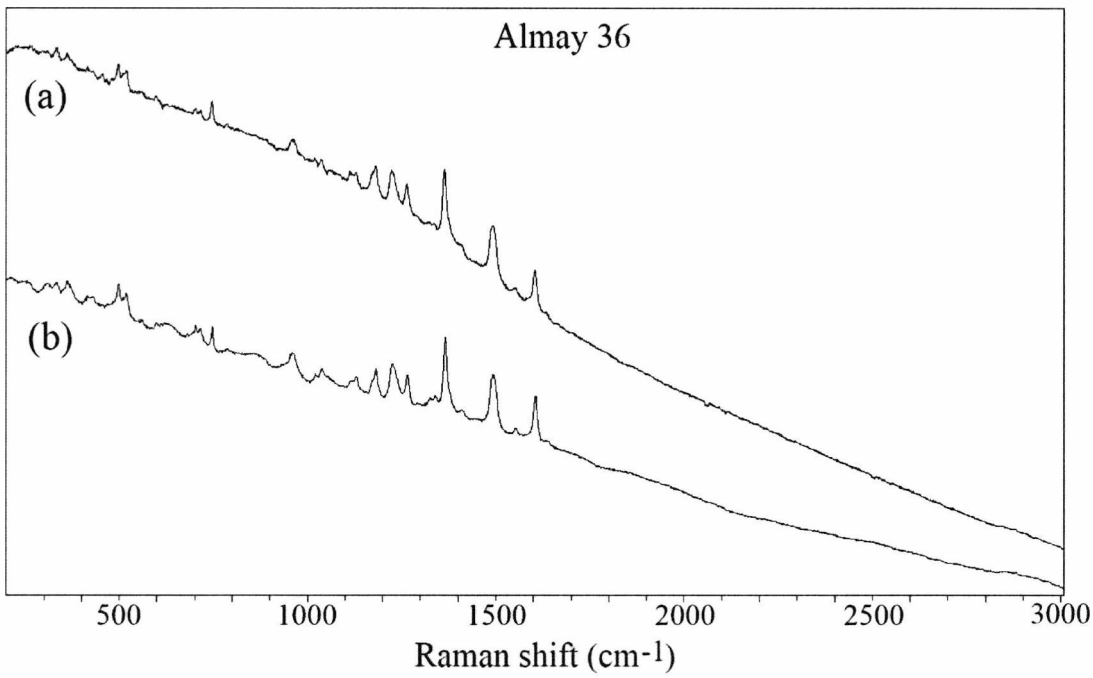

Figure 5.2. (a) Spectrum of Almay 36 obtained using *Jobin-Yvon 640* Raman spectrometer (40 accumulations for 2 seconds) **(b)** Spectrum of Almay 36 obtained using the *LabRAM-HR* (15 accumulations for 2 seconds). Both spectra were obtained using the 633 nm laser.

Despite the use of fewer accumulations for the same amount of time, the spectrum of Almay 36 lipstick acquired using the *LabRAM-HR* had a better signal-to-noise ratio. No differences were observed in terms of the positions or the relative intensities of the peaks. Therefore it was determined that the lipstick spectra obtained did not depend on the instrument used and that the same spectrum could be obtained using different spectrometers with similar setups (i.e. similar resolutions, excitation frequencies etc.).

5.3.1. Spectral range

The *LabRAM-HR* employed an edge filter that enabled the analysis of the frequency region closer to the excitation line (as low as 90 cm^{-1}). This enabled the detection of peaks that could not be observed previously with the 200 cm^{-1} cut off point of the filter on the old *Jobin-Yvon 640* spectrometer. The most significant peak observed in this region was the most intense peak of anatase observed at 143 cm^{-1} (**Fig. 5.3**). This

peak was also frequently observed in the spectra of lipsticks. No peaks were visible beyond 3100 cm^{-1}.

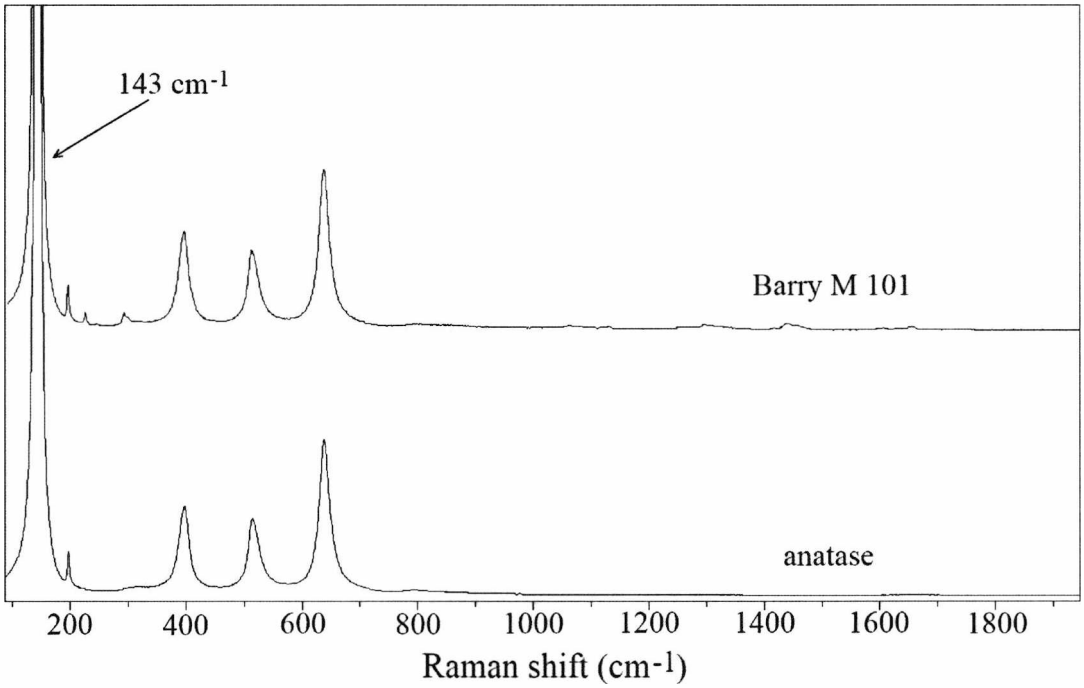

Figure 5.3. Figure comparing the spectrum of titanium dioxide (in anatase form) and the spectrum of Barry M 101 lipstick which contains anatase. The intense anatase peak at 143 cm^{-1} can be observed.

5.3.2. Spectral resolution

Increasing the spectral resolution can sometimes aid in separating overlapping peaks. This becomes very helpful in cases where the analysed sample is a complex mixture of components and the spectra are composed of overlapping peaks. A higher resolution diffraction grating gives rise to a greater dispersion of Raman scattered light, which can then resolve the overlapping peaks into their corresponding components.

The two diffraction gratings available were a 600 gr/mm and a 1800 gr/mm, which gave spectral resolutions of 2 cm^{-1} and 0.5 cm^{-1} respectively. In order to determine whether using a higher resolution grating could help differentiate between lipsticks, four lipsticks were chosen. These were Almay 36, Bourjois 16, Revlon 006 and

L'Oreal 164 lipsticks, which were placed in Group 1 in **Chapter IV** because they could not be differentiated from each other with a spectral resolution of 2 cm^{-1}. All of these lipsticks contained the dye D&C Red No. 7 Calcium lake and were placed in the same subgroup.

A comparison between the spectra of Almay 36 obtained with each diffraction grating is presented in **Fig. 5.4**. Even though the spectral resolution is four times better with the 1800 gr/mm grating, no visible differences in the separation of peaks can be observed.

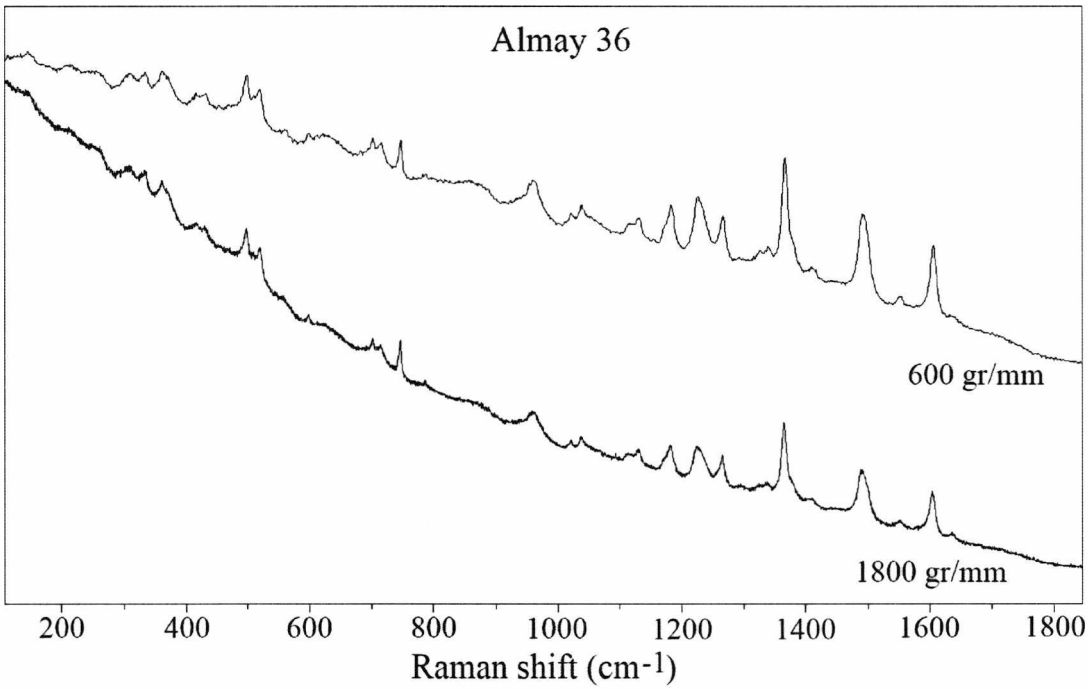

Figure 5.4. Figure comparing the spectra for Almay 36 lipstick obtained with a 600 gr/mm and an 1800 gr/mm diffraction grating using 15 accumulations for 2 seconds in both cases.

Figure 5.5 presents and compares the spectra of the four lipsticks analysed using the 1800 gr/mm diffraction grating. It can be seen that even the broader peaks, which could be composed of more than one peak overlapping with each other, were not resolved.

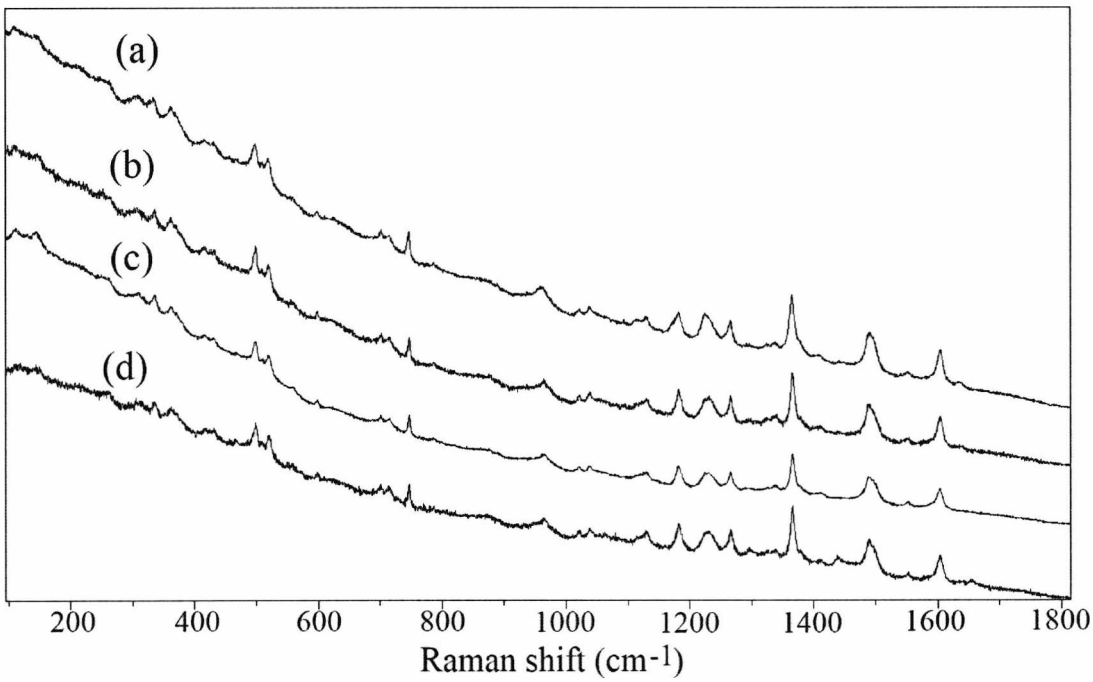

Figure 5.5. (a) Spectrum of Almay 36 lipstick **(b)** Spectrum of Bourjois 16 lipstick **(c)** Spectrum of Revlon 006 lipstick **(d)** Spectrum of L'Oreal 164 lipstick. All spectra were obtained using the 1800 gr/mm diffraction grating and the 633 nm laser.

Therefore it was still not possible to differentiate between these lipsticks by using a higher resolution diffraction grating.

5.3.3. Different excitation wavelengths

Access to different excitation wavelengths makes it easier to analyse difficult samples. Lasers of different wavelengths can be useful for resonance Raman spectroscopy if the energy gap between the electronic transitions of the analysed sample is known. They can also be used for the analysis of samples that are too fluorescent when analysed with a certain excitation wavelength. Since fluorescence occurs when the excitation source has enough energy to cause electronic transition within the sample, selecting an excitation wavelength that has a lower energy than any electronic transitions in the sample can avoid the problem.

In order to determine whether the use of different lasers could help analyse and differentiate between fluorescent lipstick samples, three lipsticks with fluorescent spectra (when illuminated with a 633 nm laser) were chosen. These were Barry M 144, Elizabeth Arden 17 and Max Factor 210. These lipsticks were analysed using the 633 nm (red) laser in **Chapter IV** and they were placed in "Group F" because they produced fluorescent spectra with no discernible peaks.

These lipsticks were analysed using the 473 nm (blue), 633 nm (red) and 784 nm (near-infrared) lasers. Each sample was smeared on a glass slide and analysed with fifteen accumulations for two seconds for each laser. The results are presented in **Figures 5.6** to **5.8**.

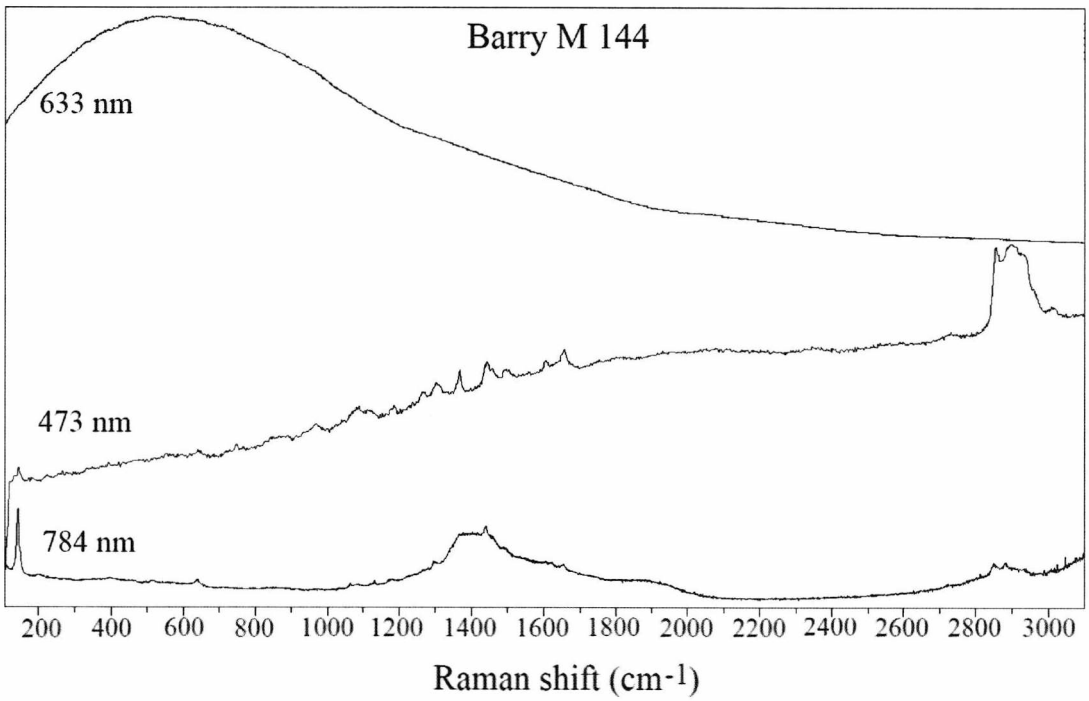

Figure 5.6. Figure comparing the spectra of Barry M 144 lipstick analysed using the red, blue and the near-infrared laser.

Barry M 144 lipstick (**Fig. 5.6**) did not produce any peaks when analysed with the red laser. However when the blue laser was used, the spectrum was significantly less fluorescent with a slightly sloping baseline. Some peaks were visible between 1000 and 1800 cm^{-1}. However, the compound(s) these peaks arose from could not be identified as they did not match the peaks in the spectra of any of the ingredients

available. The strong peak of anatase at 143 cm^{-1} could also be observed as a very weak peak, and the group of peaks between 2800 and 3000 cm^{-1} that arise due to C-H bonds was clearly visible. When the lipstick was analysed with the near-infrared laser, the anatase peak at 143 cm^{-1} appeared more intense. However, the region between 1200 and 2000 cm^{-1} displayed some fluorescence which obscured the peaks. Glass is known to fluoresce at around 1400 cm^{-1} when analysed using this excitation frequency [246]. Therefore, this fluorescence was attributed to the underlying glass slide. The C-H peaks at the high wavenumber end appeared very weak. This lack of observed C-H peaks in the 3000 cm^{-1} region is due to the insensitivity of the CCD detector at large shifts away from the near-infrared excitation line.

Elizabeth Arden 17 lipstick produced a spectrum that fluoresced beyond 2000 cm^{-1} when the blue laser was used. However, peaks belonging to anatase and some of the major peaks of D&C Red No. 7 Calcium lake dye were visible in the non-fluorescent part of the spectrum (as marked in **Fig. 5.7**). When the lipstick was analysed using the near-infrared laser, the anatase peaks were still visible but the rest of the peaks were slightly obscured by the fluorescence from the glass slide at around 1400 cm^{-1}.

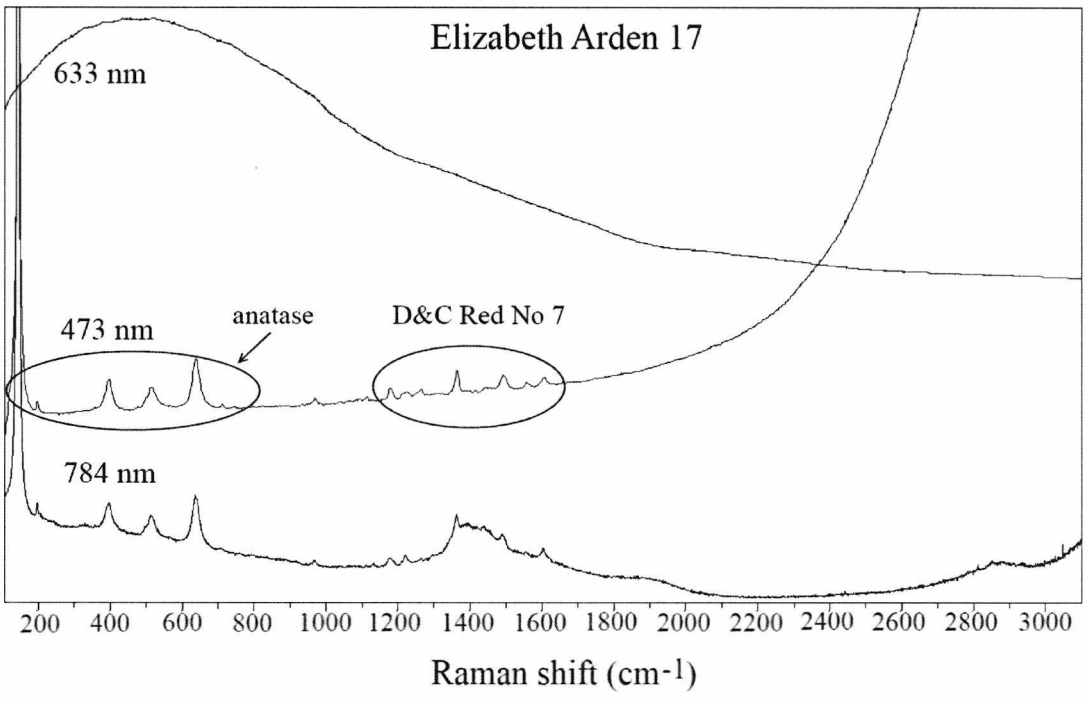

Figure 5.7. Figure comparing the spectra of Elizabeth Arden 17 lipstick analysed using the red, blue and the near-infrared laser.

Max Factor 210 lipstick produced a less fluorescent spectrum when analysed with the blue laser, with characteristic peaks between 1000 and 1800 cm^{-1}. The strong anatase peak at 143 cm^{-1} and the C-H bands between 2800 and 3000 cm^{-1} were also visible. When the near-infrared laser was used, the anatase peak was more intense than the rest of the peaks in the middle region which were obscured by fluorescence (**Fig. 5.8**).

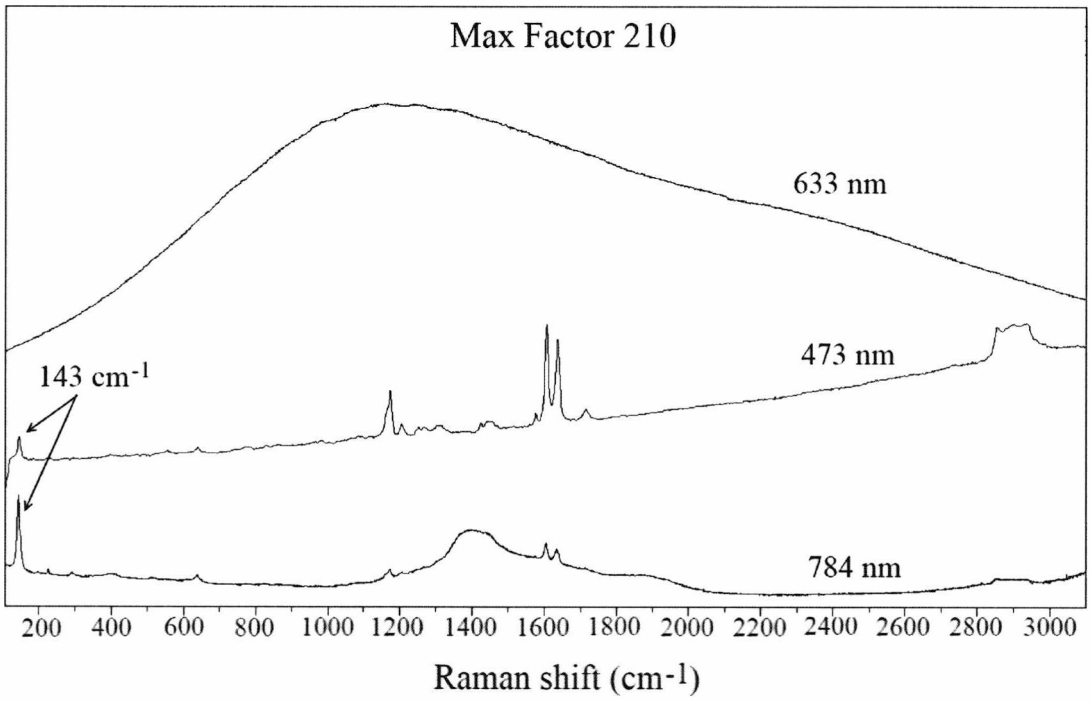

Figure 5.8. Figure comparing the spectra of Max Factor 210 lipstick analysed using the red, blue and the near-infrared laser.

A change was observed in the relative intensities of peaks for the same lipstick when different lasers were used. For example, in **Fig. 5.8**, the intensities of the peaks between 1000 and 1800 cm^{-1} are higher compared to the anatase peak at 143 cm^{-1} when the smear is analysed using the blue laser; however this is reversed when the smear is analysed using the near-infrared laser. This effect could be due to a resonance enhancement when different lasers are being used i.e. peaks of some compounds could be enhanced better with one laser frequency than the other. Resonance Raman scattering is obtained when the energy of the laser is equal or as close as possible to the energy gap between the electronic transitions within the compound. Obtaining a UV-visible spectrum of the compound could help show whether the compound is absorbing at the wavelength of the laser being used. Since

maximum resonance is obtained where there would be maximum (or near maximum) absorption, this could help explain the observed selective enhancement of the peaks when different laser frequencies are being used. To test this, a UV-Visible absorption spectrum of the lipstick Max Factor 210 was obtained. However, the spectrum showed that this lipstick did not have any absorption bands between 300 and 800 nm. Therefore, the observed change in the relative intensities of peaks could not be attributed to a significant resonance enhancement.

Overall, it was possible to obtain spectra from the samples that were too fluorescent when analysed with the red laser by using different wavelength lasers. The lipsticks analysed displayed characteristic peaks that could be used to differentiate them from each other. This demonstrated the effectiveness of using different excitation frequencies to overcome fluorescence.

In **Chapter IV**, it was mentioned that the reason the majority of lipstick peaks come from dyes could be due to resonance enhancement of the dye peaks. In order to determine whether the dye peaks were indeed being enhanced by the resonance Raman effect with the red laser, the lipstick Bourjois 16 was analysed using both red and blue lasers, and the spectra were compared (**Fig. 5.9**). This lipstick was chosen because the majority of the peaks in its spectrum arose from the dye D&C Red No. 7 Calcium lake and the concentration of dyes in lipsticks are no more than 15% by weight [218, 221, 222]. Due to the intense fluorescence observed beyond 1800 cm^{-1} when this lipstick was analysed with the blue laser, only the region up to 1800 cm^{-1} is shown. The lipstick was analysed for fifteen accumulations of two seconds for both lasers.

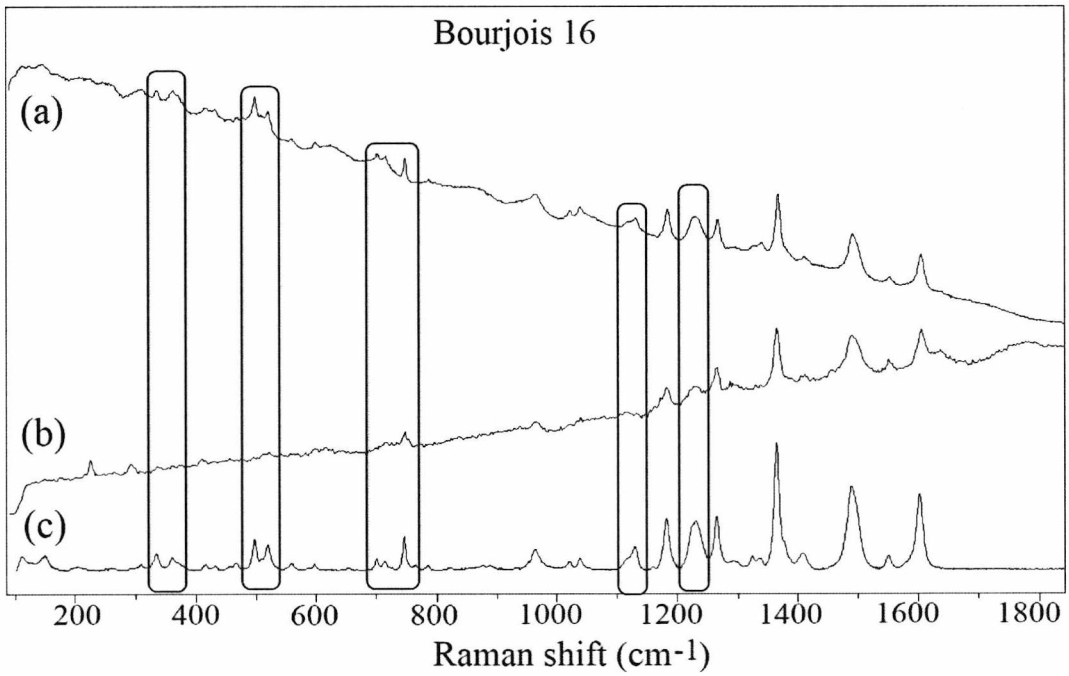

Figure 5.9. (a) Spectrum of Bourjois 16 lipstick analysed using the red (633 nm) laser **(b)** Spectrum of Bourjois 16 analysed using the blue (473 nm) laser **(c)** Spectrum of D&C Red No. 7 Calcium lake dye analysed using a near-infrared laser (obtained from http://modern.kikirpa.be). The boxes highlight areas where the relative intensities of the dye peaks are different due to the differing excitation wavelength.

When the lipstick was analysed using the blue laser, the peaks obtained were generally less intense. As presented and marked in **Fig. 5.9**, some of the peaks of the dye **(c)**, which also appear in the spectrum of the lipstick when analysed with the red laser **(a)**, are less intense or not present at all when the blue laser is used **(b)**. Therefore, it can be concluded that these peaks are probably being enhanced (to a certain degree) by the resonance Raman effect when the red laser is used.

It is important, therefore, that care is taken when comparing spectra obtained using different excitation wavelengths. Signal intensity enhancement due to the resonance Raman effect can make the spectra of the same sample appear different in terms of relative intensities of peaks. Therefore, careful consideration should be given to the use of relative intensities as being a representative fingerprint of a particular lipstick, or any other sample.

5.3.4. Raman mapping

Even though lipsticks are manufactured to have a consistent composition, microscopic examination of lipstick smears revealed that some of the lipsticks were heterogeneous. Fragments of what appeared to be colourful materials were observed distributed throughout the matrix of the lipstick. These fragments were initially believed to be thin layers of mica (muscovite) frequently used in lipsticks due to its reflective properties. However, analysis of mica using Raman spectroscopy showed that the mica peaks were not observed in the lipstick spectrum even when the laser was focused on a supposed mica fragment (**Fig. 5.10**).

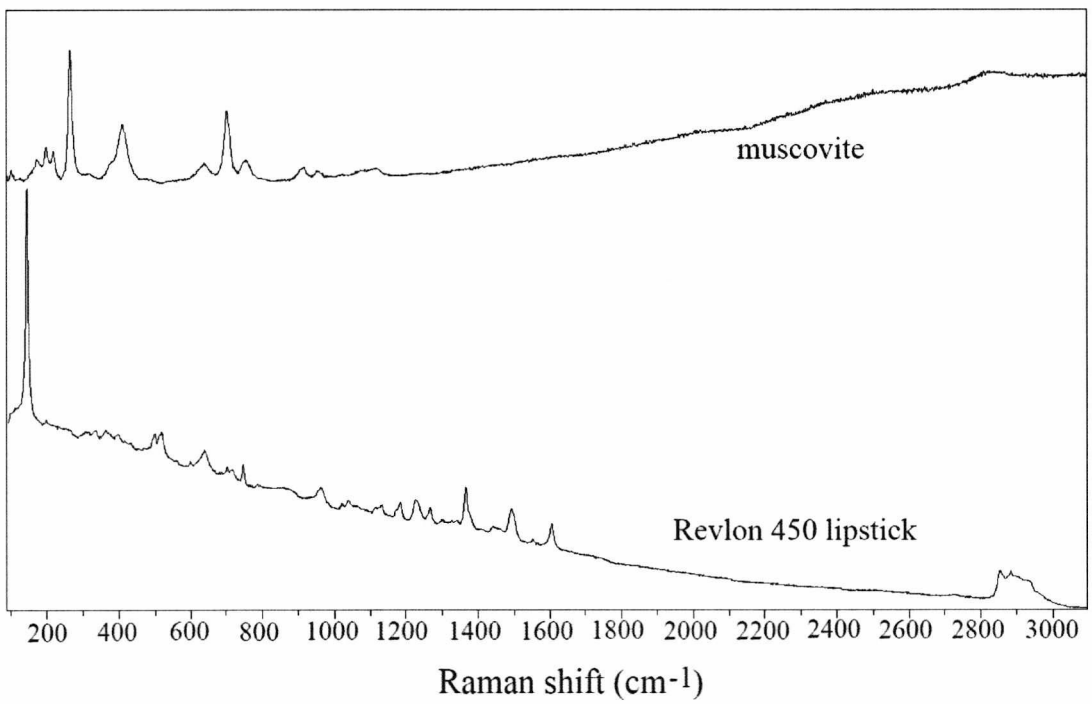

Figure 5.10. Figure comparing the spectrum of mica (muscovite) and the spectrum of Revlon 450 lipstick with the laser focused on one of the mica fragments.

Raman mapping is an invaluable tool for determining the distribution of different compounds across the top surface of a sample. In order to determine whether the spectra obtained showed any differences around such fragments within the lipstick, a Raman map of a fragment together with the granular matrix around it was obtained. The results showed that the only difference between the spectra obtained from the fragment and the surrounding matrix was the intensity of the anatase peaks. This

observation is in line with knowledge of the manufacture process of lipsticks. Layers of mica are coated with metal oxides such as titanium dioxide to obtain a required coloured shine [217, 218, 221]. Therefore it seems highly likely that these fragments in the composition of the lipstick are particles of mica coated with titanium dioxide. Thus, when the laser is focused on these particles, the spectrum obtained has more intense titanium dioxide peaks due to the higher concentration of titanium dioxide on these particles (**Fig. 5.11** and **5.12**). This also explains the lack of mica peaks from the spectra as the TiO_2 coating must be too thick for the laser to significantly excite the underlying mica.

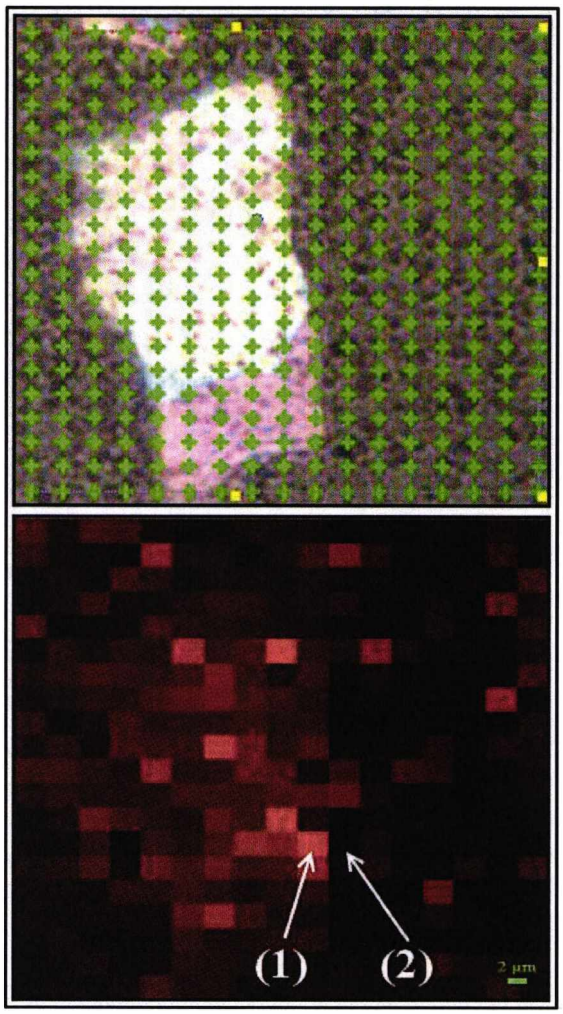

Figure 5.11. An image of the fragment as viewed under a microscope (top) and the Raman map obtained from the same area (bottom). The lighter shades of red in the map indicate higher intensities of the anatase peak at 143 cm^{-1} whereas the darker squares indicate lower peak intensities. It can be seen that in the areas corresponding to the fragment, the intensity of the anatase peak is generally higher. **Fig. 5.12** shows the spectra obtained from the squares marked as (1) and (2).

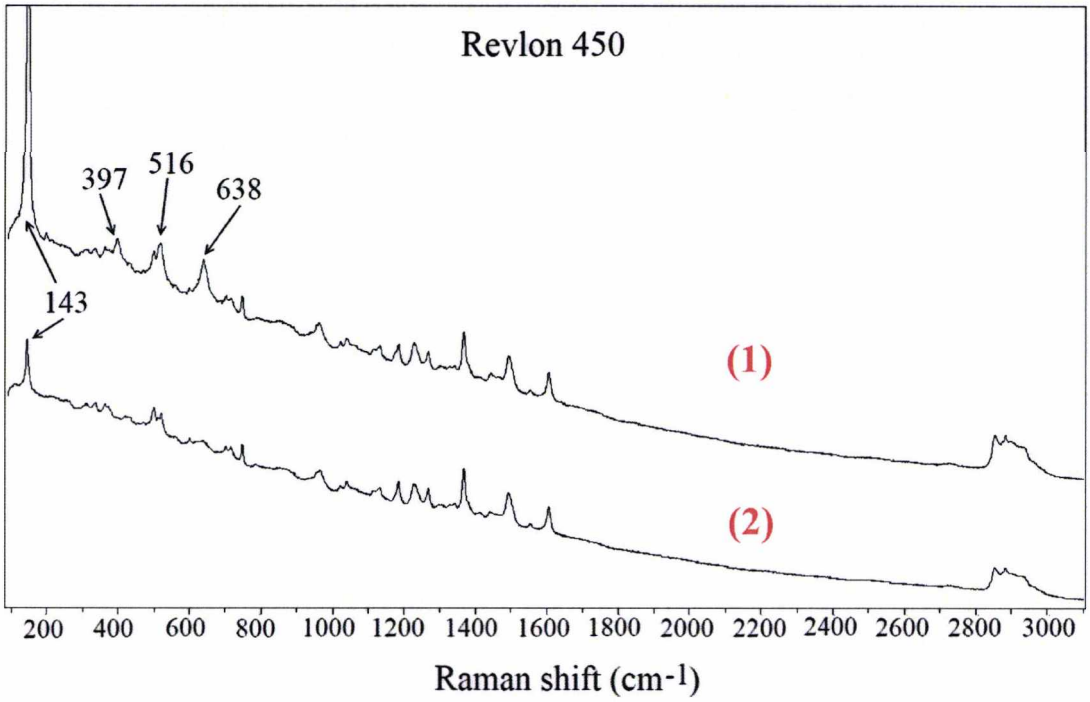

Figure 5.12. (1) Spectrum of Revlon 450 lipstick obtained from the light red square marked as '1' in **Fig. 5.11**. **(2)** Spectrum of Revlon 450 obtained from the dark red square marked as '2' in **Fig. 5.11**. It can be seen that the anatase peaks at 143, 397, 516 and 638 cm^{-1} are more intense in the spectrum taken from the anatase-coated mica particle.

As seen from **Fig. 5.12**, the intensity of the anatase peaks at 143, 397, 516 and 638 cm^{-1} is greater in the spectrum taken at position (1) than in the spectrum taken at position (2). In spectrum (2), the only peak of anatase observed is the peak at 143 cm^{-1}. The other three anatase peaks are not observed in the lipstick spectrum. However, at position (1), where the laser is focused on the fragment, the anatase peak at 143 cm^{-1} is very strong and the rest of the anatase peaks are also observed with greater intensities. The emergence of these anatase peaks in the spectrum alters the general appearance of the spectrum. Even though both spectra are taken from the same lipstick, they appear to be different due to these peaks. This was observed in several of the lipstick samples analysed throughout this study. Even though the spectra might appear slightly different, this difference is only due to the differing concentrations of anatase within the lipstick smear. Therefore, care must be taken when comparing lipstick spectra, especially of lipsticks with a heterogeneous appearance.

Another difference observed in the spectra of lipsticks is the emergence of rutile peaks instead of/together with the anatase peaks (as mentioned in **Chapter IV**). This is also observed for some of the lipsticks described in this chapter and therefore, it must be borne in mind when comparing lipstick spectra.

5.4. Effects of ageing on the Raman spectra of lipsticks

5.4.1. Introduction

A systematic investigation of the effects of ageing on evidential material can shed light onto how materials change over time, and allow any such changes to be quantified as a function of time. In forensic science it is especially important to know whether a piece of evidence undergoes changes over time, in order to be able to accurately analyse it and determine its history. In the context of Raman analyses, some materials can degrade (for example organic materials), which can cause some peaks to disappear from their Raman spectra. In the same way, the products of degradation can cause new peaks to appear in the spectra.

In order to investigate the effect of ageing on the Raman spectra of lipsticks, 20 different lipsticks were smeared on glass slides and left on a laboratory bench at room temperature, their spectra being recorded periodically. These samples were not subjected to any special storage conditions and only the effect of time on the samples was investigated.

5.4.2. Methods and materials

Five lipsticks each from four different brands were used for this study. These were:

Bourjois: Docteur Glamour 15 'Fuchsia 0 bobo', Lovely Rouge 16 'Brique Exclusif', So Rouge 32 'Fashion Rouge', Sweet Kiss 54 'Rouge Glamour' (purchased online at

www.cosmetics4less.net); Sweet Kiss 47 'Rose paré' (obtained from the local Boots store at Canterbury, Kent)

Barry M: Lip Paint No. 53, 101, 121, 136 and 140 (obtained from Boots)

Rimmel: Volume 080 'Screamer' (purchased at www.cosmetics4less.net); Colour Show Off 130 'Love Me', Lasting Finish 170 'Alarm', Lasting Finish 210 'Coral in Gold', Colour Show Off 320 'Funtime Fuchsia' (obtained from Boots)

Revlon: Matte 004 'Pink About It', Matte 009 'Fabulous Fig', Super Lustrous Pearl 430 'Softsilver Rose', Super Lustrous Pearl 450 'Gentlemen Prefer Pink' (obtained at Boots) and Absolutely Fabulous Lipcream 07 'Cherish' (purchased at www.cosmetics4less.net).

The samples were smeared on glass slides and kept at room temperature. They were all analysed using a ×50 objective lens and the 633 nm laser with the confocal hole diameter being kept constant at 200 μm. Each sample was analysed using the same parameters of fifteen accumulations and two seconds per accumulation.

5.4.3. Results and discussion

Fifteen out of the twenty analysed samples were found to give the same spectra when analysed up to two years after the deposition of the sample. An example is given in **Fig. 5.13** where the spectra for the lipstick Barry M 121 (taken over the course of twelve months) are shown. The spectra for the remaining fourteen lipsticks are presented in **Appendix III**.

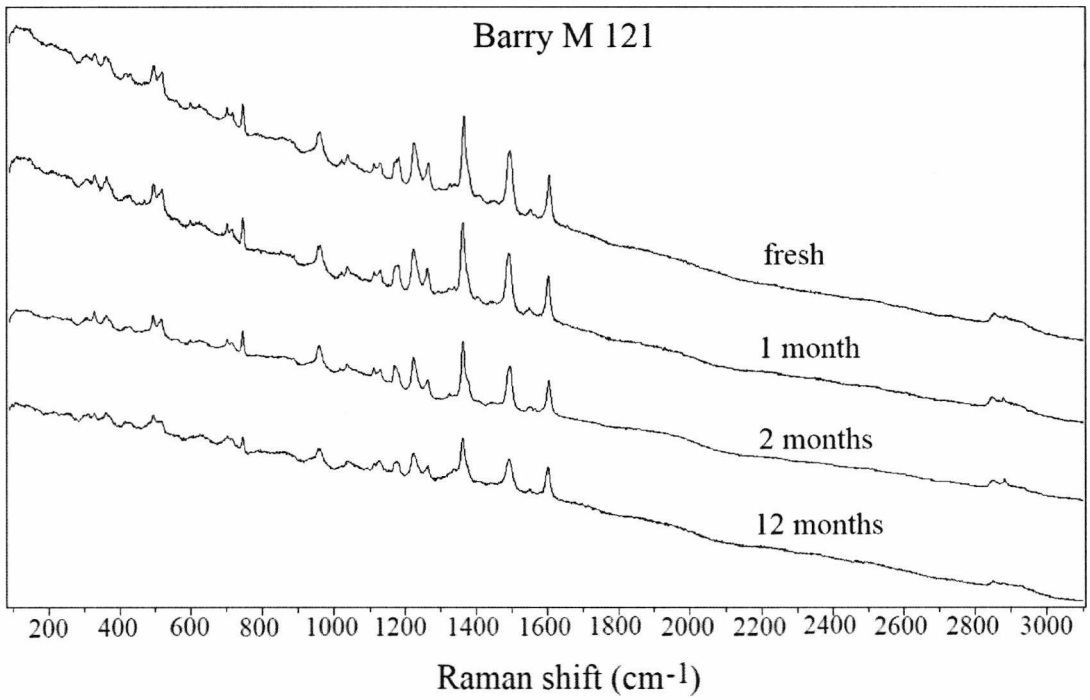

Figure 5.13. Figure showing the spectra for the Barry M 121 lipstick recorded when it was freshly deposited, and at a month, two month and twelve month periods after its deposition. The spectra for the lipstick remained the same over this time period.

However, for the lipsticks Barry M 53, Barry M 101, Barry M 136, Barry M 140 and Rimmel 210 some changes in the spectra were observed (**Figures 5.14** to **5.18**). In the spectra of these lipsticks the peak observed at 1655 cm^{-1} decreased in intensity over time. The peak at 3011 cm^{-1} found in the spectra of Barry M 53, Barry M 101, Barry M 136 and Barry M 140 also decreased in intensity and eventually disappeared within a few months. These peaks were previously attributed to beeswax in **Chapter IV**. The spectra for the fifteen lipsticks that remained unchanged did not have these two peaks.

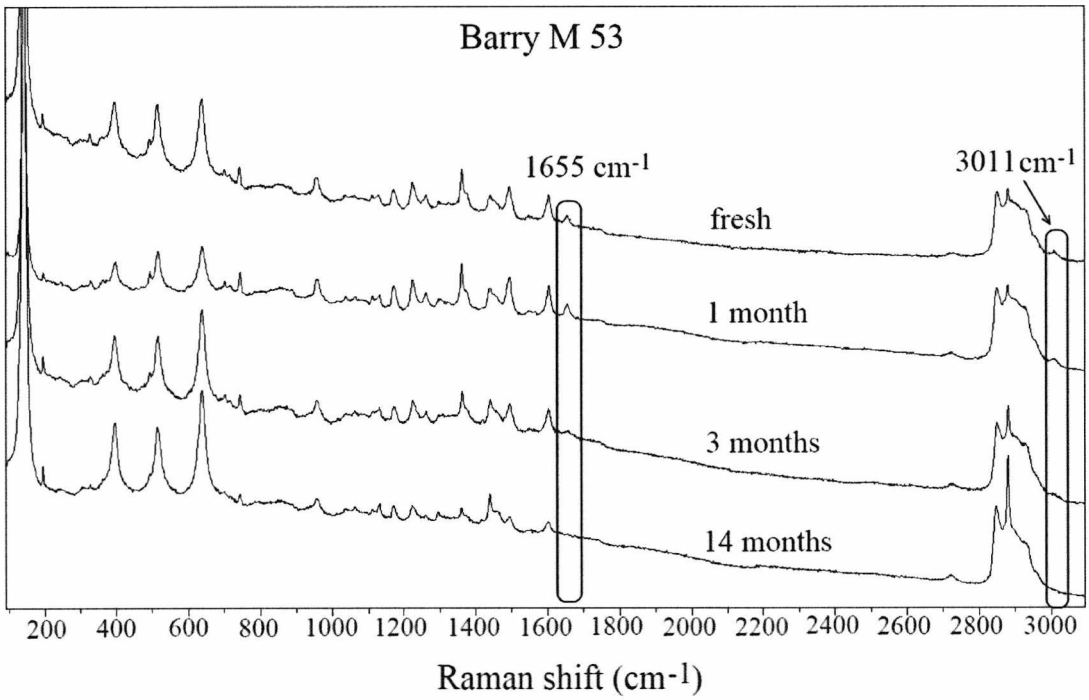

Figure 5.14. Figure showing the spectra for Barry M 53 recorded at different times after its deposition on the glass slide. The peaks at 1655 and 3011 cm^{-1} diminished significantly when the smear was around three months old, disappearing completely by the fourteenth month.

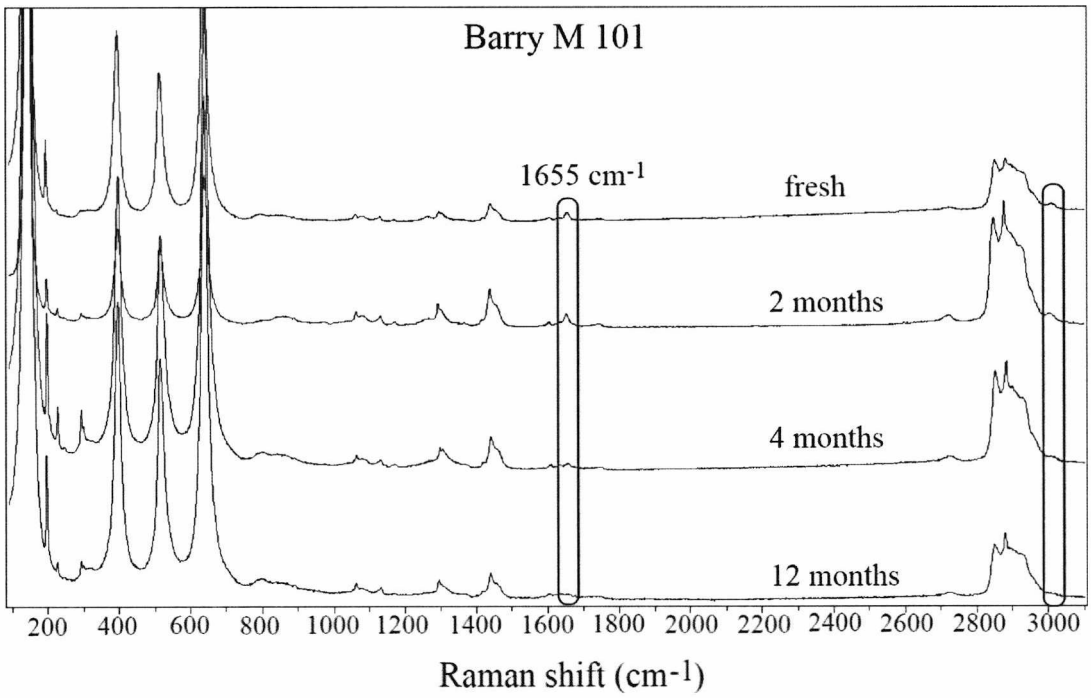

Figure 5.15. Figure showing the spectra for Barry M 101 recorded at different times after its deposition. The peaks at 1655 and 3011 cm^{-1} diminished significantly within four months.

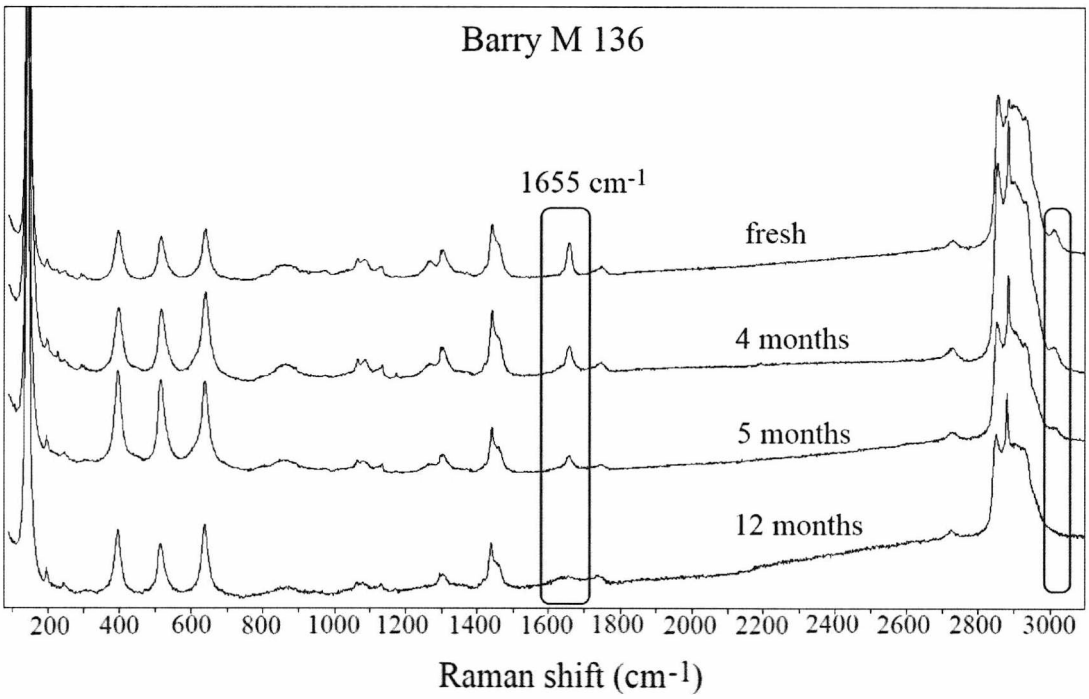

Figure 5.16. Figure showing the spectra for Barry M 136 recorded at different times after its deposition. The peaks at 1655 and 3011 cm^{-1} started diminishing by the fifth month, disappearing completely by the twelfth month.

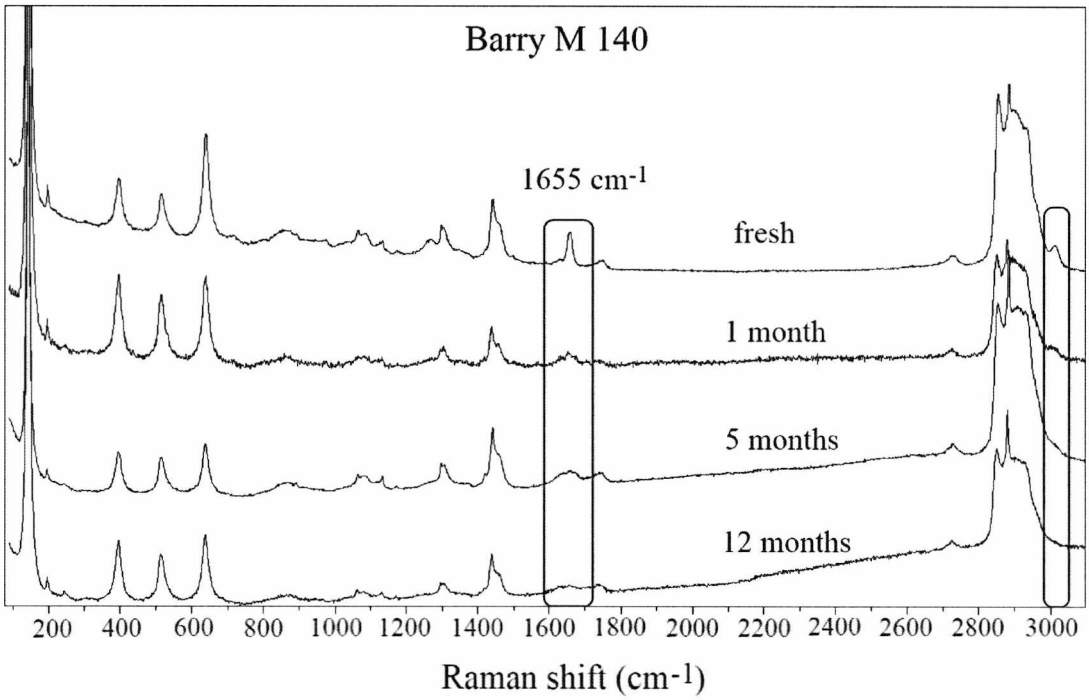

Figure 5.17. Figure showing the spectra for Barry M 140 recorded at different times after its deposition. The peak at 1655 cm^{-1} decreased in intensity significantly within a month. The peak at 3011 cm^{-1} disappeared over time starting after the first month.

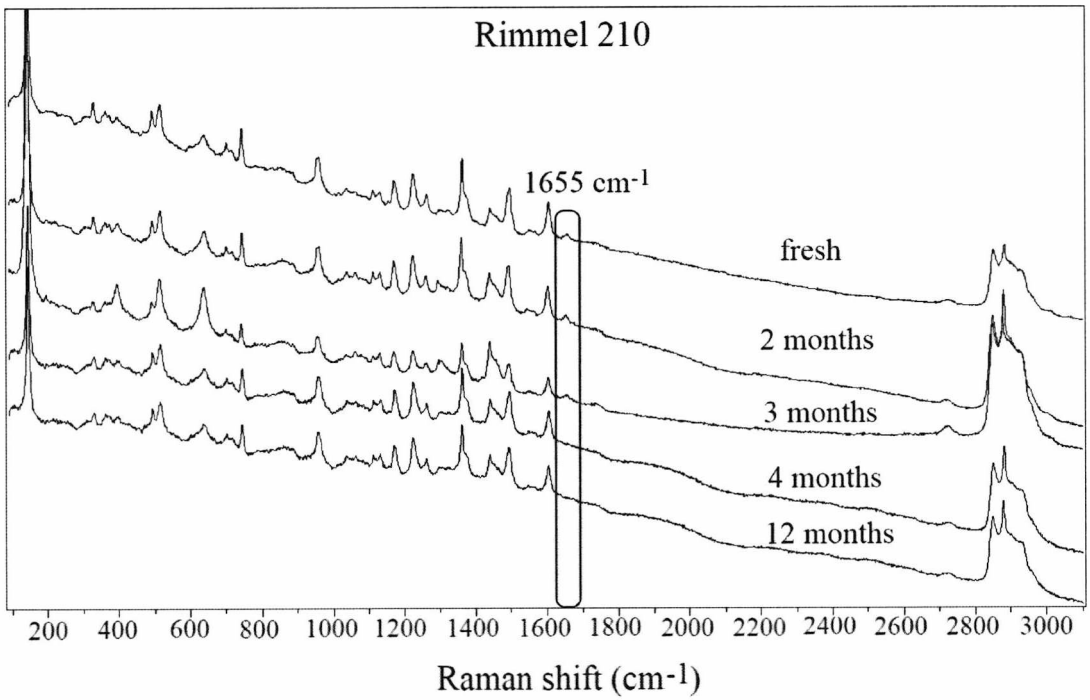

Figure 5.18. Figure showing the spectra for Rimmel 210 recorded at different times after its deposition. The peak at 1655 cm^{-1} started disappearing after the third month.

The weak peak at around 1655 cm^{-1} usually arises due to the C=C stretching in the fatty acids that are abundantly found in the waxy composition of lipsticks. It has been shown [247] that the C=C bond undergoes oxidation over time which results in the decreased intensity of its Raman band. The weak band at around 3011 cm^{-1} arises from (=CH) vibrations which has also been shown to disappear in the Raman spectra of aged lipids [247].

It was found that it was only these two peaks that changed over time. Therefore it is possible to identify and differentiate between lipstick smears even a year or two years after the deposition of the smear since the great majority of the peaks remain unchanged. With lipsticks that have peaks at around 1655 and 3011 cm^{-1}, care must be taken when making comparisons since these peaks were shown to change and eventually disappear.

This research can help to establish the approximate age of a lipstick sample. However, since this study was carried out under relatively stable environmental conditions, the effects of other factors such as changes in temperature, humidity, and exposure to sunlight needs to be taken into account. Therefore much more research could be done on how the Raman spectra of lipsticks (and other cosmetics) change under different environmental conditions.

5.5. Detection of lipstick smears on textile fibres

5.5.1. Introduction

Lipsticks are easily transferred by contact and one of the surfaces they can be encountered on is textile materials, such as clothing and bedding. Raman spectroscopy is a powerful technique for the detection and analysis of trace evidence materials on textile fibres, such as drugs-of-abuse [172, 190, 248], explosives particles [192, 193], and lipsticks [2]. These types of trace evidence materials can be analysed in situ without requiring any sample extraction or preparation. Furthermore, confocal Raman microscopy can be used to avoid interference from the fibre by selectively focusing on the sample surface and rejecting the signals that arise from the material around and underneath.

This part of the study explores the applicability of Raman spectroscopy to the analysis and differentiation of lipstick smears found on fibres.

5.5.2. Methods and materials

For the purposes of this study a variety of different types and colours of textile fibres (in the form of threads) were used. These were: DMC Laine Colbert Tapestry Wool (7785, yellow); DMC Laine Colbert Tapestry Wool (7798, light blue); DMC Laine Colbert Tapestry Wool (7309, very dark navy blue); DMC 25 Mouliné Spécial

Cotton (307, yellow); DMC 25 Mouliné Spécial Cotton (912, green); DMC Mouliné Lin Linen Embroidery Floss (L778, very light pink); and DMC Mouliné Lin Linen Embroidery Floss (L435, burnt orange).

The lipsticks used were La Femme 29 'Dream Rose' (brown-pink) and Revlon 07 'Cherish' (brown) that were purchased online at www.cosmetics4less.net; Rimmel 230 'Red Fever' (red) and Barry M 101 'Marshmallow' (flesh colour) that were obtained from the local Boots store in Canterbury, Kent. These lipsticks produced excellent, to acceptable, Raman spectra (i.e. with very flat baselines, or sloping baselines but no overwhelming fluorescence) when analysed on glass slides. These lipsticks were chosen because of the similarities in their spectra: the majority of the peaks of La Femme 29 and Rimmel 230 are common to both lipsticks, with a few clear differences in terms of the presence, or absence, of peaks (**Fig. 5.19**).

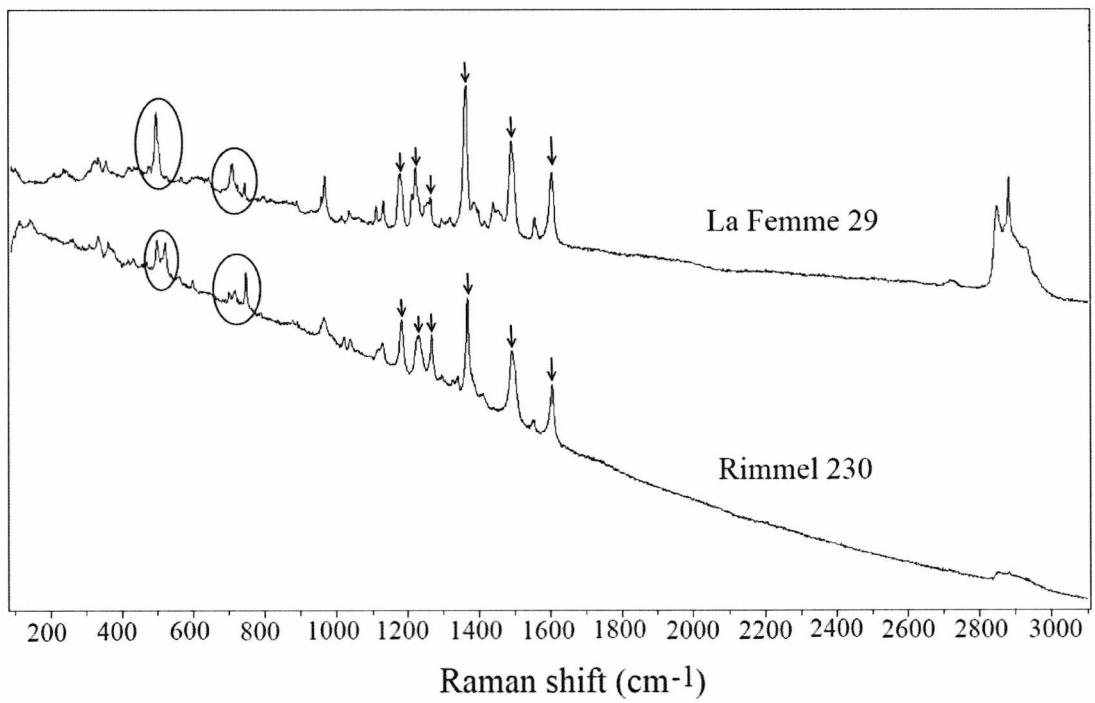

Figure 5.19. A comparison of La Femme 29 lipstick and Rimmel 230 lipstick, both analysed on a glass slide using the 633 nm laser. The arrows point at the similarities in their spectra. The major points of difference that can be used for differentiating between the two lipsticks are circled.

Barry M 101 and Revlon 07 also have peaks that are common to both, but different from the other two lipsticks (**Fig. 5.20**). This helps determine whether lipsticks with similar spectra can still be differentiated from each other when analysed on media such as textile fibres, where interference from the medium (in the form of fluorescence, or peaks from the media's own Raman spectrum) is highly probable.

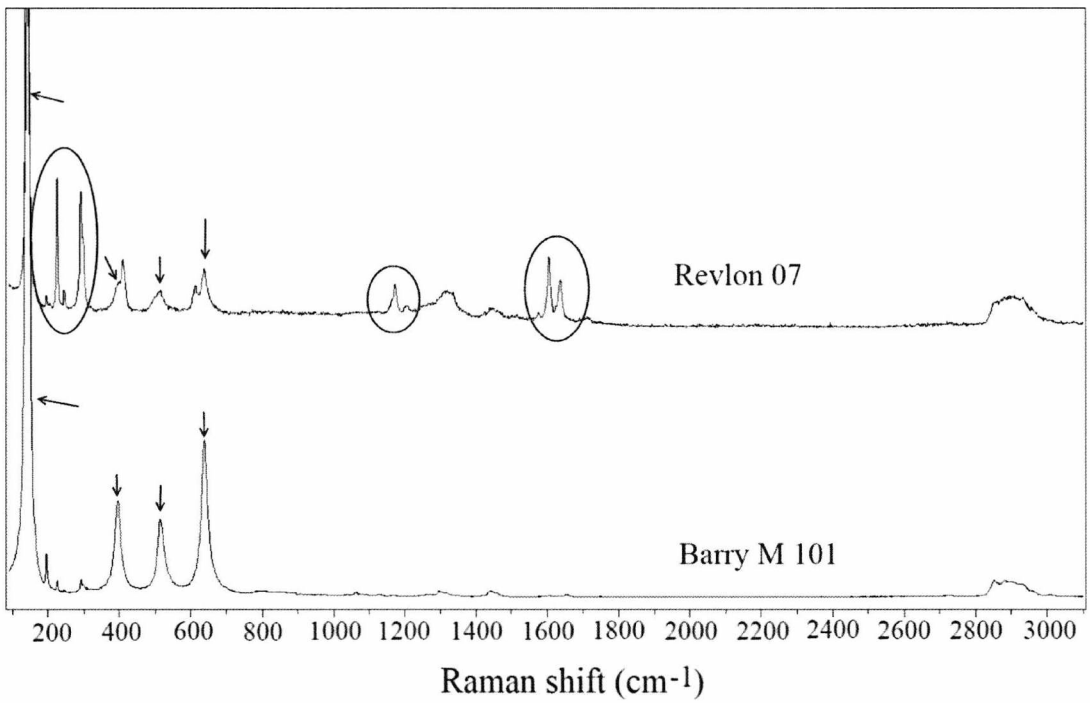

Figure 5.20. A comparison of Revlon 07 lipstick and Barry M 101 lipstick, both analysed on a glass slide using the 633 nm laser. The arrows point at the similarities in their spectra. The major points of difference are circled.

Even though the colours of the lipsticks do not exactly match, when it comes to trace amounts of smears deposited on coloured fabric, it becomes difficult to discriminate between such smears by visual comparison of colour even if the colours are different. Therefore, a more powerful technique such as Raman spectroscopy is required to differentiate between such samples.

The samples were prepared by very lightly dabbing the lipsticks onto the fibres (the piece of thread) so that only a trace amount was transferred (**Fig. 5.21**). The samples were then placed on the microscope stage, the thread being held down by glass slides placed on both ends to weigh it down and stop it moving, and then analysed. Each sample was analysed using the blue (473 nm) and the red (633 nm) laser. The

confocal hole size was adjusted where necessary: if interference from the fibre was encountered, the size of the hole was decreased. If there was little or no interference from the fibre, larger hole sizes were used.

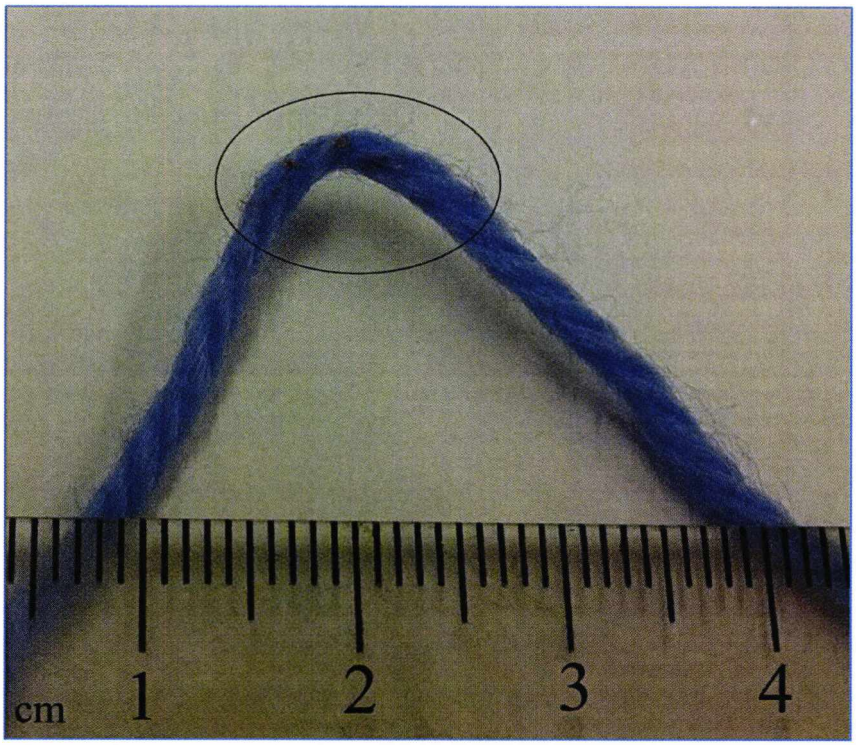

Figure 5.21 A lipstick sample deposited on blue wool in trace amounts (dark red spots as circled)

Adjusting the confocal hole aperture allowed selective sampling of different thicknesses of the sample. For example, with the 473 nm laser, a hole diameter of 200 μm (with a ×50 objective lens) gave an effective depth-of-focus, and thus detectable sample thickness, of 2.2 μm. Adjusting the diameter to 100 μm reduced the detectable sample thickness to 1.5 μm. Similarly, with the 633 nm laser, a hole diameter of 200 μm sampled about 2.3 μm of the sample, whereas a diameter of 100 μm sampled a thickness of about 1.8 μm. Therefore choosing a smaller hole aperture meant that less of the underlying fibre was being analysed. (The values are as quoted in manufacturer's technical document supplied with *LabRAM-HR* (serial # L/5/814), dated 2011).

Different neutral density filters were also used depending on sample fluorescence and degradation. The laser intensity was decreased for samples with extremely high intensity fluorescence bands which sometimes caused saturation of the detector. The intensity was also decreased if degradation of the lipstick sample occurred.

Other parameters, such as the accumulation time and accumulation number, used for each sample were varied in order to obtain the best quality spectra. **Table 5.1** gives the parameters used for each lipstick on each fibre.

Table 5.1 Table listing the accumulation time, accumulation number, confocal hole size and the filter used for each sample.

La Femme 29	473 nm Laser				633 nm Laser			
Fibre	Accumulation Time (s)	Accumulation Number	Hole size (μm)	Filter Used	Accumulation Time (s)	Accumulation Number	Hole size (μm)	Filter Used
yellow wool	3	15	200	D2	4	25	200	D1
light blue wool	2	15	200	D2	4	25	100	D2
dark navy wool	3	15	100	D2	2	15	100	D2
yellow cotton	3	15	100	D2	4	25	200	D1
green cotton	2	15	200	D2	4	25	100	D3
light pink linen	3	15	100	D2	4	25	100	D1
orange linen	3	15	200	D2	3	20	100	D1
Barry M101	**473 nm Laser**				**633 nm Laser**			
Fibre	Accumulation Time (s)	Accumulation Number	Hole size (μm)	Filter Used	Accumulation Time (s)	Accumulation Number	Hole size (μm)	Filter Used
yellow wool	2	15	100	D1	2	15	100	D0.3
light blue wool	2	15	200	D2	4	25	100	D2
dark navy wool	2	15	100	D2	2	15	100	D2
yellow cotton	2	15	100	D2	2	15	200	D0.6
green cotton	2	15	200	D2	2	15	100	D1
light pink linen	2	15	100	D2	2	15	100	D2
orange linen	2	15	100	D2	2	15	100	D1
Revlon 07	**473 nm Laser**				**633 nm Laser**			
Fibre	Accumulation Time (s)	Accumulation Number	Hole size (μm)	Filter Used	Accumulation Time (s)	Accumulation Number	Hole size (μm)	Filter Used
yellow wool	5	15	100	D2	3	20	100	D1
light blue wool	5	15	200	D2	3	15	100	D1
dark navy wool	5	15	100	D2	2	15	100	D3
yellow cotton	5	15	100	D2	3	20	100	D1
green cotton	5	15	200	D2	2	15	100	D1
light pink linen	5	15	100	D2	3	20	100	D2
orange linen	5	15	200	D2	3	15	100	D1
Rimmel 230	**473 nm Laser**				**633 nm Laser**			
Fibre	Accumulation Time (s)	Accumulation Number	Hole size (μm)	Filter Used	Accumulation Time (s)	Accumulation Number	Hole size (μm)	Filter Used
yellow wool	4	10	200	D2	4	20	100	D1
light blue wool	4	10	200	D2	4	25	100	D1
dark navy wool	4	10	200	D2	2	15	100	D2
yellow cotton	4	10	300	D2	4	20	100	D1
green cotton	4	10	200	D2	5	15	50	D1
light pink linen	4	10	200	D2	4	20	100	D1
orange linen	4	10	200	D2	4	20	100	D1

5.5.3. Results and discussion

Each sample was analysed at five different points. Difficulties arising from the detection of trace amounts of lipstick smear on fibres extended the overall time for the analyses. Fluorescent interference from the fibres was observed in many cases which made it difficult to obtain a spectrum of the lipstick, especially when the red laser (633 nm) was used. In many cases more than five spectra per sample had to be recorded in order to obtain a good spectrum of the lipstick with minimum interference from the fibre.

Representative spectra are presented below for each sample. The best five spectra per sample are provided on the accompanying CD. All the relevant figures showing spectra of lipsticks on different fibres analysed with both lasers are given in **Appendix IV**.

La Femme 29 lipstick:

This lipstick gave a good signal-to-noise ratio when analysed with the 633 nm (red) laser. However, with the 473 nm (blue) laser the spectrum started to fluoresce at a Raman shift of around 2000 cm^{-1} and the baseline intensity rose very quickly at higher Raman shifts, reaching very high intensities at approximately 3100 cm^{-1} (**Fig.5.22**). This made the spectrum effectively unusable beyond 2000 cm^{-1}. As a result, it was determined that the range to be analysed when the 473 nm laser was used (with this lipstick) would be 90 to 2000 cm^{-1}.

In general, the La Femme 29 lipstick smear could readily be analysed and identified on all types and colours of fibres with the blue laser. The fibres gave characteristic peaks when analysed with this laser. However, these peaks did not interfere with the lipstick spectra and it was possible to identify the lipstick in all cases (**Fig. 5.23**).

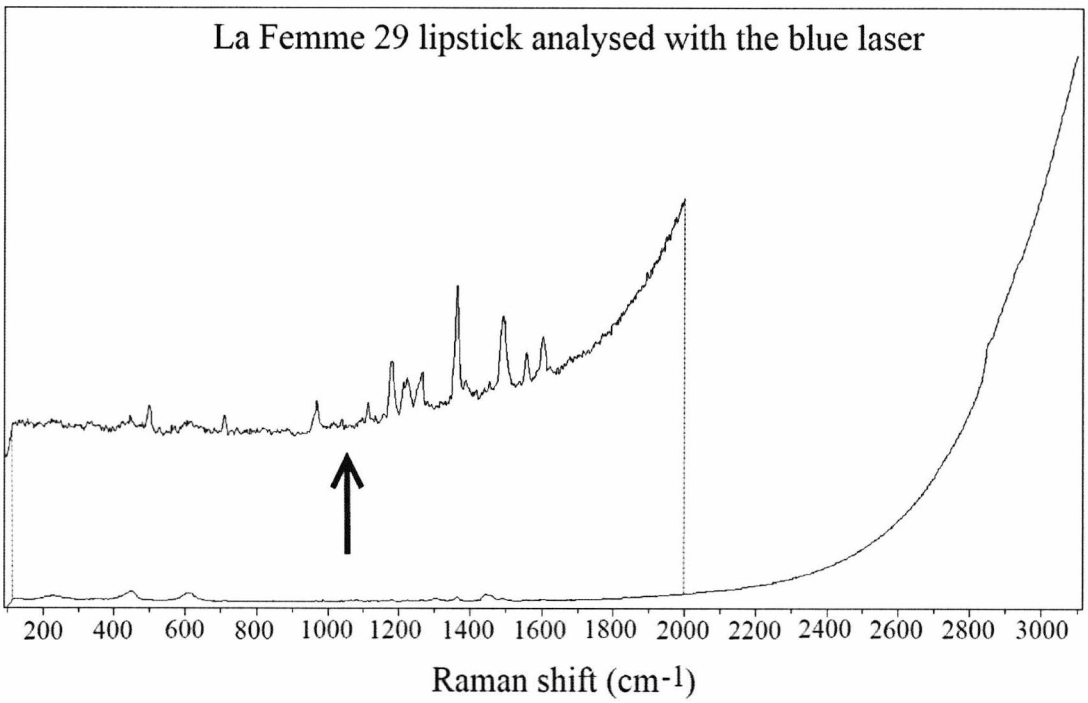

Figure 5.22. La Femme 29 lipstick analysed using the blue (473 nm) laser. The arrowed spectrum is a magnified section of the lower spectrum which shows the steep increase in fluorescence at Raman shifts >2000 cm^{-1}.

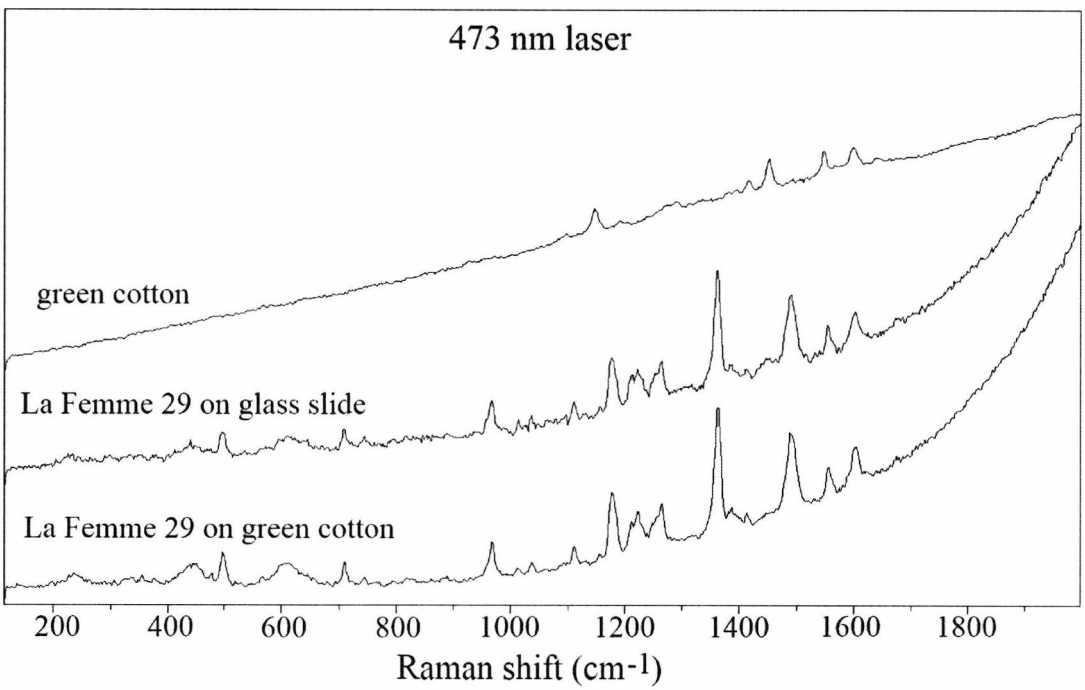

Figure 5.23. Figure comparing the spectra of clean green cotton, La Femme 29 on a glass slide, and on green cotton as analysed using the blue laser.

It was possible to analyse and identify the lipstick smear on yellow wool and yellow cotton using the red laser. Yellow cotton displayed some peaks when analysed with the red laser, but no discernible peaks were obtained from the yellow wool. In both cases, lipstick spectra could be obtained and identified with no interference from the fibres (**Fig. 5.24**).

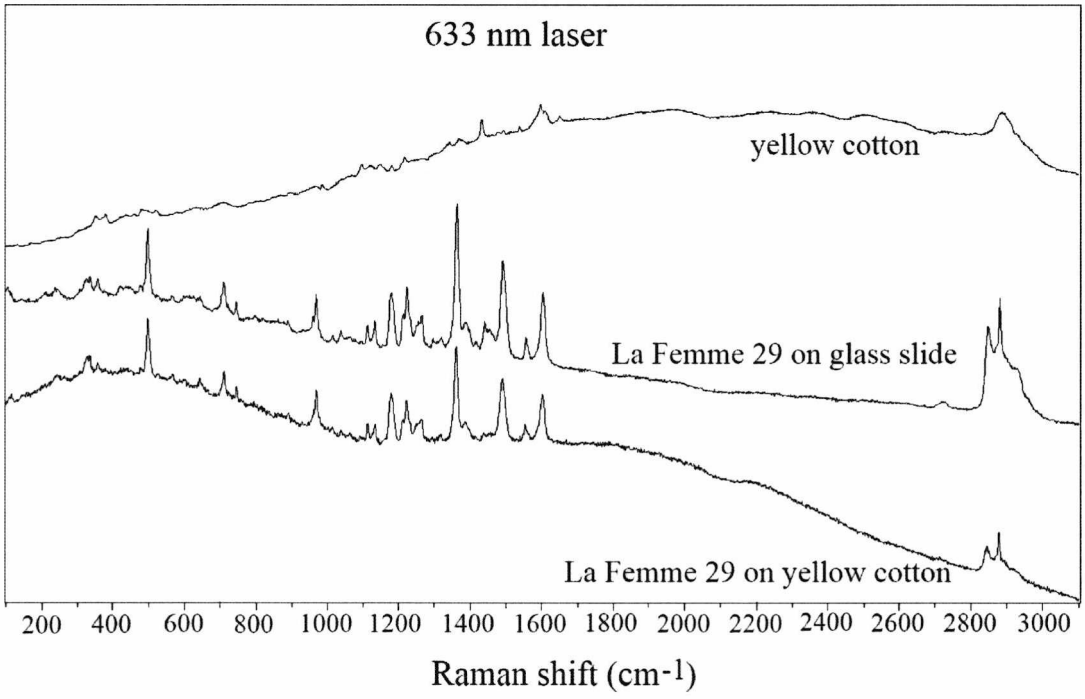

Figure 5.24. Figure comparing the spectra of yellow cotton, La Femme 29 on a glass slide and on yellow cotton, analysed using the red laser.

Pink linen displayed fluorescence when the red laser was used, but it was still possible to obtain good spectra from the lipstick smear. The orange linen sample gave a fluorescent spectrum with no discernible peaks, but the majority of the lipstick peaks could still be observed. Even though the lipstick peaks had worse signal-to-noise ratios, it was still possible to identify the lipstick. When the smear on light blue wool was analysed, however, it was not always possible to obtain a good spectrum of the lipstick due to intense fluorescent interference from the fibre.

Dark navy wool and green cotton produced very fluorescent spectra when analysed using the red laser and it was not possible to obtain a spectrum of the lipstick smear with these fibres.

All figures relating to the detection of La Femme 29 lipstick on these fibres can be found in **Appendix IV**.

When La Femme 29 smears were analysed on fibres, it was observed that the peaks found between 2800 and 3000 cm^{-1} due to C-H bond vibrations were a lot weaker (or completely absent) compared to the rest of the lipstick peaks (**Fig. 5.25**).

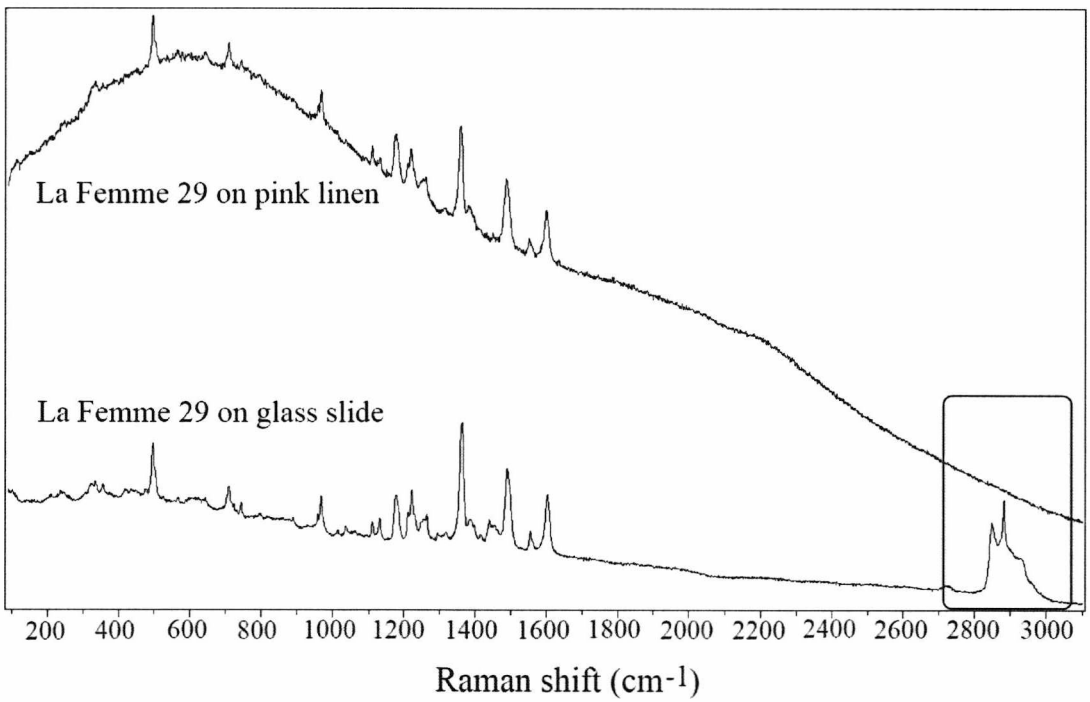

Figure 5.25. Spectrum of La Femme 29 on pink linen and on glass slide analysed using the 633 nm laser. The C-H peaks are absent in the spectrum of the lipstick on pink linen.

A theory was hypothesised to explain the observed effect, which involved localised heating of the lipstick smear. A glass slide is better at dissipating the heat energy (originating from the laser) than a textile fibre is, as it has a higher thermal conductivity. Therefore when the lipstick samples were analysed on glass slides, the samples did not heat up as much and the C-H peaks could still be detected. However, when they were deposited on fibres, the power of the laser could have caused excessive heating of the sample, which could not be dissipated by the fibre. It is possible that this localised heating caused a change in the form, or the composition, of the smear, resulting in a change in the intensity of the C-H peaks. In order to test this theory, La Femme 29 lipstick was smeared onto a circular glass coverslip and

heated up gradually in the *LabRAM-HR*'s temperature controlled heating stage, its spectrum being taken at certain temperatures. The results are presented in **Fig. 5.26**.

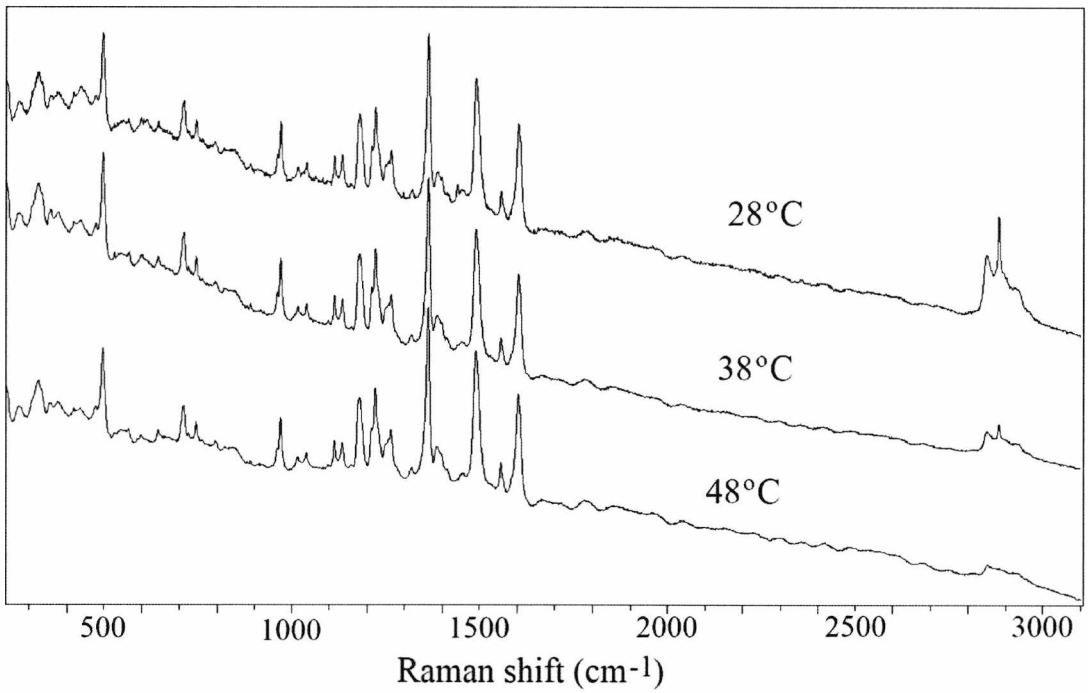

Figure 5.26. Spectra of La Femme 29 lipstick taken at 28, 38 and 48°C. It can be seen that the intensity of the peaks between 2800 and 3000 cm^{-1} decreases with increasing temperature.

It was observed that the intensity of the C-H peaks decreased as the temperature of the sample was increased, whereas the intensities of the other peaks remained the same. This suggests that the waxy components of the lipsticks started melting and changing in form whereas the dyes and pigments stayed as they were. This caused the intensity of the C-H peaks, which were due to the waxy components, to decrease with respect to the dyes and pigments, which were the components that gave rise to the rest of the peaks in the spectrum.

Rimmel 230 lipstick:

This lipstick produced a spectrum with acceptable signal-to-noise ratios with a fluorescent baseline when analysed using the red laser on a glass slide. However, when it was analysed with the blue laser, the baseline started sloping upwards steeply due to fluorescence around 2000 cm^{-1} and reached very high intensities

around 3100 cm^{-1}, in the same way La Femme 29 lipstick spectrum did. For this reason, the useable wavenumber range to be analysed with this lipstick when the blue laser was used was determined to be 90 to 2000 cm^{-1}.

Because each spectrum is taken from a different part of the lipstick smear and some of the smears are largely heterogeneous, an extra peak appears at 143 cm^{-1} in some lipstick spectra. This peak, as mentioned previously, is the most intense peak of anatase and it appears in the lipstick spectrum depending on the concentration of anatase in the analysed region of the smear (**Fig. 5.27**). This peak is visible in some of the spectra presented and it should be noted that it is a part of the lipstick spectrum rather than interference from the underlying fibres.

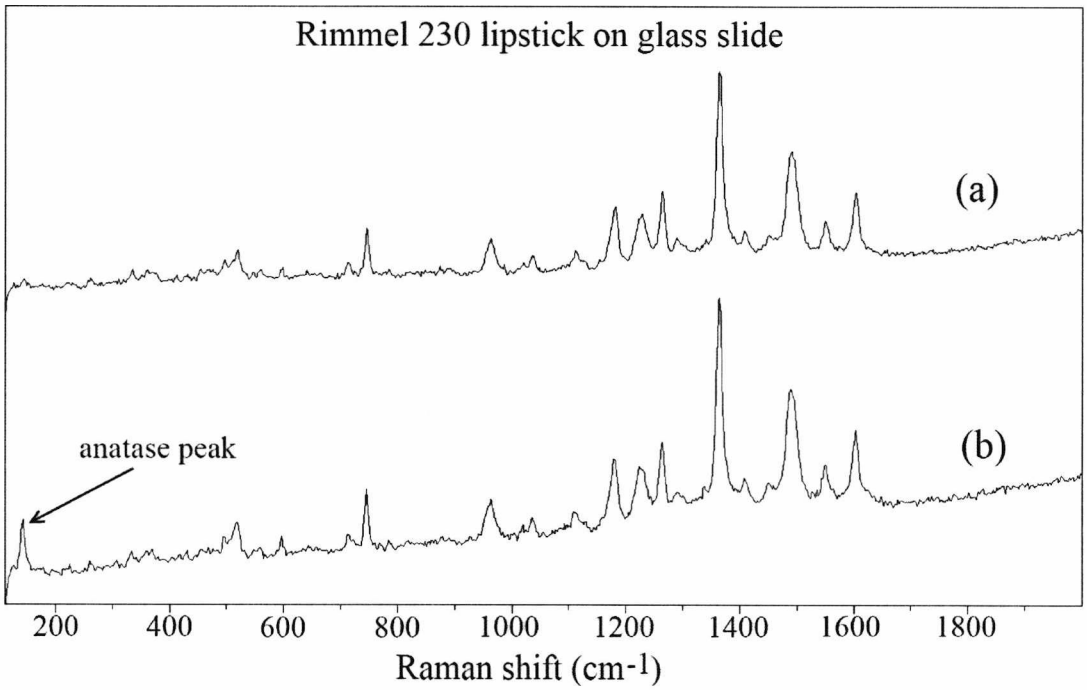

Figure 5.27. (a) and **(b)** are two spectra of Rimmel 230 lipstick recorded on two different parts of the smear on a glass slide, analysed using the blue laser.

The Rimmel 230 lipstick smear could readily be analysed and identified on all types and colours of fibres with the blue laser. The characteristic peaks observed from the fibres when they were analysed with this laser did not interfere with the lipstick spectra and it was possible to identify the lipstick in all cases.

With the red laser, it was possible to analyse and identify the lipstick smear on yellow wool, yellow cotton and orange linen. Some fluorescent interference was observed which reduced the signal-to-noise ratios of Raman peaks. This interference was greater with the smear deposited on pink linen; therefore it was more difficult to identify the lipstick smear on this fibre (**Fig. 5.28**).

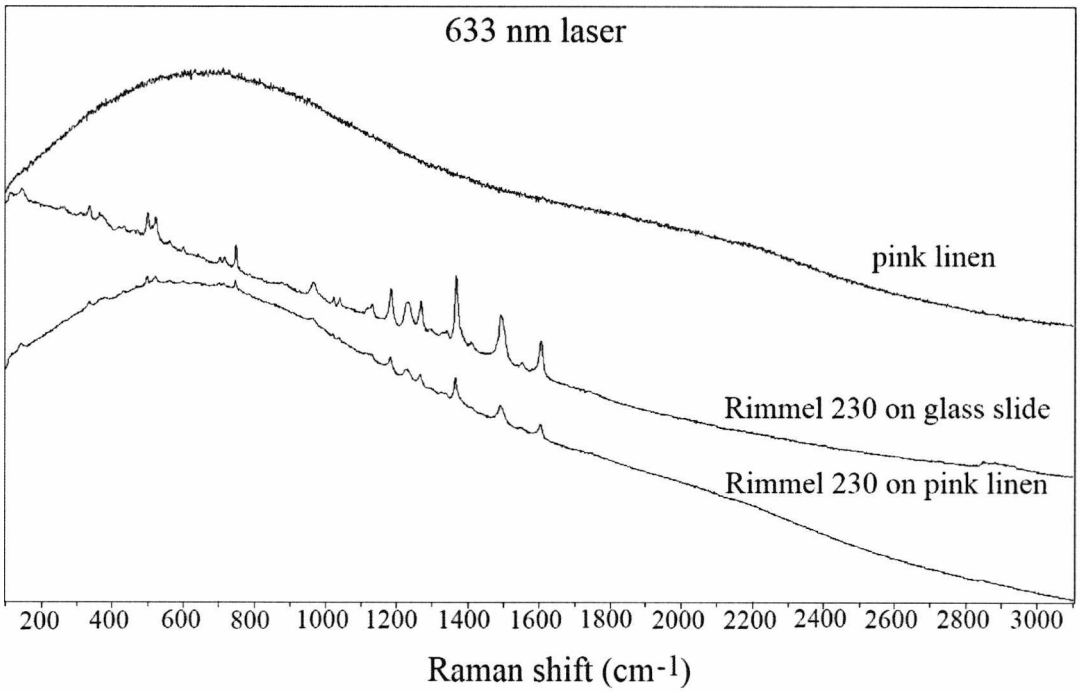

Figure 5.28. Figure comparing the spectra of pink linen, Rimmel 230 on a glass slide and on pink linen, analysed using the red laser.

Due to intense fluorescent interference from the light blue wool, dark navy wool and green cotton, it was not possible to obtain distinguishable spectra of the lipstick smear on these fibres.

All figures relating to the detection of Rimmel 230 lipstick on fibres can be found in **Appendix IV**.

Barry M 101 lipstick:

This lipstick gave excellent spectra when analysed on glass slides using both lasers. The full wavenumber range of 90 to 3100 cm^{-1} was used in both cases.

This lipstick smear could readily be analysed and identified with the blue laser on all types and colours of fibres. With the red laser, the smear deposited on yellow cotton was found to be the easiest to analyse and identify. It was also possible to identify the smear deposited on yellow wool and orange linen using this laser. However, due to fluorescent interference from the fibres, it was not possible to identify the smear deposited on pink linen, light blue wool, dark navy wool and green cotton. In most cases, the only peak visible in the spectrum of the lipstick smear was the anatase peak at 143 cm^{-1} (**Fig. 5.29**).

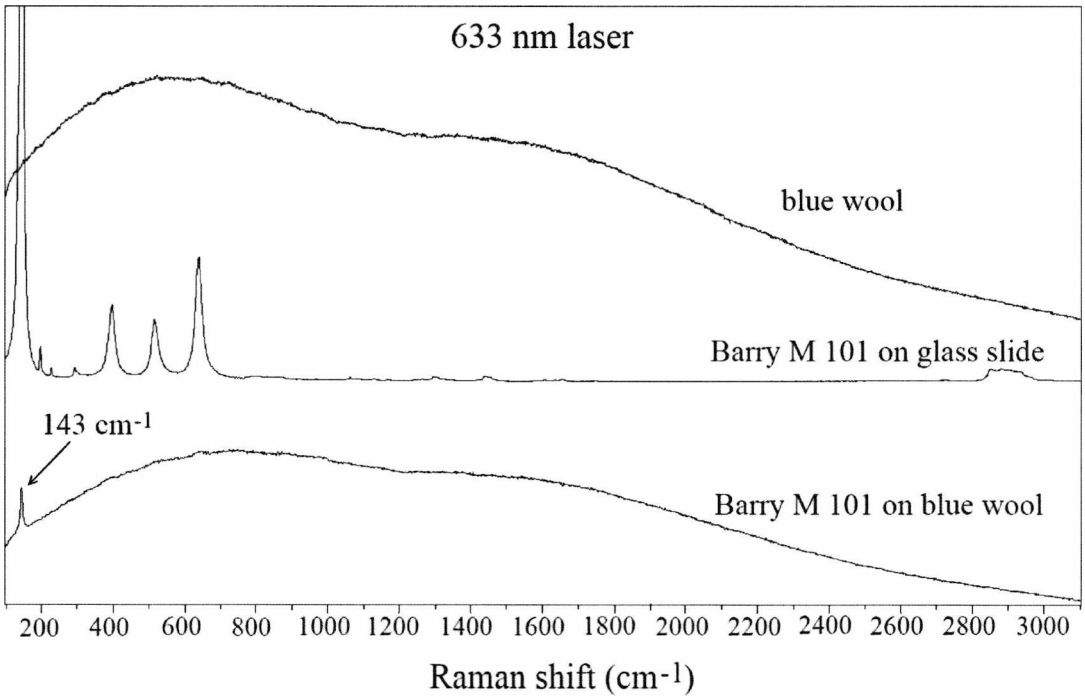

Figure 5.29. Figure comparing the spectra of blue wool, Barry M 101 on a glass slide and on blue wool, analysed using the red laser.

All figures relating to the detection of Barry M 101 lipstick on fibres can be found in **Appendix IV**.

Revlon 07 lipstick:

This lipstick could readily be analysed on glass slides using both lasers and it produced peaks with large signal-to-noise ratios. Even though it had a slightly fluorescent baseline when analysed with the blue laser, the baseline was flat with near-zero intensity when analysed with the red laser.

It was possible to readily analyse and identify this lipstick smear on yellow wool, blue wool and dark navy wool using the blue laser. The intensity of peaks of the smear between 1000 and 1800 cm^{-1} were significantly reduced compared to the rest of the peaks when the smear was deposited on pink linen, yellow cotton and green cotton. However, it was still possible to identify the smear on these fibres using the blue laser (**Fig. 5.30**). This selective loss of peaks could be due to the compounds giving rise to these peaks getting soaked into the fibre, or burning or decomposition of these compounds because of the energy of the laser.

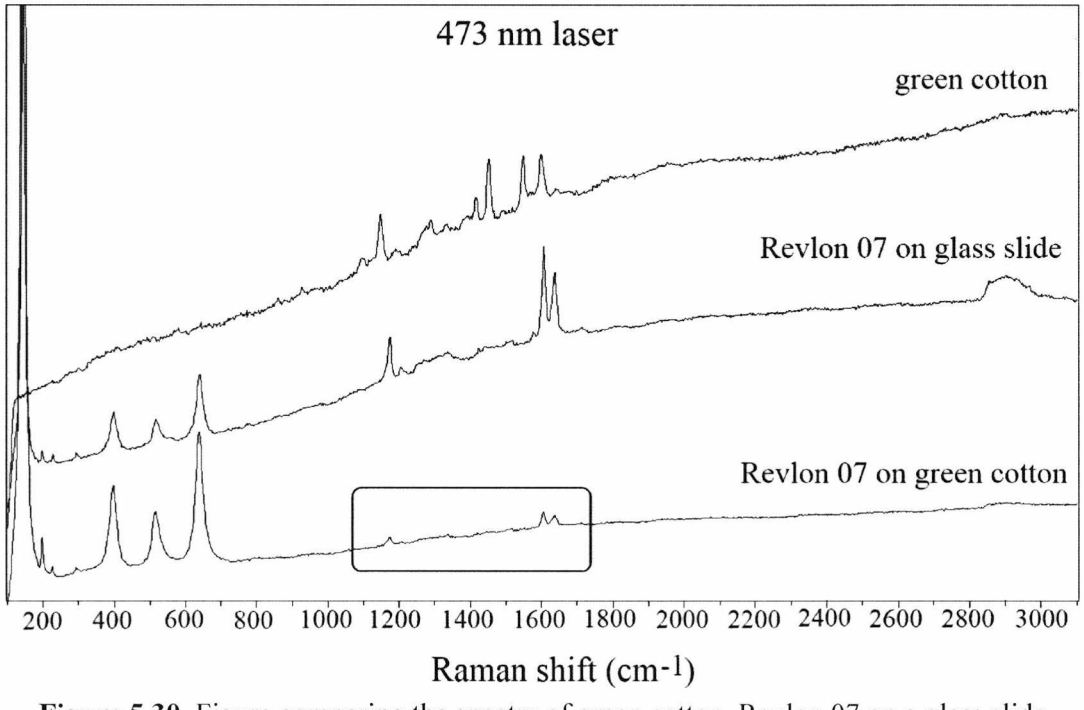

Figure 5.30. Figure comparing the spectra of green cotton, Revlon 07 on a glass slide and on green cotton, analysed using the blue laser. The intensity of the peaks between 1000 and 1800 cm^{-1} is lower compared to the rest of the peaks in the lipstick spectrum.

It was more difficult to analyse the smear deposited on orange linen using the blue laser. Sometimes peaks from the orange linen were observed in the spectrum of the lipstick smear (**Fig. 5.31**). It was not always possible to obtain a good spectrum of the smear on this fibre using the blue laser.

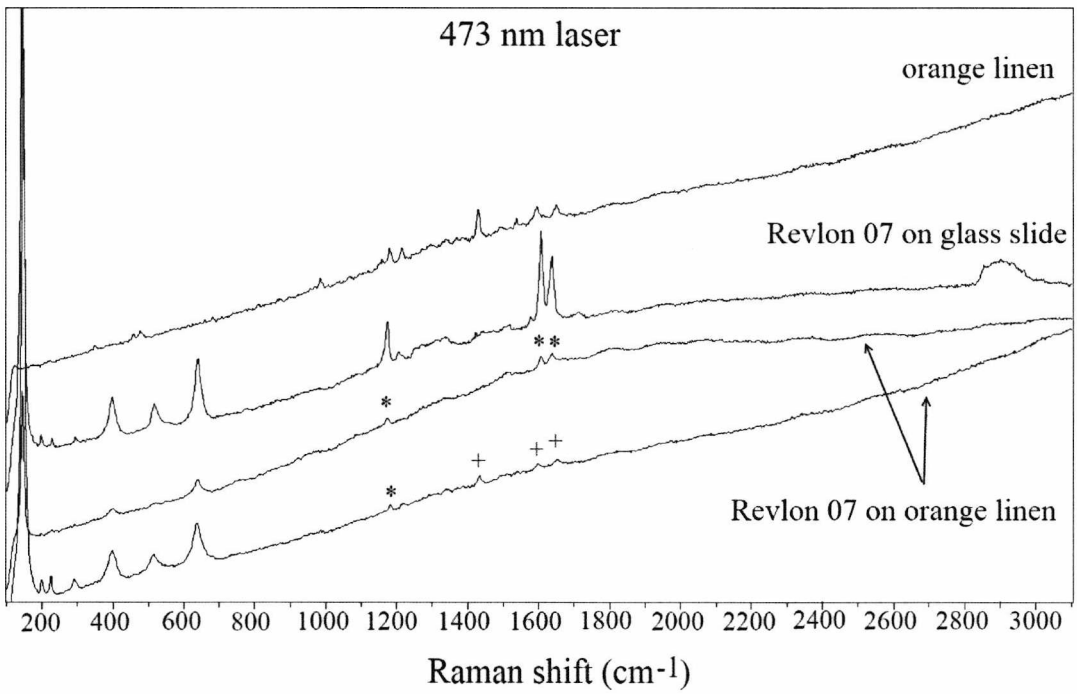

Figure 5.31. Figure comparing the spectra of orange linen, Revlon 07 on a glass slide and on orange linen, analysed using the blue laser. A '*' denotes the peaks that arise from the lipstick, and a '+' indicates those that arise from the orange linen.

When the red laser was used, the Revlon 07 smear could readily be analysed and identified on yellow cotton and orange linen. Despite some fluorescent interference from the yellow wool, it was also possible to identify the smear deposited on this fibre using the red laser. Some of the lipstick peaks were observed in the spectrum of the smear deposited on green cotton, providing identification of the lipstick smear to a certain degree. With the smears deposited on blue wool and pink linen, only some of the anatase peaks could be observed. No spectrum with discernible peaks could be obtained from the smear deposited on dark navy wool.

All figures relating to the detection of Revlon 07 lipstick on fibres can be found in **Appendix IV**.

Overall, it was found that the blue laser was more suitable for the analysis of trace amounts of lipstick smears on fibres. All of the smears could be analysed and identified without any interference from the fibre using the blue laser (except in the case of Revlon 07 deposited on orange linen). The only disadvantage of the blue laser was found to be the very intense fluorescence it caused between 2000 and 3100 cm^{-1} with two of the lipsticks, which made it impossible to determine any spectral peaks within this region. However, the peaks of interest were found between 90 and 1800 cm^{-1}, therefore this was not a major impediment. Analyses with the red laser on the other hand were more difficult to perform due to intense fluorescent interference from the fibres. The smears were analysed the best with this laser when they were found on yellow fibres. The results are summarised in **Table 5.2**.

Table 5.2. A table summarising the results of **Chapter 5.5**. A '✓' indicates that the smear could be analysed and identified on the corresponding fibre with the laser used. A '×' indicates that the smear could not be analysed or identified. A '*' indicates that the smear could sometimes be identified, or identified to a certain degree (i.e. could not detect all of the peaks in the spectrum).

473 nm Laser							
	yellow wool	light blue wool	dark navy wool	yellow cotton	green cotton	light pink linen	orange linen
La Femme 29	✓	✓	✓	✓	✓	✓	✓
Rimmel 230	✓	✓	✓	✓	✓	✓	✓
Barry M 101	✓	✓	✓	✓	✓	✓	✓
Revlon 07	✓	✓	✓	✓	✓	✓	*
633 nm Laser							
	yellow wool	light blue wool	dark navy wool	yellow cotton	green cotton	light pink linen	orange linen
La Femme 29	✓	×	×	✓	×	✓	✓
Rimmel 230	✓	×	×	✓	×	*	✓
Barry M 101	✓	×	×	✓	×	×	✓
Revlon 07	✓	×	×	✓	*	×	✓

It was possible to differentiate between La Femme 29 and Rimmel 230 deposited on fibres. When good spectra could be obtained using the red laser, differentiation between the two lipsticks could be achieved (**Fig. 5.32**).

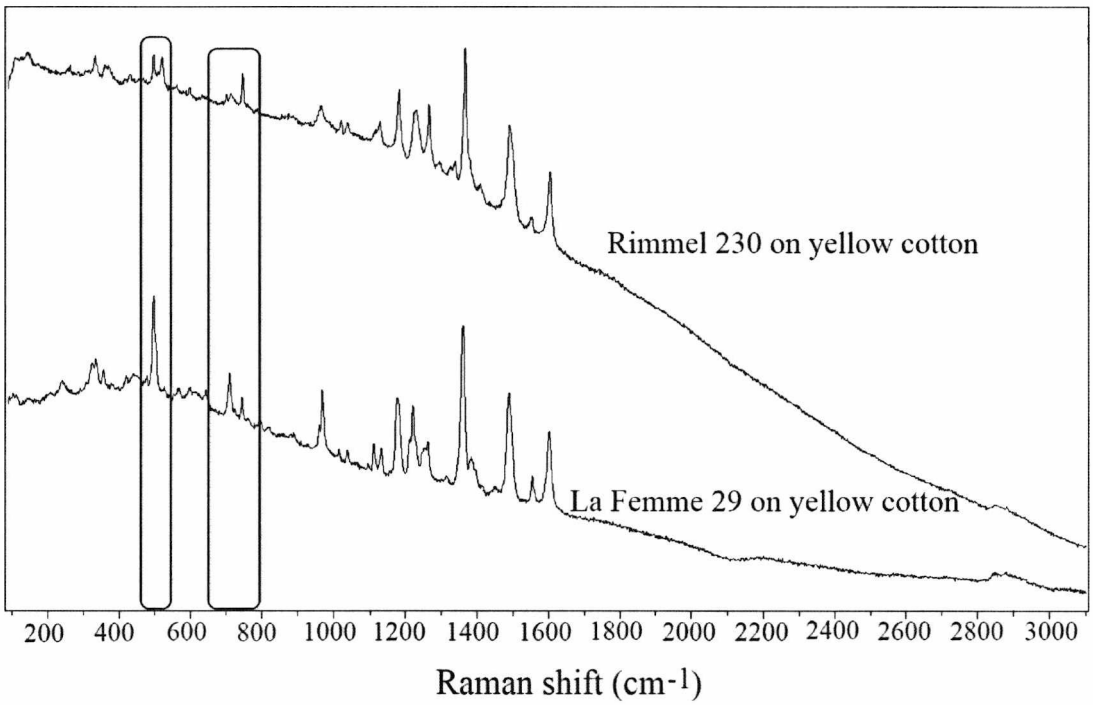

Figure 5.32. Figure comparing the spectra of Rimmel 230 and La Femme 29 on yellow cotton, analysed using the red laser. The main points of difference between the two spectra are marked. It was possible to differentiate between the two lipstick smears.

In cases where the red laser could not be used to obtain spectra from the smears, differentiation of the lipsticks using the blue laser could be achieved (**Fig. 5.33**).

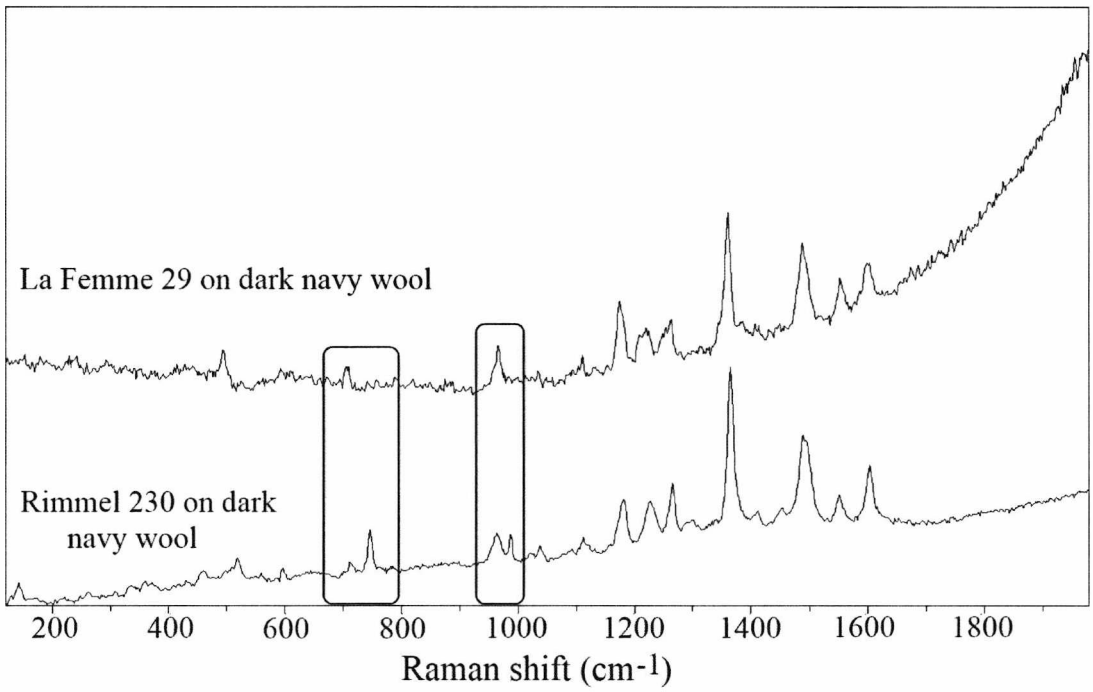

Figure 5.33. Figure comparing the spectra of La Femme 29 and Rimmel 230 on dark navy wool, analysed using the blue laser. The main points of difference between the two spectra are marked.

It was also possible to differentiate between Barry M 101 and Revlon 07 using the red laser when good lipstick spectra could be obtained with this laser (**Fig. 5.34**).

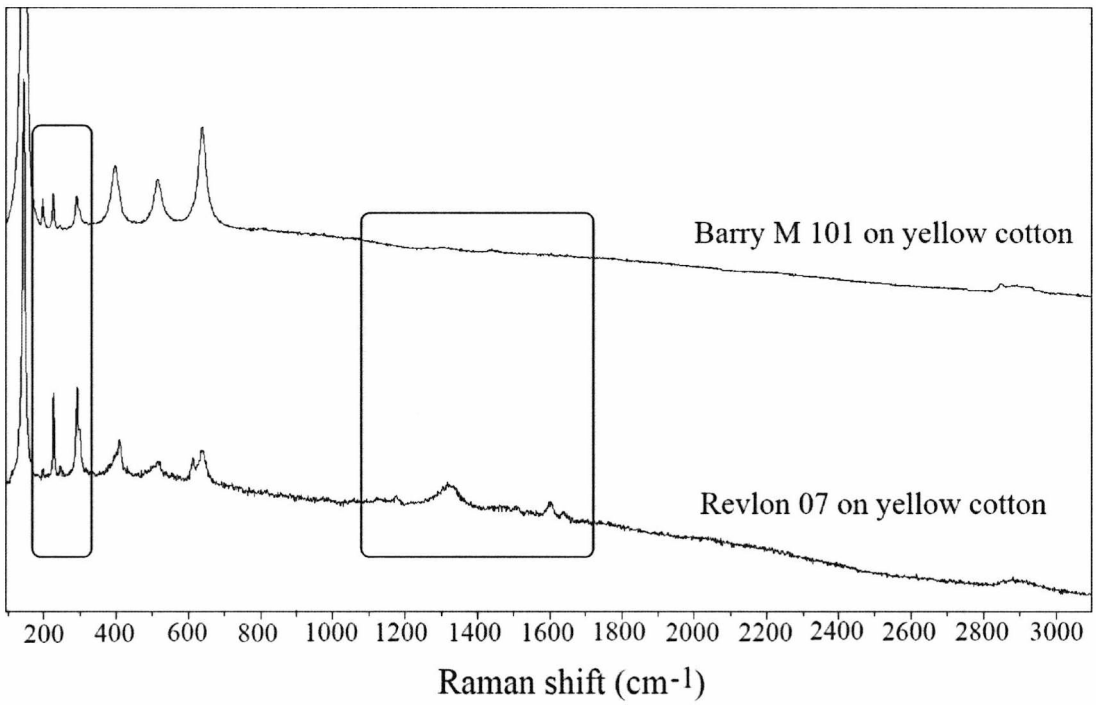

Figure 5.34. Figure comparing the spectra of Barry M 101 and Revlon 07 on yellow cotton, analysed using the red laser. The main points of difference between the two spectra are marked.

In cases where lipstick spectra with discernible peaks could not be obtained with the red laser, spectra obtained using the blue laser were compared and differentiation between the two lipsticks was achieved (**Fig. 5.35**).

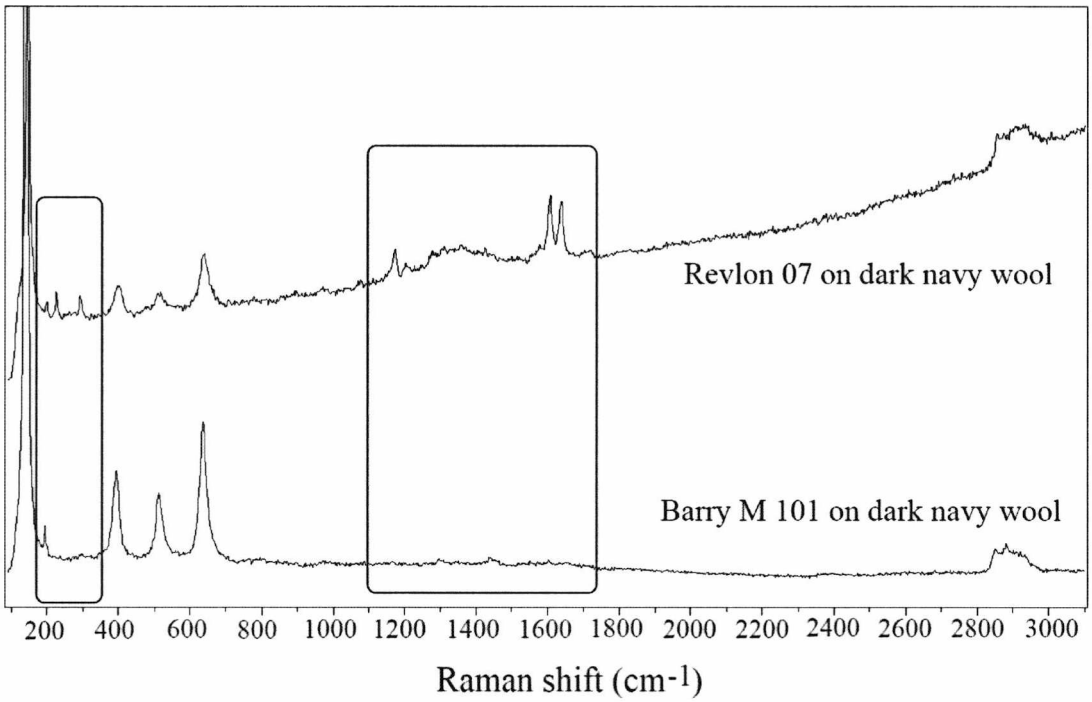

Figure 5.35. Figure comparing the spectra of Revlon 07 and Barry M 101 on dark navy wool, analysed using the blue laser. The main points of difference between the two spectra are marked.

It was found that all of the samples could be analysed and identified when both lasers were used together. It has been shown that it is possible to differentiate between lipsticks with similar spectra even when they are deposited in trace amounts on a variety of fibres. Therefore it has been demonstrated that Raman spectroscopy is a powerful technique for the analysis and differentiation of trace amounts of lipstick smears on fibres.

5.6. Detection of lipstick smears on cigarette butts

5.6.1. Introduction

One of the surfaces lipstick smears are commonly encountered on is cigarette butts, which have been recognised as forensic evidence for a long time. A variety of evidential materials can be found on a cigarette butt, such as saliva, which is used for DNA analysis [249], and fingerprints [250]. Lipstick is easily transferred onto the cigarette butt during smoking, leaving another source of evidence on the butt.

Analysis and identification of these smears can therefore provide valuable information for use in a forensic investigation. Therefore, this part of the study explores the applicability of Raman spectroscopy to the analysis and differentiation of lipstick smears found on cigarette butts.

5.6.2. Methods and materials

The same four lipsticks used in Chapter 5.5 were chosen for this part of the study. These were La Femme 29 'Dream Rose', Rimmel 230 'Red Fever', Barry M 101 'Marshmallow' and Revlon 07 'Cherish'. These lipsticks were chosen because of the similarities in their spectra: La Femme 29 and Rimmel 230 have very similar spectra with some small differences, and Barry M 101 and Revlon 07 have some similarities as well as some differences in terms of their spectra.

Volunteers were asked to smoke cigarettes after putting on a given lipstick. The smoked cigarette butts were then collected and analysed. Spectra of the lipstick smears on cigarette butts, as well as that of 'blank' cigarette butts, were obtained and the results were compared. Each sample was analysed at five different points using the 633 nm laser. The parameters used for each sample are given in **Table 5.3**.

Table 5.3. Table listing the accumulation times, accumulation numbers, confocal hole sizes and the neutral density filter used for each sample.

Lipstick	Cigarette Butt	Accumulation Time (s)	Accumulation Number	Filter Used	Hole size (μm)
La Femme 29	Pall Mall	4	20	D1	100
Rimmel 230	Silk Cut Silver	3	20	D1	100
Revlon 07	Pall Mall	4	20	D1	100
Barry M 101	B&H Silver	2	15	D0.6	100
--	Silk Cut Silver	2	15	D1	200
--	Pall Mall	2	15	D2	200
--	B&H Silver	2	15	D1	200

Every spectrum from each sample is supplied on the accompanying CD.

5.6.3. Results and discussion

The filter of a cigarette is made up of cellulose acetate fibres. Each fibre is treated with titanium dioxide (whitening agent) and over 15000 fibres are packed tightly together to create a single filter. This is then wrapped with paper and/or rayon wrapping, which is also treated with chemicals such as glues and alkali metal salts [251-253].

The analysis of cigarette butts using Raman spectroscopy revealed that the most intense peaks found in their spectra were those of titanium dioxide in anatase form (**Fig. 5.36**).

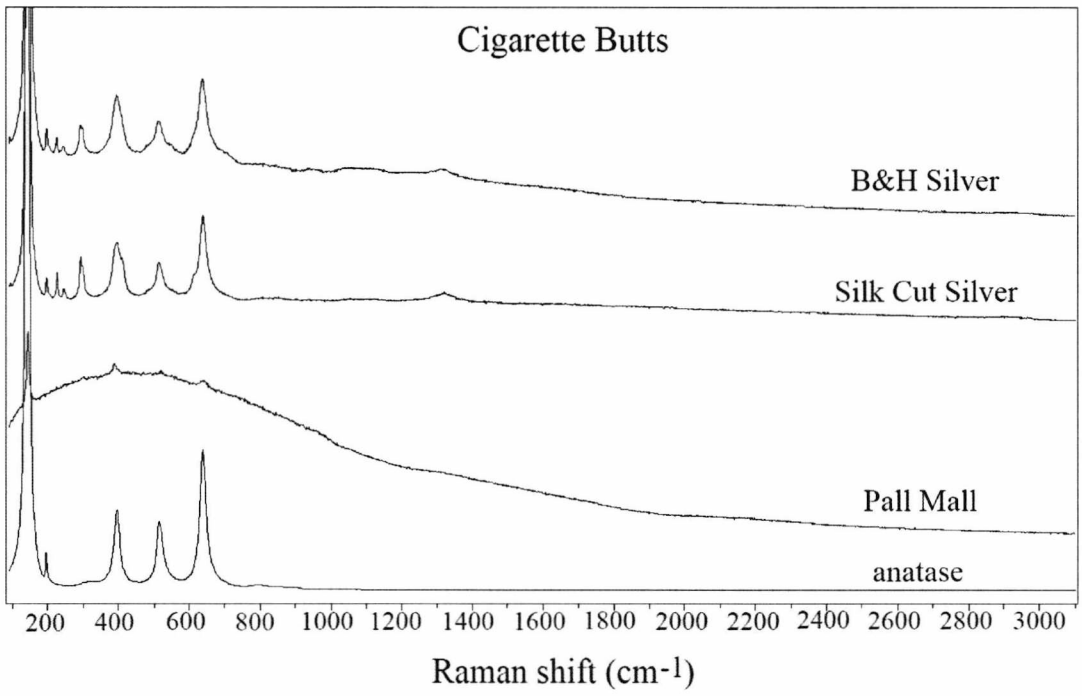

Figure 5.36. Figure comparing the spectra of B&H Silver, Silk Cut Silver and Pall Mall cigarette butts with that of titanium dioxide in anatase form.

The strong presence of titanium dioxide in the spectra of cigarette butts presented a challenge in terms of the analysis of lipsticks that had titanium dioxide as the main peaks in their spectra. **Fig. 5.37** presents the spectrum of Barry M 101 on a B&H Silver cigarette butt.

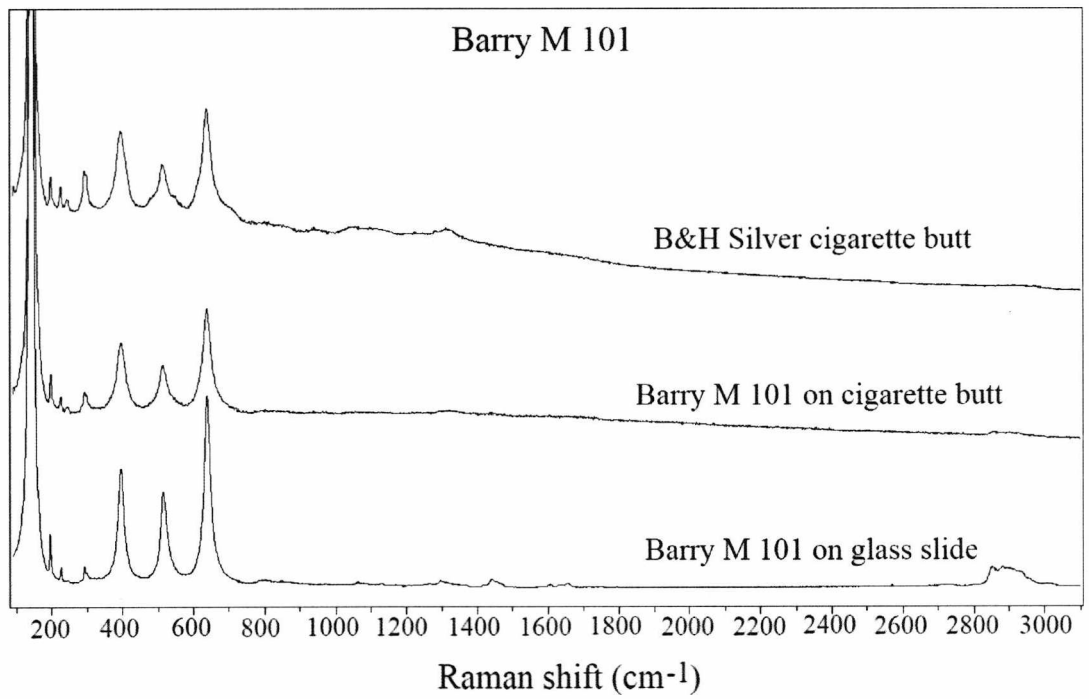

Figure 5.37. Figure comparing the spectra of B&H Silver cigarette butt, Barry M 101 on the cigarette butt and on glass slide.

Due to the similarities between the spectrum of the cigarette butt and the Barry M 101 lipstick, it was not possible to reach a valid conclusion in terms of detection of this lipstick smear on the cigarette butt using Raman spectroscopy.

Revlon 07 was also one of the lipsticks that had titanium dioxide peaks as the major peaks in its spectrum. However, it was still possible to analyse and identify the lipstick smear because the spectrum of the cigarette butt used did not contain strong peaks (**Fig. 5.38**).

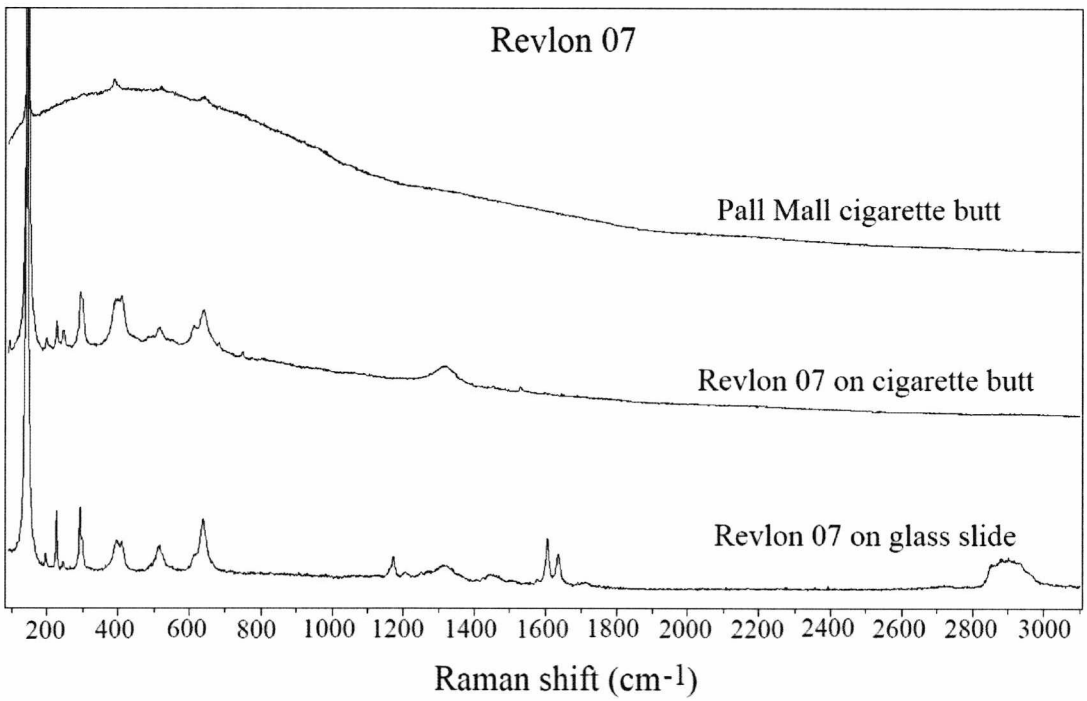

Figure 5.38. Figure comparing the spectra of Pall Mall cigarette butt, Revlon 07 on the cigarette butt and on glass slide.

Even though it was possible to detect the lipstick peaks between 90 and 800 cm^{-1}, some of the characteristic peaks between 1000 and 1800 cm^{-1}, as well as the C-H peaks between 2800 and 3000 cm^{-1}, could not be detected with the smear on the cigarette butt. This selective loss of peaks could be arising from some components reacting with, or soaking into, the cigarette butt; or, as observed with some of the fibres previously, it could be due to the burning or decomposition of the components responsible for those peaks.

With the lipsticks La Femme 29 and Rimmel 230, the spectra of the cigarette butts did not cause as much interference. In the case of La Femme 29, the cigarette butt used did not have strong peaks except for the most intense peak of titanium dioxide at 143 cm^{-1}, which was also detected in the spectrum of the lipstick (**Fig. 5.39**).

In the case of Rimmel 230, even though the spectrum of the cigarette butt contained strong peaks, these did not interfere with the lipstick spectrum, except for the anatase peak at 143 cm^{-1} (**Fig. 5.40**).

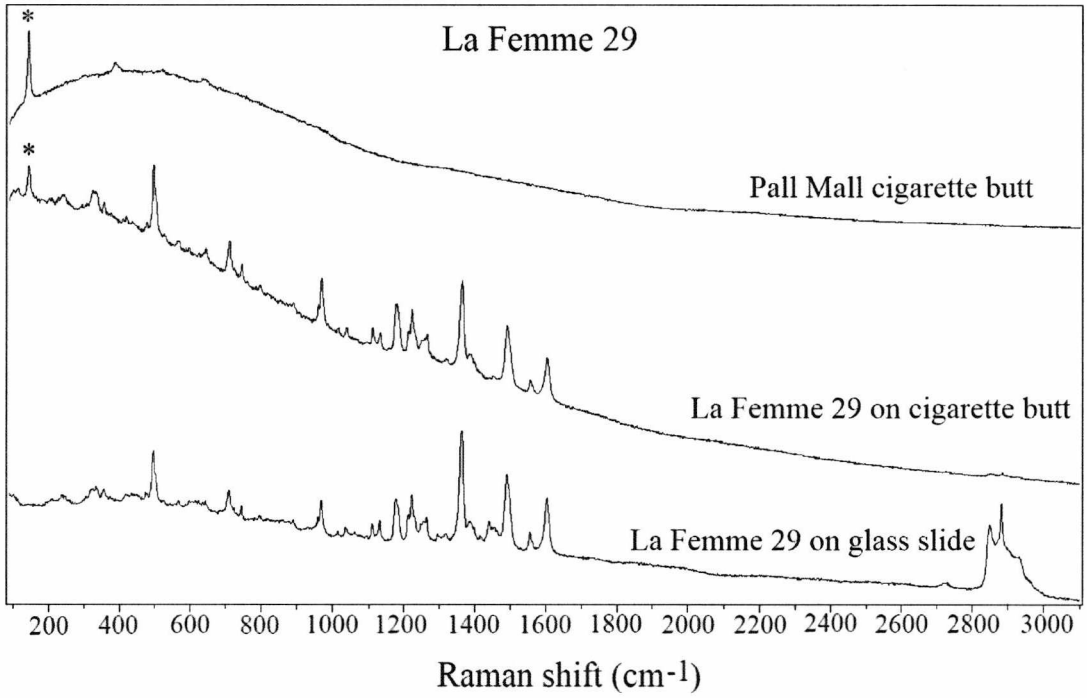

Figure 5.39. Figure comparing the spectra of Pall Mall cigarette butt, La Femme 29 on the cigarette butt and on glass slide. The anatase peak at 143 cm^{-1} that is also observed in the lipstick spectrum is marked with a '*'.

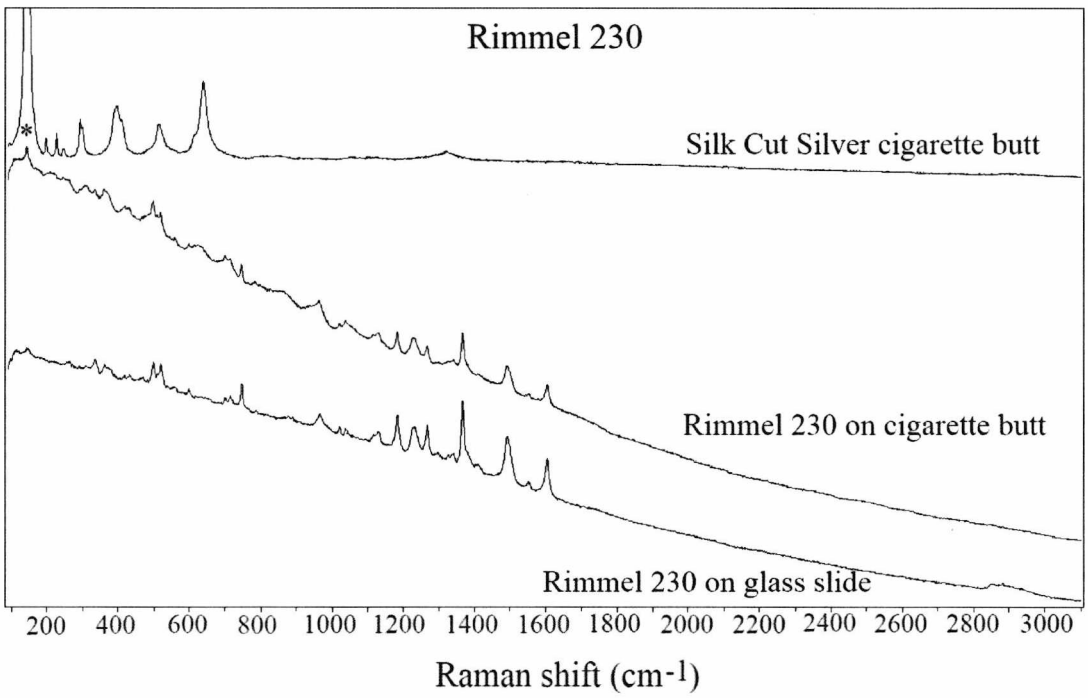

Figure 5.40. Figure comparing the spectra of Silk Cut Silver cigarette butt, Rimmel 230 on the cigarette butt and on glass slide. The intense anatase peak from the cigarette butt at 143 cm^{-1} can be observed in the lipstick spectrum (marked with a '*').

Even though the strong titanium dioxide peaks present in the spectra of the cigarette butts interfered with the analysis of some lipsticks, it was still possible to detect and identify the rest. La Femme 29 and Rimmel 230 lipsticks were chosen because they produced similar spectra with some differences. A comparison of the spectra of these lipsticks on cigarette butts showed that it was possible to differentiate between lipsticks with similar spectra even when they are found on cigarette butts (**Fig. 5.41**).

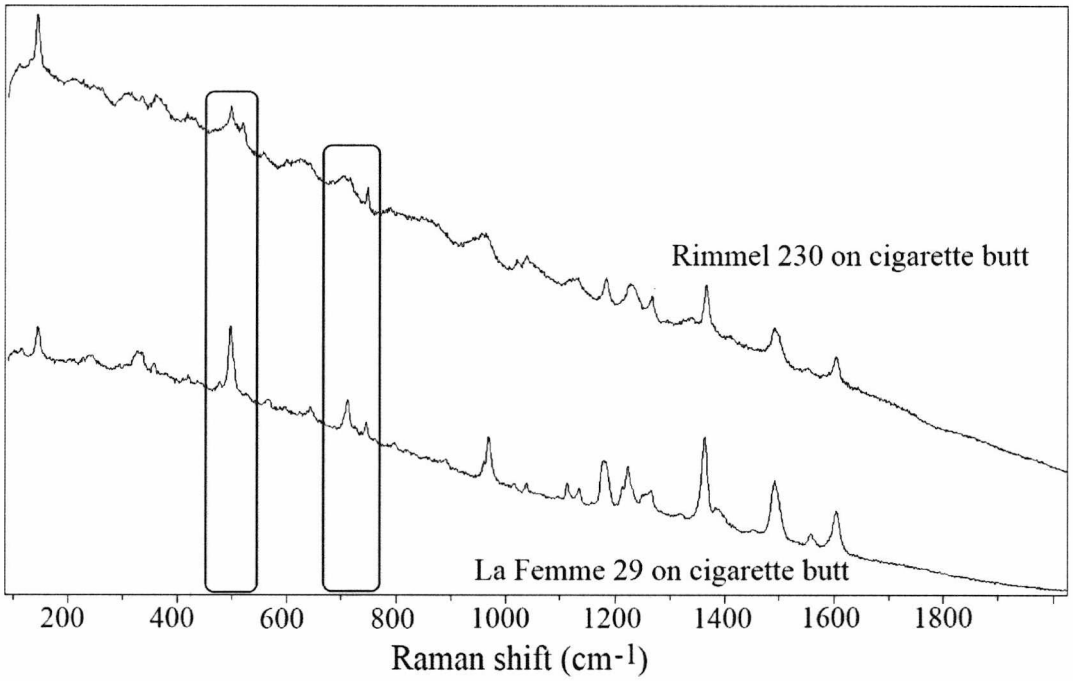

Figure 5.41. Figure comparing the spectra of Rimmel 230 and La Femme 29 on cigarette butts. The main points of difference between the two lipsticks are highlighted in the boxes.

It was shown that it is possible to analyse and differentiate between lipstick smears found on cigarette butts using Raman spectroscopy. However, care must be taken when lipsticks with strong anatase peaks are concerned since the cigarette butts display strong anatase peaks as well. Therefore, it is concluded that the presence (or absence) of anatase peaks should not be used as a discriminator when trying to match an unknown lipstick found on a cigarette butt.

5.7. Detection of lipstick smears on tissues

5.7.1. Introduction

Tissues and handkerchiefs are frequently used in daily life. Lipstick smears can be transferred onto tissues when the mouth is wiped onto the tissue after a meal or when tissues are used to remove makeup. Therefore the identification and characterisation of lipstick smears on tissues could potentially aid in a forensic investigation by linking the evidence to a suspect or a victim.

This part of the study explores the applicability of Raman spectroscopy to the analysis and differentiation of lipstick smears found on tissues.

5.7.2. Methods and materials

The lipsticks used for this study were La Femme 29, Rimmel 230, Barry M 101 and Revlon 07. As mentioned in the previous sections, these lipsticks were chosen due to the similarities in their spectra. Each sample was prepared by lightly dabbing a piece of tissue (Tempo Petit Jasmine Handkerchiefs) onto the lips with lipstick on. Spectra were taken from five different positions on each sample using the 633 nm laser. Both the 'blank' tissue and the lipstick smear on the tissue were analysed and compared. The parameters used for each sample are given **Table 5.4**.

Table 5.4. Table listing the accumulation times, accumulation numbers, confocal hole sizes and the neutral density filter used for each sample.

Sample	Accumulation Time (s)	Accumulation Number	Filter Used	Hole size (μm)
Blank tissue	3	20	--	200
La Femme 29 on tissue	3	20	D0.3	100
Rimmel 230 on tissue	3	20	D0.6	100
Barry M 101 on tissue	3	20	D0.3	100
Revlon 07 on tissue	4	20	D0.6	100

Every spectrum from each sample is presented on the accompanying CD.

5.7.3. Results and discussion

The Raman spectrum of the blank tissue displayed peaks that arose from cellulose found in the makeup of the tissue (**Fig. 5.42**). The peaks at 380, 1098 and 2900 cm^{-1} are characteristic peaks of cellulose [254].

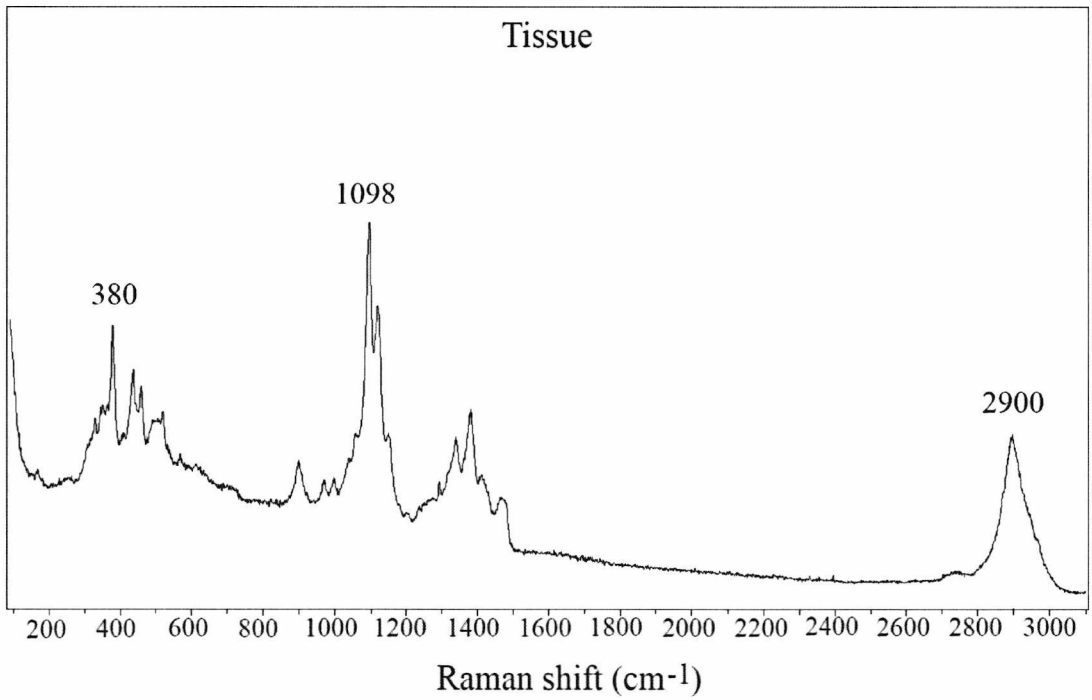

Figure 5.42. Raman spectrum of Tempo Petit Jasmine Handkerchief.

Despite some interference from the tissue, Raman spectra of the lipstick smears could still be obtained. La Femme 29 and Rimmel 230 lipsticks were easier to analyse on the tissues and they produced spectra without interference from the underlying tissue (**Fig. 5.43** and **5.44**).

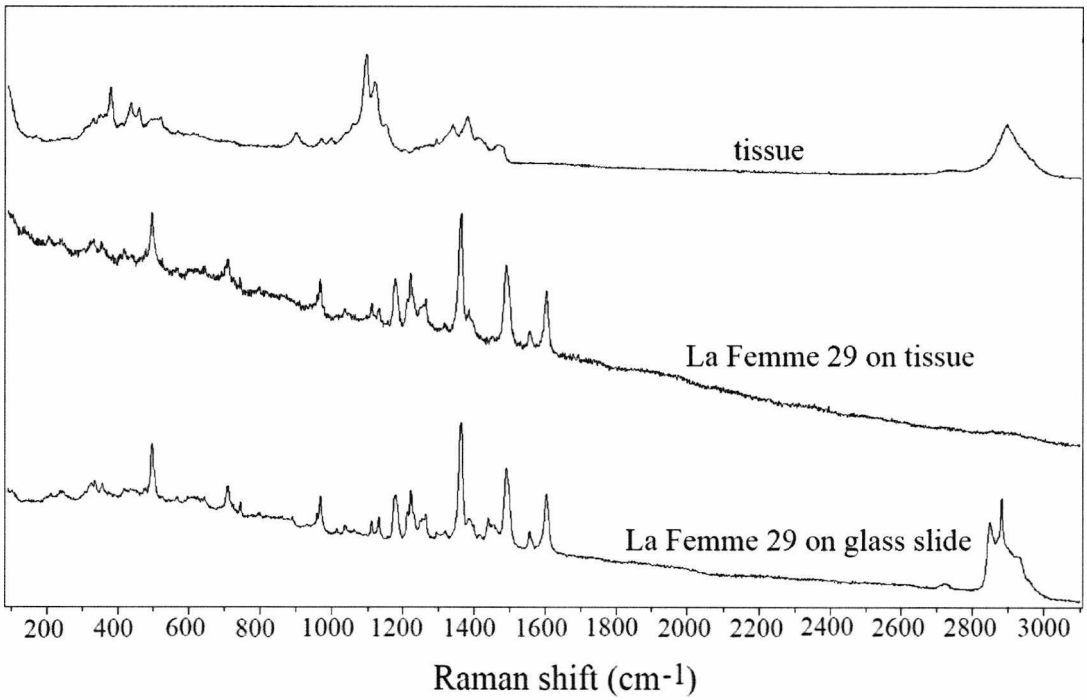

Figure 5.43. Figure comparing the Raman spectra of the tissue, La Femme 29 on the tissue and on glass slide.

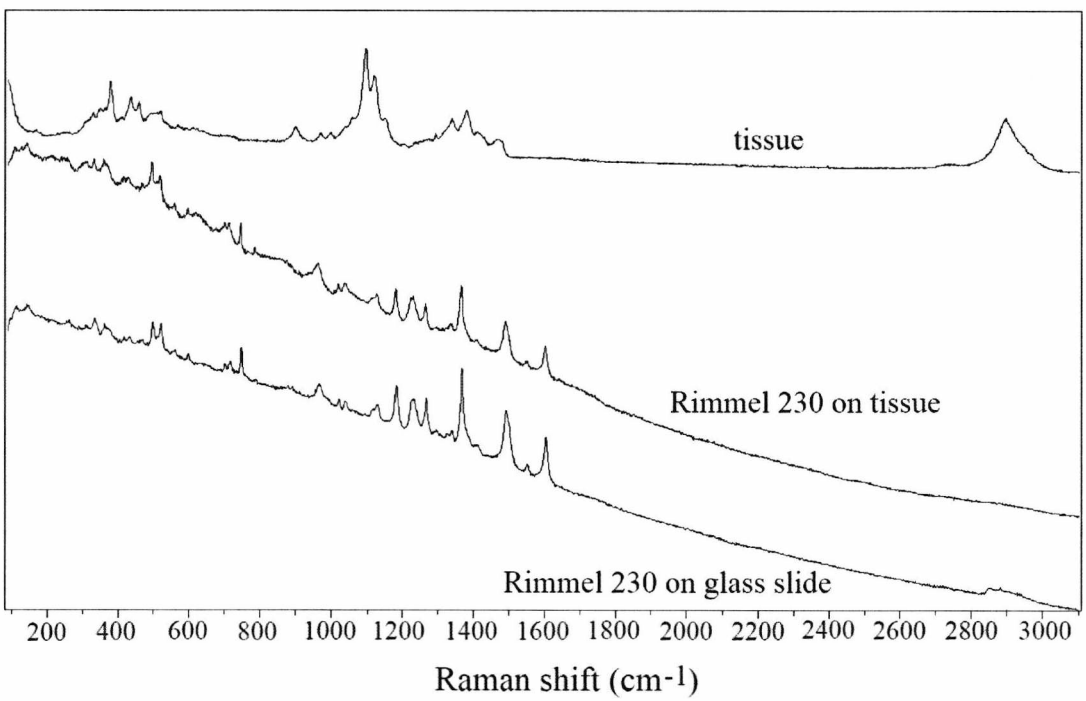

Figure 5.44. Figure comparing the Raman spectra of the tissue, Rimmel 230 on the tissue and on glass slide.

The disappearance of the C-H peaks between 2800 and 3000 cm^{-1} was also observed with these samples. When the spectra for the two lipstick smears on tissues were compared, it was possible to differentiate between the two lipsticks (**Fig. 5.45**).

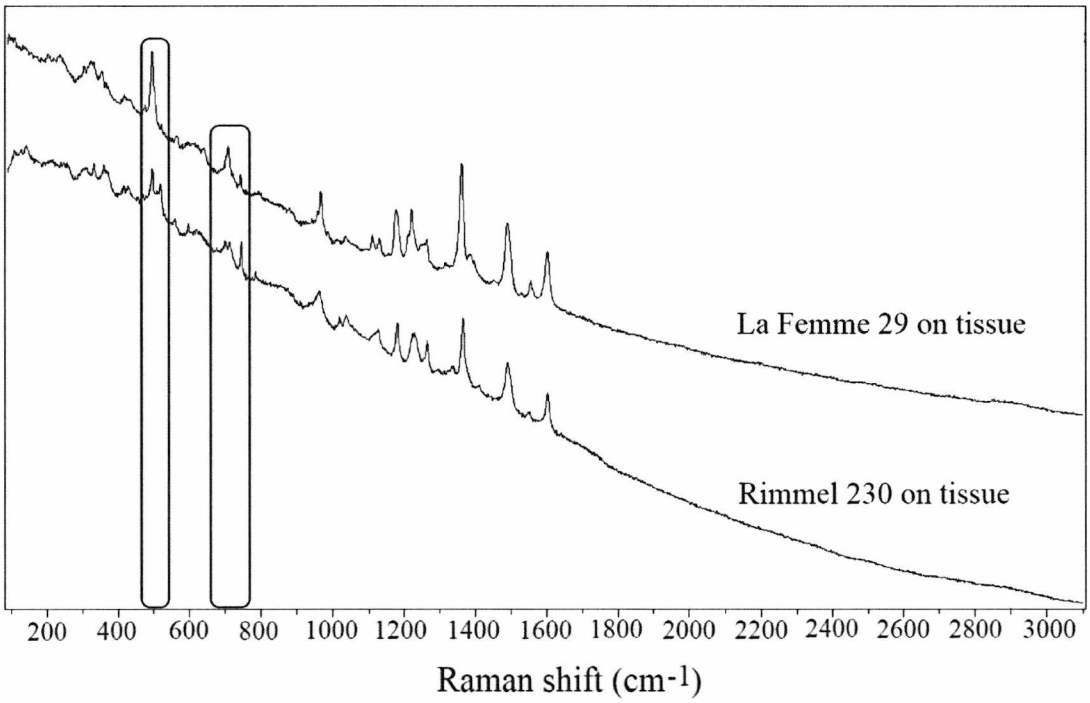

Figure 5.45. Figure comparing the spectra of La Femme 29 and Rimmel 230 on tissues. The main points of difference between the two lipstick spectra are indicated.

The Barry M 101 lipstick could also be analysed without much interference from the tissue (**Fig. 5.46**). However, it was more difficult to obtain a good spectrum of Revlon 07 on the tissue. Some of the characteristic peaks of this lipstick between 1100 and 1700 cm^{-1}, and the C-H bond vibrations between 2800 and 3000 cm^{-1} could not be detected when the smear deposited on the tissue was analysed (**Fig. 5.47**). This effect was also observed when this lipstick smear was deposited on cigarette butts (**Chapter 5.6**).

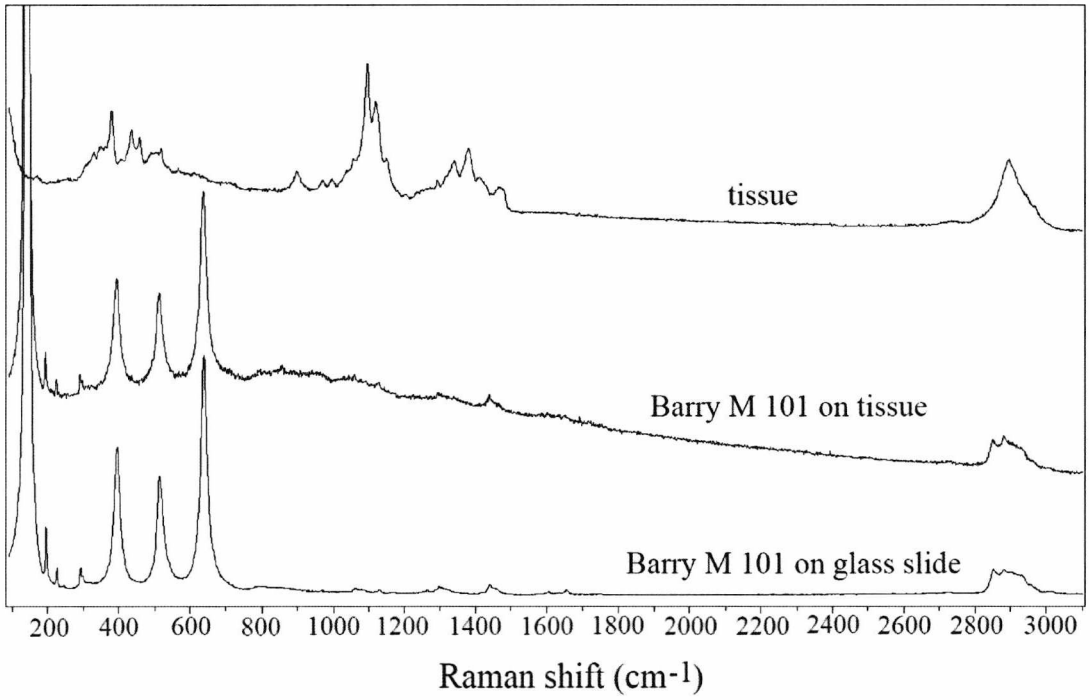

Figure 5.46. Figure comparing the Raman spectra of the tissue, Barry M 101 on the tissue and on glass slide.

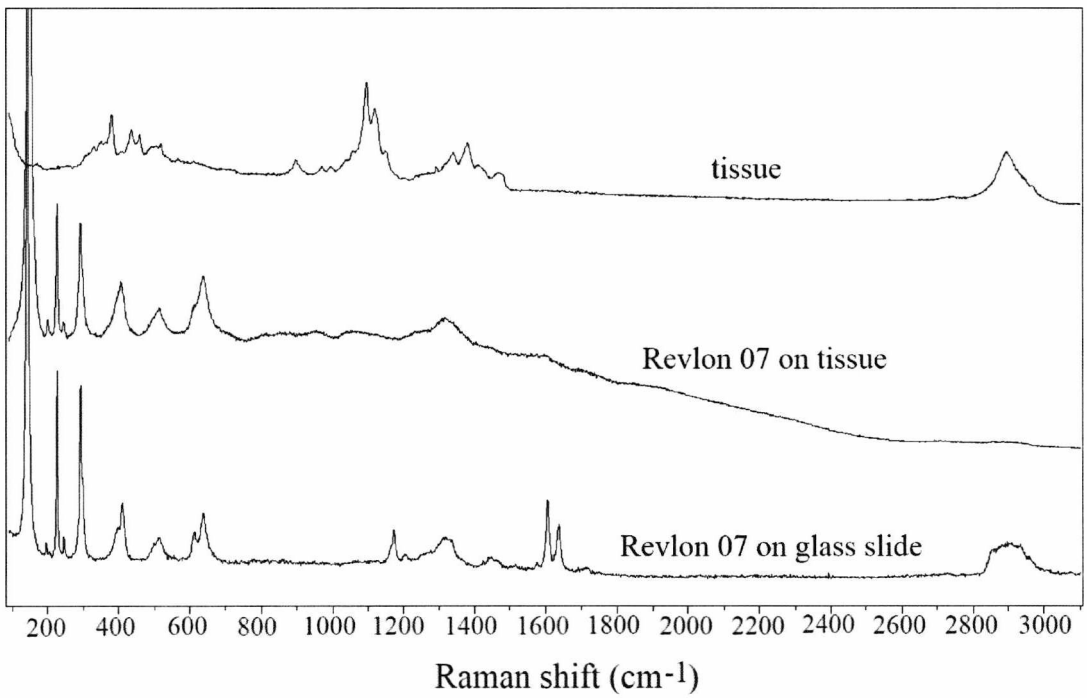

Figure 5.47. Figure comparing the Raman spectra of the tissue, Revlon 07 on the tissue and on glass slide. The characteristic peaks of the lipstick between 1100 and 1700 cm^{-1} could not be observed.

Despite the difficulty in obtaining a characteristic spectrum for the lipstick Revlon 07, it was still possible to differentiate between the smears of Barry M 101 and Revlon 07 deposited on tissues (**Fig. 5.48**).

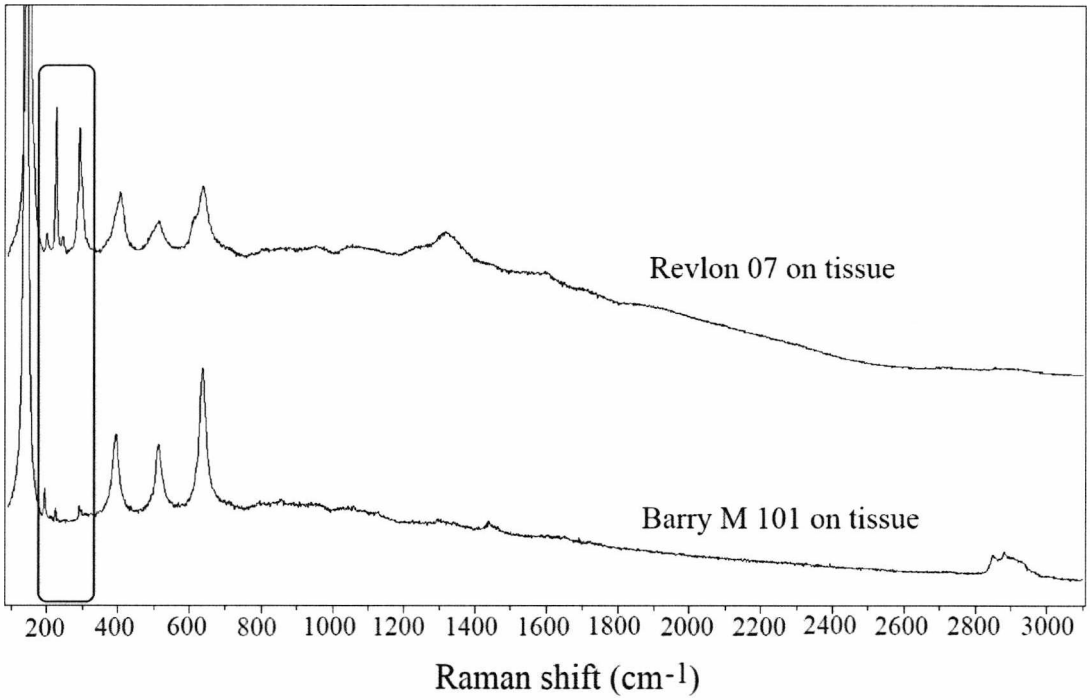

Figure 5.48. Figure comparing the spectra for Revlon 07 and Barry M 101 on the tissue. One of the main points of difference between the two is indicated.

Therefore, it has been shown that it is possible to analyse lipstick smears deposited from lips onto tissues with little or no interference from the underlying tissue. It has also been demonstrated that differentiation can be achieved between lipstick smears (with similar spectra) deposited on tissues using Raman spectroscopy.

5.8. Analysis of lipstick smears through evidence bags

5.8.1. Introduction

In forensic science, it is very important to preserve the integrity of evidential material. Recovered evidence is stored in evidence bags to allow secure transit and to preserve the chain of custody. It is therefore extremely valuable to be able to analyse

the evidence without removing it from the evidence bag in order to minimise the risk of contamination.

Raman spectroscopy is a powerful technique that can be used to identify materials by looking at their characteristic spectral patterns. It is a non-contact technique that can analyse samples contained within packaging materials and evidence bags that are transparent to the exiting laser [99, 100, 170, 171].

This part of the study looks at the applicability of Raman spectroscopy to the analysis of lipstick smears found on glass slides, cigarette butts and tissues through evidence bags.

5.8.2. Methods and materials

The evidence bag used in this study was a polyethylene Tek-Niche Police Evidence Bag (a standard evidence bag, kindly donated by the Kent Police) and the lipstick used was La Femme 29. Each sample was placed in the evidence bag and analysed under the Raman microscope without any sample preparation or treatment (**Fig. 5.49**). Each sample was analysed using the 633 nm laser and a ×50 objective lens. Five spectra were obtained from different parts of each sample. The spectra are supplied on the accompanying CD.

The samples prepared and analysed were: La Femme 29 lipstick smear on a glass slide, La Femme 29 lipstick smear on a Pall Mall cigarette butt, and La Femme 29 lipstick smear on a piece of Tempo Petit Jasmine Handkerchiefs tissue. The parameters used for each sample are given in T**able 5.5**.

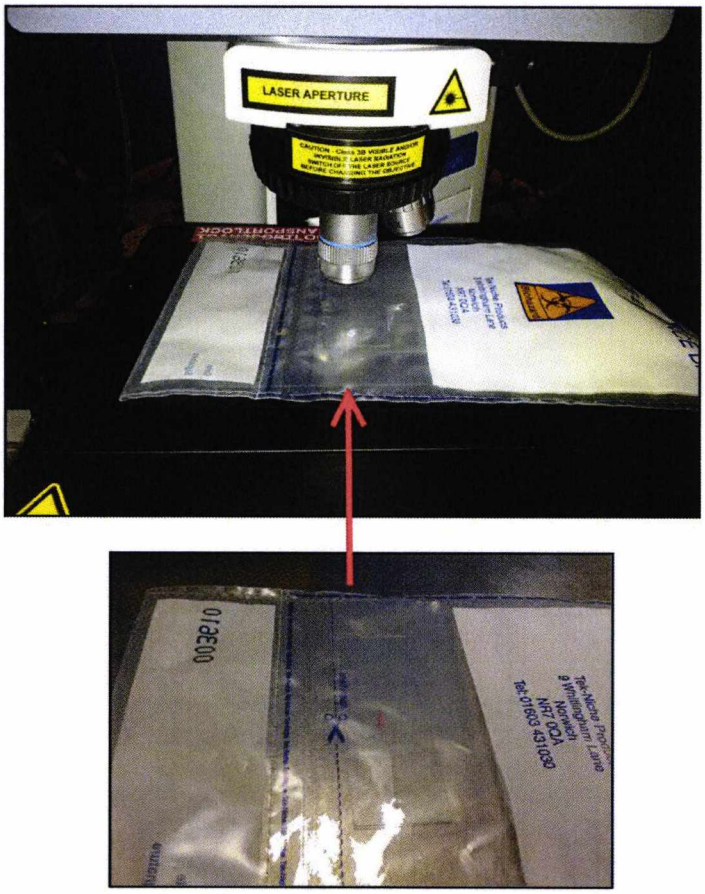

Figure 5.49. A picture showing how the samples were prepared and analysed. In the picture, the lipstick smear on a glass slide was placed in the clear part of the evidence bag, which was then placed on the microscope stage for analysis.

Table 5.5. Table listing the accumulation times, accumulation numbers, confocal hole sizes and the filter used for each sample.

Sample	Accumulation Time (s)	Accumulation Number	Filter Used	Hole size (μm)
Evidence bag	4	20	D0.6	100
La Femme 29 on glass slide, through bag	5	25	--	100
La Femme 29 on cigarette butt, through bag	4	20	D1	100
La Femme 29 on tissue, through bag	5	25	--	100

5.8.3. Results and discussion

The polyethylene evidence bag displayed strong Raman peaks. However, this could mostly be avoided by ensuring that the laser was properly focused on the sample rather than the evidence bag. The laser was focused through the clear part of the evidence bag. It was easier to focus on the sample when the sample and the bag were not in contact with each other. However, a large gap between the sample and the bag resulted in less intense Raman signals being acquired from the sample. In cases where the sample was in contact with the evidence bag, very small interference from the polyethylene bag was observed.

Figure 5.50 compares the spectrum of La Femme 29 on glass slide with and without the evidence bag. The lipstick smear could easily be detected and identified through the evidence bag without interference from the polyethylene peaks.

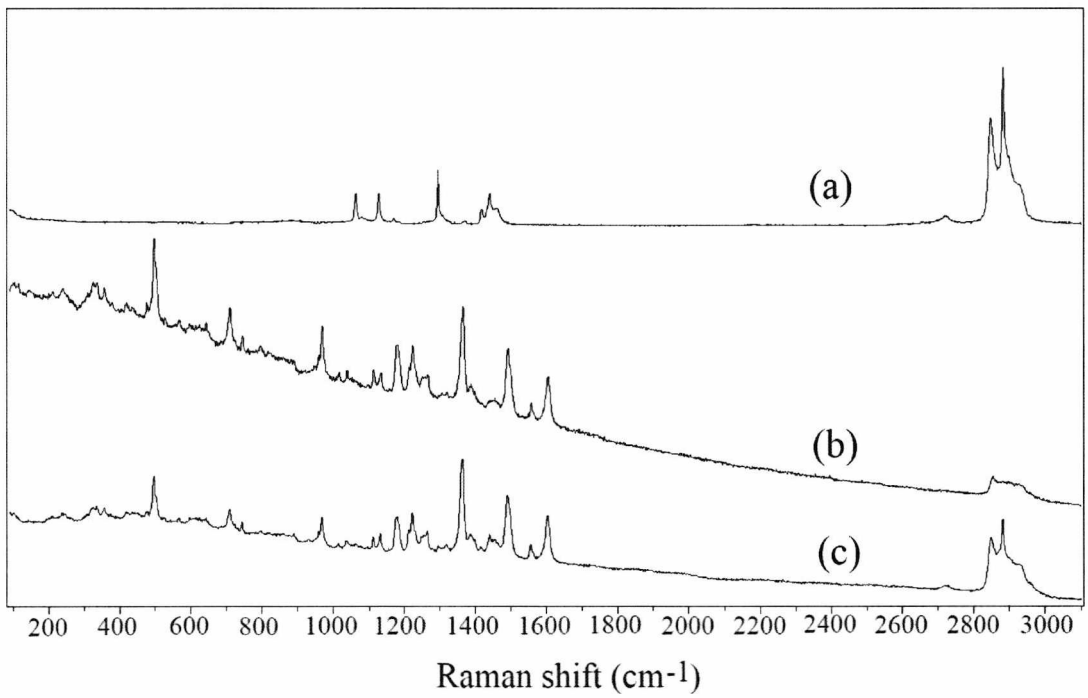

Figure 5.50. (a) Spectrum of the evidence bag (polyethylene) **(b)** Spectrum of La Femme 29 on glass slide through the evidence bag **(c)** Spectrum of La Femme 29 on glass slide without the evidence bag.

During the analysis of the smear deposited on the cigarette butt, the evidence bag frequently came in contact with the cigarette butt. Therefore, the spectra obtained of the lipstick smear had some interference from the evidence bag (as indicated in **Fig. 5.51**).

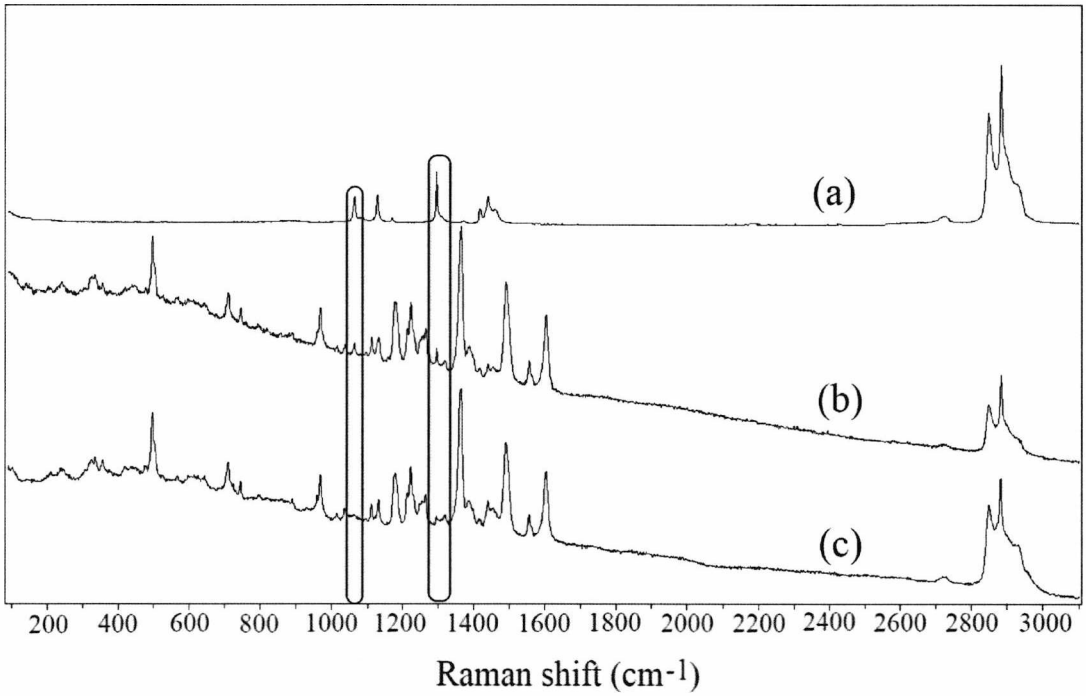

Figure 5.51. (a) Spectrum of the evidence bag **(b)** Spectrum of La Femme 29 on cigarette butt through evidence bag **(c)** Spectrum of La Femme 29 on glass slide without the evidence bag. Polyethylene peaks can be detected in the lipstick spectrum analysed through the bag (as marked).

Figure 5.52 shows the spectrum of La Femme 29 on a tissue analysed through the evidence bag. Even though the Raman signals from the lipstick are less intense, a comparison with the lipstick on glass slide shows that it can still be identified as La Femme 29.

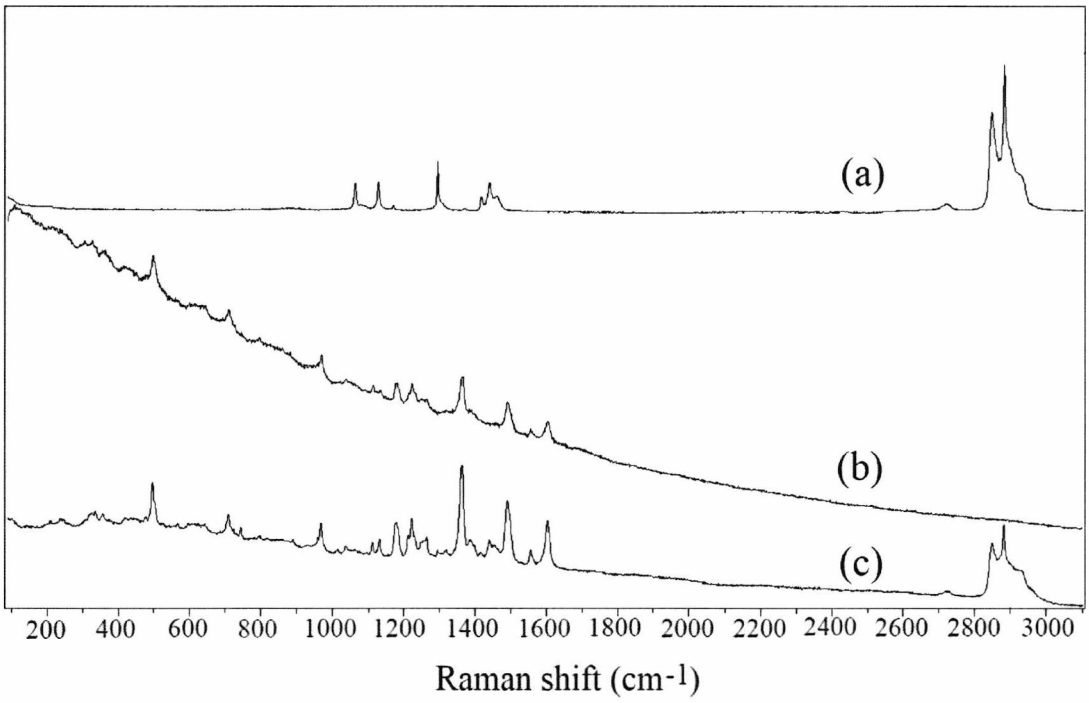

Figure 5.52. (a) Spectrum of the evidence bag **(b)** Spectrum of La Femme 29 on tissue through evidence bag **(c)** Spectrum of La Femme 29 on glass slide without the evidence bag.

Therefore, this study demonstrated the applicability of Raman spectroscopy to the analysis of lipstick smears on different media, such as glass slides, cigarette butts and tissues, through police evidence bags.

5.9. Summary

The study presented in this section has demonstrated that the Raman spectra obtained are independent of the instrument used. Use of different excitation wavelengths were shown to help with the discrimination of fluorescent lipstick samples. Some lipstick samples were found to be prone to getting damaged with high power lasers, so neutral density filters were used where necessary. It was found that the use of a higher resolution diffraction grating did not help differentiate between lipsticks with similar spectra. It was demonstrated that the majority of the lipstick spectra did not change over time, and the only change observed was the decrease in the intensity of peaks at 1655 and 3011 cm^{-1}, which were attributed to C=C and (=CH) vibrations of the waxy composition of lipsticks.

This study has also demonstrated the viability of using Raman spectroscopy for the analysis and differentiation of trace amounts of lipstick smears on potential crime scene surfaces and materials such as fibres, cigarette butts and tissues, even through evidence bags. It was found that lipstick smears on these surfaces could be analysed and identified using Raman spectroscopy with little or no interference from the underlying media.

5.10. Use of chemometrics for the characterisation of lipstick spectra

(The following work was carried out in collaboration with Dr. Stuart J. Gibson at the University of Kent, Canterbury.)

5.10.1. Introduction

Modern Raman spectrometers can acquire a large number of high quality spectra in a very short amount of time, decreasing the analysis time and leading to quick identification of samples. However, this also means that a large volume of data is collected that needs to be analysed and characterised.

Quick and reliable analysis of large amounts of data can be achieved by applying chemometrics to the data. Chemometrics is a discipline that applies mathematical and statistical methods to the solution of chemical problems [244].

Raman spectroscopy combined with chemometrics is becoming a widespread technique for the analysis and characterisation of a variety of materials across a range of disciplines. Studies on the application of chemometric methods to the analysis of spectra include discrimination of carbon nanotubes [255], detection of counterfeit medicines [256], discrimination between authentic and counterfeit banknotes [257], quantitative analysis of narcotics in mixtures [258, 259], discrimination between synthetic and natural artist's pigments [260] as well as historic pigments used in ancient paintings [261], and forensic analysis of paint samples [262] and lipsticks [3].

Spectroscopic methods provide data on many components of a single sample. Different bonds within the sample give peaks at different Raman shifts (cm^{-1}). These shifts collectively form a spectrum which is the fingerprint of the analysed sample. This Raman fingerprint contains vibrational information on all components of the sample. Also, a Raman spectrum is typically recorded over hundreds of wavenumbers. This means that there are hundreds of data points, each with their own measurement of wavenumbers and intensity values. Therefore each Raman spectrum provides a large amount of data for a single sample. When more than one measurement can be made on a single specimen, such as in a Raman spectrum, multivariate data is obtained [244, 263].

If each Raman shift (i.e. wavenumber point, m) is considered as having its own dimension with its own wavenumber and intensity measurements, then for n number of spectra, each Raman shift would exist at a specific position in an n-dimensional space. For n number of spectra, this would give an enormous amount of data with a large number of dimensions. It is extremely difficult to visualise such a large number of dimensions. Therefore, a data reduction method is required to reduce the dimensionality of the multivariate data.

One of the most commonly used techniques for data reduction is principal components analysis (PCA). PCA is a technique that reduces the number of dimensions without significant loss of the original information. It calculates a new set of uncorrelated variables called principal components (PCs) from the original set of variables (i.e. each wavenumber is a variable). The PCs can be thought of as vectors in multidimensional space, each one representing an axis. So, the first PC is created along the direction that has the largest variance within the data; the second PC is created at a right angle to the first PC along the direction with the second largest variance and so on. This results in PCs that are orthogonal to each other. There can be as many PCs created as the number of data in the data set[1]. However, the way the PCs are calculated means that the first few PCs will account for the

[1] i.e. m, which is the number of variables (wavenumbers), or n, which is the number of observations (spectra). In this study, m is greater than n, so there can be at most n number of PCs created.

majority of the variation in the data while still containing the original information. By choosing only these significant (or 'useful') PCs, the amount of data is reduced to the number of PCs chosen [244, 263, 264].

The PCs are calculated using matrix algorithms. The original spectrum is treated as a multivariate data matrix and its covariance matrix is calculated. This is a square matrix which gives the relationship between the dimensions in the data, and how they vary from the mean of the data with respect to each other. The formula for calculating the covariance is given as:

$$cov(X,Y) = \frac{\sum_{i=1}^{n}(X_i - \bar{X})(Y_i - \bar{Y})}{(n-1)}$$

where X and Y are the dimensions of the data; n is the number of samples; $\bar{X}$ is the mean of data in the X dimension; and $\bar{Y}$ is the mean of the data in the Y dimension. To form a covariance matrix, the covariance between data in each dimension is calculated and put in the form of a matrix. If the variables in the raw data change dramatically (for example, if the absolute intensity values for each wavenumber differ greatly between spectra of the same sample due to a fluorescent baseline), then the raw data must first be standardised. Otherwise, if one variable has a greater variance, it will dominate the first principal component (PC) created. Standardising makes all variables carry equal weight. Data is standardised by calculating the correlation matrix instead of the covariance matrix. Correlation gives the amount of linear relationship between variables and its values vary from -1 to +1, where a negative value represents a negative link between the variables (i.e. when one variable increases, the other one decreases), and a positive value represents a positive link (i.e. when one variable increases, the other increases too). Correlation is calculated by taking the square root of the covariance between two variables, and dividing it by the product of their variances (i.e. standard deviation squared gives variance) [244, 263-265]. In this study, the correlation matrix of the data was used.

Algorithms are then used to determine eigenvectors within the matrix. Eigenvectors are vectors that, when multiplied by the matrix, give an integer multiple of the original vector.

So, matrices and vectors are multiplied in this way:

$$\underset{\text{Matrix}}{\begin{pmatrix} A & B \\ C & D \end{pmatrix}} \times \underset{\text{Vector}}{\begin{pmatrix} P \\ Q \end{pmatrix}} = \begin{pmatrix} (A \times P) + (B \times Q) \\ (C \times P) + (D \times Q) \end{pmatrix}$$

Therefore, the example matrix and the vector below will be multiplied giving:

$$\begin{pmatrix} 2 & 3 \\ 2 & 1 \end{pmatrix} \times \begin{pmatrix} 3 \\ 2 \end{pmatrix} = \begin{pmatrix} (2 \times 3) + (3 \times 2) \\ (2 \times 3) + (1 \times 2) \end{pmatrix} = \begin{pmatrix} 12 \\ 8 \end{pmatrix}$$

The resultant vector $\begin{pmatrix} 12 \\ 8 \end{pmatrix}$ is a multiple of the original vector $\begin{pmatrix} 3 \\ 2 \end{pmatrix}$:

$$\begin{pmatrix} 12 \\ 8 \end{pmatrix} = 4 \times \begin{pmatrix} 3 \\ 2 \end{pmatrix}$$

Therefore, $\begin{pmatrix} 3 \\ 2 \end{pmatrix}$ is an eigenvector that has been multiplied by a constant, 4, which is called the eigenvalue. Eigenvectors give the principal components (PCs) of the correlation matrix and the size of each PC is given by the corresponding eigenvalue. The larger the eigenvalue, the more variation the eigenvector (or the PC) accounts for [244, 265].

As a result of PCA, a scree plot can be obtained that shows the amount of variance (given by the eigenvalues) described by each principal component. From this plot the number of 'useful' PCs can be determined by looking at how much of the variance they account for. Usually, the first few PCs account for the majority of the variance; hence they have the highest eigenvalues. **Fig. 5.53** shows an example scree plot. The elbow of the scree plot (as marked) indicates the cut off point for the number of useful PCs.

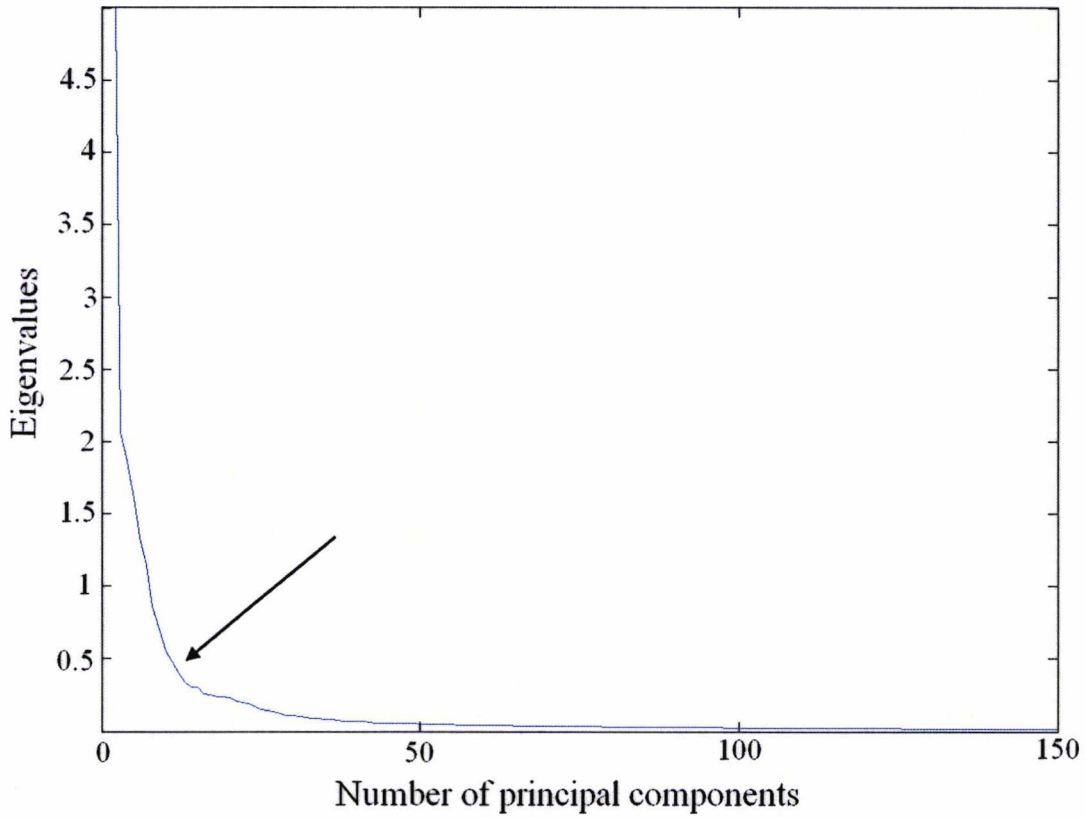

Figure 5.53. A scree plot of eigenvalues against the number of principal components. The first few PCs account for the majority of the variation in the data. The elbow (shown by the arrow) indicates the number of useful PCs.

By choosing only the PCs that account for the majority of the variation in the data, reduction of the dimensionality of the original data is achieved. Therefore, if the first three components are responsible for the majority of variation, then the data can be plotted in three dimensions i.e. along the axes of the first three principal components. Each observation (i.e. spectrum) can then be represented as a point in the multidimensional space defined by the chosen PCs. These points indicate the 'score' of each spectrum on each of the PCs.

The resultant plot may reveal patterns within the original data that were otherwise undetectable. In a PCA plot, samples can group together on the basis of the similarity of their spectra, and formation of separate groups can help differentiate between the samples (**Fig. 5.54**) [244, 263].

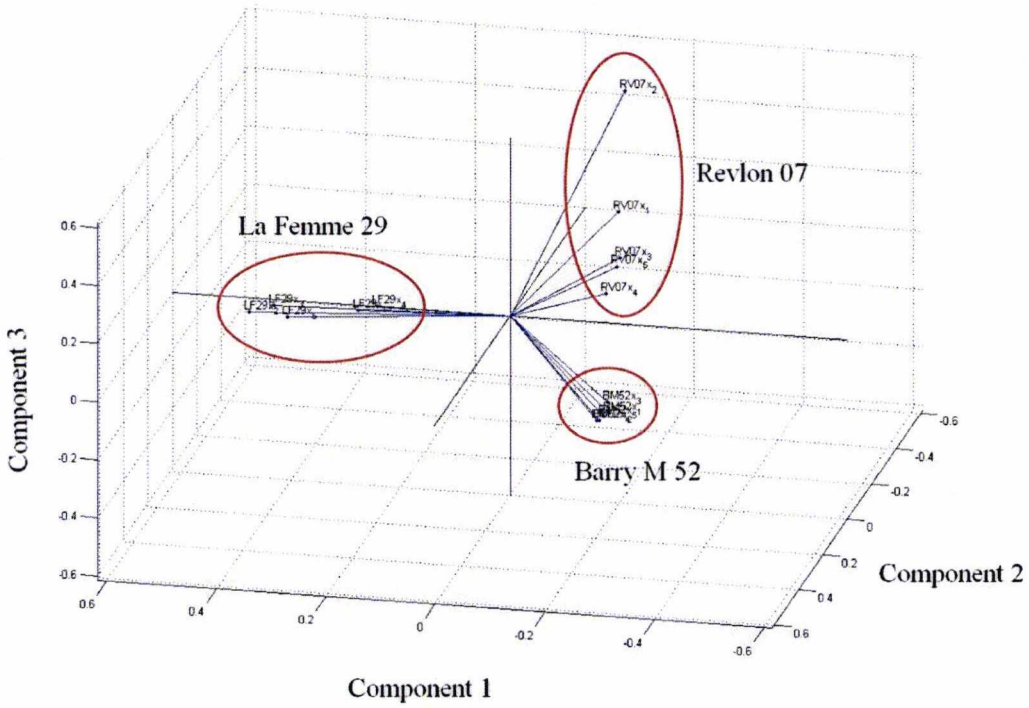

Figure 5.54. An example three dimensional PCA plot of five spectra each from three different lipsticks. The scores for the first three principal components per sample were plotted. Distinct grouping of lipsticks of the same brand can be seen as circled in red.

In **Figure 5.54**, each point with a name attached to it represents the spectrum of a lipstick that has undergone PCA and has been plotted in three dimensions using the scores of each spectrum on the first three principal components. Each spectrum per lipstick can be seen grouped closely together, and separate from the other two lipsticks in the three dimensional space.

Several classifier methods exist that can classify an unknown spectrum, which then helps with the identification of the unknown by determining the group it belongs to. An example method is the *K*-Nearest Neighbours (KNN) classifier. KNN is a method that classifies samples by looking at their distance to the surrounding neighbours. For example, if an unknown is analysed by PCA and plotted with groups of other samples, KNN will measure the distance of the unknown to the samples around it in the plot. If the nearest number of neighbours, *K*, is set to five, the unknown will be put in the same class as its nearest five neighbours. In the case of more than one class of neighbours being present, the unknown is classified by a

majority voting rule which puts the unknown in the same class as the majority of its K nearest neighbours (**Fig. 5.55**) [244, 263].

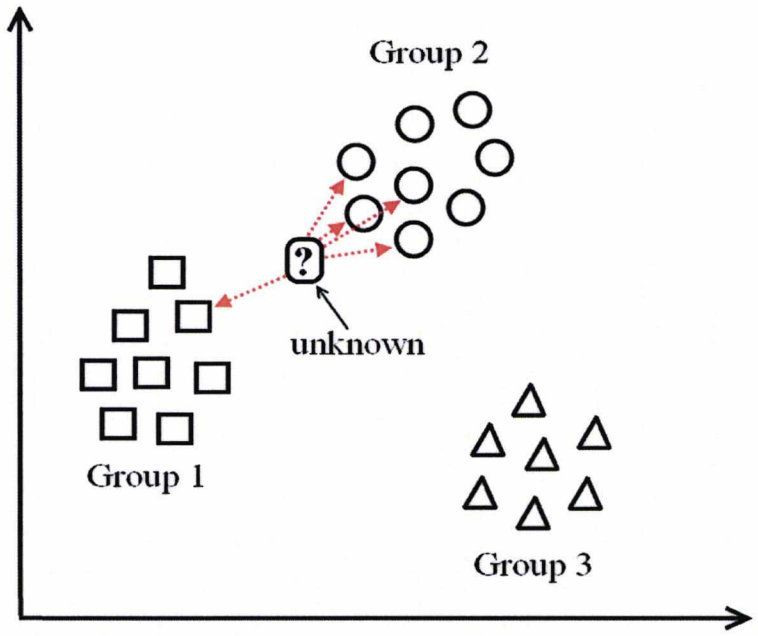

Figure 5.55. An example plot showing how KNN method classifies unknown samples.

In **Fig. 5.55**, three different groups of compounds can be seen. If the nearest neighbours to search for is set to five (i.e. $K = 5$), then the distances of the unknown to the surrounding compounds will be calculated, and the nearest five neighbours will be determined. In the example, four of the five nearest neighbours belong to Group 2, whereas one of the nearest neighbours is a Group 1 compound. Since the majority of the nearest five neighbours are from Group 2, with the majority voting rule the unknown will be classified as belonging to Group 2 [244, 263].

Data reduction methods such as PCA, and subsequent algorithms that classify the data obtained using PCA, can help identify large amounts of unknown samples, such as forensic evidence, efficiently. This part of the study explores the applicability of principal components analysis (PCA) to the quick and effective discrimination of large numbers of lipstick spectra.

5.10.2. Methods and materials

For the purposes of this study, ten different lipsticks of various colours and brands were chosen. These were: Barry M 52 'Shocking Pink', Barry M 53 ' Coral', Barry M 121 ' Pillar Box Red', La Femme 29 'Dream Rose', Rimmel Moisture Renew 210 'Fancy', Rimmel Lasting Finish 272 'Frosted', Revlon Matte 006 'Really Red', Revlon Colorburst 025 'Carnation', Revlon Colorburst 075 'Peach', Revlon Absolutely Fabulous Lipcream 07 'Cherish'. These lipsticks were chosen because their spectra had strong similarities as well as varying degrees of differences. This helps determine whether PCA can be used to differentiate between lipsticks with similar spectra. An example spectrum for each lipstick is given in **Figures 5.56** and **5.57**.

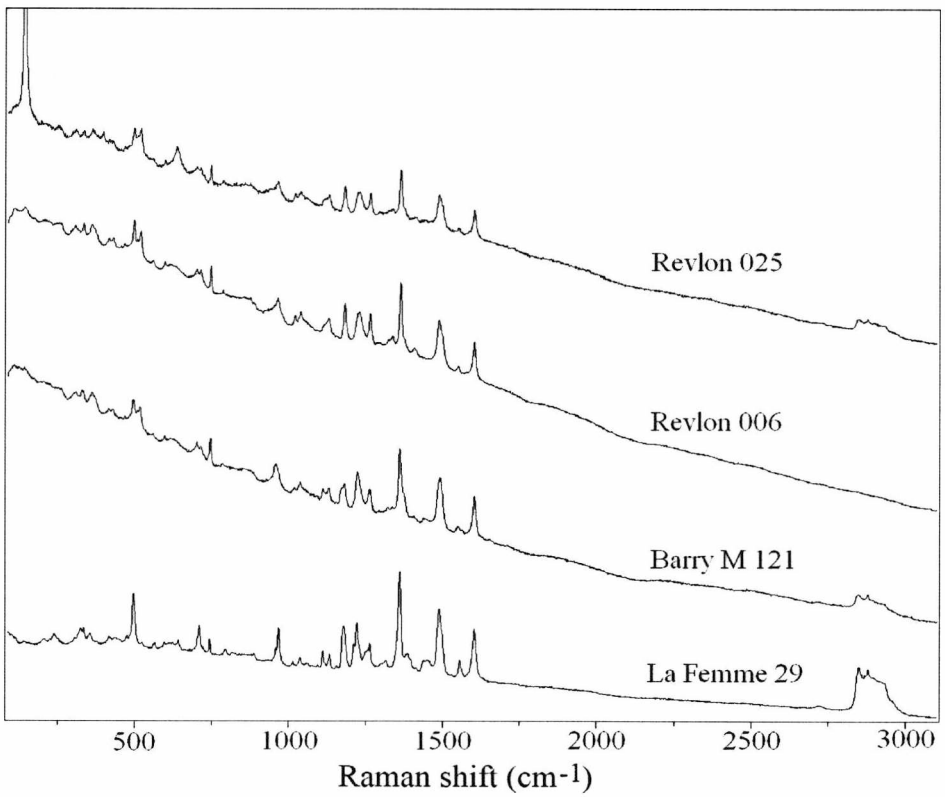

Figure 5.56. Example Raman spectra for the lipsticks Revlon 025, Revlon 006, Barry M 121 and La Femme 29. Strong similarities between spectra can be seen.

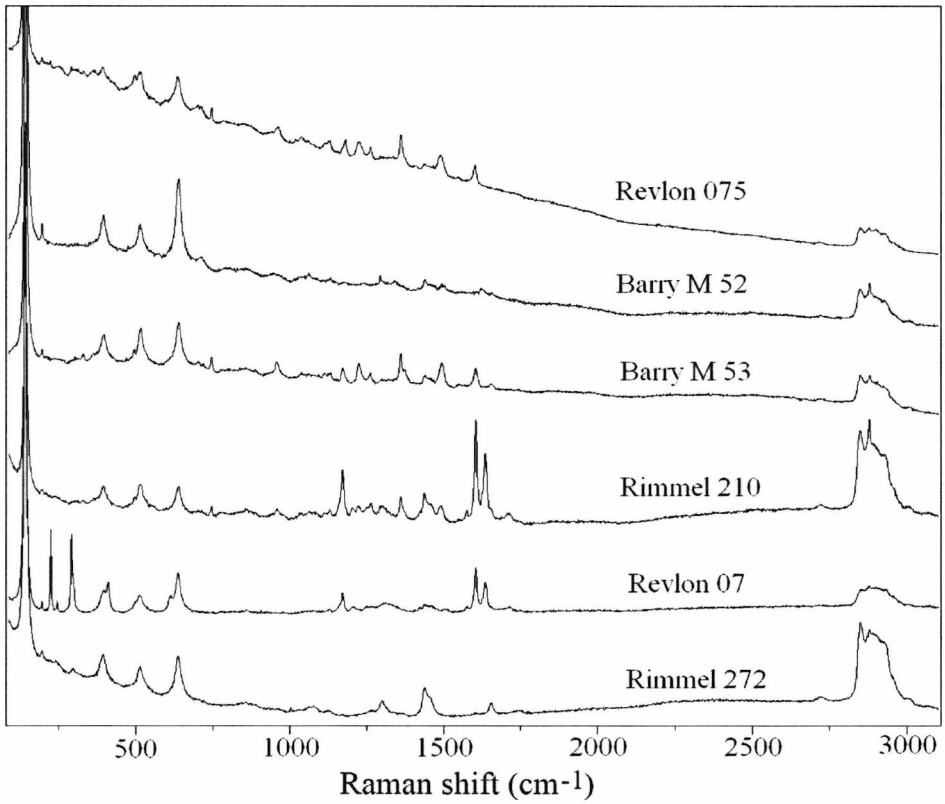

Figure 5.57. Example Raman spectra for the lipsticks Revlon 075, Revlon 07, Barry M 52, Barry M 53, Rimmel 210 and Rimmel 272. Similarities as well as some differences between the spectra can be observed.

Thirty spectra per lipstick were obtained using the Horiba *LabRAM-HR* Raman spectrometer, giving a total of 300 spectra. A ×50 objective lens and an excitation wavelength of 633 nm were employed. Each spectrum was acquired from different positions on the lipstick smear (on a glass slide) using fifteen accumulations for two seconds. The spectra were obtained using Labspec version 5 and the files were saved in .TXT format, which were then imported into MATLAB. The MATLAB code required for performing the principal components analysis was written by Dr. Stuart Gibson.

Since there can be large differences in the absolute intensities of Raman signals between spectra originating from the same sample, some form of normalisation must be performed before undertaking PCA. The majority of the spectra obtained displayed fluorescent baselines, and the absolute intensities of the baselines and the peaks varied greatly between spectra. For this reason, the spectra were pre-processed

by smoothing and subtracting the estimated baseline to obtain baseline-corrected spectra. This was achieved by applying a MATLAB smoothing function to the data. For each spectrum, gentle smoothing was used to remove the high frequency noise and to improve the clarity of the peaks. Strong smoothing was then applied to estimate the baseline, which was subsequently subtracted from the spectrum (**Fig. 5.58**).

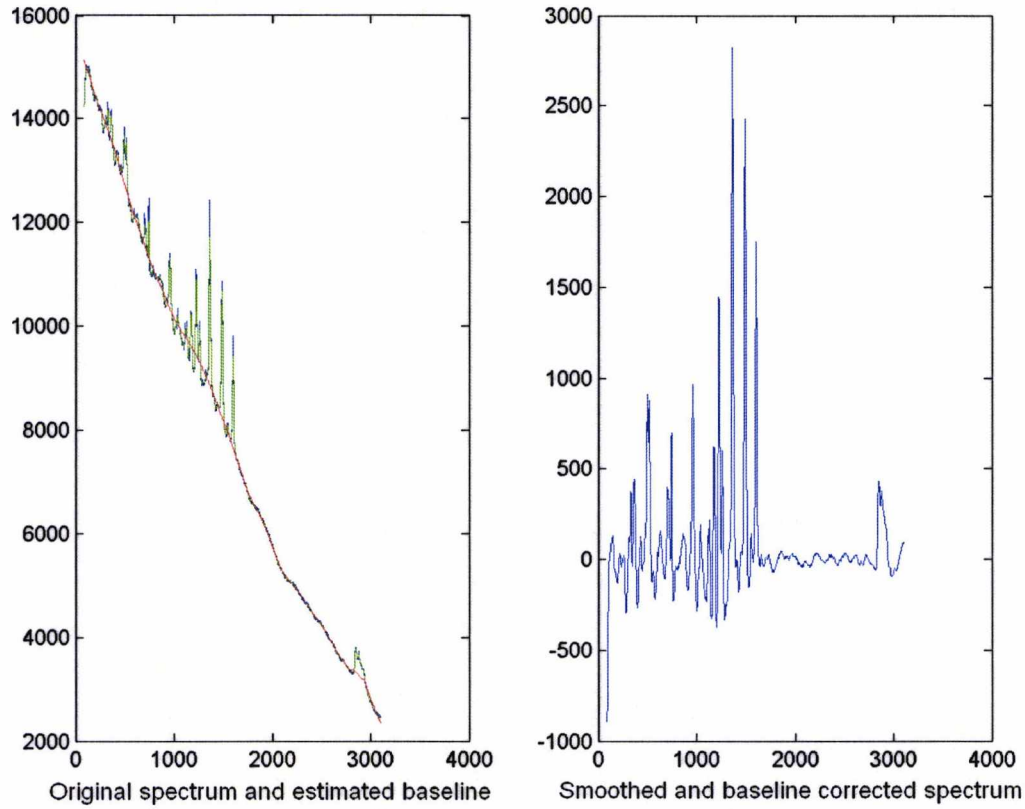

Figure 5.58. An example of pre-processing of the spectra. The raw data (blue line on the left plot) was smoothed (green line) and the baseline was estimated (red line). The baseline was then subtracted from the smoothed spectrum giving the spectrum on the right.

Principal components analysis (PCA) was then performed on the pre-processed spectra. The resulting scree plot showed that the first 10 principal components (PCs) accounted for the majority of the variance in the original data (**Fig. 5.59**).

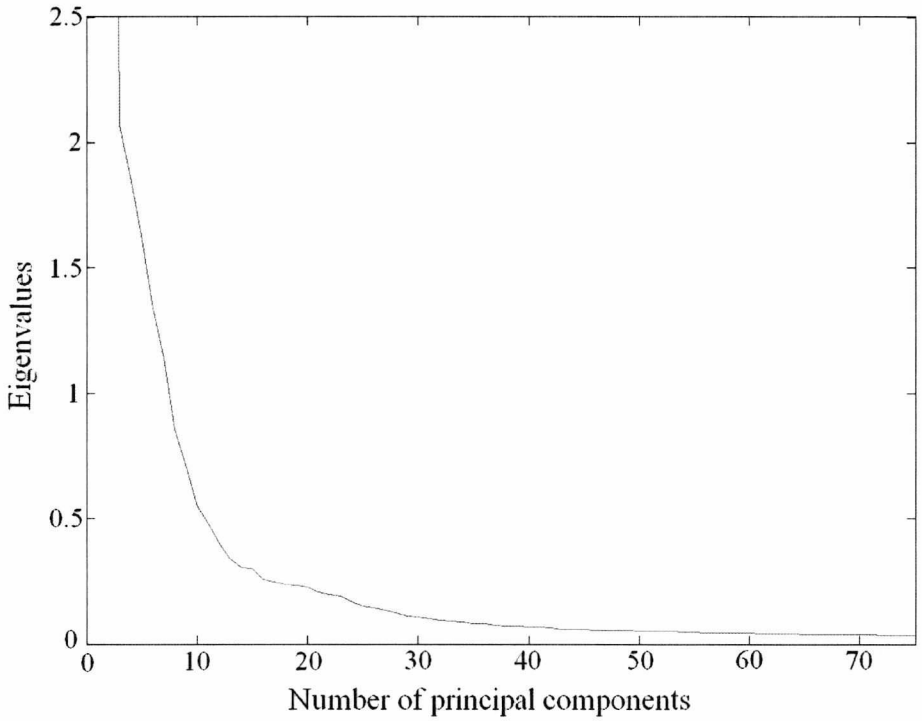

Figure 5.59. The eigenvalue plot of the data. The majority of the variance is accounted for by the first 10 principal components (the elbow of the scree plot).

Therefore the first 10 PCs were chosen for each lipstick spectrum and the results were plotted in ten-dimensional space. Due to the extreme difficulty in the visualisation and representation of a ten-dimensional plot, the resultant plot cannot be displayed.

In order to classify the lipstick spectra, the *K*-Nearest Neighbours (KNN) method was employed (as described previously). The distances between the neighbours were calculated using the Euclidean distance metric. The Euclidean distance is calculated by the formula:

$$d = \sqrt{(x_1 - y_1)^2 + (x_2 - y_2)^2 + \cdots + (x_n - y_n)^2}$$

where d is the distance, x and y are the coordinates of the PCs and n is the number of dimensions (in this case, 10) [244].

Each lipstick sample was analysed and classified using the leave-one-out cross validation method with KNN. This is a method where one of samples in the sample

set is kept out and used for classification; and this process is repeated until all of the samples have been left out once [264]. For the total of 300 spectra used, this meant that each classification was performed with 299 spectra, with the left out spectra being treated as the 'unknown' and the group it belongs to was predicted using KNN. This was applied to each spectrum in the set, resulting in a total of 300 classifications. If the majority of the K nearest neighbours of the 'unknown' corresponded to the spectra of the same lipstick as the 'unknown', then the classification was accepted as correct. If the majority of the neighbours were spectra of a different lipstick than the 'unknown', the classification was incorrect. At the end of the classification, the percentage of correct classifications was calculated.

5.10.3. Results and discussion

When the full range of the spectra (90 – 3100 cm^{-1}) was analysed with the number of nearest neighbours set to five (i.e. $K = 5$), the percentage of correct classifications was found to be 95.3%. This meant that if an unknown sample spectrum was analysed using PCA and classified with the KNN method, it would be correctly identified with a confidence level of 95.3% (provided that the unknown belongs to one of the groups of samples within the analysed set).

In some of the lipstick spectra, the most intense peak in the spectrum was that of titanium dioxide (in anatase form) found at 143 cm^{-1}. In most cases this peak was several times more intense than the rest of the peaks in the spectrum. Due to the high intensity of this peak, it is possible that the spectra that contained this peak did not show as great a variation as the other spectra. Even though the rest of the peaks showed differences, because the intensity of the anatase peak was a lot greater than the other peaks in the spectrum, those differences may not have appeared as significant during PCA. Also, the intensity of anatase peaks can vary for the same sample depending on the position on the lipstick smear the spectrum is acquired from. For this reason, it was decided to perform the PCA analysis and the

classification by disregarding the intense anatase peak at 143 cm^{-1}. Therefore the region to be analysed was set to 180 – 3100 cm^{-1} and PCA was performed again.

With K set to 5, the analysis yielded 96.3% correct classifications. In order to improve the classification results, the number of nearest neighbours, K, was increased. This enabled more of the surrounding neighbours to be included in the classification, which provided a better classification. It was found that:

- when $K = 7$, the percentage of correct classifications increased to 97.6%
- when $K = 9$, the percentage of correct classifications was 98%
- when $K = 11$, the percentage of correct classifications was 98.3%
- when $K = 15$, the percentage of correct classifications was 98.7%

When the anatase peak was included and the full range of 90 – 3100 cm^{-1} was analysed with $K = 15$, the percentage of correct classifications was 97.7%. This was still a lower percentage than the classification without the anatase peak with $K = 15$. Therefore, it was evident that disregarding the intense anatase peak provided a better classification of the lipstick samples.

In order to test the applicability of PCA to the classification of lipstick smears found not only on glass, but also on forensic evidential materials such as fibres, spectra obtained from lipstick smears found on fibres were also analysed and classified using the same method. These included:

- Two spectra of La Femme 29 smear on orange linen
- Three spectra of La Femme 29 smear on pink linen
- Three spectra of La Femme 29 smear on yellow cotton
- Three spectra of La Femme 29 smear on yellow wool
- One spectrum of Revlon 07 on orange linen
- One spectrum of Revlon 07 on yellow cotton

These spectra were the same spectra used in **Chapter 5.5**, obtained using the 633 nm laser and a ×50 objective lens, with the parameters as described in the mentioned section. These spectra will be referred to as the 'evidential samples' in this section for convenience.

The evidential samples were included in the PCA model and they were classified using the KNN method. All of the evidential samples were correctly classified when K was set to 5 with the full 90 – 3100 cm^{-1} range being included in the analysis. 100% correct classification of the evidential samples was also obtained when K was set to 15 and the anatase peak at 143 cm^{-1} was disregarded.

5.10.4. Summary

This study demonstrated that Raman spectroscopy combined with chemometrics is a powerful technique for the non-destructive analysis and characterisation of large numbers of lipstick spectra. It also showed that principal components analysis (PCA) is an effective way of reducing the dimensionality of data while preserving the variance within the data. PCA combined with K-nearest neighbours (KNN) method provided an effective tool for the classification of lipstick spectra with a confidence level of up to 98.7%. It was shown that this technique is useful for the characterisation of spectra obtained from lipstick smears on glass slides as well as on fluorescent materials like fibres. Therefore, this demonstrates that PCA could be an invaluable forensic tool for the identification of lipstick smears recovered from crime scenes.

It is possible to improve the results and provide a better confidence level by making some changes to the techniques used. The first issue that can improve the results is the auto fitting of the baseline. The current method allows the correction of the baseline by subtracting the estimated baseline (obtained by using the smoothing function of MATLAB) from the original spectrum. Even though the baseline

estimated this way worked well for the majority of the spectra, in some cases the estimated baseline was not a correct representation of the actual baseline (**Fig. 5.60**).

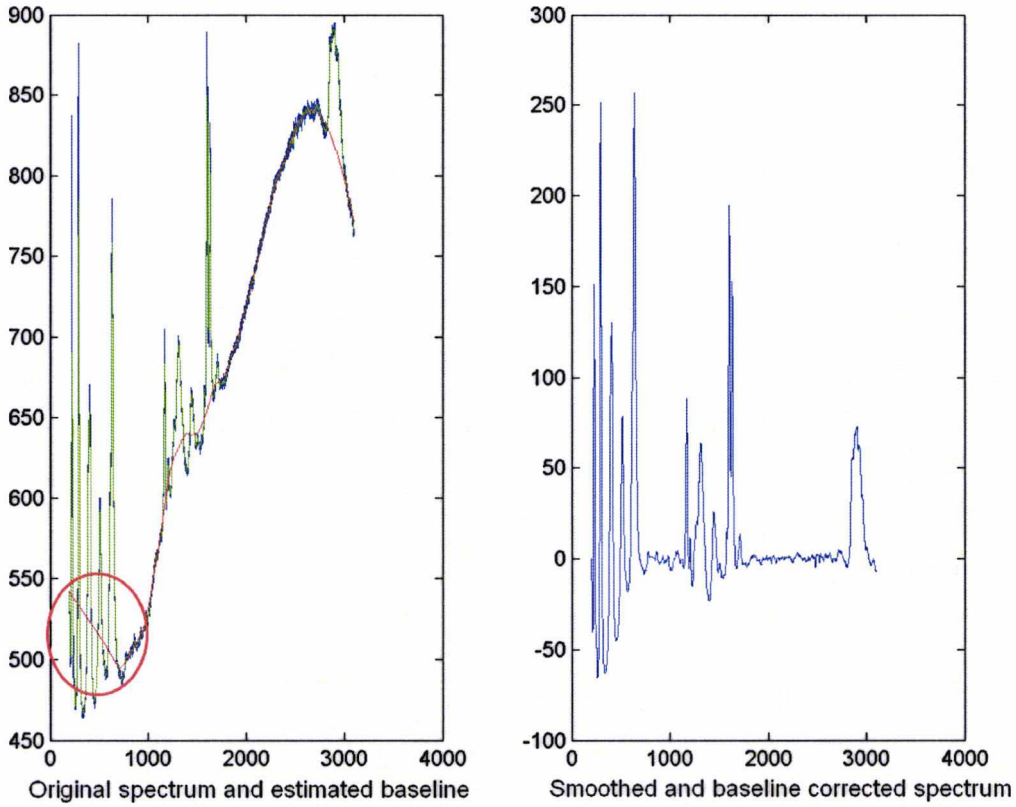

Figure 5.60. Figure showing the baseline correction of a spectrum. The estimated baseline (red line on the left plot) does not always give an accurate representation of the actual baseline of the spectrum (as circled in red).

This can be improved by using a different algorithm to calculate and auto-fit the baseline to ensure a better baseline correction for all samples. A manual fitting of the baseline can also provide a more accurate baseline correction; however, this approach would increase the analysis time greatly.

The use of different classifier methods can also be explored instead of the K-nearest neighbours (KNN) method used. KNN is a simple and useful method for classification of samples; however, it has some limitations. Because it operates on a majority voting system, the number of samples in each group or class has to be approximately equal so that the 'votes' are not biased towards the group with most members. Also, outliers in the data can cause problems with the correct classification

of the data. Employing other methods that classify samples in different ways can circumvent these limitations [263].

Additionally, a larger number of lipsticks can be used and the study can also be expanded to include the spectra of lipstick smears found on a variety of other crime scene surfaces or materials.

CHAPTER VI

Conclusions

Raman spectroscopy has been recognised as a powerful analytical technique with important applications in multiple disciplines, including forensic science. Analysis of evidential material is important in forensic science in order to establish the source of the evidence and to form a link between suspects, victims and crime scenes. Many types of evidence can be encountered in a forensic investigation and one of these is cosmetic evidence such as lipstick smears. Even though lipstick smears have been recognised as forensic evidence for many years, very little research has been done on the analysis and differentiation of lipsticks using Raman spectroscopy. The aim of this research, therefore, was to explore the application of Raman spectroscopy to the differentiation of lipstick smears as forensic evidence.

Raman spectroscopy was applied to the analysis and differentiation of 73 different lipsticks. Visual examination of lipstick spectra allowed the lipsticks to be categorised into different groups. Eight out of the 73 lipsticks (11%) were too fluorescent to obtain spectra from using the 633 nm laser (Group F). 16 out of the 73 lipsticks (21.9%) gave spectra that were unique to each lipstick and could be used to differentiate them from each other and the lipsticks of the other groups (Group U). The remaining 49 lipsticks (67.1%) could be categorised into seven different groups (Groups 1 to 7), each group with spectra characteristic to that group. The lipsticks of different groups could be differentiated from each other. However, no differentiation between the lipsticks of the same group could be achieved.

Identification of the peaks in the lipstick spectra allowed further classification of the lipsticks. This showed that the majority of the lipstick peaks arose due to the dyes found in the composition of lipsticks. Two dyes in particular, D&C Red No. 6 Barium lake and D&C Red No. 7 Calcium lake, were found to be responsible for the peaks in the majority of the lipstick samples analysed. This allowed further

classification of the lipsticks according to which of the dye peaks, if any at all, their spectra contained. Further differentiation of lipsticks with similar spectra was also achieved by comparing the relative intensities of peaks arising from different compounds in the spectrum. This increased the overall level of discrimination achieved between lipsticks.

A comprehensive library of 65 lipsticks was constructed. The library included the average peak positions (cm^{-1}), signal strengths, standard deviation from the average position, and the identity of each peak (if known). This library has the potential to be a database against which 'unknown' lipstick spectra could be compared in order to find a match, or to identify some of the peaks in the lipstick spectrum.

Availability of a modern Raman spectrometer allowed for more experiments to be conducted. It was found that the lipstick spectra obtained were independent of the instrument used. It was determined that using a higher resolution diffraction grating did not improve the lipstick spectra or resolve the broad peaks. Therefore increasing the resolution did not help with the differentiation of lipsticks with similar spectra.

It was found that the lipsticks that were previously too fluorescent to analyse using the 633 nm laser could be analysed and differentiated using the 473 and 784 nm lasers. Employment of the Raman mapping feature uncovered that the coloured fragments seen in the composition of some of the lipstick smears under the microscope could possibly be mica particles coated with titanium dioxide.

Effects of ageing on the spectra of lipsticks were investigated. It was found that the spectra of 15 out of the 20 samples analysed did not change over the course of up to two years. In the spectra of five of the lipsticks analysed, changes were observed in terms of the intensity of peaks found at 1655 and 3011 cm^{-1}, which were attributed to C=C and (=CH) vibrations of fatty acids (found in the waxy composition of lipsticks) respectively. It was determined that these peaks decreased in intensity and

disappeared over the course of a few months. This has the potential of establishing the approximate age of a lipstick smear using Raman spectroscopy. However, the study was carried out under relatively stable environmental conditions; therefore more research is required on how the Raman spectra of lipsticks change under different environmental conditions.

Raman spectroscopy was also applied to the detection and analysis of trace amounts of lipstick smears on textile fibres. It was found that the analyses were more difficult with the 633 nm laser due to intense fluorescent interference from the fibres. However, almost all of the samples could be analysed and differentiated from each other using the 473 nm laser. It was determined that each sample could easily be analysed and differentiated from each other by using both lasers together. Therefore, Raman spectroscopy was found to be an effective tool for the analysis of trace amounts of lipsticks on fibres.

Lipstick smears on smoked cigarette butts were also analysed using Raman spectroscopy. The presence of titanium dioxide peaks in the spectra of cigarette butts presented a challenge during the analysis of lipsticks with strong titanium dioxide peaks. However, it was possible to identify and differentiate between lipstick smears that did not have titanium dioxide peaks as the main peaks in their spectra. Therefore Raman spectroscopy was found to be effective for the analysis of lipstick smears on cigarette butts, where either (a) the lipstick spectrum does not contain strong titanium dioxide peaks, or (b) the cigarette butt spectrum does not have strong titanium dioxide peaks.

Lipstick smears deposited on tissues were analysed using Raman spectroscopy. The smears could be identified and differentiated from each other with minimum interference from the tissue. Therefore Raman spectroscopy was found to be effective for the analysis and discrimination of trace amounts of lipsticks deposited on tissues.

Applicability of Raman spectroscopy to the analysis of lipstick smears deposited on glass slides, cigarette butts and tissues through evidence bags was investigated. It was found that Raman spectroscopy could be used to obtain spectra of the lipstick smears deposited on a variety of surfaces even through evidence bags, with little or no interference from the bag.

Use of chemometrics for the characterisation of large numbers of lipstick spectra was explored. Thirty spectra each from ten different lipsticks were obtained for analysis and characterisation. It was found that Principal Components Analysis (PCA) was an effective technique for reducing the dimensionality of data while preserving the variance within the data. The spectra were classified using the *K*-Nearest Neighbours (KNN) method depending on their distances from each other in the ten-dimensional plot obtained. Up to 98.7% correct classification was achieved. Spectra from trace amounts of lipstick smears deposited on fibres were also analysed and classified using the same technique. 100% correct classification of these samples was achieved. This demonstrated that Raman spectroscopy combined with PCA could be a potentially powerful forensic technique for the characterisation and identification of lipstick smears recovered from crime scenes.

In conclusion, Raman spectroscopy has been found to be a useful tool for the discrimination of lipstick samples and this study reports on a comprehensive exploration of its use in a forensic context. Identification of the dye components was found to increase the level of discrimination achieved between samples. The first compilation of a library of well characterised lipstick spectra was reported.

Lipstick samples were found to be prone to getting damaged with high powered lasers, so the use of neutral density filters is recommended. The spectra obtained were found to be independent of the instrument used, and the employment of different excitation frequencies were found to help with the analysis and

characterisation of fluorescent samples. It was established that some lipstick spectra can change as a function of time, as well as a function of the underlying surface due to interferences. In the case of smears deposited on cigarette butts, it was determined that the presence (or absence) of titanium dioxide peaks should not be used as a discriminator when trying to match unknown lipstick smears deposited on cigarette butts. Therefore, care needs to be taken when making comparisons with smears deposited on different media. In the case of smears deposited on textile fibres, it was found that using different excitation frequencies can facilitate the identification and differentiation of lipstick smears on such surfaces. The combination of Raman spectroscopy with chemometric methods such as Principal Components Analysis (PCA) was found to be effective for the characterisation of large numbers of lipstick spectra, and it was found to be potentially useful in a forensic context.

This study has also opened up other areas for research which are given in the following section.

Future work

A database of lipstick spectra can be useful in forensic investigations. It can aid in the identification of a lipstick smear recovered from a crime scene. The limitation of a database, though, is its content: a suspect sample can be identified by searching the database only if its 'standard' sample is present in the database. The larger a database is, the better are the chances of getting a more accurate match. Therefore, a better database can be built by including more lipsticks from more brands. This can also be expanded to include other lip cosmetics such as lip balms and lip glosses, as well as other potential cosmetic evidence materials such as eye shadows, powder and cream foundations and nail varnishes.

Manufacturers produce their products in batches, so it is important to know whether same brand, same number lipsticks from different batches show any differences in

terms of their Raman spectra. Due to a lack of lipstick samples from different batches, such a study could not be carried out. However, it is forensically important to investigate how, if at all, lipstick spectra change between different batches. This information would be very useful in a database of lipstick spectra because it would provide more accurate results for comparison.

Infrared spectroscopy is a complimentary technique to Raman spectroscopy, and the two techniques are frequently used together for the identification of compounds. Therefore, research can be done to explore the application of infrared spectroscopy to the differentiation of lipsticks that have identical Raman spectra. A combination of infrared and Raman spectroscopy could provide a better level of differentiation for lipstick samples. Furthermore, UV-Visible absorption spectroscopy could help determine the maximum absorption wavelengths for the analysed samples which can either help with choosing an excitation frequency appropriate for resonance enhancement, or help explain any differences observed in terms of relative intensities of peaks for the same compound when analysed using different excitation frequencies.

Since forensic evidence is not always found and recovered under ideal conditions, investigation of the effects of environmental conditions on the Raman spectra of lipsticks (or any other cosmetic evidence) is an important area for research. This can include the effects of varying the temperature and humidity of the immediate surroundings of a lipstick smear; exposing the smear to different weather conditions; and investigating the effects of ageing under different environmental conditions using a larger number of samples.

A lipstick smear can be found on a variety of surfaces such as drinking glasses, cigarette butts and clothing materials. It is, therefore, essential to investigate the applicability of Raman spectroscopy for the analysis and differentiation of lipstick smears on such materials. More research in this area can include the use of a larger number of lipstick samples and a wider range of materials, such as mixtures of

different colours and types of textile materials, different brands of cigarette butts and tissues.

Lipsticks are typically worn for extended periods (hours) throughout the day. Eating, drinking, or simply wearing the lipstick can cause some components of the lipstick to be dissolved due to coming into contact with saliva. This could result in variations in the Raman spectra of the deposited lipstick smear. Therefore it is important to investigate the effects of wear time on the Raman spectra of lipsticks.

Chemometrics combined with Raman spectroscopy is a powerful technique for quick and effective analysis and characterisation of hundreds of spectra. Principal components analysis (PCA) is a widely used method for reducing the dimensionality of data. It can present the data in such a way as to highlight the similarities and differences between samples, which makes the classification of samples easier. Many algorithms can be used to classify different samples and each one has its own advantages and disadvantages. In forensic science it is important that an analytical technique gives the highest level of confidence possible for the accurate analysis of evidential samples. Therefore, investigation of different algorithms and chemometric methods for the characterisation of lipstick spectra with the highest level of confidence is another important area for research.

BIBLIOGRAPHY

[1] E. Smith, G. Dent, Modern Raman Spectroscopy: A Practical Approach, Wiley, England, 2005.

[2] C. Rodger, V. Rutherford, D. Broughton, P.C. White, W.E. Smith, The in-situ analysis of lipsticks by surface enhanced resonance Raman scattering, Analyst. 123 (1998) 1823-1826.

[3] R. Goodacre, N. Kaderbhai, A.C. McGovern, E.A. Goodacre, Chemometric analyses with self organising feature maps: a worked example of the analysis of cosmetics using Raman spectroscopy, in: Oja E., Kaski S. (Eds.), Kohonen Maps, Elsevier Science B.V., Netherlands, 1999, pp. 335-347.

[4] C.V. Raman, K.S. Krishnan, A new type of secondary radiation, Nature. 121 (1928) 501-502.

[5] R. Singh, C. V. Raman and the Discovery of the Raman Effect, Phys. Perspect. 4 (2002) 399-420.

[6] C.V. Raman, A new radiation, Indian J. Phys. 2 (1928) 387-398.

[7] J.M. Chalmers, P.R. Griffiths, Handbook of Vibrational Spectroscopy, John Wiley & Sons Ltd., Chichester, UK, 2002.

[8] R.L. McCreery, Raman Spectroscopy for Chemical Analysis, John Wiley & Sons Inc., USA, 2000.

[9] I.R. Lewis, H.G.M. Edwards, Handbook of Raman Spectroscopy, Marcel Dekker Inc., New York, 2001.

[10] B. Schrader, Infrared and Raman Spectroscopy: Methods and Applications, Wiley-VCH, Weinheim, 1995.

[11] J. Jehlicka, A. Culka, P. Vandenabeele, H.G.M. Edwards, Critical evaluation of a handheld Raman spectrometer with near infrared (785 nm) excitation for field identification of minerals, Spectrochim. Acta, Part A. 80 (2011) 36-40.

[12] P. Vandenabeele, T.L. Weis, E.R. Grant, L.J. Moens, A new instrument adapted to in situ Raman analysis of objects of art, Anal. Bioanal. Chem. 379 (2004) 137-142.

[13] B. Schrader, A. Hoffmann, S. Keller, Near-infrared Fourier transform Raman spectroscopy: Facing absorption and background, Spectrochim. Acta, Part A. 47 (1991) 1135-1148.

[14] F.C. Thorley, K.J. Baldwin, D.C. Lee, D.N. Batchelder, Dependence of the Raman spectra of drug substances upon laser excitation wavelength, J. Raman Spectrosc. 37 (2006) 335-341.

[15] P.C. Lee, D. Meisel, Adsorption and Surface-Enhanced Raman of Dyes on Silver and Gold Sols, J. Phys. Chem. 86 (1982) 3391-3395.

[16] M. Leona, J. Stenger, E. Ferloni, Application of surface-enhanced Raman scattering techniques to the ultrasensitive identification of natural dyes in works of art, J. Raman Spectrosc. 37 (2006) 981-992.

[17] K. Chen , K. Vo-Dinh, F. Yan, M.B. Wabuyele, T. Vo-Dinh, Direct identification of alizarin and lac dye on painting fragments using surface-enhanced Raman scattering, Anal. Chim. Acta. 569 (2006) 234-237.

[18] Z. Jurasekova, C. Domingo, J.V. Garcia-Ramos, S. Sanchez-Cortes, In situ detection of flavonoids in weld-dyed wool and silk textiles by surface-enhanced Raman scattering, J. Raman Spectrosc. 39 (2008) 1309-1312.

[19] S. Bruni, V. Guglielmi, F. Pozzi, Surface-enhanced Raman spectroscopy (SERS) on silver colloids for the identification of ancient textile dyes: Tyrian purple and madder, J. Raman Spectrosc. 41 (2010) 175-180.

[20] S. Bruni, V. Guglielmi, F. Pozzi, A.M. Mercuri, Surface-enhanced Raman spectroscopy (SERS) on silver colloids for the identification of ancient textile dyes. Part II: pomegranate and sumac, J. Raman Spectrosc. 42 (2010) 465-473.

[21] A.V. Whitney, R.P. Van Duyne, F. Casadio, An innovative surface-enhanced Raman spectroscopy (SERS) method for the identification of six historical red lakes and dyestuffs, J. Raman Spectrosc. 37 (2006) 993-1002.

[22] I.T. Shadi, B.Z. Chowdhry, M.J. Snowden, R. Withnall, Semi-quantitative analysis of alizarin and purpurin by surface-enhanced resonance Raman spectroscopy (SERRS) using silver colloids, J. Raman Spectrosc. 35 (2004) 800-807.

[23] N. Peica, W. Kiefer, Characterization of indigo carmine with surface-enhanced resonance Raman spectroscopy (SERRS) using silver colloids and island films, and theoretical calculations, J. Raman Spectrosc. 39 (2008) 47-60.

[24] I.T. Shadi, B.Z. Chowdhry, M.J. Snowden, R. Withnall, Semi-quantitative analysis of indigo by surface enhanced resonance Raman spectroscopy (SERRS) using silver colloids, Spectrochim. Acta, Part A. 59 (2003) 2213-2220.

[25] P.C. White, C.H. Munro, W.E. Smith, In situ surface enhanced resonance Raman scattering analysis of a reactive dye covalently bound to cotton, Analyst. 121 (1996) 835-838.

[26] C.H. Munro, W.E. Smith, P.C. White, Qualitative and semi-quantitative trace analysis of acidic monoazo dyes by surface enhanced resonance Raman scattering, Analyst. 120 (1995) 993-1003.

[27] C.H. Munro, W.E. Smith, P.C. White, Use of poly(L-lysine) and ascorbic acid for surface enhanced resonance Raman scattering analysis of acidic monoazo dyes, Analyst. 118 (1993) 731-733.

[28] I. Geiman, M. Leona, J.R. Lombardi, Application of Raman Spectroscopy and Surface-Enhanced Raman Scattering to the Analysis of Synthetic Dyes Found in Ballpoint Pen Inks, J. Forensic Sci. 54 (2009) 947-952.

[29] C.J. McHugh, W.E. Smith, R. Lacey, D. Graham, The first controlled reduction of the high explosive RDX, Chem. Commun. 21 (2002) 2514-2515.

[30] C.J. McHugh, R. Keir, D. Graham, W.E. Smith, Selective functionalisation of TNT for sensitive detection by SERRS Chem. Commun. 6 (2002) 580-581.

[31] S. Botti, L. Cantarini, A. Palucci, Surface-enhanced Raman spectroscopy for trace-level detection of explosives, J. Raman Spectrosc. 41 (2010) 866-869.

[32] T. Vo-Dinh, F. Yan, M.B. Wabuyele, Surface-enhanced Raman scattering for medical diagnostics and biological imaging, J. Raman Spectrosc. 36 (2005) 640-647.

[33] K. Faulds, R.P. Barbagallo, J.T. Keer, W.E. Smith, D. Graham, SERRS as a more sensitive technique for the detection of labelled oligonucleotides compared to fluorescence, Analyst. 129 (2004) 567-568.

[34] A. Baran, B. Wrzosek, J. Bukowska, L.M. Proniewicz, M. Baranska, Analysis of alizarin by surface-enhanced and FT-Raman spectroscopy, J. Raman Spectrosc. 40 (2009) 436-441.

[35] M. Sackmann, A. Materny, Surface enhanced Raman scattering (SERS) – a quantitative analytical tool? J. Raman Spectrosc. 37 (2006) 305-310.

[36] T. Vosgrone, A.J. Meixner, Surface- and Resonance-Enhanced Micro-Raman Spectroscopy of Xanthene Dyes: From the Ensemble to Single Molecules, Chem. Phys. Chem. 6 (2005) 154-163.

[37] M. Fan, G.F.S. Andrade, A.G. Brolo, A review on the fabrication of substrates for surface enhanced Raman spectroscopy and their applications in analytical chemistry, Anal. Chim. Acta. 693 (2011) 7-25.

[38] J. Fang, Y. Huang, X. Li, X. Dou, Aggregation and surface-enhanced Raman activity study of dye-coated mixed silver–gold colloids, J. Raman Spectrosc. 35 (2004) 914-920.

[39] B. Sharma, R.R. Frontiera, A. Henry, E. Ringe, R.P. Van Duyne, SERS: Materials, applications, and the future, Mater. Today. 15 (2012) 16-25.

[40] P.C. White, SERRS Spectroscopy – a new technique for forensic science? Sci. Justice. 40 (2000) 113-119.

[41] N.J. Cherepy, A.R. Holzwarth, R.A. Mathies, Near-Infrared Resonance Raman Spectra of Chloroflexus aurantiacus Photosynthetic Reaction Centers, Biochemistry. 34 (1995) 5288-5293.

[42] N.J. Cherepy, M. Du, A.R. Holzwarth, R.A. Mathies, Near-Infrared Resonance Raman Spectra of Chlorosomes: Probing Nuclear Coupling in Electronic Energy Transfer, J. Phys. Chem. 100 (1996) 4662-4671.

[43] N.J. Cherepy, A.P. Shreve, L.J. Moore, S. Franzen, S.G. Boxer, R.A. Mathies, Near-Infrared Resonance Raman Spectroscopy of the Special Pair and the Accessory Bacteriochlorophylls in Photosynthetic Reaction Centers, J. Phys. Chem. 98 (1994) 6023-6029.

[44] A.P. Shreve, N.J. Cherepy, S. Franzen, S.G. Boxer, R.A. Mathies, Rapid-flow resonance Raman spectroscopy of bacterial photosynthetic reaction centers, Proc. Natl. Acad. Sci. USA. 88 (1991) 11207-11211.

[45] P.A. Mosier-Boss, S.H. Lieberman, R. Newbery, Fluorescence Rejection in Raman Spectroscopy by Shifted-Spectra, Edge Detection, and FFT Filtering Techniques, Appl. Spectrosc. 49 (1995) 630-638.

[46] S.E.J. Bell, E.S.O. Bourguignon, A. Dennis, Analysis of luminescent samples using subtracted shifted Raman spectroscopy, Analyst. 123 (1998) 1729-1734.

[47] F. Rosi, M. Paolantoni, C. Clementi, B. Doherty, C. Miliani, B.G. Brunetti, et al., Subtracted shifted Raman spectroscopy of organic dyes and lakes, J. Raman Spectrosc. 41 (2010) 452-458.

[48] S.E.J. Bell, E.S.O. Bourguignon, A.C. Dennis, J.A. Fields, J.J. McGarvey, K.R. Seddon, Identification of Dyes on Ancient Chinese Paper Samples Using the Subtracted Shifted Raman Spectroscopy Method, Anal. Chem. 72 (2000) 234-239.

[49] I. Osticioli, A. Zoppi, E.M. Castellucci, Fluorescence and Raman spectra on painting materials: reconstruction of spectra with mathematical methods, J. Raman Spectrosc. 37 (2006) 974-980.

[50] S.E.J. Bell, E.S.O. Bourguignon, A. O'Grady, J. Villaumie, A.C. Dennis, Extracting Raman spectra from highly fluorescent samples with "Scissors" (SSRS, Shifted-Subtracted Raman Spectroscopy), Spectrosc. Eur. 14 (2002) 17-20.

[51] A.M. Macdonald, P. Wyeth, On the use of photobleaching to reduce fluorescence background in Raman spectroscopy to improve the reliability of pigment identification on painted textiles, J. Raman Spectrosc. 37 (2006) 830-835.

[52] D.L.A. De Faria, M.A. De Souza, Raman Spectra of Human Skin and Nail Excited in the Visible Region, J. Raman Spectrosc. 30 (1999) 169-171.

[53] P. Buzzini, G. Massonnet, F.M. Sermier, The micro Raman analysis of paint evidence in criminalistics: case studies, J. Raman Spectrosc. 37 (2006) 922-931.

[54] Z. Zhang, S. Chen, Y. Liang, Z. Liu, Q. Zhang, L. Ding, et al., An intelligent background-correction algorithm for highly fluorescent samples in Raman spectroscopy, J. Raman Spectrosc. 41 (2010) 659-669.

[55] W. Min, S. Lu, G.R. Holtom, X.S. Xie, Triple-Resonance Coherent Anti-Stokes Raman Scattering Microspectroscopy, Chem. Phys. Chem. 10 (2009) 344-347.

[56] C.L. Evans, X.S. Xie, Coherent Anti-Stokes Raman Scattering Microscopy: Chemical Imaging for Biology and Medicine, Annu. Rev. Anal. Chem. 1 (2008) 883-909.

[57] J. Cheng, X.S. Xie, Coherent Anti-Stokes Raman Scattering Microscopy: Instrumentation, Theory, and Applications, J. Phys. Chem. 108 (2004) 827-840.

[58] A. Cao, A.K. Pandya, G.K. Serhatkulu, R.E. Weber, H. Dai, J.S. Thakur, et al., A robust method for automated background subtraction of tissue fluorescence, J. Raman Spectrosc. 38 (2007) 1199-1205.

[59] P.M. Ramos, I. Ruisanchez, Noise and background removal in Raman spectra of ancient pigments using wavelet transform, J. Raman Spectrosc. 36 (2005) 848-856.

[60] L. Raffaelly, B. Champagnon, High temperature experiments: a way to observe Raman scattering in luminescent samples, J. Raman Spectrosc. 38 (2007) 1242-1245.

[61] P. Matousek, M. Towrie, A.W. Parker, Fluorescence background suppression in Raman spectroscopy using combined Kerr gated and shifted excitation Raman difference techniques, J. Raman Spectrosc. 33 (2002) 238-242.

[62] P. Matousek, M. Towrie, C. Ma, W.M. Kwok, D. Phillips, W.T. Toner, et al., Fluorescence suppression in resonance Raman spectroscopy using a high-performance picosecond Kerr gate, J. Raman Spectrosc. 32 (2001) 983-988.

[63] T.L. Gustafson, F.E. Lytle, Time-resolved rejection of fluorescence from Raman spectra via high repetition rate gated photon counting, Anal. Chem. 54 (1982) 634-637.

[64] R.S. Das, Y.K. Agrawal, Raman spectroscopy: Recent advancements, techniques and applications, Vib. Spectrosc. 57 (2011) 163-176.

[65] W. Kiefer, Recent advances in linear and non-linear Raman spectroscopy. Part III, J. Raman Spectrosc. 40 (2009) 1766-1779.

[66] W. Kiefer, Recent Advances in linear and nonlinear Raman spectroscopy I, J. Raman Spectrosc. 38 (2007) 1538-1553.

[67] W. Kiefer, Recent advances in linear and nonlinear Raman spectroscopy II, J. Raman Spectrosc. 39 (2008) 1710-1725.

[68] A. Torreggiani, G. Bottura, G. Fini, Interaction of biotin and biotinyl derivatives with avidin: conformational changes upon binding, J. Raman Spectrosc. 31 (2000) 445-450.

[69] N. Howell, E. Li-Chan, Elucidation of interactions of lysozyme with whey proteins by Raman spectroscopy, Int. J. Food Sci. Tech. 31 (1996) 439-451.

[70] W.L. Peticolas, Applications of Raman Spectroscopy to biological macromolecules, Biochimie. 54 (1975) 417-428.

[71] P.R. Carey, Raman Spectroscopy in Enzymology: the First 25 Years, J. Raman Spectrosc. 29 (1998) 7-14.

[72] H.A. Rinia, M. Bonn, E.M. Vartiainen, C.B. Schaffer, M. Müller, Spectroscopic analysis of the oxygenation state of hemoglobin using coherent anti-Stokes Raman scattering, J. Biomed. Opt. 11 (2006) 050502-1-050502-3.

[73] L. Chiu, M. Ando, H. Hamaguchi, Study of the 'Raman spectroscopic signature of life' in mitochondria isolated from budding yeast, J. Raman Spectrosc. 41 (2010) 2-3.

[74] C. Medina-Gutiérrez, J.L. Quintanar, C. Frausto-Reyes, R. Sato-Berrú, The application of NIR Raman spectroscopy in the assessment of serum thyroid-stimulating hormone in rats, Spectrochim. Acta, Part A. 61 (2005) 87-91.

[75] S. Wessel, M. Gniadecka, G.B.E. Jemec, H.C. Wulf, Hydration of human nails investigated by NIR-FT-Raman spectroscopy, Biochim. Biophys. Acta. 1433 (1999) 210-216.

[76] A.M. Herrero, Raman spectroscopy a promising technique for quality assessment of meat and fish: A review, Food Chem. 107 (2008) 1642-1651.

[77] C. Xie, D. Chen, Y. Li, Raman sorting and identification of single living micro-organisms with optical tweezers, Opt. Lett. 30 (2005) 1800-1802.

[78] R. Tuma, G.J. Thomas Jr, Mechanisms of virus assembly probed by Raman spectroscopy: the icosahedral bacteriophage P22, Biophys. Chem. 68 (1997) 17-31.

[79] S.A. Overman, G.J. Thomas Jr, Novel Vibrational Assignments for Proteins from Raman Spectra of Viruses, J. Raman Spectrosc. 29 (1998) 23-29.

[80] D. Pestov, M. Zhi, Z. Sariyanni, N.G. Kalugin, A.A. Kolomenskii, R. Murawski, et al., Visible and UV coherent Raman spectroscopy of dipicolinic acid, P. Natl. Acad. Sci. USA. 102 (2005) 14976-14981.

[81] M.V.P. Chowdary, K.K. Kumar, K. Thakur, A. Anand, J. Kurien, C.M. Krishna, et al., Discrimination of Normal and Malignant Mucosal Tissues of the Colon by Raman Spectroscopy, Photomed. Laser Surg. 25 (2007) 269-274.

[82] M.V.P. Chowdary, K.K. Kumar, S. Mathew, L. Rao, C.M. Krishna, J. Kurien, Biochemical Correlation of Raman Spectra of Normal, Benign and Malignant Breast Tissues: A Spectral Deconvolution Study, Biopolymers. 91 (2009) 539-546.

[83] C.J. Frank, D.C.B. Redd, T.S. Gansler, R.L. McCreery, Characterization of Human Breast Biopsy Specimens with Near-IR Raman Spectroscopy, Anal. Chem. 66 (1994) 319-326.

[84] P.R.T. Jess, D.D.W. Smith, M. Mazilu, K. Dholakia, A.C. Riches, C.S. Herrington, Early detection of cervical neoplasia by Raman spectroscopy, Int. J. Cancer. 121 (2007) 2723-2728.

[85] K. Bensalah, J. Fleureau, D. Rolland, O. Lavastre, N. Rioux-Leclercq, F. Guille, et al., Raman Spectroscopy: A Novel Experimental Approach to Evaluating Renal Tumours, Eur. Urol. 58 (2010) 602-608.

[86] V. Vrabie, C. Gobinet, O. Piot, A. Tfayli, P. Bernard, R. Huez, et al., Independent component analysis of Raman spectra: Application on paraffin-embedded skin biopsies, Biomed. Signal Proces. 2 (2007) 40-50.

[87] C.W. Ong, Z.X. Shen, Y. He, T. Lee, S.H. Tang, Raman Microspectroscopy of the Brain Tissues in the Substantia Nigra and MPTP-induced Parkinson's Disease, J. Raman Spectrosc. 30 (1999) 91-96.

[88] A.R. de Paula Jr., S. Sathaiah, Raman spectroscopy for diagnosis of atherosclerosis: a rapid analysis using neural networks, Med. Eng. Phys. 27 (2005) 237-244.

[89] C.J. Frank, R.L. McCreery, D.C.B. Redd, T.S. Gansler, Detection of Silicone in Lymph Node Biopsy Specimens by Near-Infrared Raman Spectroscopy, Appl. Spectrosc. 47 (1993) 387-390.

[90] J.P. Salenius, J.F. Brennan, A. Miller, Y. Wang, T. Aretz, B. Sacks, et al., Biochemical composition of human peripheral arteries examined with near-infrared Raman spectroscopy, J. Vasc. Surg. 27 (1998) 710-719.

[91] K.R. Ward, R.W. Barbee, P.S. Reynolds, I.P.T. Filho, M.H. Tiba, L. Torres, et al., Oxygenation Monitoring of Tissue Vasculature by Resonance Raman Spectroscopy, Anal. Chem. 79 (2007) 1514-1518.

[92] I. Notingher, Raman Spectroscopy Cell-based Biosensors, Sensors. 7 (2007) 1343-1358.

[93] D. Pappas, B.W. Smith, J.D. Winefordner, Raman spectroscopy in bioanalysis, Talanta. 51 (2000) 131-144.

[94] Y. Roggo, K. Degardin, P. Margot, Identification of pharmaceutical tablets by Raman spectroscopy and chemometrics, Talanta. 81 (2010) 988-995.

[95] A.O. Izolani, M.T. de Moraes, C.A. Tellez S., Fourier transform Raman spectroscopy of drugs: quantitative analysis of 1-phenyl-2,3-dimethyl-5-pyrazolone-4-methylaminomethane sodium sulfonate: (dipyrone), J. Raman Spectrosc. 34 (2003) 837-843.

[96] M.G. Orkoula, C.G. Kontoyannis, C.K. Markopoulou, J.E. Koundourellis, Validation of a direct non-destructive quantitative analysis of amiodarone hydrochloride in Angoron® formulations using FT-Raman spectroscopy, Talanta. 73 (2007) 258-261.

[97] W. Bonawi-Tan, J.A.S. Williams, Online Quality Control with Raman Spectroscopy in Pharmaceutical Tablet Manufacturing, J. Manuf. Syst. 23 (2004) 299-308.

[98] M.T. Islam, N. Rodriguez-Hornedo, S. Ciotti, C. Ackermann, The Potential of Raman Spectroscopy as a Process Analytical Technique During Formulations of Topical Gels and Emulsions, Pharm. Res. 21 (2004) 1844-1851.

[99] A.K. Deisingh, Pharmaceutical counterfeiting, Analyst. 130 (2005) 271-279.

[100] C. Eliasson, P. Matousek, Noninvasive Authentication of Pharmaceutical Products through Packaging Using Spatially Offset Raman Spectroscopy, Anal. Chem. 79 (2007) 1696-1701.

[101] A. Weselucha-Birczynska, K. Nakamoto, Study of the Interaction of the Antimalarial Drug Cinchonine with Nucleic Acids by Raman Spectroscopy, J. Raman Spectrosc. 27 (1996) 915-919.

[102] C.A. Butler, R.P. Cooney, W.A. Denny, Resonance Raman Study of the Binding of the Anticancer Drug Amsacrine to DNA, Appl. Spectrosc. 48 (1994) 822-826.

[103] M.M. Glice, A. Les, K. Bajdor, IR, Raman and theoretical ab initio RHF study of aminoglutethimide — an anticancer drug, J Mol Struct. 450 (1998) 141-153.

[104] G. Fini, Applications of Raman spectroscopy to pharmacy, J. Raman Spectrosc. 35 (2004) 335-337.

[105] R.A. Barrio, F.L. Galeener, E. Martinez, Dihedral-angle-averaged Bethe lattice for vibrations in glasses, Phys. Rev. B. 31 (1985) 7779-7787.

[106] R.B. Laughlin, J.D. Joannopoulos, Phonons in amorphous silica, Phys. Rev. B. 16 (1977) 2942-2952.

[107] M. Oussaid, P. Becker, C. Carabatos-Nedelec, Raman and Infrared Spectra of Bis(Thiourea)Zinc Chloride $Zn[CS(NH_2)_2]^2Cl_2$ Single Crystal, Phys. Stat. Sol. 207 (1998) 499-507.

[108] K. Mouaine, P. Becker, C. Carabatos-Nedelec, Thermal and spectroscopic study of dehydration of lithium formate monohydrate single-crystals, J. Therm. Anal. Calorim. 55 (1999) 807-816.

[109] M.L. Fish, O. Massler, J.A. Reid, R. MacGregor, J.D. Comins, The application of photoluminescence and Raman spectroscopy of synthetic diamond, Diam. Relat. Mater. 8 (1999) 1511-1514.

[110] R.L. Frost, M.C. Hales, D.L. Wain, Raman spectroscopy of smithsonite, J. Raman Spectrosc. 39 (2008) 108-114.

[111] S.J. Palmer, R.L. Frost, G. Ayoko, T. Nguyen, Synthesis and Raman spectroscopic characterisation of hydrotalcite with CO_3^{2-} and $(MoO_4)^{2-}$ anions in the interlayer, J. Raman Spectrosc. 39 (2008) 395-401.

[112] I. El-Harrad, A. Ridah, C. Carabatos-Nedelec, P. Becker, J. Handerek, Z. Ujma, et al., Raman Scattering Investigation with Temperature of Phase Transitions in $(Pb_{1-x}Ba_x)ZrO_3$ Ceramics at Critical Compositions x= 0.175 and 0.35, J. Raman Spectrosc. 29 (1998) 123-129.

[113] S.S. Potgieter-Vermaak, J.H. Potgieter, R. Van Grieken, The application of Raman spectrometry to investigate and characterize cement, Part I: A review, Cement Concrete Res. 36 (2006) 656-662.

[114] A. Garton, D.N. Batchelder, C. Cheng, Raman microscopy of polymer blends, Appl. Spectrosc. 47 (1993) 922-927.

[115] K.D.O. Jackson, M.J.R. Loadman, Fourier transform Raman spectroscopy of elastomers: An overview, Spectrochim. Acta, Part A. 46 (1990) 217-226.

[116] K. Tashiro, S. Sasaki, Y. Ueno, A. Yoshioka, M. Kobayashi, Crystallization Behavior of Polymers as Viewed from the Molecular Level, Korea Polym. J. 8 (2000) 103-115.

[117] S.W. Cornell, J.L. Koenig, The Raman Spectra of Polybutadiene Rubbers, Macromolecules. 2 (1969) 540-545.

[118] F. Cerdeira, T.A. Fjeldly, M. Cardona, Effect of Free Carriers on Zone-Center Vibrational Modes in Heavily Doped p-type Si. II. Optical Modes, Phys. Rev. B. 8 (1973) 4734-4745.

[119] S.J. Sandoval, Micro-Raman spectroscopy: a powerful technique for materials research, Microelectr. J. 31 (2000) 419-427.

[120] J. Zhu, F. Xu, S.J. Schofer, C.A. Mirkin, The First Raman Spectrum of an Organic Monolayer on a High-Temperature Superconductor: Direct Spectroscopic Evidence for a Chemical Interaction between an Amine and $YBa_2Cu_3O_{7-\delta}$, J. Am. Chem. Soc. 119 (1997) 235-236.

[121] F. Adar, R. Geiger, J. Nooan, Raman Spectroscopy for Process/Quality Control, Appl. Spectrosc. Rev. 32 (1997) 45-101.

[122] B. Gu, J. Tio, W. Wang, Y. Ku, S. Dai, Raman Spectroscopic Detection for Perchlorate at Low Concentrations, Appl. Spectrosc. 58 (2004) 741-744.

[123] A. Ianoul, T. Coleman, S.A. Asher, UV Resonance Raman Spectroscopic Detection of Nitrate and Nitrite in Wastewater Treatment Processes, Anal. Chem. 74 (2002) 1458-1461.

[124] C. Ruan, W. Luo, W. Wang, B. Gu, Surface-enhanced Raman spectroscopy for uranium detection and analysis in environmental samples, Anal. Chim. Acta. 605 (2007) 80-86.

[125] K.S. Kalasinsky, T. Hadfield, A.A. Shea, V.F. Kalasinsky, M.P. Nelson, J. Neiss, et al., Raman Chemical Imaging Spectroscopy Reagentless Detection and Identification of Pathogens: Signature Development and Evaluation, Anal. Chem. 79 (2007) 2658-2673.

[126] S.A. Centeno, J. Shamir, Surface enhanced Raman scattering (SERS) and FTIR characterization of the sepia melanin pigment used in works of art, J Mol Struct. 873 (2008) 149-159.

[127] R.J.H. Clark, Pigment identification by spectroscopic means: an arts/science interface, C. R. Chimie. 5 (2002) 7-20.

[128] H.G.M. Edwards, Analytical Raman spectroscopic discrimination between yellow pigments of the Renaissance, Spectrochim. Acta, Part A. 80 (2011) 14-20.

[129] K. Chen , M. Leona, K. Vo-Dinh, F. Yan, M.B. Wabuyele, T. Vo-Dinh, Application of surface-enhanced Raman scattering (SERS) for the identification of anthraquinone dyes used in works of art, J. Raman Spectrosc. 37 (2006) 520-527.

[130] Z. Jurasekova, E. del Puerto, G. Bruno, J.V. García-Ramos, S. Sanchez-Cortes, C. Domingo, Extractionless non-hydrolysis surface-enhanced Raman spectroscopic detection of historical mordant dyes on textile fibers, J. Raman Spectrosc. 41 (2010) 1455-1461.

[131] K.L. Brown, R.J.H. Clark, Analysis of Pigmentary Materials on the Vinland Map and Tartar Relation by Raman Microprobe Spectroscopy, Anal. Chem. 74 (2002) 3658-3661.

[132] R.J.H. Clark, P.J. Gibbs, K.R. Seddon, N.M. Brovenko, Y.A. Petrosyan, Non-Destructive In Situ Identification of Cinnabar on Ancient Chinese Manuscripts, J. Raman Spectrosc. 28 (1997) 91-94.

[133] L. Burgio, R.J.H. Clark, P.J. Gibbs, Pigment Identification Studies In Situ of Javanese, Thai, Korean, Chinese and Uighur Manuscripts by Raman Microscopy, J. Raman Spectrosc. 30 (1999) 181-184.

[134] S. Bioletti, R. Leahy, J. Fields, B. Meehan, W. Blau, The examination of the Book of Kells using micro-Raman spectroscopy, J. Raman Spectrosc. 40 (2009) 1043-1049.

[135] F.R. Perez, H.G.M. Edwards, A. Rivas, L. Drummond, Fourier Transform Raman Spectroscopic Characterization of Pigments in the Mediaeval Frescoes at Convento de la Peregrina, Sahagun, Leon, Spain. Part 1—Preliminary Study, J. Raman Spectrosc. 30 (1999) 301-305.

[136] H.G.M. Edwards, C.J. Brooke, J.K.F. Tait, Fourier Transform Raman Spectroscopic Study of Pigments from English Mediaeval Wall Paintings, J. Raman Spectrosc. 28 (1997) 95-98.

[137] D.C. Smith, A. Barbet, A Preliminary Raman Microscopic Exploration of Pigments in Wall Paintings in the Roman Tomb Discovered at Kertch, Ukraine, in 1891, J. Raman Spectrosc. 30 (1999) 319-324.

[138] A. Derbyshire, R. Withnall, Pigment Analysis of Portrait Miniatures Using Raman Microscopy, J. Raman Spectrosc. 30 (1999) 185-188.

[139] R.J.H. Clark, L. Curri, G.S. Henshaw, Characterization of Brown–Black and Blue Pigments in Glazed Pottery Fragments from Castel Fiorentino (Foggia, Italy) by Raman Microscopy, X-Ray Powder Diffractometry and X-Ray Photoelectron Spectroscopy, J. Raman Spectrosc. 28 (1997) 105-109.

[140] J. Zuo, C. Xu, C. Wang, Z. Yushi, Identification of the Pigment in Painted Pottery from the Xishan Site by Raman Microscopy, J. Raman Spectrosc. 30 (1999) 1053-1055.

[141] R.J.H. Clark, P.J. Gibbs, Non-Destructive In Situ Study of Ancient Egyptian Faience by Raman Microscopy, J. Raman Spectrosc. 28 (1997) 99-103.

[142] H.G.M. Edwards, E.R. Gwyer, J.K.F. Tait, Fourier Transform Raman Analysis of Paint Fragments from Biodeteriorated Renaissance Frescoes, J. Raman Spectrosc. 28 (1997) 677-684.

[143] M.M. Naumova, S.A. Pisareva, G.O. Nechiporenko, Green Copper Pigments of Old Russian Frescoes, Stud. Conserv. 35 (1990) 81-88.

[144] D.C. Smith, M. Bouchard, M. Lorblanchet, An Initial Raman Microscopic Investigation of Prehistoric Rock Art in Caves of the Quercy District, S. W. France, J.Raman Spectrosc. 30 (1999) 347-354.

[145] H.G.M. Edwards, L. Drummond, J. Russ, Fourier Transform Raman Spectroscopic Study of Prehistoric Rock Paintings from the Big Bend Region, Texas, J. Raman Spectrosc. 30 (1999) 421-428.

[146] H.G.M. Edwards, D.W. Farwell, E.M. Newton, F.R. Perez, S.J. Villar, Raman spectroscopic studies of a 13th century polychrome statue: identification of a 'forgotten' pigment, J. Raman Spectrosc. 31 (2000) 407-413.

[147] L. Burgio, R.J.H. Clark, Comparative pigment analysis of six modern Egyptian papyri and an authentic one of the 13th century BC by Raman microscopy and other techniques, J. Raman Spectrosc. 31 (2000) 395-401.

[148] I.M. Bell, R.J.H. Clark, P.J. Gibbs, Raman spectroscopic library of natural and synthetic pigments (pre- ~ 1850 AD), Spectrochim. Acta, Part A. 53 (1997) 2159-2179.

[149] M. Bouchard, D.C. Smith, Catalogue of 45 reference Raman spectra of minerals concerning research in art history or archaeology, especially on corroded metals and coloured glass, Spectrochim. Acta, Part A. 59 (2003) 2247-2266.

[150] P. Vandenabeele, L. Moens, H.G.M. Edwards, R. Dams, Raman spectroscopic database of azo pigments and application to modern art studies, J. Raman Spectrosc. 31 (2000) 509-517.

[151] F. Schulte, K. Brzezinka, K. Lutzenberger, H. Stege, U. Panne, Raman spectroscopy of synthetic organic pigments used in 20th century works of art, J. Raman Spectrosc. 39 (2008) 1455-1463.

[152] F. Froment, A. Tournie, P. Colomban, Raman identification of natural red to yellow pigments: ochre and iron-containing ores, J. Raman Spectrosc. 39 (2008) 560-568.

[153] L. Burgio, R.J.H. Clark, Library of FT-Raman spectra of pigments, minerals, pigment media and varnishes, and supplement to existing library of Raman spectra of pigments with visible excitation, Spectrochim. Acta, Part A. 57 (2001) 1491-1521.

[154] K. Castro, M. Perez-Alonso, M.D. Rodríguez-Laso, L.A. Fernandez, J.M. Madariaga, On-line FT-Raman and dispersive Raman spectra database of artists' materials (e-VISART database), Anal. Bioanal. Chem. 382 (2005) 248-258.

[155] G. Burrafato, M. Calabrese, A. Cosentino, A.M. Gueli, S.O. Troja, A. Zuccarello, ColoRaman project: Raman and fluorescence spectroscopy of oil, tempera and fresco paint pigments, J. Raman Spectrosc. 35 (2004) 879-886.

[156] P. Vandenabeele, H.G.M. Edwards, L. Moens, A Decade of Raman Spectroscopy in Art and Archaeology, Chem. Rev. 107 (2007) 675-686.

[157] H.G.M. Edwards, D.W. Farwell, A. Quye, 'Dragon's Blood' I - Characterization of an Ancient Resin Using Fourier Transform Raman Spectroscopy, J. Raman Spectrosc. 28 (1997) 243-249.

[158] C. Daher, C. Paris, A.L. Ho, L. Bellot-Gurlet, J. Echard, A joint use of Raman and infrared spectroscopies for the identification of natural organic media used in ancient varnishes, J. Raman Spectrosc. 41 (2010) 1494-1499.

[159] W. Winkler, E.C. Kirchner, A. Asenbaum, M. Musso, A Raman spectroscopic approach to the maturation process of fossil resins, J. Raman Spectrosc. 32 (2001) 59-63.

[160] A. Bertoluzza, P. Brasili, L. Castri, F. Facchini, C. Fagnano, A. Tinti, Preliminary Results in Dating Human Skeletal Remains by Raman Spectroscopy, J. Raman Spectrosc. 28 (1997) 185-188.

[161] M.H. Schweitzer, M. Marshall, K. Carron, D.S. Bohle, S.C. Busse, E.V. Arnold, et al., Heme compounds in dinosaur trabecular bone, Proc. Natl. Acad. Sci. USA. 94 (1997) 6291-6296.

[162] P. Vandenabeele, Raman spectroscopy in art and archaeology, J. Raman Spectrosc. 35 (2004) 607-609.

[163] G.D. Smith, R.J.H. Clark, Raman microscopy in archaeological science, J Archaeol Sci. 31 (2004) 1137-1160.

[164] D. Roy, M. Chhowalla, H. Wang, N. Sano, I. Alexandrou, T.W. Clyne, et al., Characterisation of carbon nano-onions using Raman spectroscopy, Chem. Phys. Lett. 373 (2003) 52-56.

[165] C. Fantini, A. Jorio, A.P. Santos, V.S.T. Peressinotto, M.A. Pimenta, Characterization of DNA-wrapped carbon nanotubes by resonance Raman and optical absorption spectroscopies, Chem. Phys. Lett. 439 (2007) 138-142.

[166] M.S. Dresselhaus, G. Dresselhaus, R. Saito, A. Jorio, Raman spectroscopy of carbon nanotubes, Phys. Rep. 409 (2005) 47-99.

[167] R. Graupner, Raman spectroscopy of covalently functionalized single-wall carbon nanotubes, J. Raman Spectrosc. 38 (2007) 673-683.

[168] P. Puech, A. Bassil, J. Gonzalez, C. Power, E. Flahaut, S. Barrau, et al., Similarities in the Raman RBM and D bands in double-wall carbon nanotubes, Phys. Rev. B. 72 (2005) 155436-1--155436-6.

[169] A. Jorio, A.P. Santos, H.B. Ribeiro, C. Fantini, M. Souza, J.P.M. Vieira, et al., Quantifying carbon-nanotube species with resonance Raman scattering, Phys. Rev. B. 72 (2005) 075207-1--075207-5.

[170] M.J. West, M.J. Went, The spectroscopic detection of drugs of abuse in fingerprints after development with powders and recovery with adhesive lifters, Spectrochim. Acta, Part A. 71 (2009) 1984-1988.

[171] M.J. West, M.J. Went, The spectroscopic detection of exogenous material in fingerprints after development with powders and recovery with adhesive lifters, Forensic Sci. Int. 174 (2008) 1-5.

[172] M.J. West, M.J. Went, The spectroscopic detection of drugs of abuse on textile fibres after recovery with adhesive lifters, Forensic Sci. Int. 189 (2009) 100-103.

[173] J.D. Gelder, P. Vandenabeele, F. Govaert, L. Moens, Forensic analysis of automotive paints by Raman spectroscopy, J. Raman Spectrosc. 36 (2005) 1059-1067.

[174] J. Zieba-Palus, J. Was-Gubała, An investigation into the use of micro-Raman spectroscopy for the analysis of car paints and single textile fibres, J Mol Struct. 993 (2011) 127-133.

[175] J. Zieba-Palus, A. Michalska, A. Weselucha-Birczynska, Characterisation of paint samples by infrared and Raman spectroscopy for criminalistic purposes, J Mol Struct. 993 (2011) 134-141.

[176] J. Zieba-Palus, R. Borusiewicz, Examination of multilayer paint coats by the use of infrared, Raman and XRF spectroscopy for forensic purposes, J Mol Struct. 792-793 (2006) 286-292.

[177] S.E.J. Bell, L.A. Fido, S.J. Speers, W.J. Armstrong, Rapid Forensic Analysis and Identification of "Lilac" Architectural Finishes Using Raman Spectroscopy, Appl. Spectrosc. 59 (2005) 100-108.

[178] M. Claybourn, M. Ansell, Using Raman Spectroscopy to solve crime: inks, questioned documents and fraud, Sci. Justice. 40 (2000) 261-271.

[179] X. Wang, J. Yu, A. Zhang, D. Zhou, M. Xie, Nondestructive identification for red ink entries of seals by Raman and Fourier transform infrared spectrometry, Spectrochim. Acta, Part A. 97 (2012) 986-994.

[180] L. Heudt, D. Debois, T.A. Zimmerman, L. Kohler, F. Bano, F. Partouche, et al., Raman spectroscopy and laser desorption mass spectrometry for minimal destructive forensic analysis of black and color inkjet printed documents, Forensic Sci. Int. 219 (2012) 64-75.

[181] C. Rodger, G. Dent, J. Watkinson, W.E. Smith, Surface-Enhanced Resonance Raman Scattering and Near-Infrared Fourier Transform Raman Scattering as in situ Probes of Ink Jet Dyes Printed on Paper, Appl. Spectrosc. 54 (2000) 1567-1576.

[182] P.C. White, In situ Surface Enhanced Resonance Raman Scattering (SERRS) spectroscopy of biro inks - long term stability of colloid treated samples, Sci. Justice. 43 (2003) 149-152.

[183] L. Lepot, K. De Wael, F. Gason, B. Gilbert, Application of Raman spectroscopy to forensic fibre cases, Sci. Justice. 48 (2008) 109-117.

[184] G. Massonnet, P. Buzzini, G. Jochem, M. Stauber, T. Coyle, C. Roux, et al., Evaluation of Raman Spectroscopy for the Analysis of Colored Fibers: A Collaborative Study, J. Forensic Sci. 50 (2005) 1-11.

[185] J. Thomas, P. Buzzini, G. Massonnet, B. Reedy, C. Roux, Raman spectroscopy and the forensic analysis of black/grey and blue cotton fibres Part 1. Investigation of the effects of varying laser wavelength, Forensic Sci. Int. 152 (2005) 189-197.

[186] L.C. Abbott, S.N. Batchelor, J.R.L. Smith, J.N. Moore, Resonance Raman and UV–visible spectroscopy of black dyes on textiles, Forensic Sci. Int. 202 (2010) 54-63.

[187] I.P. Keen, G.W. White, P.M. Fredericks, Characterization of Fibers by Raman Microprobe Spectroscopy, J. Forensic Sci. 43 (1998) 82-89.

[188] G. Massonnet, P. Buzzini, F. Monard, G. Jochem, L. Fido, S. Bell, et al., Raman spectroscopy and microspectrophotometry of reactive dyes on cotton fibres: Analysis and detection limits, Forensic Sci. Int. in press (2012).

[189] C. Weyermann, Y. Mimoune, F. Anglada, G. Massonnet, P. Esseiva, P. Buzzini, Applications of a transportable Raman spectrometer for the in situ detection of controlled substances at border controls, Forensic Sci. Int. 209 (2011) 21-28.

[190] E.M.A. Ali, H.G.M. Edwards, M.D. Hargreaves, I.J. Scowen, In-situ detection of drugs-of-abuse on clothing using confocal Raman microscopy, Anal. Chim. Acta. 615 (2008) 63-72.

[191] J.S. Day, H.G.M. Edwards, S.A. Dobrowski, A.M. Voice, The detection of drugs of abuse in fingerprints using Raman spectroscopy II: cyanoacrylate-fumed fingerprints, Spectrochim. Acta, Part A. 60 (2004) 1725-1730.

[192] E.M.A. Ali, H.G.M. Edwards, I.J. Scowen, In-situ detection of single particles of explosive on clothing with confocal Raman microscopy, Talanta. 78 (2009) 1201-1203.

[193] E.M.A. Ali, H.G.M. Edwards, I.J. Scowen, Raman spectroscopy and security applications: the detection of explosives and precursors on clothing, J. Raman Spectrosc. 40 (2009) 2009-2014.

[194] C. Eliasson, N.A. Macleod, P. Matousek, Noninvasive Detection of Concealed Liquid Explosives Using Raman Spectroscopy, Anal. Chim. Acta. 79 (2007) 8185-8189.

[195] N.A. Hatab, G. Eres, P.B. Hatzinger, B. Gu, Detection and analysis of cyclotrimethylenetrinitramine (RDX) in environmental samples by surface-enhanced Raman spectroscopy, J. Raman Spectrosc. 41 (2010) 1131-1136.

[196] Z. Xu, X. Meng, Detection of 3-nitro-1, 2, 4-triazol-3-one (NTO) by surface-enhanced Raman spectroscopy, Vib. Spectrosc. (in press).

[197] I.P. Hayward, T.E. Kirkbride, D.N. Batchelder, R.J. Lacey, Use of a Fiber Optic Probe for the Detection and Identification of Explosive Materials by Raman Spectroscopy, J. Forensic Sci. 40 (1995) 883-884.

[198] M. López-López, J.L. Ferrando, C. García-Ruiz, Comparative analysis of smokeless gunpowders by Fourier transform infrared and Raman spectroscopy, Anal. Chim. Acta. 717 (2012) 92-99.

[199] M.K. Kumar, N.G. Prabhakar, G. Chandrika, B.M. Mohan, G. Nagendrappa, Microscopic and spectrometric characterizations of trace evidence materials present on the discharged lead bullet and shot—A case report, Journal of Saudi Chemical Society. 15 (2011) 11-18.

[200] K. Virkler, I.K. Lednev, Raman spectroscopy offers great potential for the nondestructive confirmatory identification of body fluids, Forensic Sci. Int. 181 (2008) e1-e5.

[201] V. Sikirzhytski, A. Sikirzhytskaya, I.K. Lednev, Multidimensional Raman spectroscopic signature of sweat and its potential application to forensic body fluid identification, Anal. Chim. Acta. 718 (2012) 78-83.

[202] K. Virkler, I.K. Lednev, Raman spectroscopic signature of semen and its potential application to forensic body fluid identification, Forensic Sci. Int. 193 (2009) 56-62.

[203] A. Sikirzhytskaya, V. Sikirzhytski, I.K. Lednev, Raman spectroscopic signature of vaginal fluid and its potential application in forensic body fluid identification, Forensic Sci. Int. 216 (2012) 44-48.

[204] K. Virkler, I.K. Lednev, Raman spectroscopic signature of blood and its potential application to forensic body fluid identification, Anal. Bioanal. Chem. 396 (2010) 525-534.

[205] S. Boyd, M.F. Bertino, S.J. Seashols, Raman spectroscopy of blood samples for forensic applications, Forensic Sci. Int. 208 (2011) 124-128.

[206] V. Sikirzhytski, A. Sikirzhytskaya, I.K. Lednev, Advanced statistical analysis of Raman spectroscopic data for the identification of body fluid traces: Semen and blood mixtures, Forensic Sci. Int. (in press).

[207] K. Virkler, I.K. Lednev, Analysis of body fluids for forensic purposes: From laboratory testing to non-destructive rapid confirmatory identification at a crime scene, Forensic Sci. Int. 188 (2009) 1-17.

[208] J. Zieba-Palus, R. Borusiewicz, M. Kunicki, PRAXIS—combined μ-Raman and μ-XRF spectrometers in the examination of forensic samples, Forensic Sci. Int. 175 (2008) 1-10.

[209] V. Otieno-Alego, Some forensic applications of a combined micro-Raman and scanning electron microscopy system, J. Raman Spectrosc. 40 (2009) 948-953.

[210] R.D. Blackledge, E.L. Jones Jr., All that Glitters Is Gold, in: Blackledge R.D. (Ed.), Forensic Analysis on the Cutting Edge: New Methods for TRace Evidence Analysis, John Wiley & Sons Inc., New Jersey, 2007, pp. 1-31.

[211] F. Gunn, The Artificial Face: A History of Cosmetics, Ebenezer Baylis & Son Ltd, Great Britain, 1973.

[212] S. Pointer, The Artifice of Beauty: A History and Practical Guide to Perfumes and Cosmetics, Sutton Publishing, U.K., 2005.

[213] J. Pallingston, Lipstick: A Celebration of a Girl's Best Friend, Simon & Schuster UK Ltd, London, 1999.

[214] M.C. Ragas, K. Kozlowski, Read My Lips: A Cultural History of Lipstick, Chronicle Books, Hong Kong, 1998.

[215] J. Toedt, D. Koza, K. Van Cleef-Toedt, Chemical Composition of Everyday Products, Greenwood Press, Westport - USA, 2005.

[216] J. Stenger, E.E. Kwan, K. Eremin, S. Speakman, D. Kirby, H. Stewart, et al., Lithol Red Salts: Charaterization and Deterioration, E-Preservation Science. 7 (2010) 147-157.

[217] R. Winter, A Consumer's Dictionary of Cosmetic Ingredients, 7th ed., Three Rivers Press, New York, 2009.

[218] A. Salvador, A. Chisvert, Analysis of Cosmetic Products, Elsevier, Amsterdam, 2007.

[219] http://rimmel.rimmellondon.com/sites/all/themes/rimmel/images/uk/en/NEW_RIMMEL_INCI_BOOK.pdf, Date accessed: 08/06/12.

[220] http://www.barrym.com/products/ingredients.asp?id=82, Date accessed: 08/06/12.

[221] A.O. Barel, M. Paye, H.I. Maibach, Handbook of Cosmetic Science and Technology, Marcel Dekker, Inc., New York, 2001.

[222] L.D. Rhein, A. O'Lenick, M. Schlossman, P. Somasundaran, Surfactants in Personal Care Products and Decorative Cosmetics, 3rd ed., CRC Press, USA, 2007.

[223] M. Ogilvie, P. Kristensen-Bach, Why Women Wear Lipstick: Preliminary Findings, ECU Publications, under review. (2001).

[224] *State v. Johnson* [1933] 37 N.M. 280, 21 P.2d 813, 815,.

[225] E.P. Coffey, The Importance of Scientific Analysis of Evidence in the Prosecution of Crime, Indiana Law J. 11 (1935) 105-115.

[226] F.E. Inbau, The Admissibility of Scientific Evidence in Criminal Cases, Law & Contemp. Probs. 2 (1935) 495-503.

[227] *Fishburn v. Fishburn* [1955] 2 W.L.R. 236,.

[228] G. Falcon, 'Lipstick Killer' behind bars since 1946, http://edition.cnn.com/2009/CRIME/10/24/illinois.lipstick.murders/index.html. Date accessed: 18/07/2012 (Updated: October 2009).

[229] C. Simmonds, Suspect Arrested in Connection with Bank of the West Robbery, http://www.fbi.gov/oklahomacity/press-releases/2012/suspect-arrested-in-connection-with-bank-of-the-west-robbery. Date accessed: 12/07/2012 (Updated: April 2012).

[230] S. Dunlap, "Rasta Robber" Dons Dreadlocks in Houston Bank Robbery, http://www.fbi.gov/houston/press-releases/2010/ho010610.htm. Date accessed: 18/07/2012 (Updated: January 2010).

[231] L.W. Russell, A.E. Welch, Analysis of lipsticks, Forensic Sci. Int. 25 (1984) 105-116.

[232] J. Andrasko, Forensic analysis of lipsticks, Forensic Sci. Int. 17 (1981) 235-251.

[233] D.J. Reuland, W.A. Trinler, A Comparison of Lipstick Smears by High Performance Liquid Chromatography, J. Forensic Sci. Soc. 20 (1980) 111-120.

[234] Y. Ehara, Y. Marumo, Identification of lipstick smears by fluorescence observation and purge-and-trap gas chromatography, Forensic Sci. Int. 96 (1998) 1-10.

[235] D.M. Lucas, G. Eijgelaar, An evaluation of a technique for the examination of lipstick stains, J. Forensic Sci. 6 (1961) 354-362.

[236] M.Y. Choudhry, Comparison of Minute Smears of Lipstick by Microspectrophotometry and Scanning Electron Microscopy/Energy-Dispersive Spectroscopy, J. Forensic Sci. 36 (1991) 366-375.

[237] R.L. Keagy, Examination of Cosmetic Smudges Including Transesterification and Gas Chromatographic/Mass Spectrometric Analysis, J. Forensic Sci. 28 (1982) 623-631.

[238] G. Misra, V.K. Mittal, Neutron activation analysis of lipsticks using γ-ray spectrometry, J. Appl. Spectrosc. 71 (2004) 270-274.

[239] J.T. Abraham, S.K. Shukla, A.K. Singh, Application of X-Ray Diffraction Techniques in Forensic Science, FBI Forensic Science Communications. 9 (2007) 18/07/2012.

[240] C. Desiderio, C. Marra, S. Fanali, Quantitative analysis of synthetic dyes in lipstick by micellar electrokinetic capillary chromatography, Electrophoresis. 19 (1998) 1478-1483.

[241] G. Socrates, Infrared and Raman Characteristic Group Frequencies, 3rd ed., John Wiley & Sons Ltd, England, 2010.

[242] I. Basson, E.C. Reynhardt, An investigation of the structures and molecular dynamics of natural waxes: II. Carnauba wax, J. Phys. D: Appl. Phys. 21 (1988) 1429-1433.

[243] I. Basson, E.C. Reynhardt, An investigation of the structures and molecular dynamics of natural waxes: I. Beeswax, J. Phys. D: Appl. Phys. 21 (1988) 1421-1428.

[244] J.N. Miller, J.C. Miller, Statistics and Chemometrics for Analytical Chemistry, 4th ed., Pearson Education Ltd, Great Britain, 2000.

[245] F. Salahioglu, M.J. Went, Differentiation of lipsticks by Raman spectroscopy, Forensic Sci. Int. 223 (2012) 148-152.

[246] The non-destructive and in-situ identification of controlled drugs and narcotics, HORIBA Scientific Application Note. Raman (RA19).

[247] M.S. Maier, D.L.A. de Faria, M.T. Boschín, S.D. Parera, Characterization of reference lipids and their degradation products by Raman spectroscopy, nuclear magnetic resonance and gas chromatography-mass spectrometry, ARKIVOC. 12 (2005) 311-318.

[248] E.M.A. Ali, H.G.M. Edwards, M.D. Hargreaves, I.J. Scowen, *In situ* detection of cocaine hydrochloride in clothing impregnated with the drug using benchtop and portable Raman spectroscopy, J. Raman Spectrosc. 41 (2010) 938-943.

[249] S.A. Montpetit, I.T. Fitch, P.T. O'Donnell, A Simple Automated Instrument for DNA Extraction in Forensic Casework, J. Forensic Sci. 50 (2005) 1-9.

[250] N.J. Crane, E.G. Bartick, R.S. Perlman, S. Huffman, Infrared Spectroscopic Imaging for Noninvasive Detection of Latent Fingerprints, J. Forensic Sci. 52 (2007) 48-53.

[251] E. Slaughter, R.M. Gersberg, K. Watanabe, J. Rudolph, C. Stransky, T.E. Novotny, Toxicity of cigarette butts, and their chemical components, to marine and freshwater fish, Tobacco Control. 20 (2011) i25-i29.

[252] E. Slaughter, Toxicity of cigarette butts and their chemical components to the marine and freshwater fishes, atherinops affinis and pimephales promelas, Master's Thesis. (2010).

[253] O. Geiss, D. Kotzias, Tobacco, Cigarettes and Cigarette Smoke: An Overview, European Communities, Italy, 2007.

[254] U.P. Agarwal, Raman imaging to investigate ultrastructure and composition of plant cell walls: distribution of lignin and cellulose in black spruce wood (*Picea mariana*), Planta. 224 (2006) 1141-1153.

[255] R.Y. Sato-Berru, E.V. Basiuk, J.M. Saniger, Application of principal component analysis to discriminate the Raman spectra of functionalized multiwalled carbon nanotubes, J. Raman Spectrosc. 37 (2006) 1302-1306.

[256] K. Dégardin, Y. Roggo, F. Been, P. Margot, Detection and chemical profiling of medicine counterfeits by Raman spectroscopy and chemometrics, Anal. Chim. Acta. 705 (2011) 334-341.

[257] M.R. de Almeida, D.N. Correa, W.F.C. Rocha, F.J.O. Scafi, R.J. Poppi, Discrimination between authentic and counterfeit banknotes using Raman spectroscopy and PLS-DA with uncertainty estimation, Microchem. J. (in press).

[258] A.G. Ryder, G.M. O'Connor, T.J. Glynn, Identifications and Quantitative Measurement of Narcotics in Solid Mixtures Using Near-IR Raman Spectroscopy and Multivariate Analysis, J. Forensic Sci. 44 (1999) 1013-1019.

[259] A.G. Ryder, G.M. O'Connor, T.J. Glynn, Quantitative analysis of cocaine in solid mixtures using Raman spectroscopy and chemometric methods, J. Raman Spectrosc. 31 (2000) 221-227.

[260] P. Vandenabeele, L. Moens, Micro-Raman spectroscopy of natural and synthetic indigo samples, Analyst. 128 (2003) 187-193.

[261] N. Navas, J. Romero-Pastor, E. Manzano, C. Cardell, Raman spectroscopic discrimination of pigments and tempera paintmodel samples by principal component analysis on first-derivative spectra, J. Raman Spectrosc. 41 (2010) 1486-1493.

[262] C. Muehlethaler, G. Massonnet, P. Esseiva, The application of chemometrics on Infrared and Raman spectra as a tool for the forensic analysis of paints, Forensic Sci. Int. 209 (2011) 173-182.

[263] R.G. Brereton, Chemometrics: Data Analysis for the Laboratory and Chemical Plant, John Wiley & Sons Ltd, England, 2006.

[264] K.H. Esbensen, Multivariate Data Analysis - In Practice, 5th ed., CAMO Software, USA, 2010.

[265] L.I. Smith, http://www.cs.otago.ac.nz/cosc453/student_tutorials/principal_components.pdf, Date accessed: 19/10/2012.

APPENDIX I

List of Lipsticks

Table A1. Table listing the brand, type, labelled colour and the visual colour of the lipsticks used in Chapter IV.

BRAND	VARIANT	COLOUR (as on label)	MAIN COLOUR	SHADE
Almay		36 Lip Vitality	Red	
Barry M	Lip Paint	52 Shocking Pink	Pink	
Barry M	Lip Paint	53 Coral	Orange	Peach
Barry M	Lip Paint	54 Peach	Orange	Peach
Barry M	Lip Paint	62 Vibrant Pink	Pink	
Barry M	Lip Paint	101 Marshmallow	Flesh	
Barry M	Lip Paint	113 Sheer Pink	Pink	Shimmery, Light
Barry M	Lip Paint	117 Orange	Orange	
Barry M	Lip Paint	121 Pillar Box Red	Red	
Barry M	Lip Paint	136 Golden Bronze	Brown	Shimmery, Light
Barry M	Lip Paint	140 Pink Sparkle	Pink	Shimmery
Barry M	Lip Paint	141 Royal Raspberry	Burgundy	
Barry M	Lip Paint	144 Cerise Pink	Pink	Very Dark
Barry M	Lip Paint	145 Punky Pink	Pink	Dark
Barry M	Lip Paint	146 Dolly Pink	Pink	
Bourjois	Docteur Glamour	15 Fuchsia 0 bobo	Pink	
Bourjois	Lovely Rouge	16 Brique Exclusif	Red	
Bourjois	So Rouge	32 Fashion Rouge	Red	Dark
Bourjois	Sweet Kiss	54 Rouge Glamour	Red	
Coty Mainz	Colour Sensation	070 Golden Terracotta	Brown	
Elizabeth Arden	Exceptional Lipstick	17 Breathless	Brown	Pink
La Femme		29 Dream Rose	Brown	Pink
L'Oreal	Color Riche	164 Concorde Red	Red	Light
L'Oreal	Color Riche	243 Velvet Gold	Brown	Light, Pink
L'Oreal	Color Riche	345 Cherry Crystal	Brown	Red, Shimmery
L'Oreal	Crème	524 Tendre Mauve	Brown	
L'Oreal	Invincible Platinum	900 Platinum Candy	Brown	Pink
Max Factor	Hyperfull	210 Vigorous	Brown	
Max Factor	Lipfinity Everlites	30 Curious	Brown	Pink, Lipgloss
Maybelline	Watershine	18 Cherry Pie	Burgundy	

Prestige		CL-78A Pout	Brown	Light
Prestige		PL-28A Fever	Orange	Peach
Prestige		PL-38A Spunky	Brown	Very Light
Prestige		PL-49A Pink Sands	Brown	Pink
Prestige		CL-93A Aftershock	Pink	Very Dark
Revlon	Matte	004 Pink About It	Pink	Dark, Peach
Revlon	Matte	005 Strawberry Suede	Peach	Red
Revlon	Matte	006 Really Red	Red	Dark
Revlon	Absolutely Fabulous Lipcream	07 Cherish	Brown	
Revlon	Matte	008 Cocoa Craving	Brown	
Revlon	Matte	009 Fabulous Fig	Red	Matt, Brown
Revlon	Colorburst	020 Baby Pink	Pink	Shimmery
Revlon	Colorburst	025 Carnation	Pink	
Revlon	Colorburst	030 Fuchsia	Pink	Very Dark
Revlon	Colorburst	035 Blush	Brown	
Revlon	Colorburst	045 Raspberry	Brown	Dark Pink
Revlon	Moon Drops Moisture Frost	46 Nude Shimmer	Brown	
Revlon	Colorburst	075 Peach	Peach	
Revlon	Colorburst	080 Coral	Red	Bright
Revlon	Colorburst	090 True Red	Red	
Revlon	Colorburst	095 Crimson	Red	Very Dark
Revlon	Super Lustrous (Pearl)	103 Caramel Glace	Brown	Shimmery
Revlon	Super Lustrous (Pearl)	353 Cappuccino	Brown	Shimmery, Light
Revlon	Super Lustrous (Creme)	359 Naturally Nude	Brown	
Revlon	Super Lustrous (Pearl)	371 Copper Frost	Brown	Peach
Revlon	Super Lustrous (Pearl)	430 Softsilver Rose	Pink	Dark, Shimmery
Revlon	Super Lustrous (Pearl)	450 Gentlemen Prefer Pink	Pink	Shimmery
Revlon	Super Lustrous (Pearl)	455 Paparazzi Pink	Pink	Shimmery
Revlon	Super Lustrous (Creme)	663 Va Va Violet	Violet	Very Dark
Revlon	Super Lustrous (Creme)	675 Volcanic Red	Red	
Revlon	Super Lustrous (Creme)	750 Kiss Me Coral	Red	Orange
UNE	Lip-toned Colour	L02	Brown	
UNE	Lip-toned Colour	L05	Brown	
UNE	Lip-toned Colour	L07	Brown	
UNE	Lip-toned Colour	L09	Brown	

UNE	Sheer Lips Balm	S03	Brown	
UNE	Sheer Lips Balm	S05	Brown	
UNE	Sheer Lips Balm	S07	Brown	
UNE	Sheer Lips Balm	S08	Brown	
UNE	Sheer Lips Balm	S12	Brown	
UNE	Sheer Lips Balm	S15	Brown	
UNE	Sheer Lips Balm	S17	Brown	
UNE	Sheer Lips Balm	S19	Brown	

APPENDIX II

Group U Lipsticks

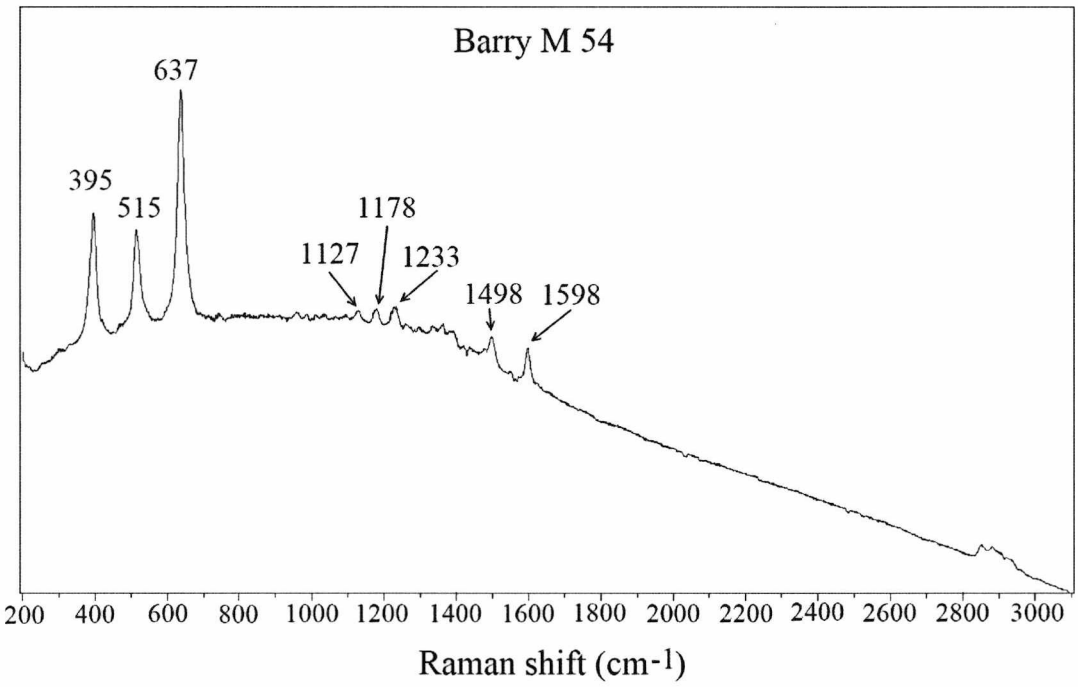

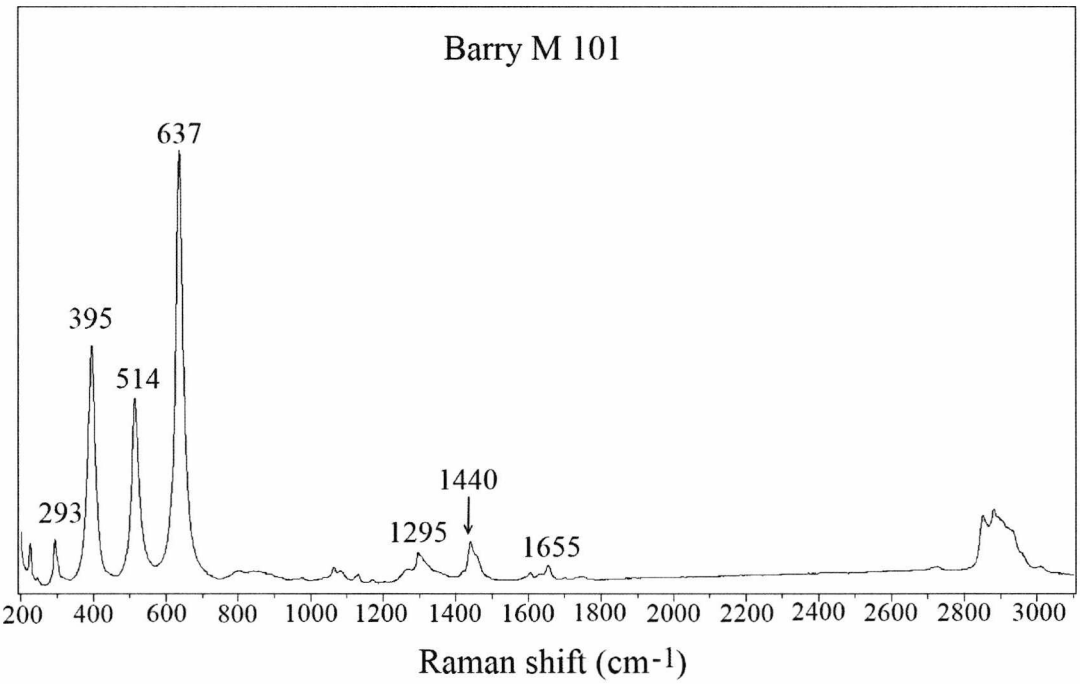

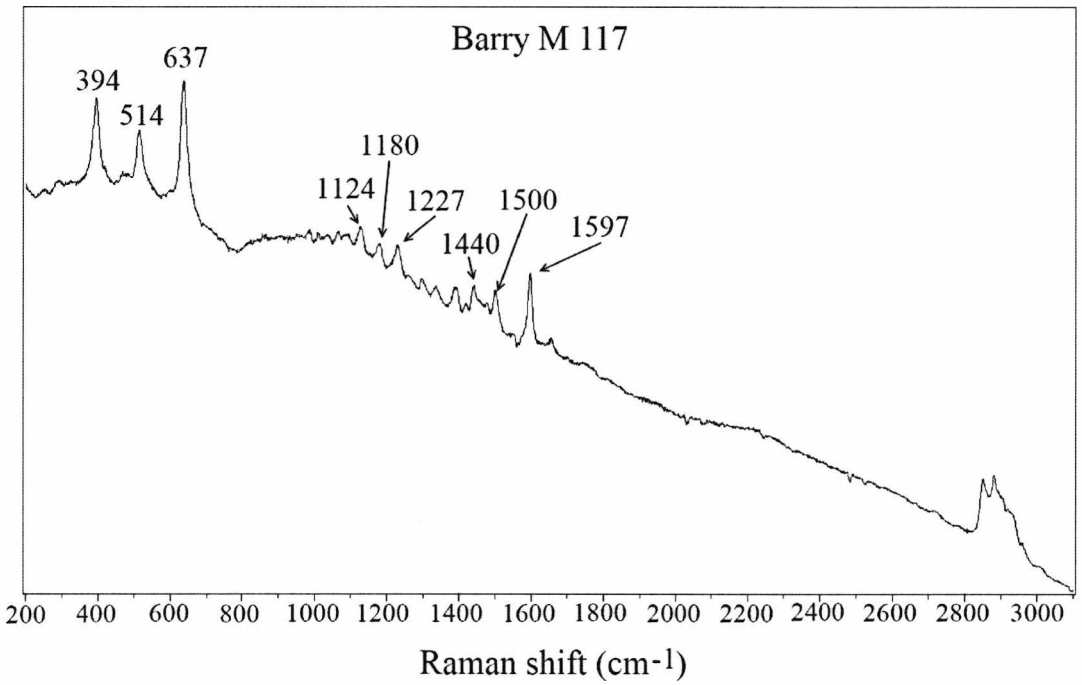
Barry M 117
394
514
637
1124
1180
1227
1440
1500
1597
200 400 600 800 1000 1200 1400 1600 1800 2000 2200 2400 2600 2800 3000
Raman shift (cm-1)

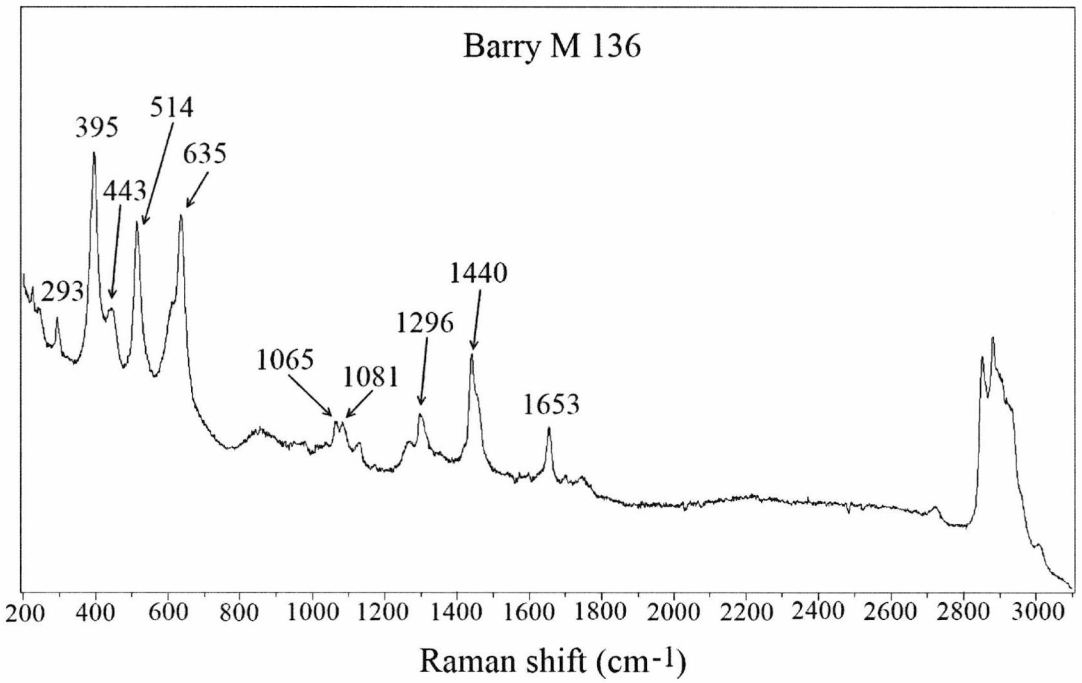
Barry M 136
293
395
443
514
635
1065
1081
1296
1440
1653
200 400 600 800 1000 1200 1400 1600 1800 2000 2200 2400 2600 2800 3000
Raman shift (cm-1)

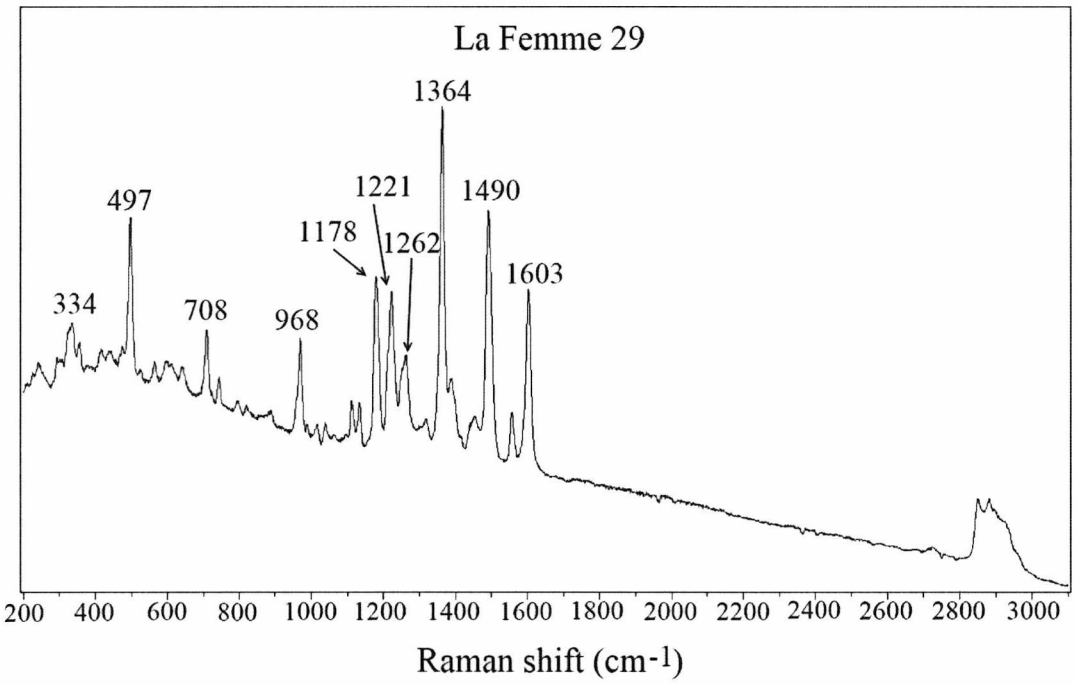
La Femme 29
1364
497
1221
1490
1178
1262
1603
334
708
968
200 400 600 800 1000 1200 1400 1600 1800 2000 2200 2400 2600 2800 3000
Raman shift (cm-1)

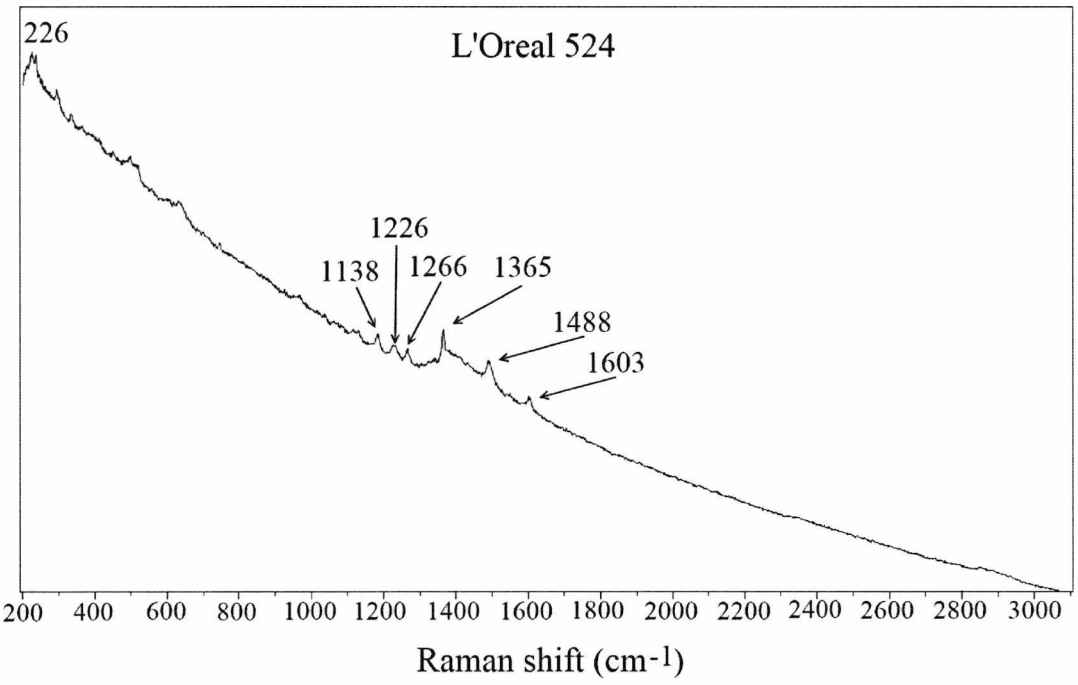
226
L'Oreal 524
1226
1138
1266
1365
1488
1603
200 400 600 800 1000 1200 1400 1600 1800 2000 2200 2400 2600 2800 3000
Raman shift (cm-1)

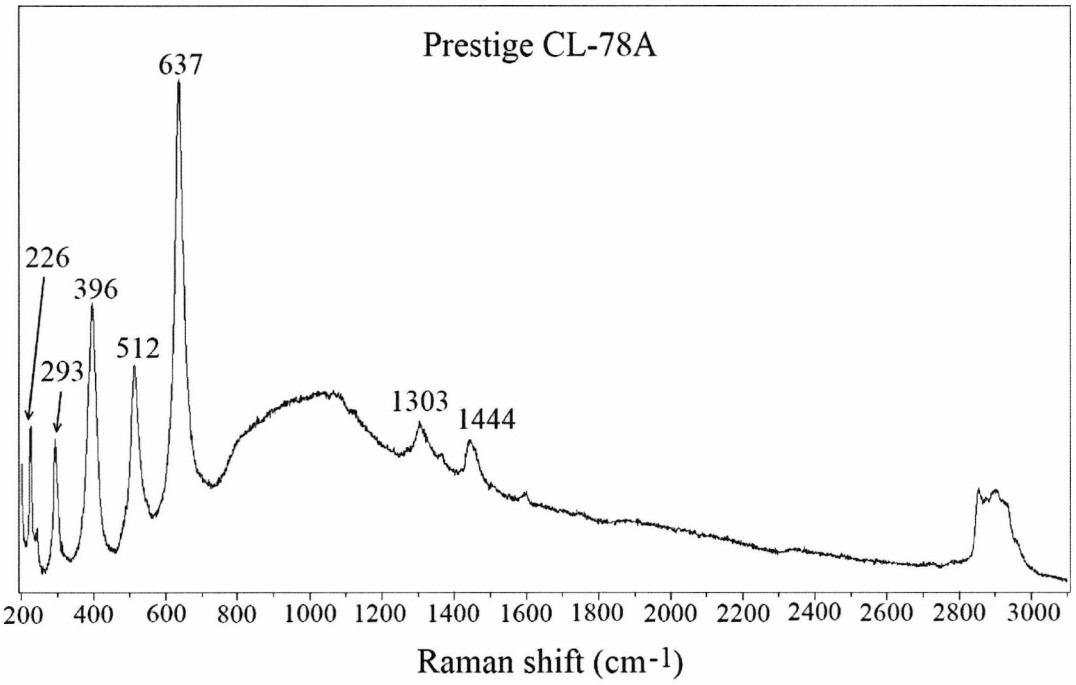
Prestige CL-78A
637
226
396
512
293
1303
1444
200 400 600 800 1000 1200 1400 1600 1800 2000 2200 2400 2600 2800 3000
Raman shift (cm-1)

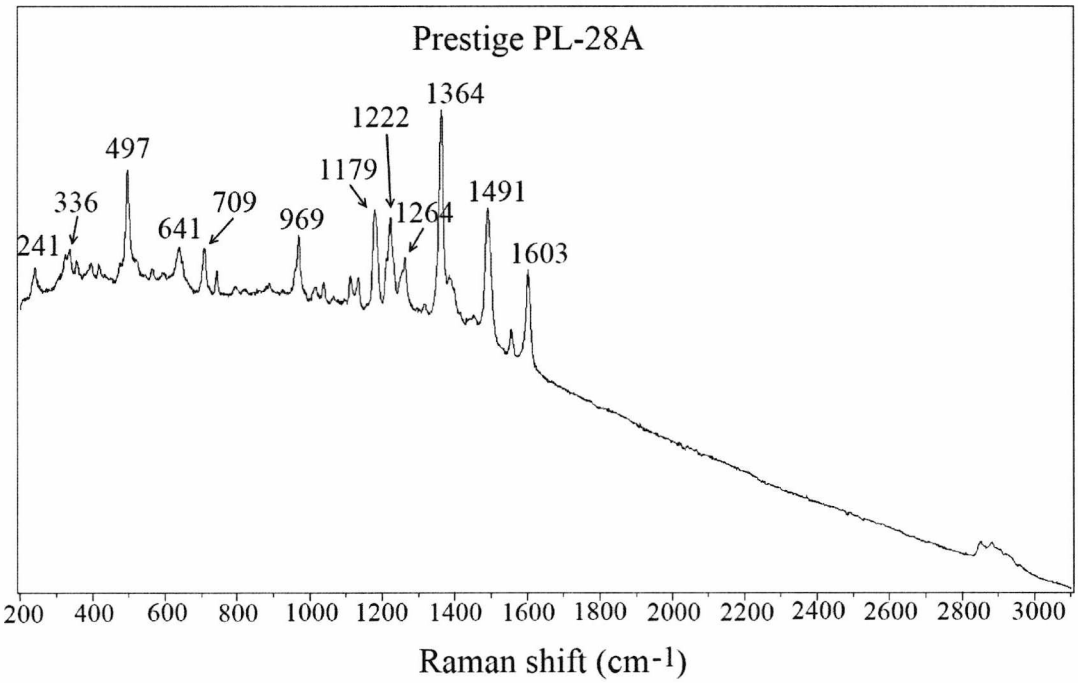
Prestige PL-28A
1364
1222
497
1179
1491
336
709
641
969
1264
241
1603
200 400 600 800 1000 1200 1400 1600 1800 2000 2200 2400 2600 2800 3000
Raman shift (cm-1)

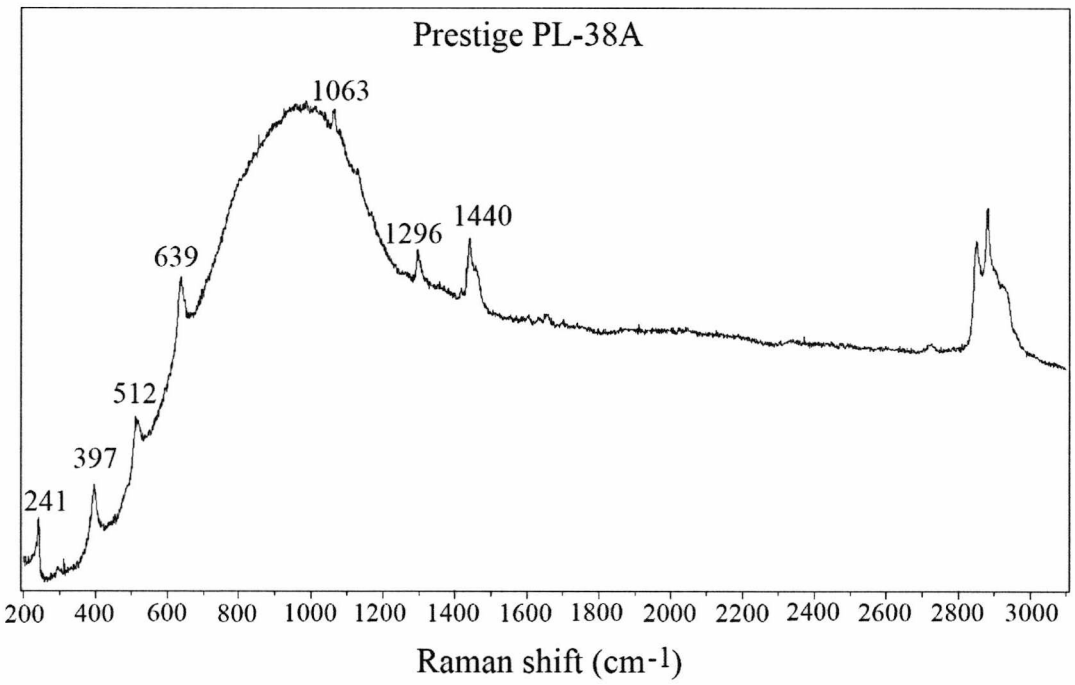
Prestige PL-38A
1063
1296
1440
639
512
397
241
200 400 600 800 1000 1200 1400 1600 1800 2000 2200 2400 2600 2800 3000
Raman shift (cm-1)

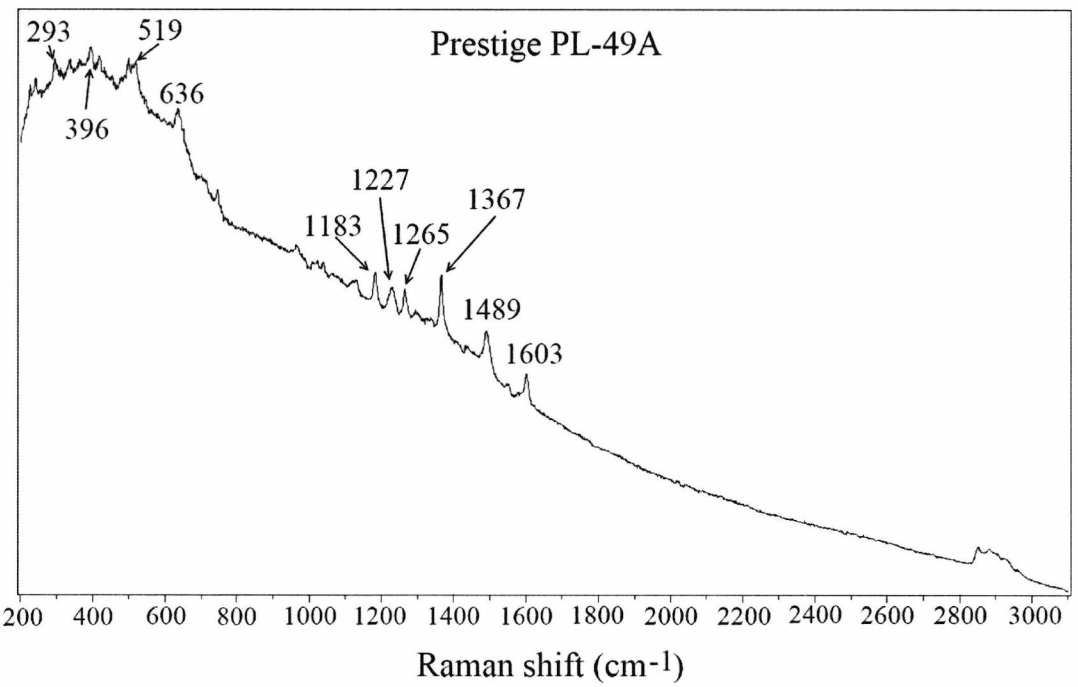
Prestige PL-49A
293
519
636
396
1227
1367
1183
1265
1489
1603
200 400 600 800 1000 1200 1400 1600 1800 2000 2200 2400 2600 2800 3000
Raman shift (cm-1)

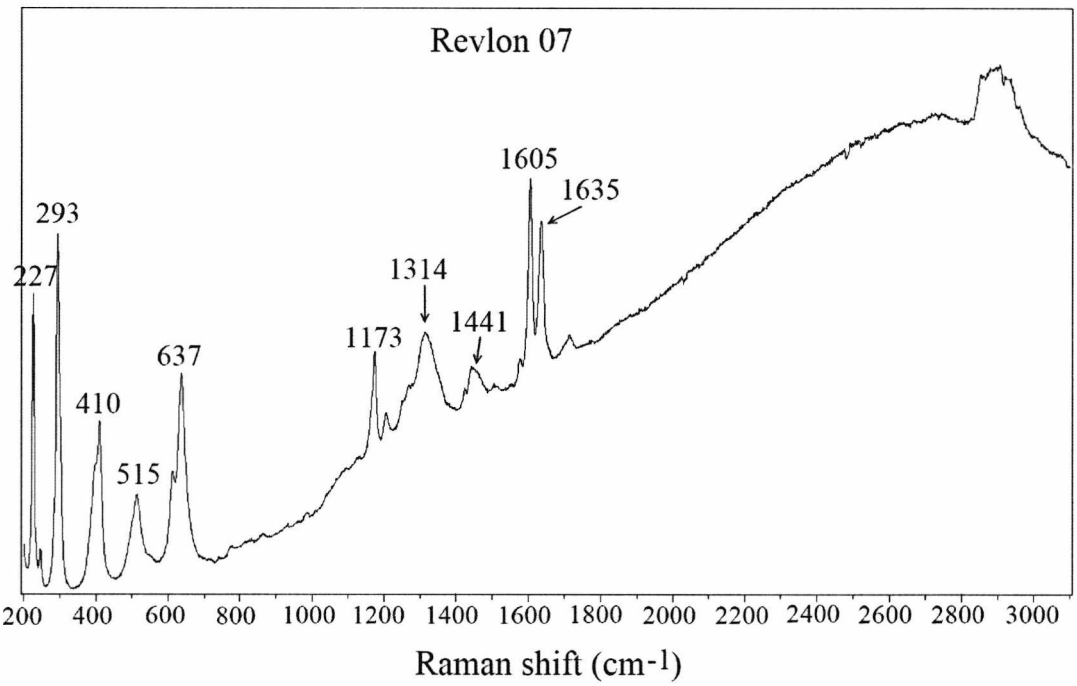
Revlon 07
227
293
410
515
637
1173
1314
1441
1605
1635
200 400 600 800 1000 1200 1400 1600 1800 2000 2200 2400 2600 2800 3000
Raman shift (cm-1)

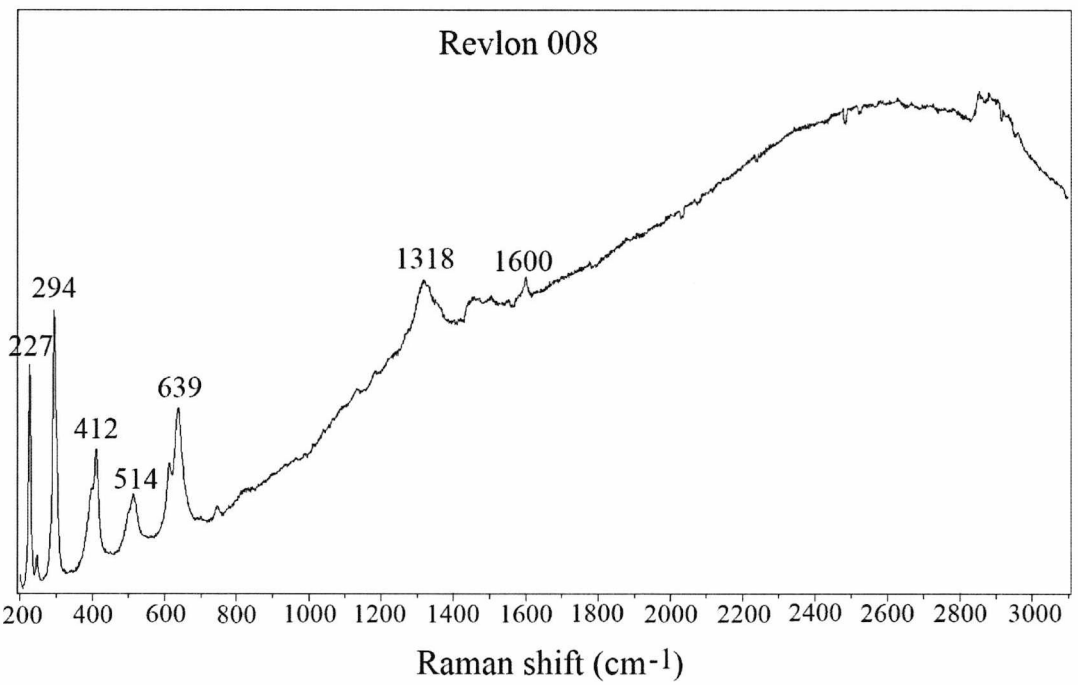
Revlon 008
227
294
412
514
639
1318
1600
200 400 600 800 1000 1200 1400 1600 1800 2000 2200 2400 2600 2800 3000
Raman shift (cm-1)

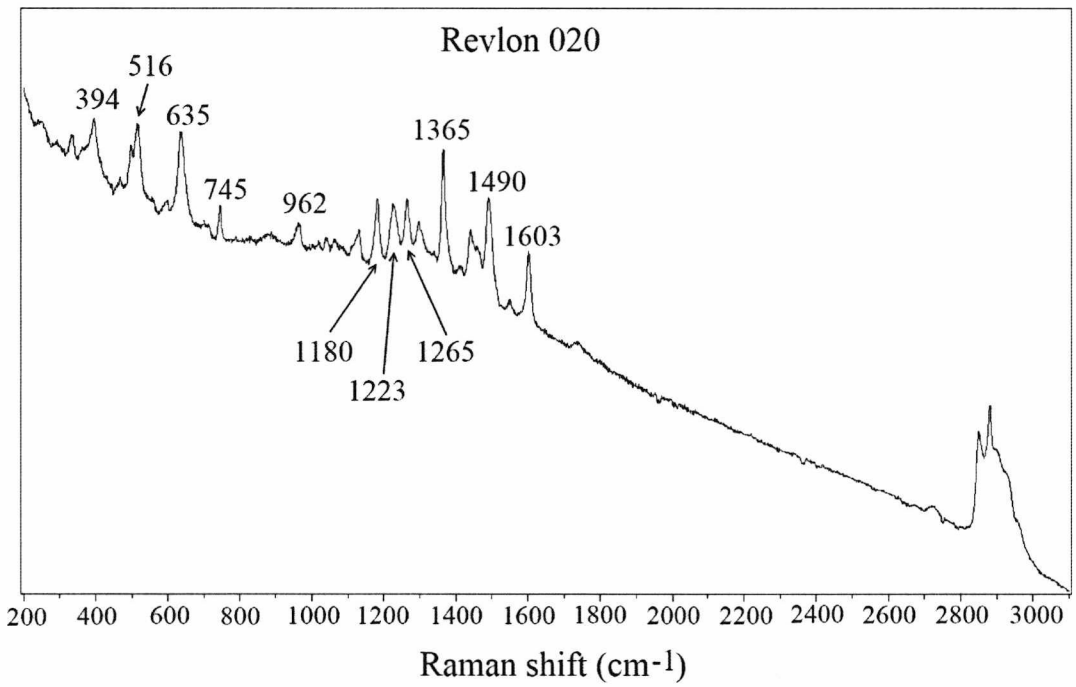
Revlon 020
516
394
635
745
962
1365
1490
1603
1180
1265
1223
200 400 600 800 1000 1200 1400 1600 1800 2000 2200 2400 2600 2800 3000
Raman shift (cm-1)

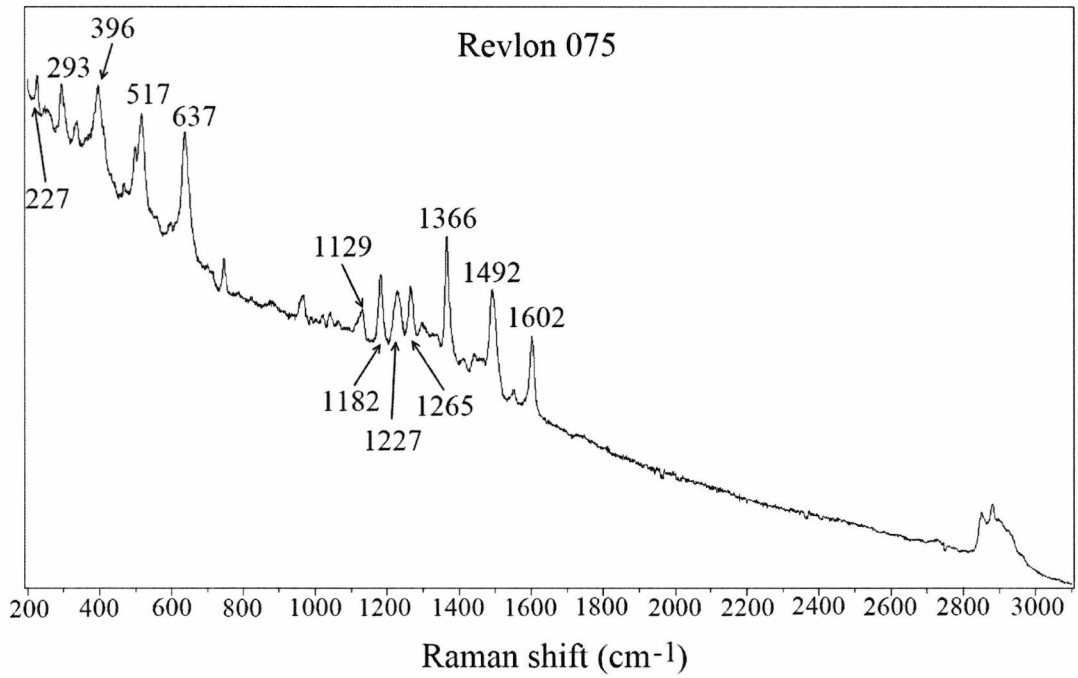
Revlon 075
396
293
517
637
227
1366
1129
1492
1602
1182
1265
1227
200 400 600 800 1000 1200 1400 1600 1800 2000 2200 2400 2600 2800 3000
Raman shift (cm-1)

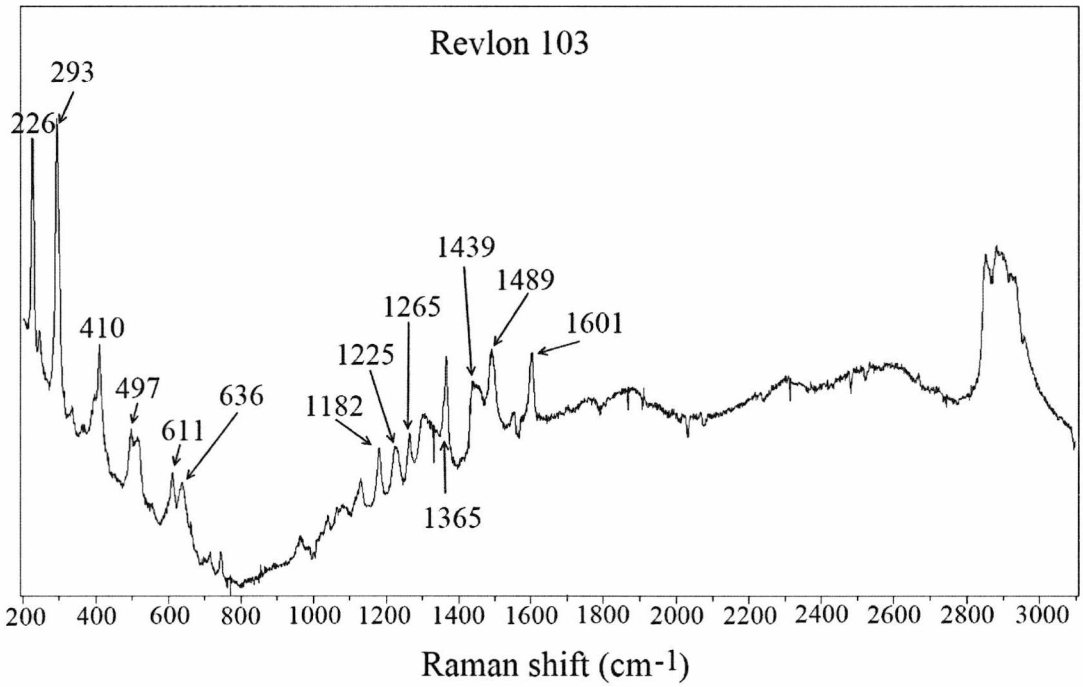
Revlon 103
293
226
410
497
636
611
1182
1225
1265
1439
1489
1601
1365
200 400 600 800 1000 1200 1400 1600 1800 2000 2200 2400 2600 2800 3000
Raman shift (cm-1)

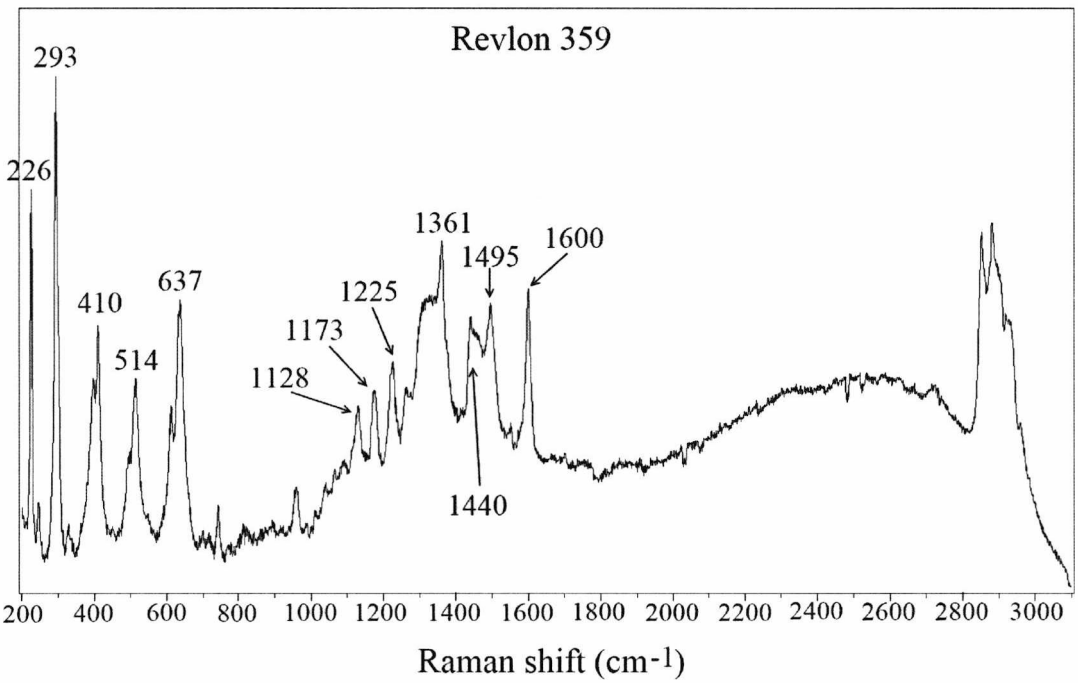
Revlon 359
293
226
410
514
637
1128
1173
1225
1361
1495
1600
1440
200 400 600 800 1000 1200 1400 1600 1800 2000 2200 2400 2600 2800 3000
Raman shift (cm-1)

APPENDIX III

Effects of Ageing on the Lipstick Spectra

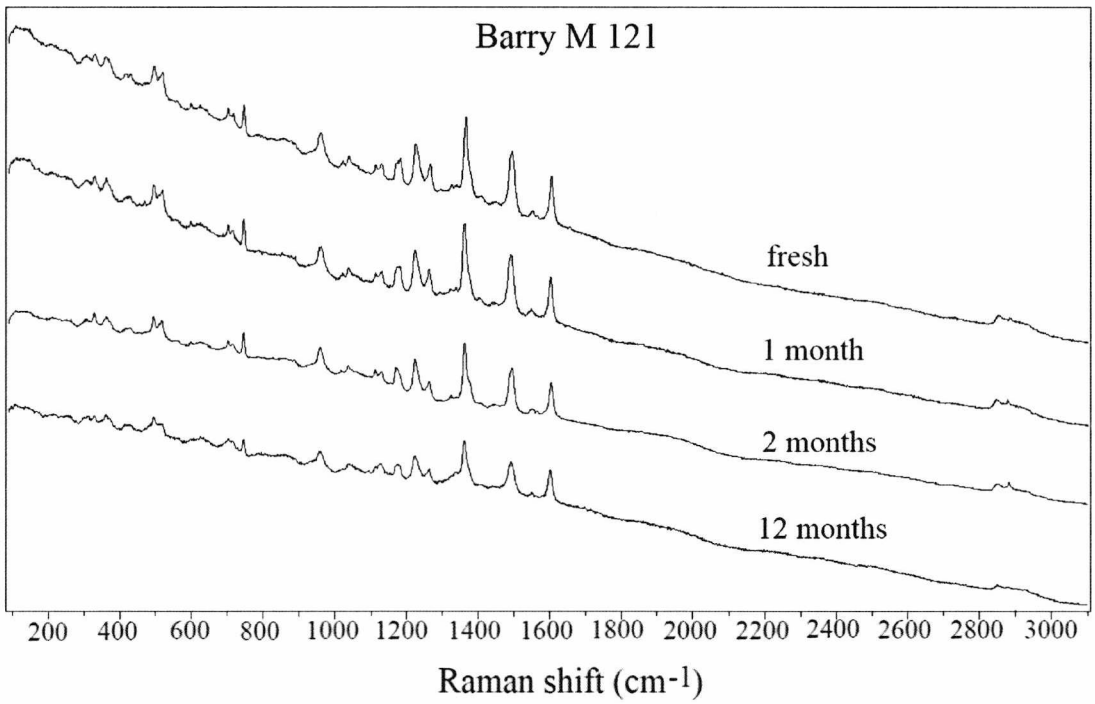

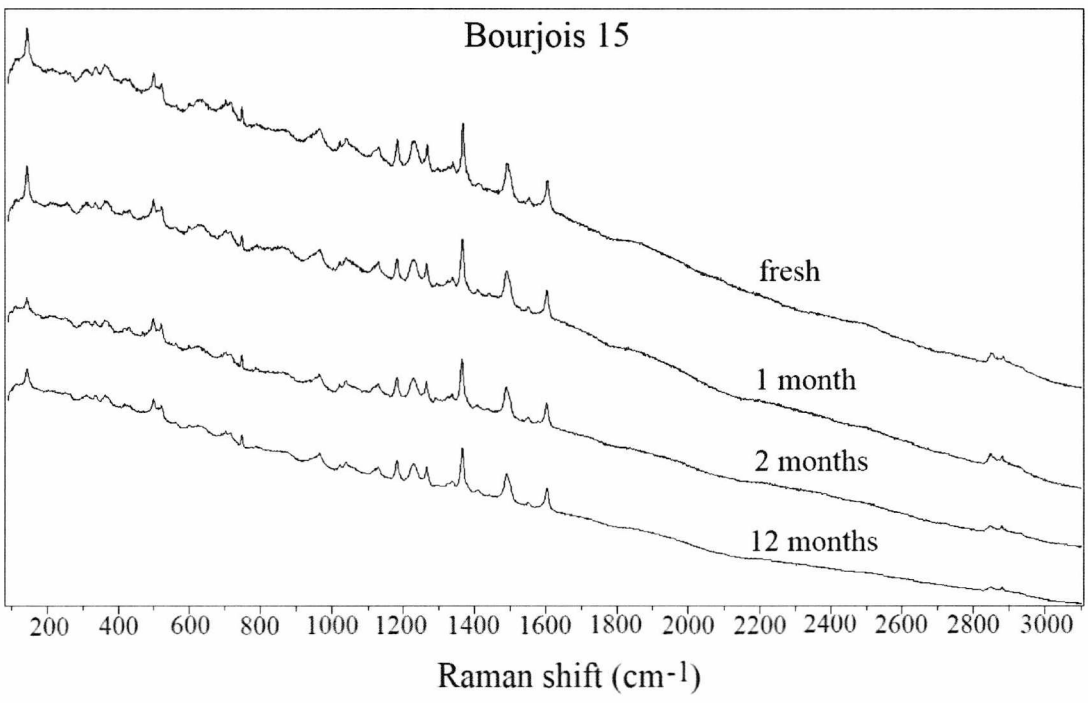

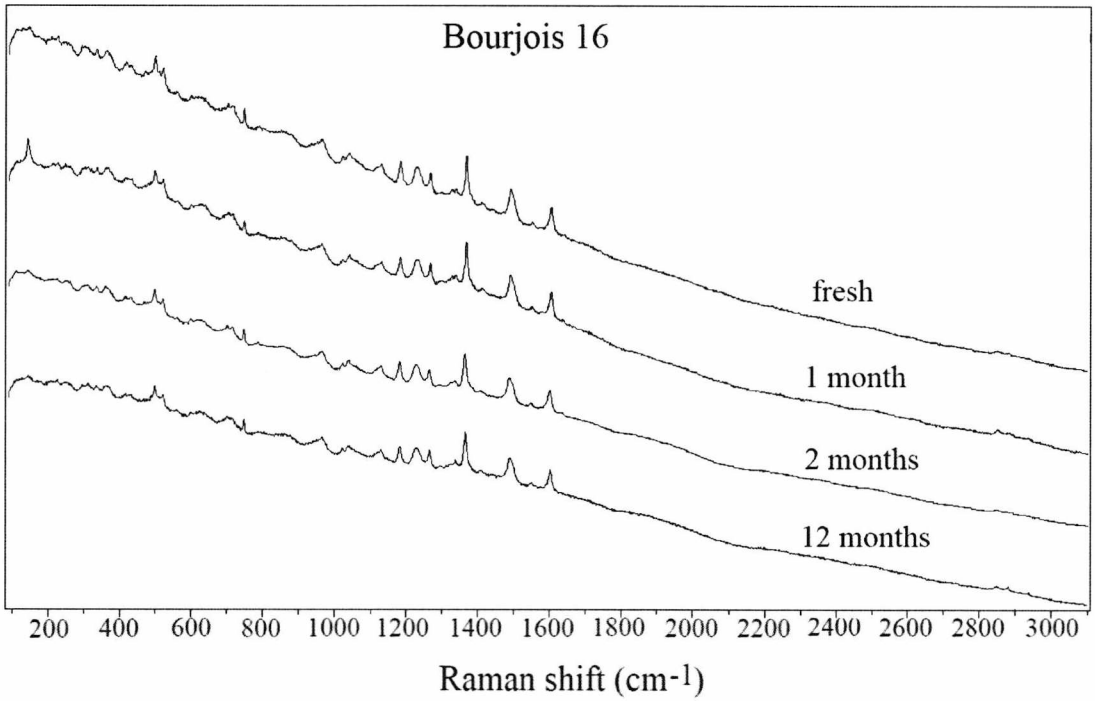
Bourjois 16
fresh
1 month
2 months
12 months
200 400 600 800 1000 1200 1400 1600 1800 2000 2200 2400 2600 2800 3000
Raman shift (cm-1)

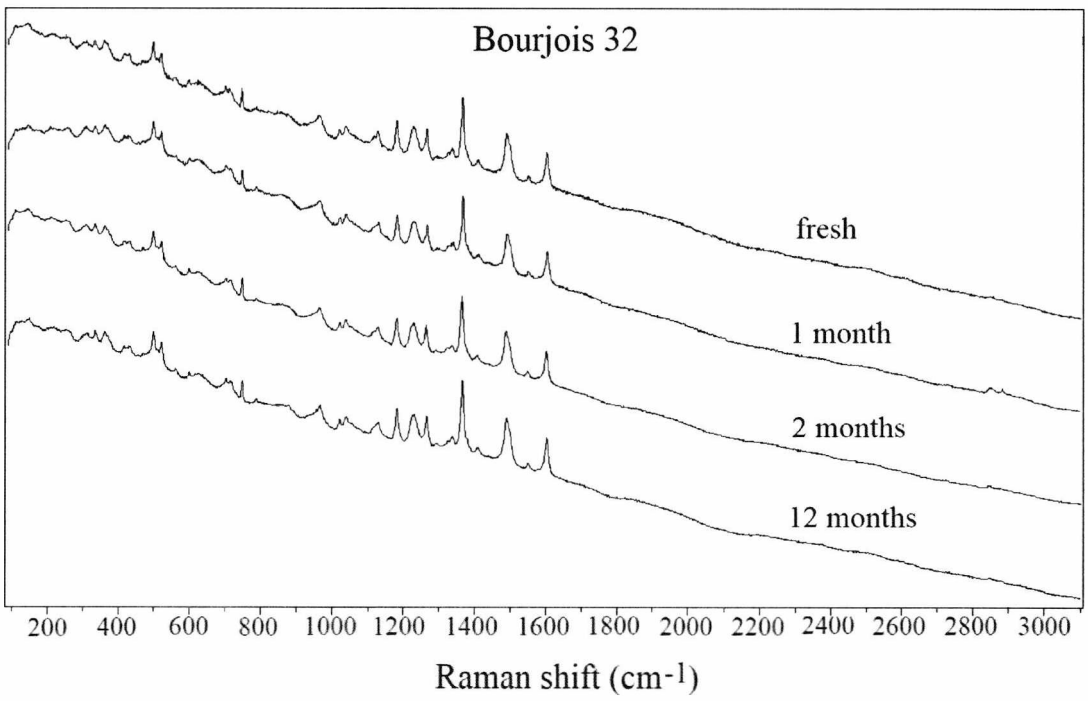
Bourjois 32
fresh
1 month
2 months
12 months
200 400 600 800 1000 1200 1400 1600 1800 2000 2200 2400 2600 2800 3000
Raman shift (cm-1)

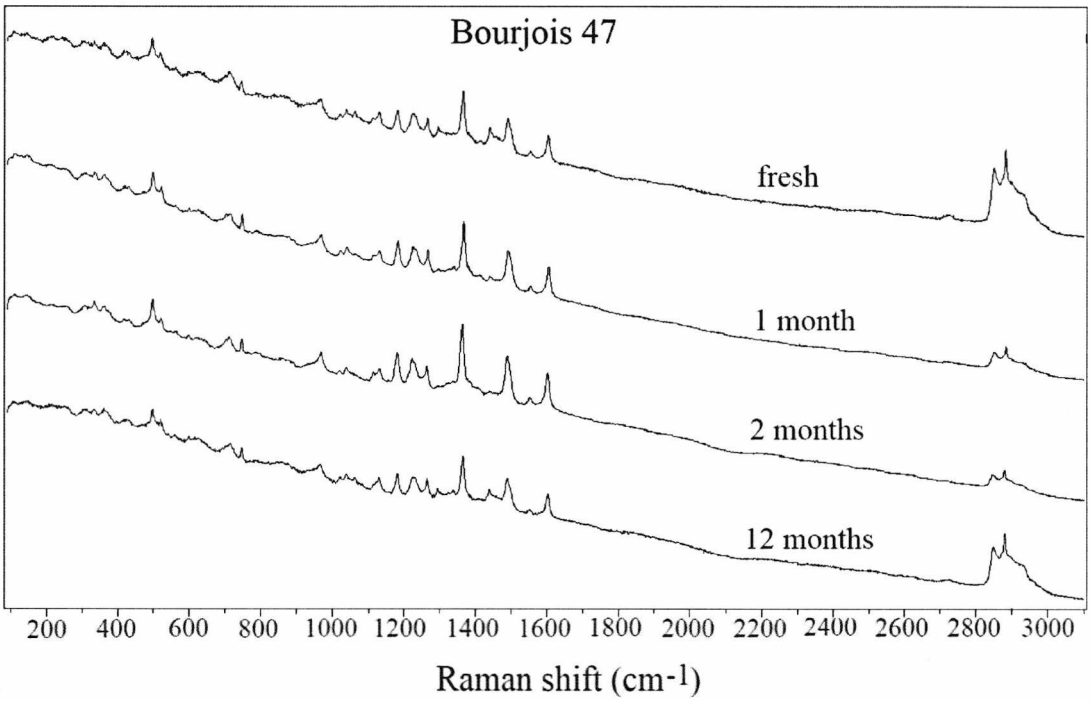
Bourjois 47
fresh
1 month
2 months
12 months
200 400 600 800 1000 1200 1400 1600 1800 2000 2200 2400 2600 2800 3000
Raman shift (cm-1)

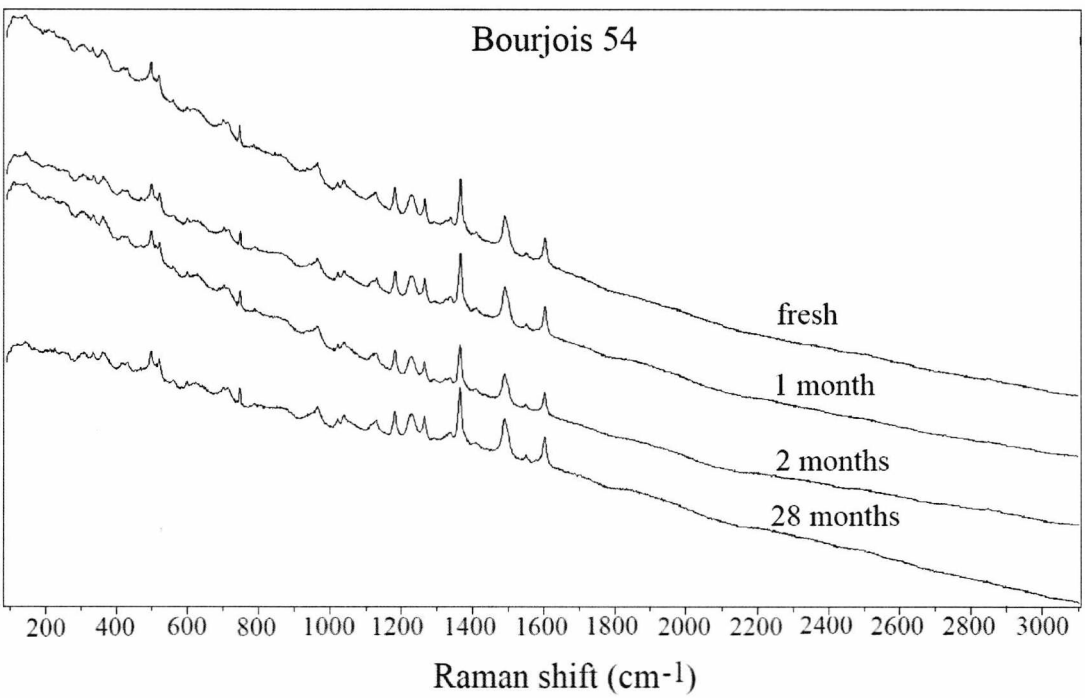
Bourjois 54
fresh
1 month
2 months
28 months
200 400 600 800 1000 1200 1400 1600 1800 2000 2200 2400 2600 2800 3000
Raman shift (cm-1)

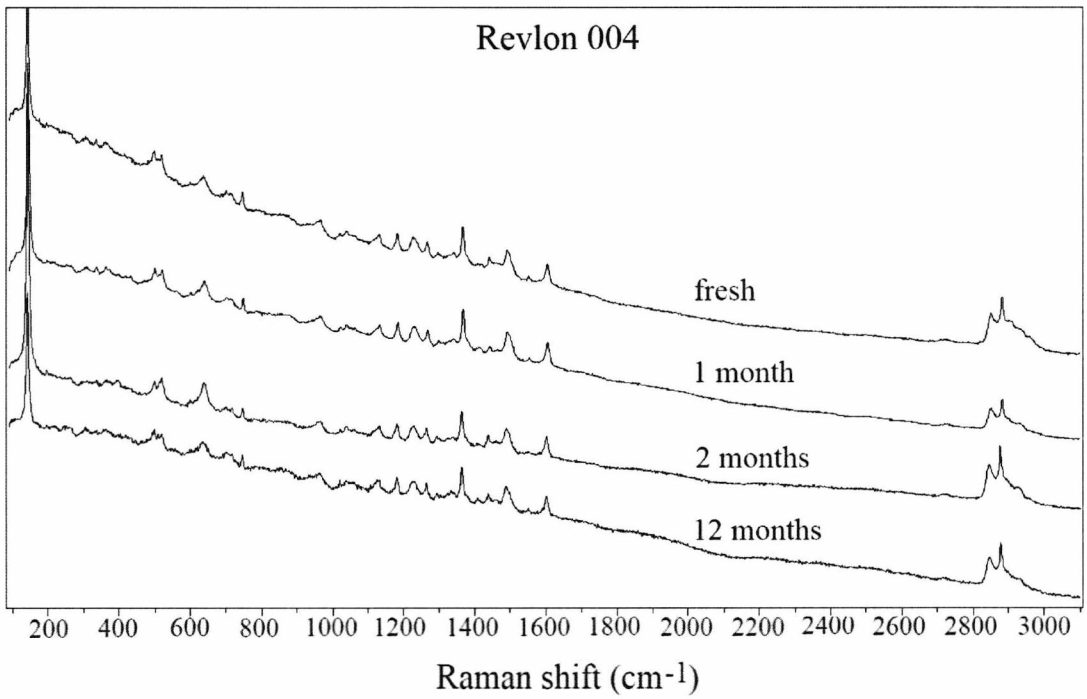
Revlon 004
fresh
1 month
2 months
12 months
200 400 600 800 1000 1200 1400 1600 1800 2000 2200 2400 2600 2800 3000
Raman shift (cm-1)

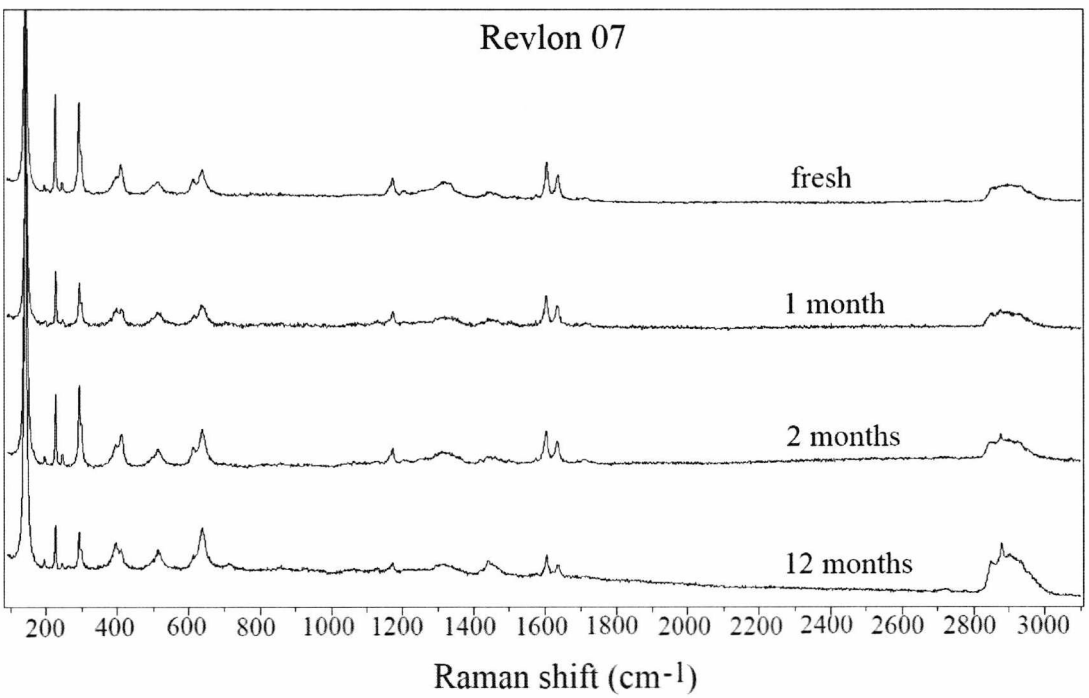
Revlon 07
fresh
1 month
2 months
12 months
200 400 600 800 1000 1200 1400 1600 1800 2000 2200 2400 2600 2800 3000
Raman shift (cm-1)

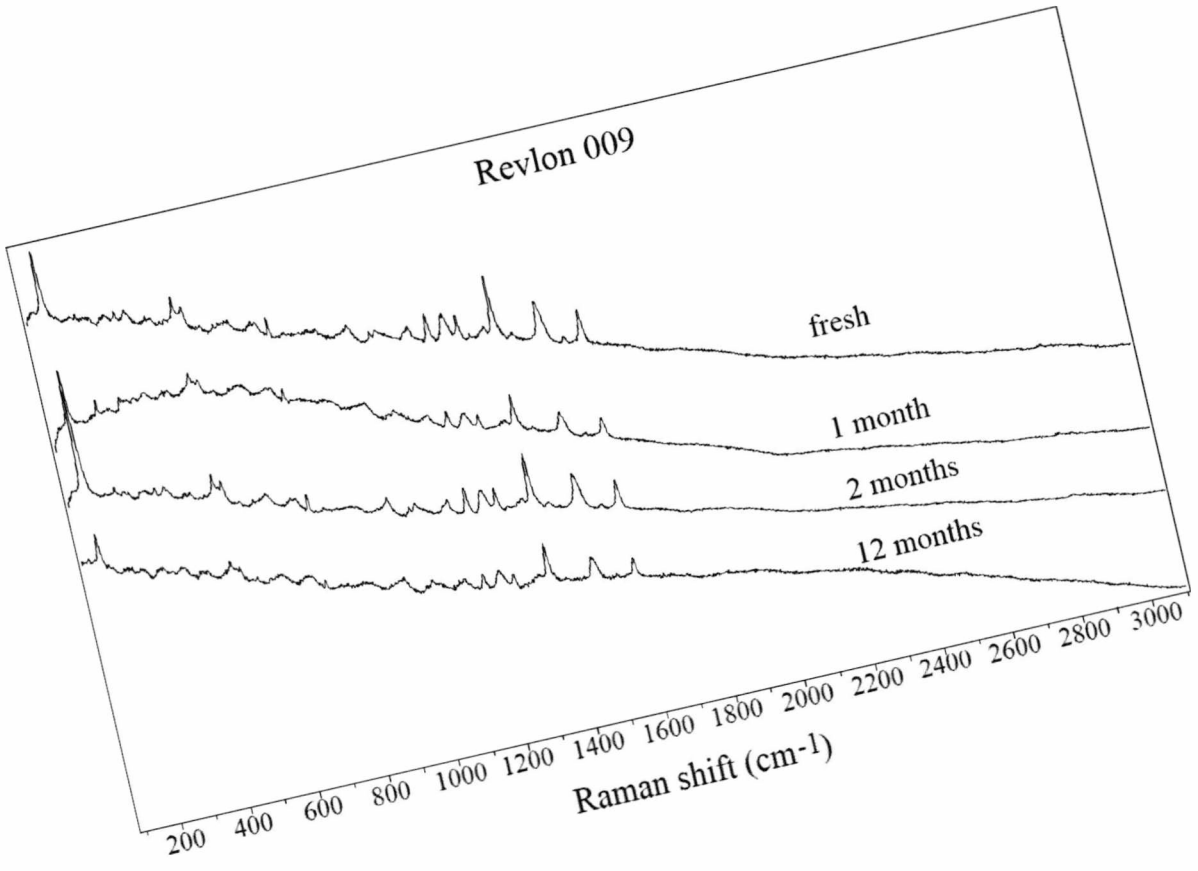
Revlon 009
fresh
1 month
2 months
12 months
200
400
600
800
1000
1200
1400
1600
1800
2000
2200
2400
2600
2800
3000
Raman shift (cm-1)

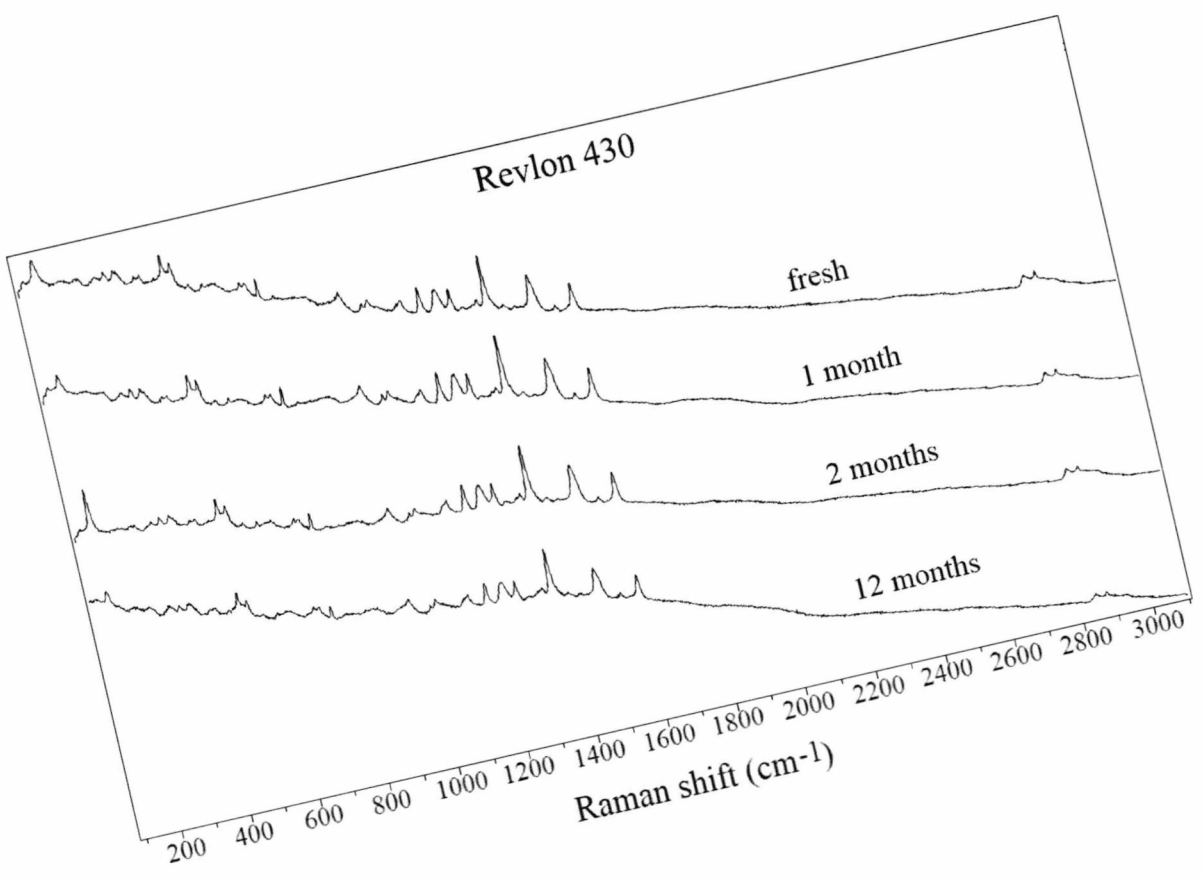
Revlon 430
fresh
1 month
2 months
12 months
200
400
600
800
1000
1200
1400
1600
1800
2000
2200
2400
2600
2800
3000
Raman shift (cm-1)

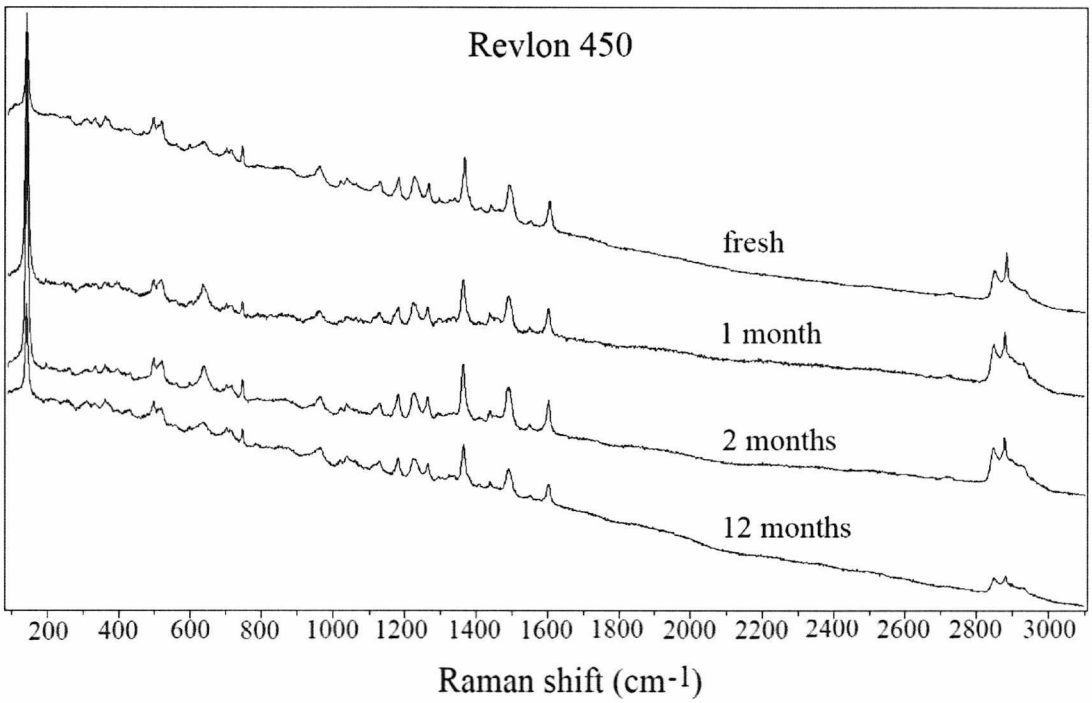
Revlon 450
fresh
1 month
2 months
12 months
200 400 600 800 1000 1200 1400 1600 1800 2000 2200 2400 2600 2800 3000
Raman shift (cm-1)

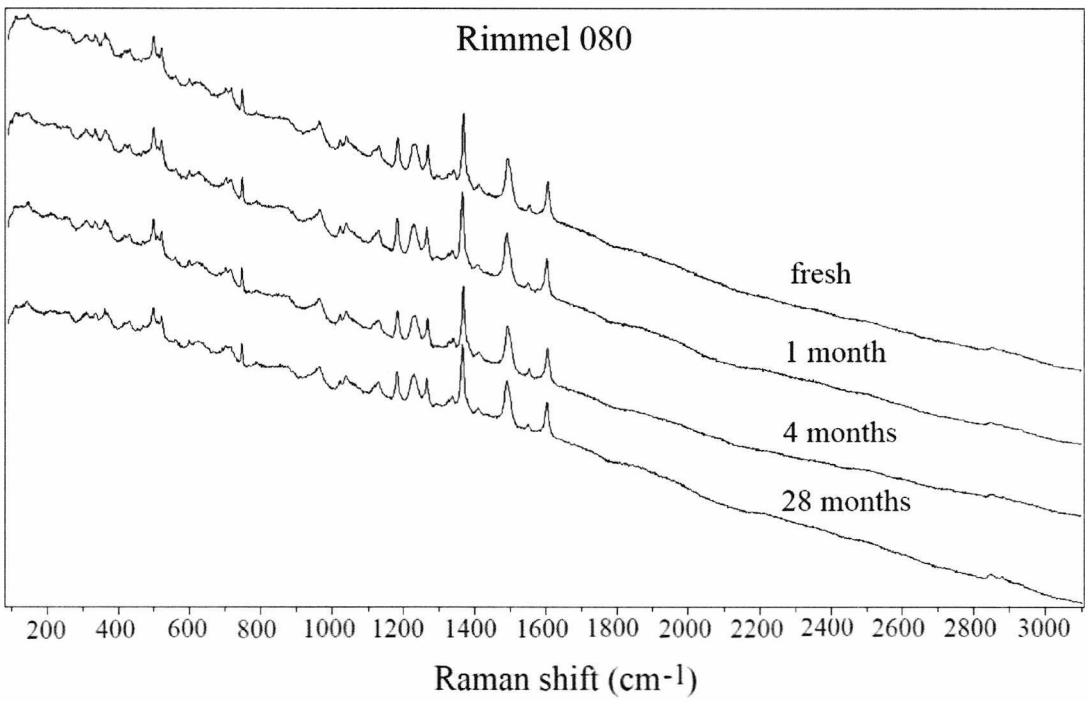
Rimmel 080
fresh
1 month
4 months
28 months
200 400 600 800 1000 1200 1400 1600 1800 2000 2200 2400 2600 2800 3000
Raman shift (cm-1)

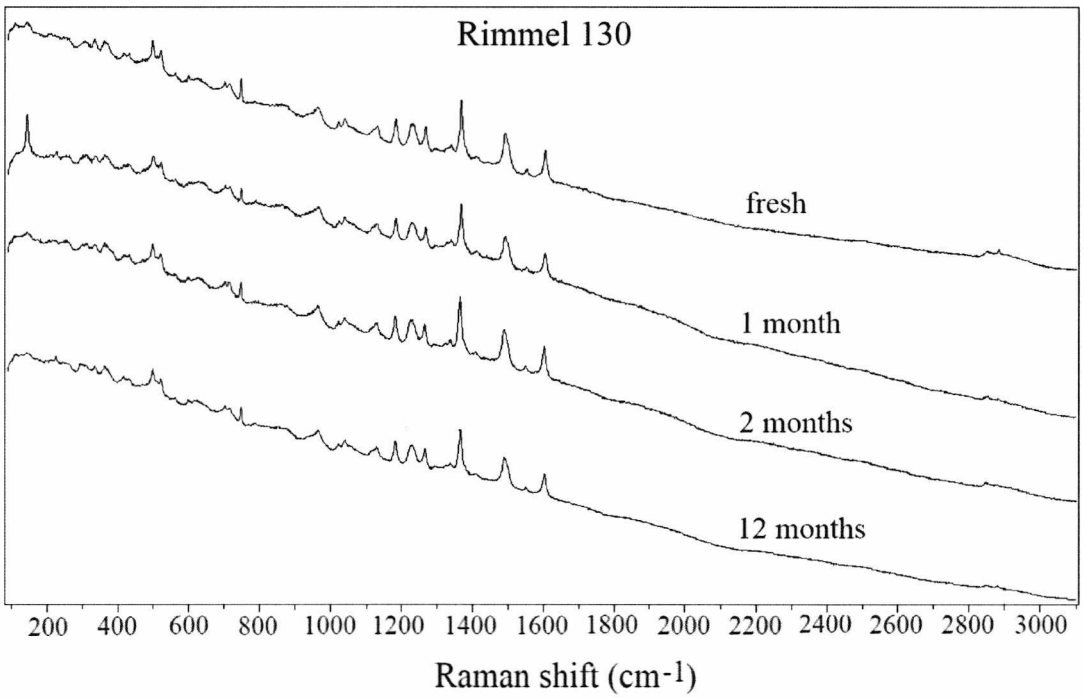
Rimmel 130
fresh
1 month
2 months
12 months
200 400 600 800 1000 1200 1400 1600 1800 2000 2200 2400 2600 2800 3000
Raman shift (cm-1)

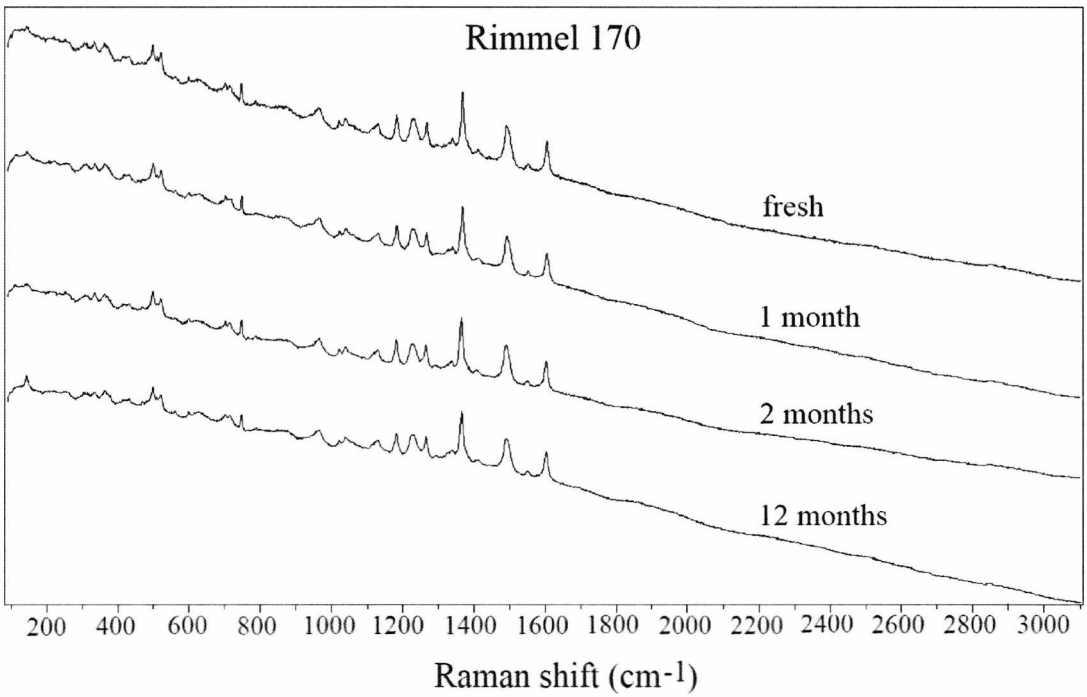
Rimmel 170
fresh
1 month
2 months
12 months
200 400 600 800 1000 1200 1400 1600 1800 2000 2200 2400 2600 2800 3000
Raman shift (cm-1)

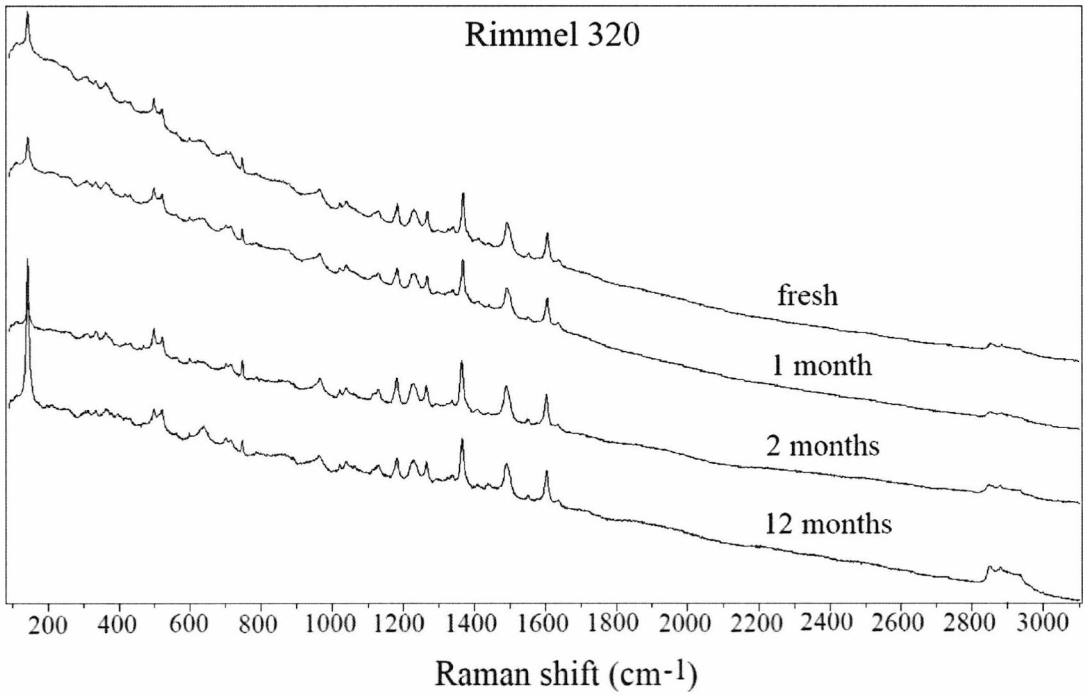
Rimmel 320
fresh
1 month
2 months
12 months
200 400 600 800 1000 1200 1400 1600 1800 2000 2200 2400 2600 2800 3000
Raman shift (cm-1)

APPENDIX IV

Detection of lipstick smears on textile fibres

La Femme 29 on yellow wool

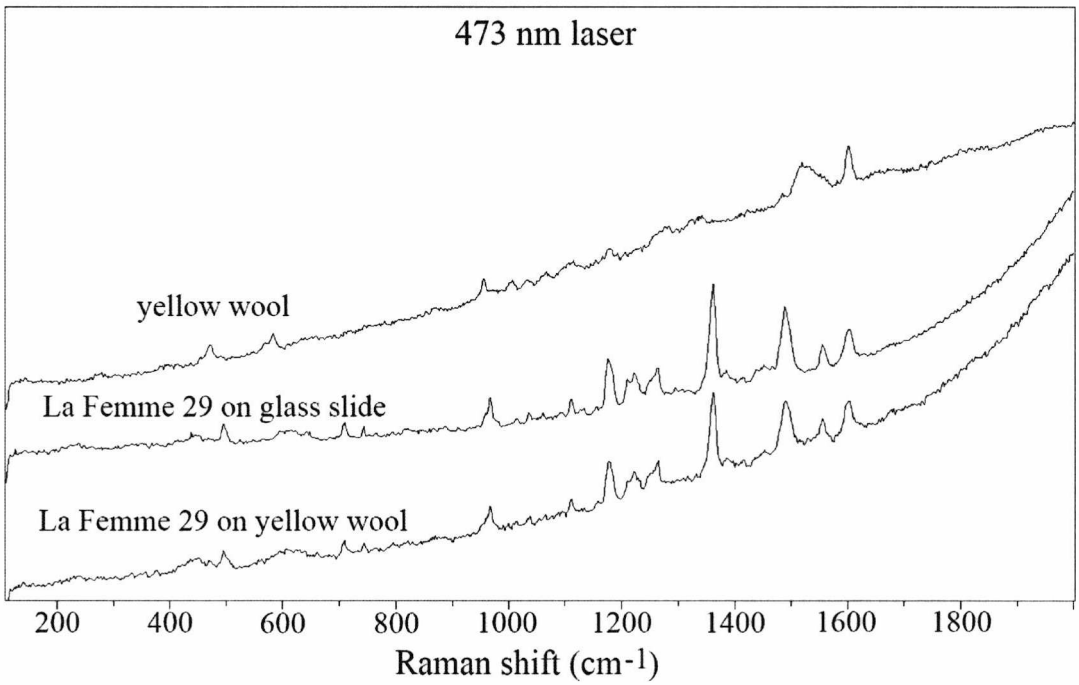

Figure A4.1. Figure comparing the spectra of yellow wool, La Femme 29 on glass slide and on yellow wool, obtained using the blue laser.

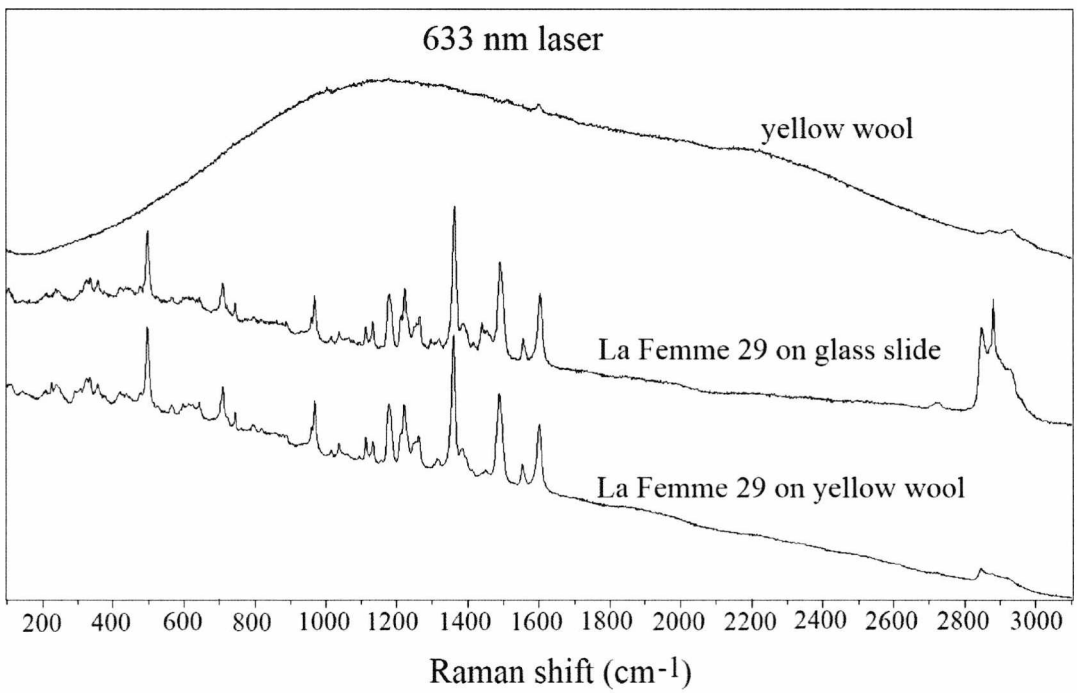

Figure A4.2. Figure comparing the spectra of yellow wool, La Femme 29 on glass slide and on yellow wool, obtained using the red laser.

La Femme 29 on (light) blue wool

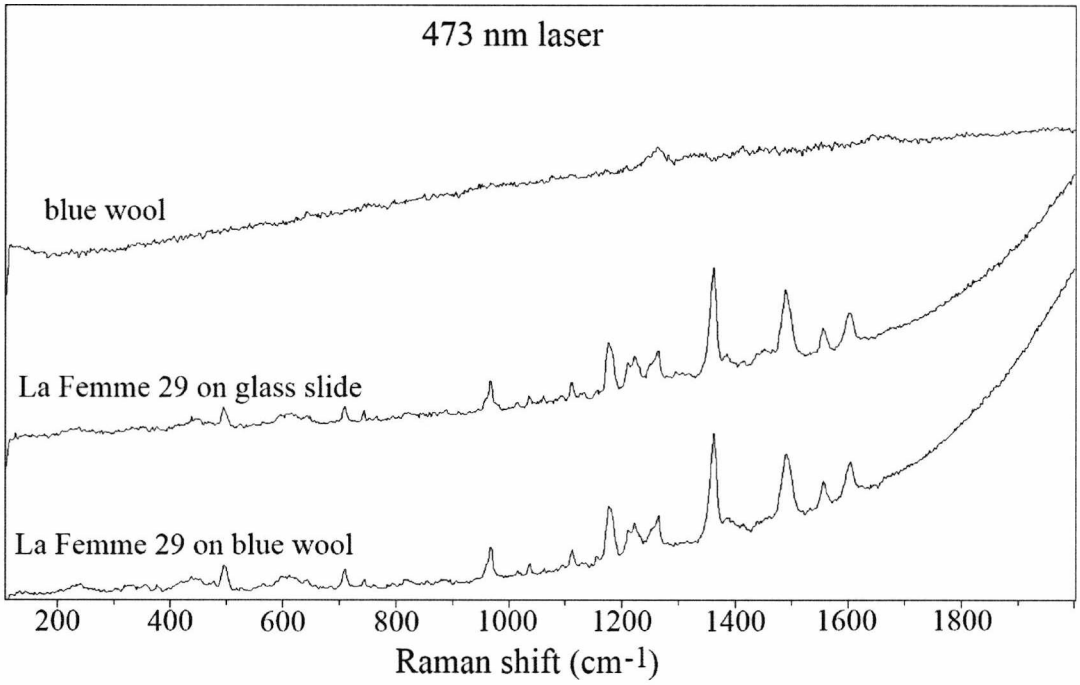

Figure A4.3. Figure comparing the spectra of blue wool, La Femme 29 on a glass slide and on blue wool, analysed using the blue laser.

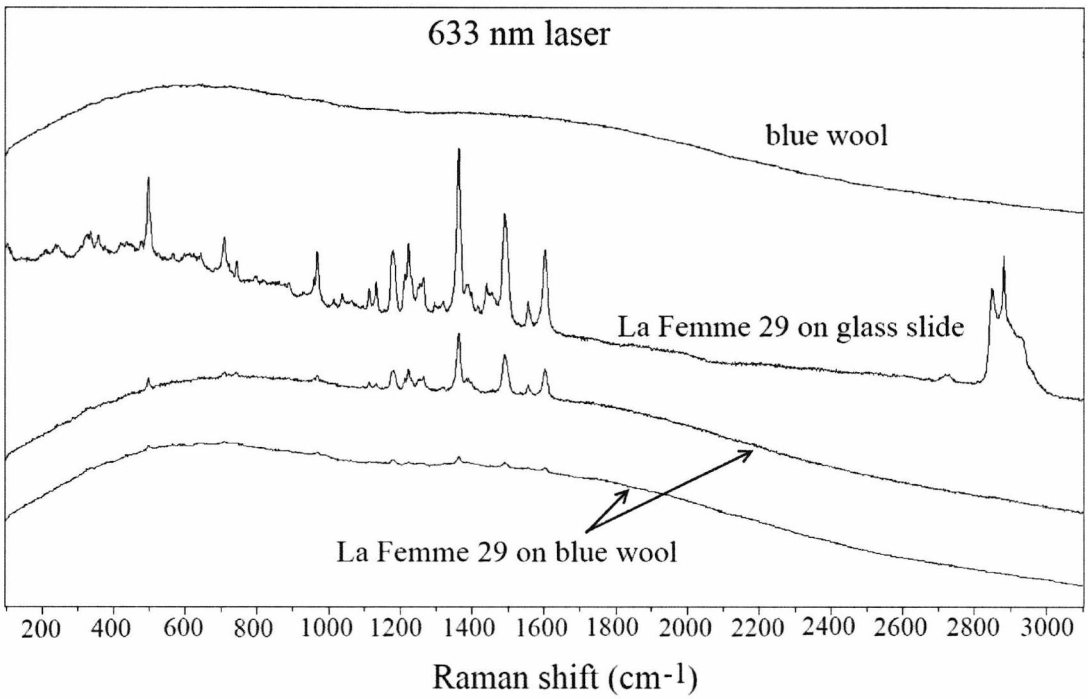

Figure A4.4. Figure comparing the spectra of blue wool, La Femme 29 on a glass slide and on blue wool, analysed using the red laser. Due to fluorescence interference from the blue wool, it was not always possible to obtain an acceptable signal-to-noise ratio for the lipstick spectra.

La Femme 29 on dark navy wool

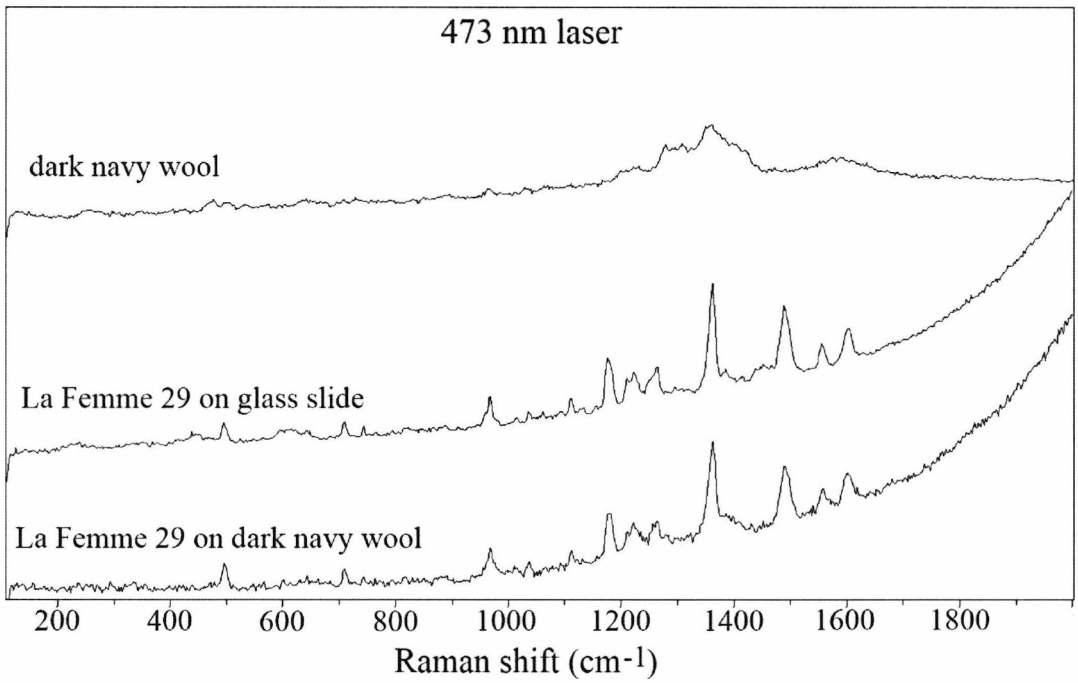

Figure A4.5. Figure comparing the spectra of dark navy wool, La Femme 29 on a glass slide and on dark navy wool, analysed using the blue laser.

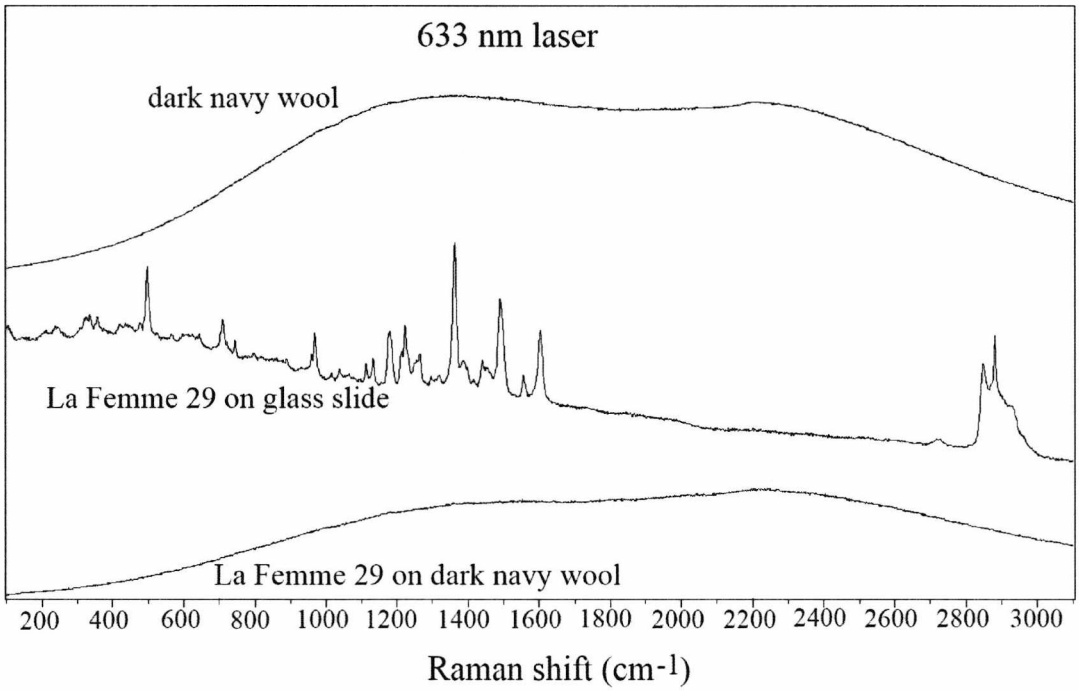

Figure A4.6. Figure comparing the spectra of dark navy wool, La Femme 29 on a glass slide and on dark navy wool, analysed using the red laser. It can be seen that the spectrum of the lipstick on the fibre displays the same fluorescent band shape as the fibre.

La Femme 29 on yellow cotton

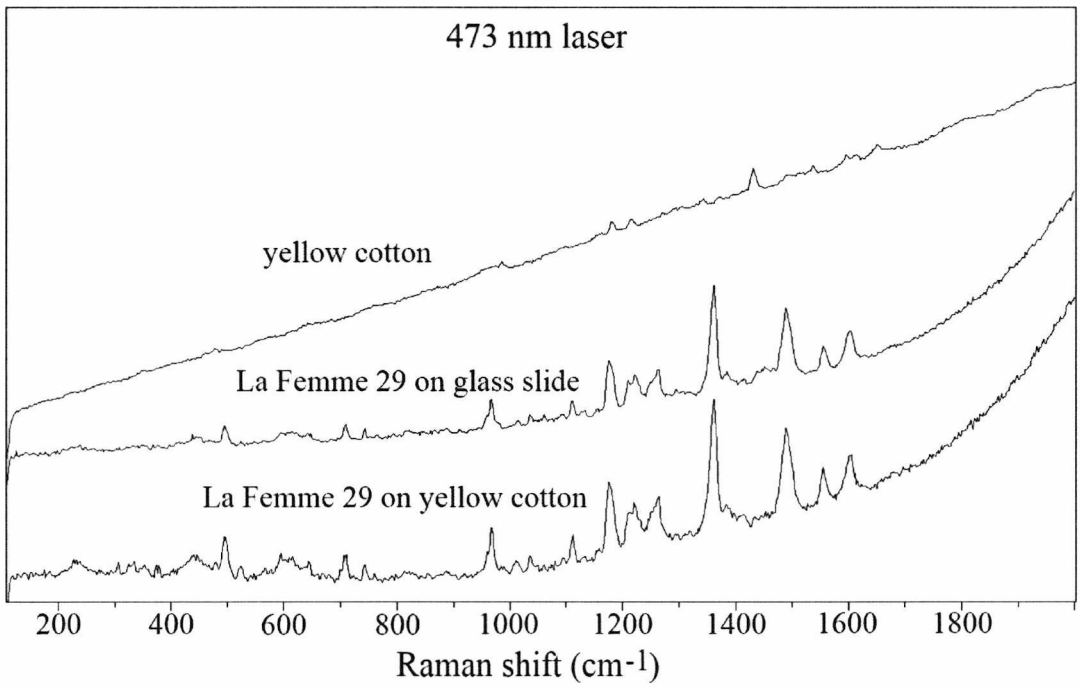

Figure A4.7. Figure comparing the spectra yellow cotton, La Femme 29 on a glass slide and on yellow cotton, analysed using the blue laser.

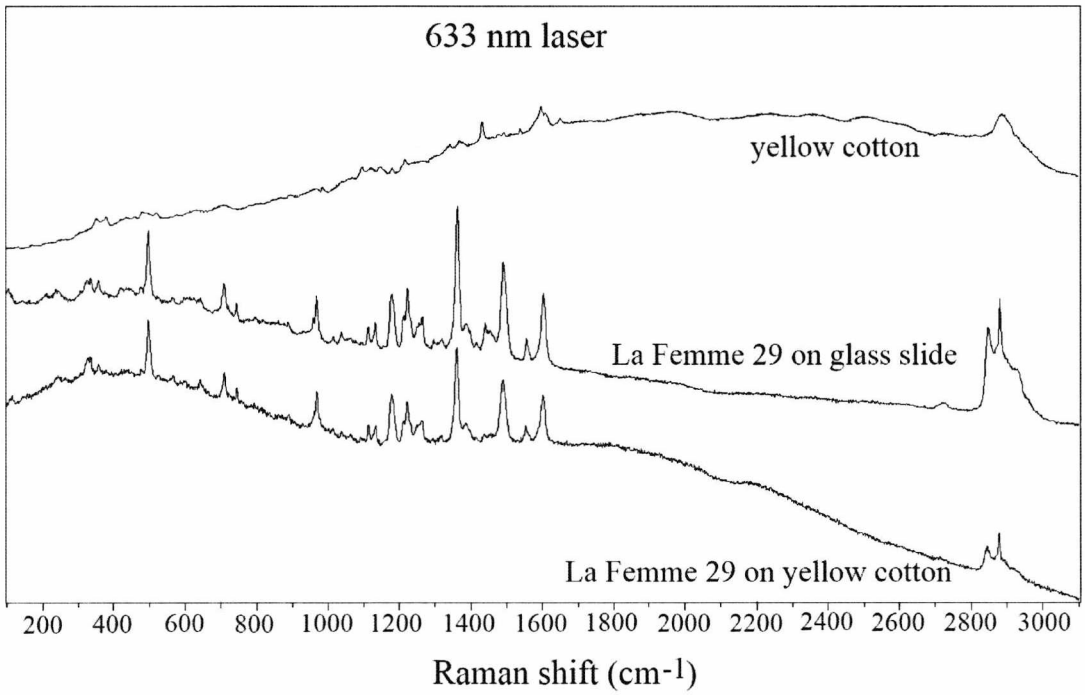

Figure A4.8. Figure comparing the spectra of yellow cotton, La Femme 29 on a glass slide and on yellow cotton, analysed using the red laser.

La Femme 29 on green cotton

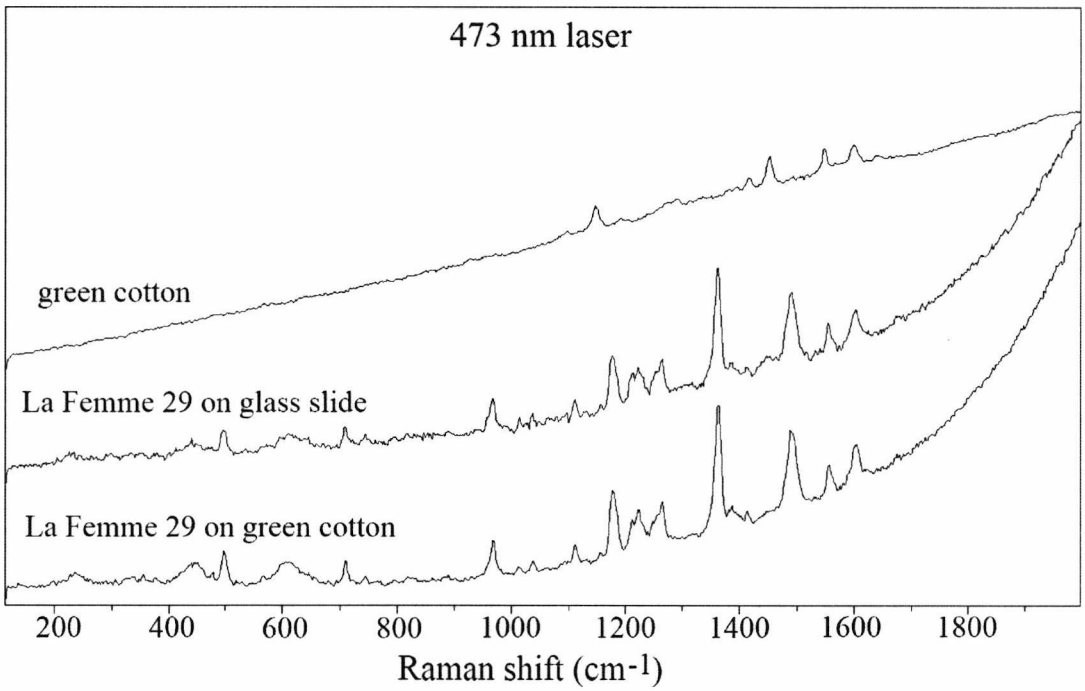

Figure A4.9. Figure comparing the spectra of green cotton, La Femme 29 on a glass slide and on green cotton, analysed using the blue laser.

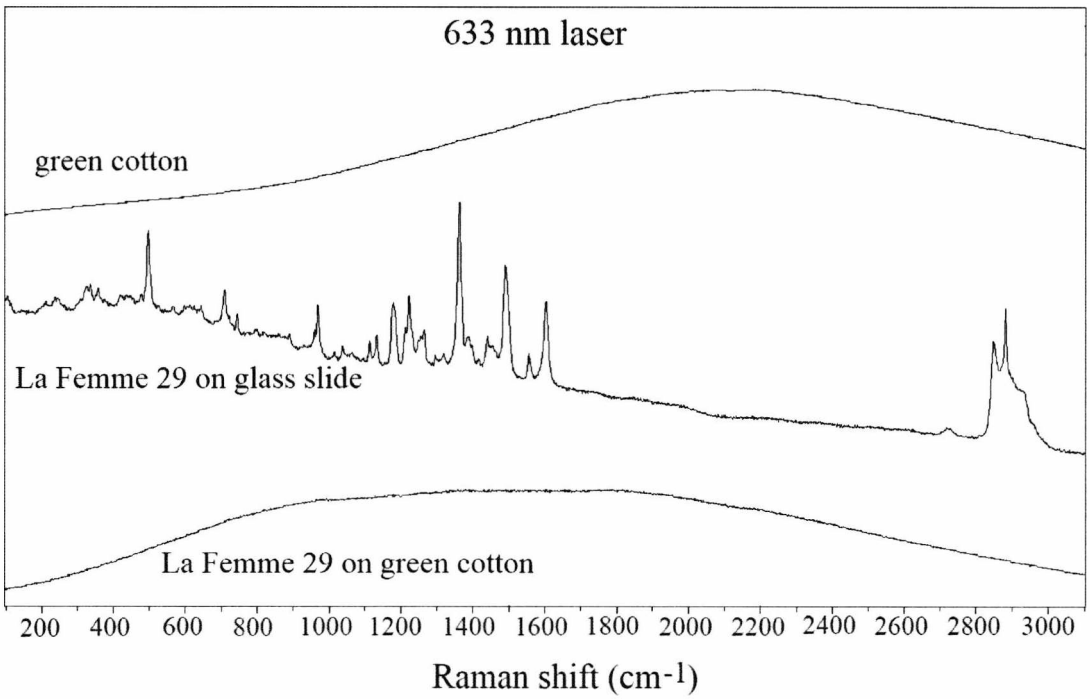

Figure A4.10. Figure comparing the spectra of green cotton, La Femme 29 on a glass slide and on green cotton, analysed using the red laser. The fluorescence from the fibre prevents the analysis of the lipstick smear on the fibre.

La Femme 29 on pink linen

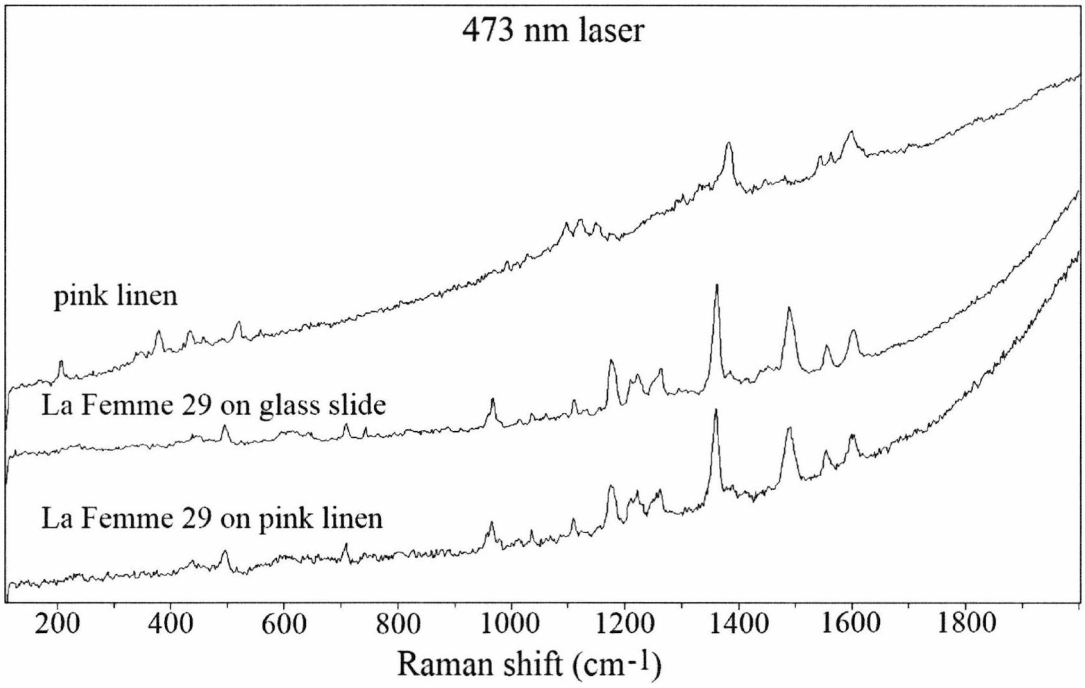

Figure A4.11. Figure comparing the spectra of pink linen, La Femme 29 on a glass slide and on pink linen, analysed using the blue laser.

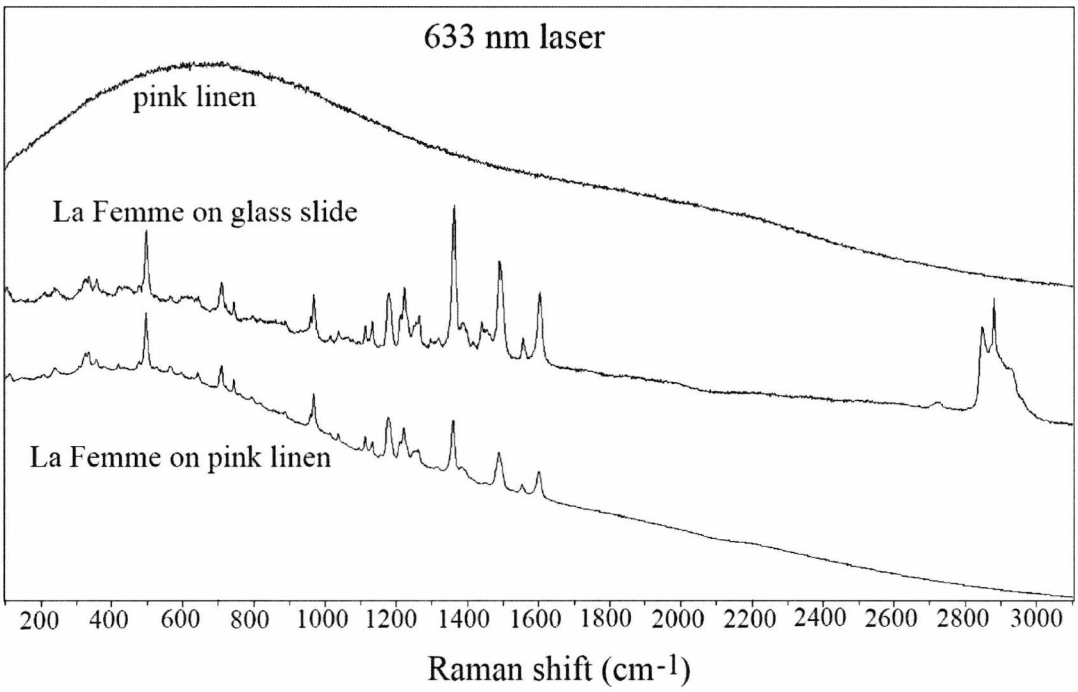

Figure A4.12. Figure comparing the spectra of pink linen, La Femme 29 on a glass slide and on pink linen, analysed using the red laser.

La Femme 29 on orange linen

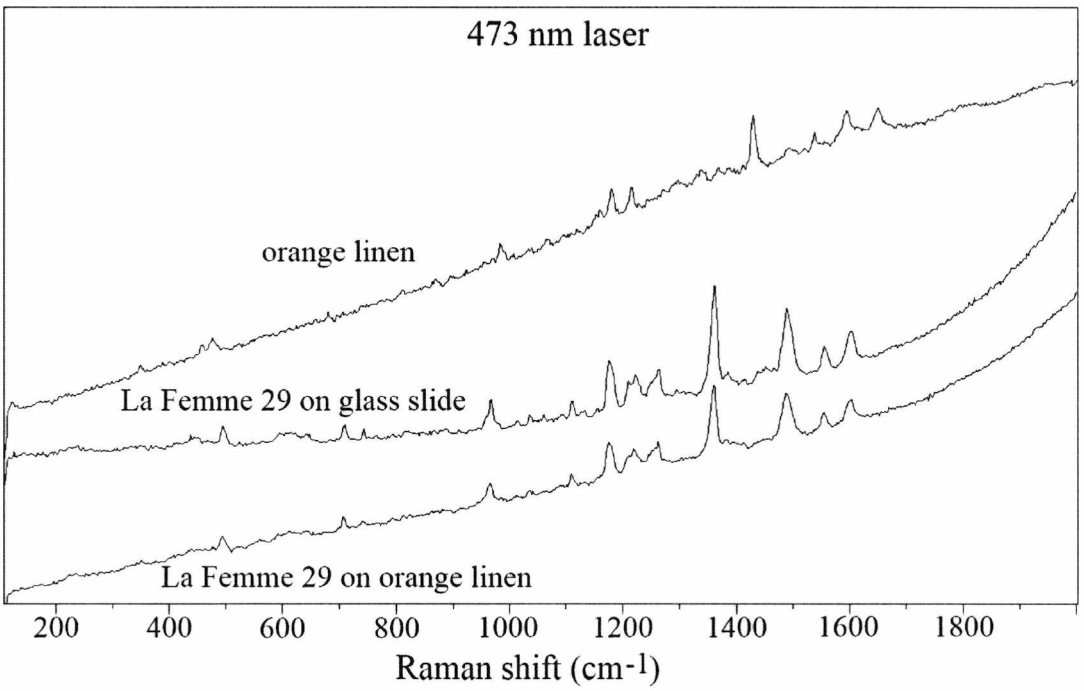

Figure A4.13. Figure comparing the spectra of orange linen, La Femme 29 on a glass slide and on orange linen, analysed using the blue laser.

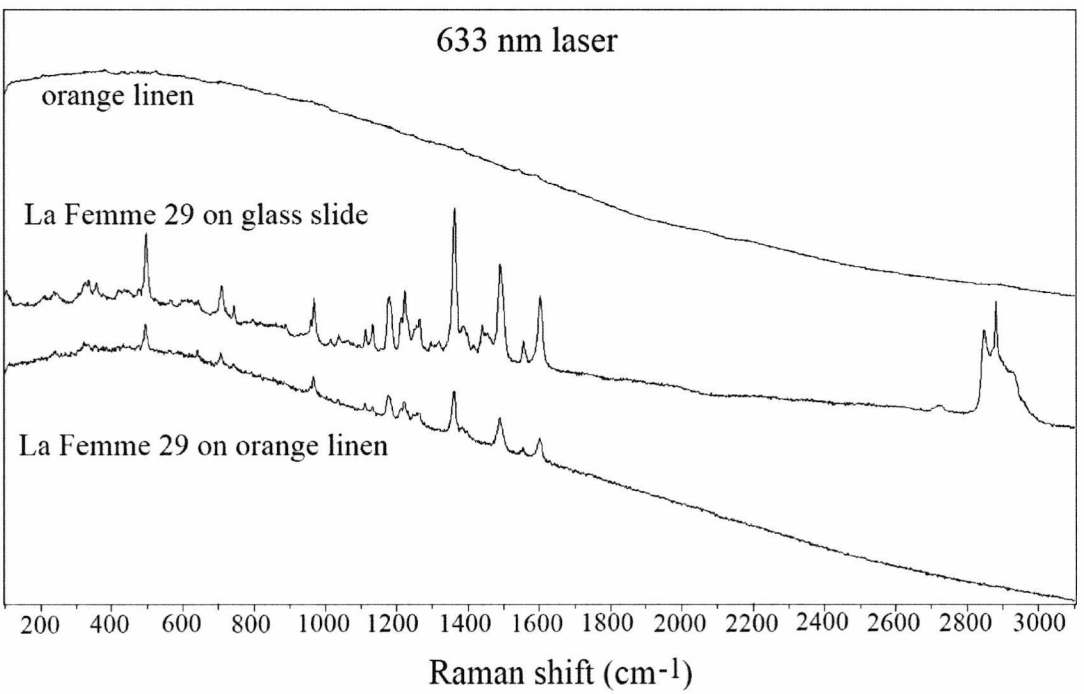

Figure A4.14. Figure comparing the spectra of orange linen, La Femme 29 on a glass slide and on orange linen, analysed using the red laser.

Rimmel 230 on yellow wool

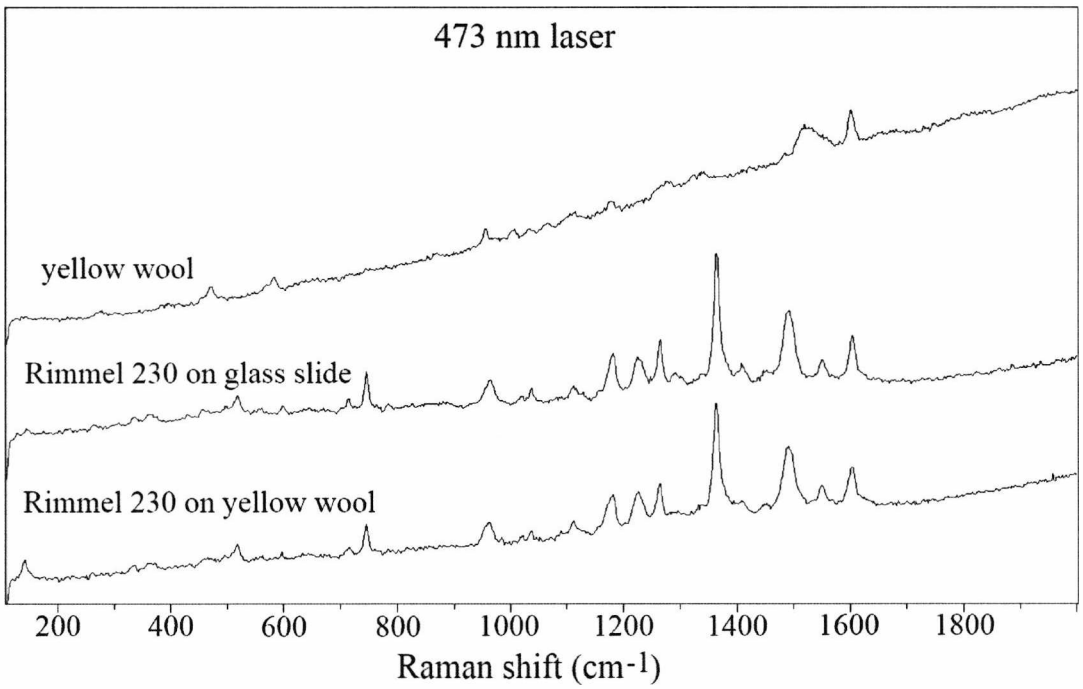

Figure A4.15. Figure comparing the spectra of yellow wool, Rimmel 230 on a glass slide and on yellow wool, analysed using the blue laser.

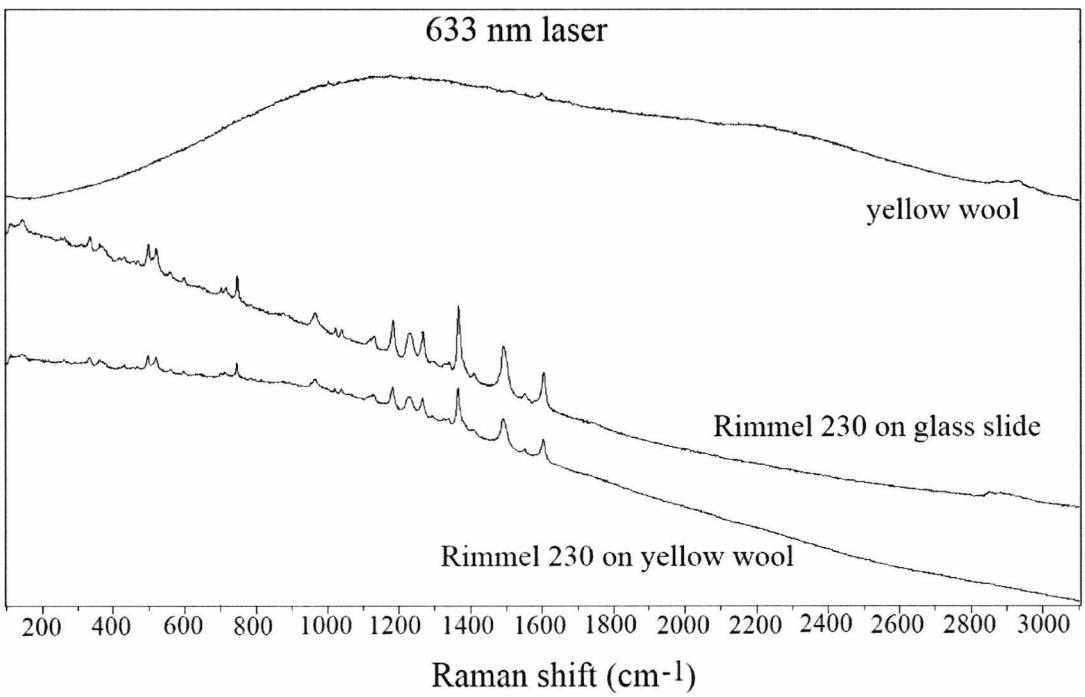

Figure A4.16. Figure comparing the spectra of yellow wool, Rimmel 230 on a glass slide and on yellow wool, analysed using the red laser.

Rimmel 230 on (light) blue wool

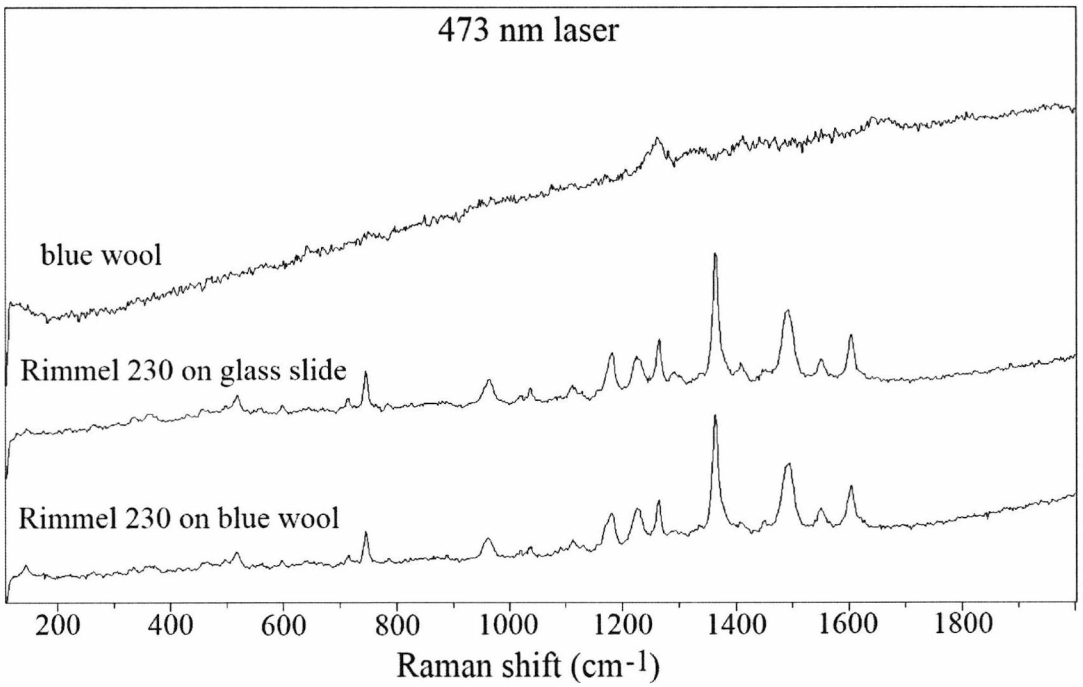

Figure A4.17. Figure comparing the spectra of blue wool, Rimmel 230 on a glass slide and on blue wool, analysed using the blue laser.

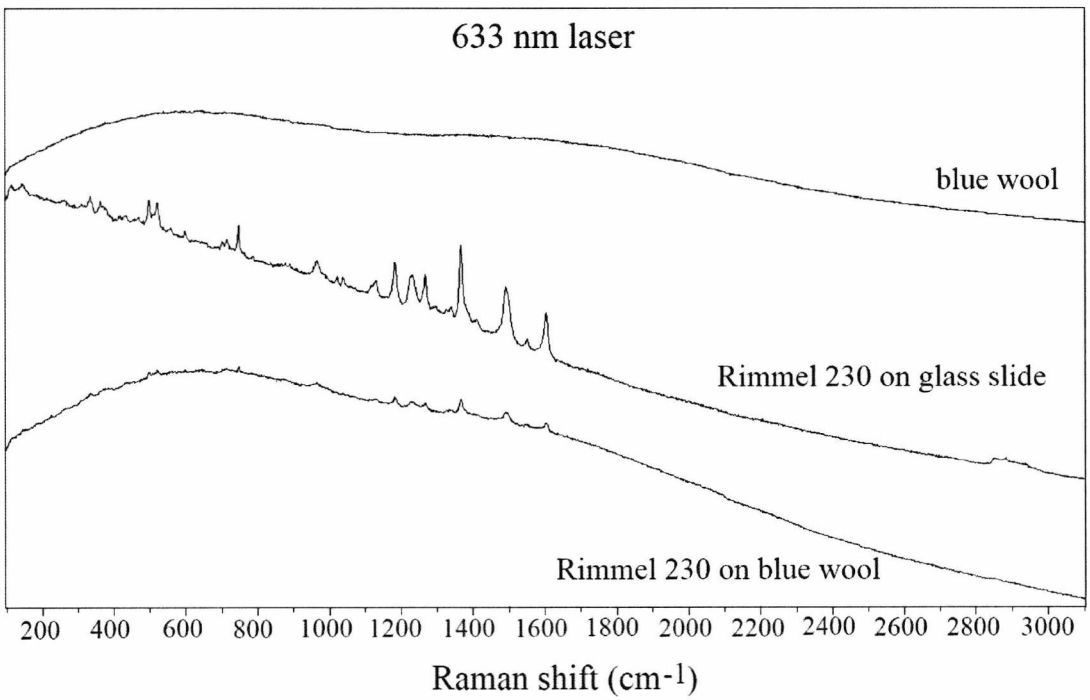

Figure A4.18. Figure comparing the spectra of blue wool, Rimmel 230 on a glass slide and on blue wool, analysed using the red laser.

Rimmel 230 on dark navy wool

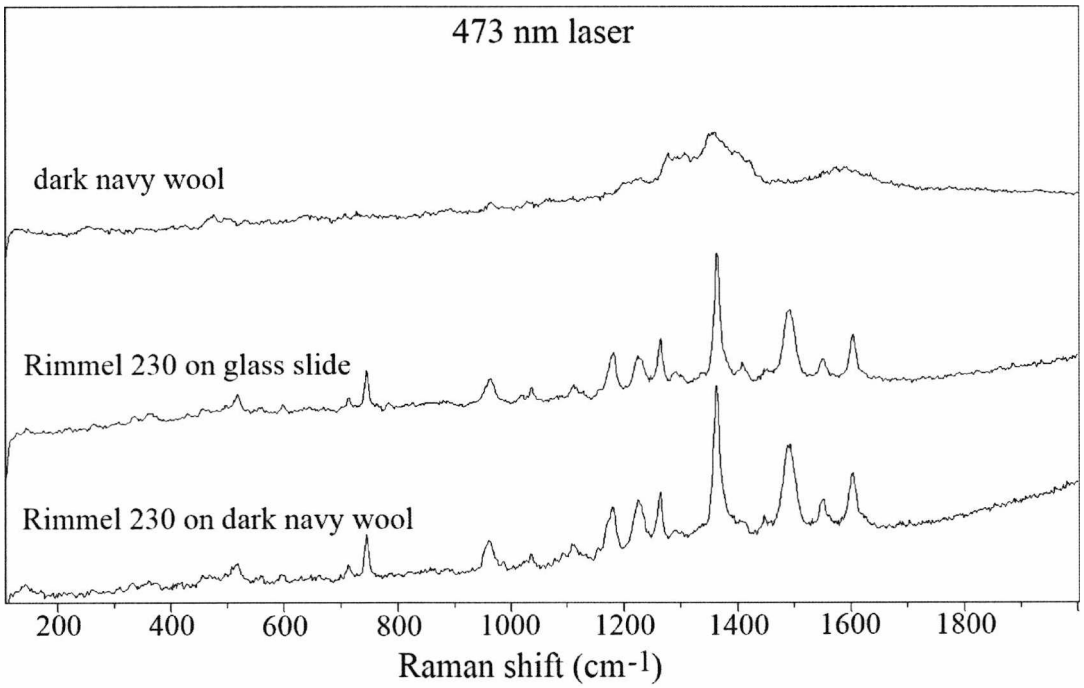

Figure A4.19. Figure comparing the spectra of dark navy wool, Rimmel 230 on a glass slide and on dark navy wool, analysed using the blue laser.

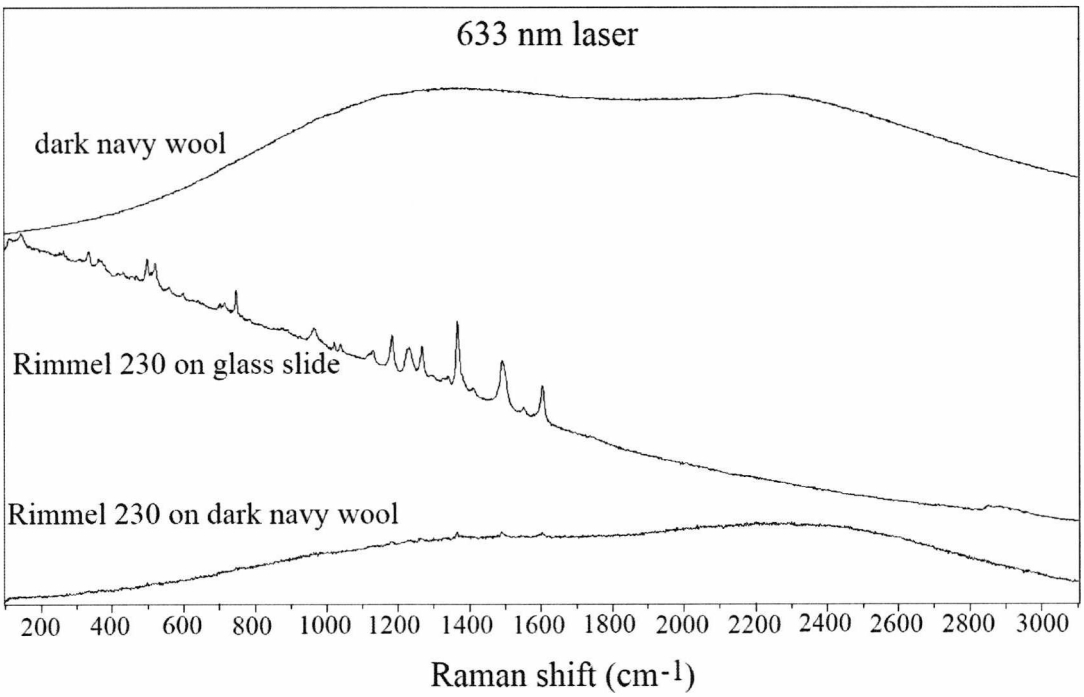

Figure A4.20. Figure comparing the spectra of dark navy wool, Rimmel 230 on a glass slide and on dark navy wool, analysed using the red laser.

Rimmel 230 on yellow cotton

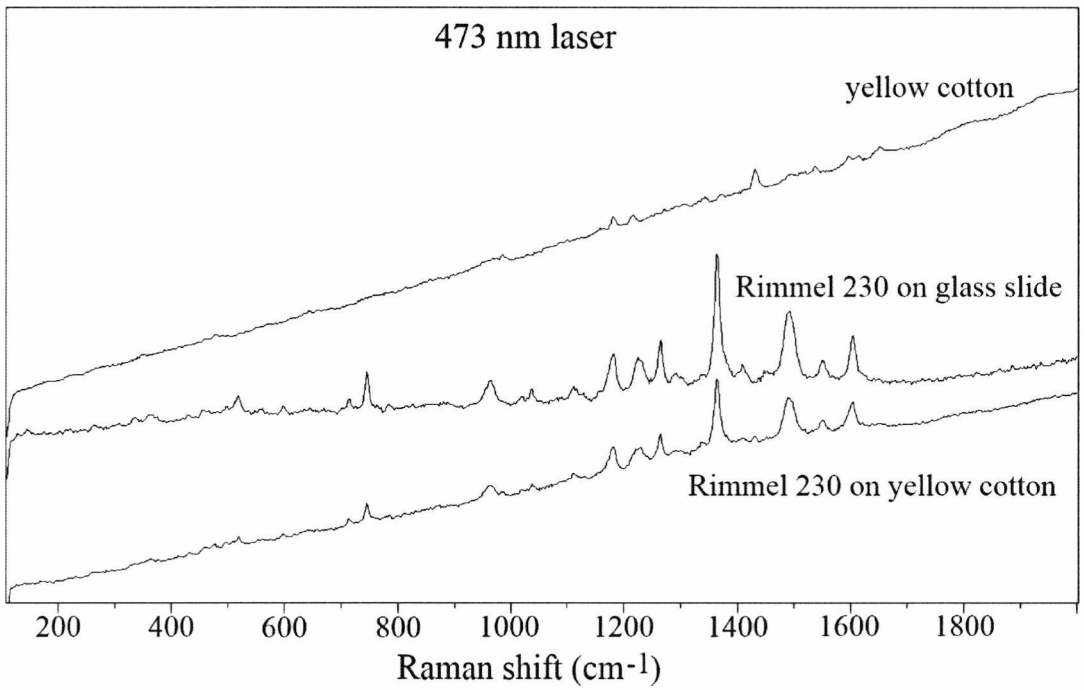

Figure A4.21. Figure comparing the spectra of yellow cotton, Rimmel 230 on a glass slide and on yellow cotton, analysed using the blue laser.

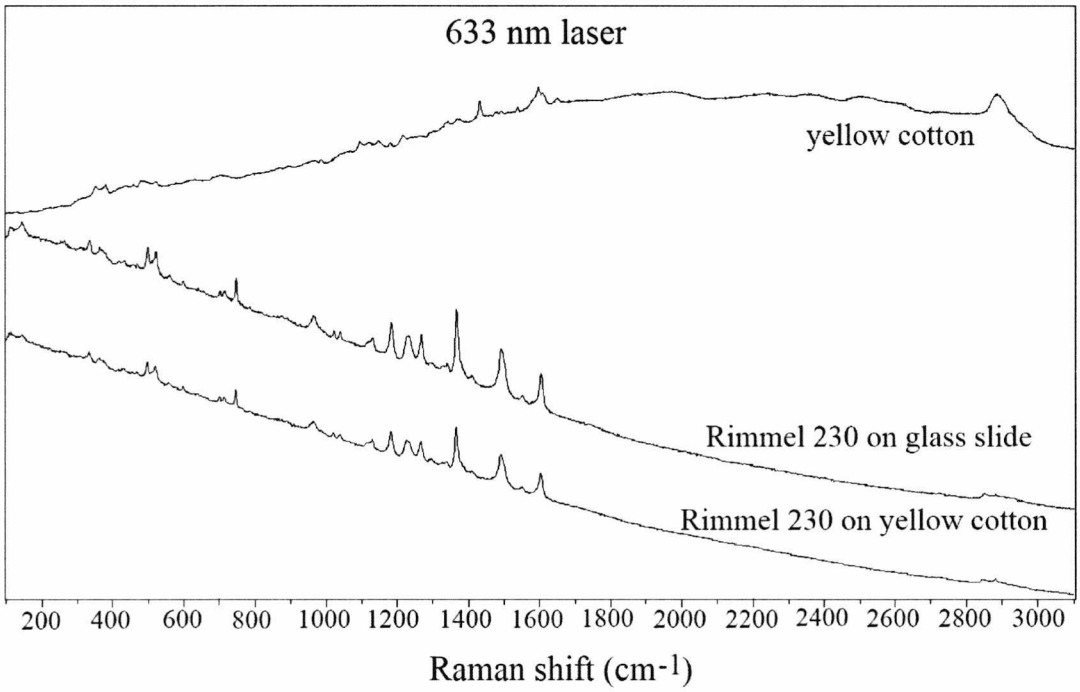

Figure A4.22. Figure comparing the spectra of yellow cotton, Rimmel 230 on a glass slide and on yellow cotton, analysed using the red laser.

Rimmel 230 on green cotton

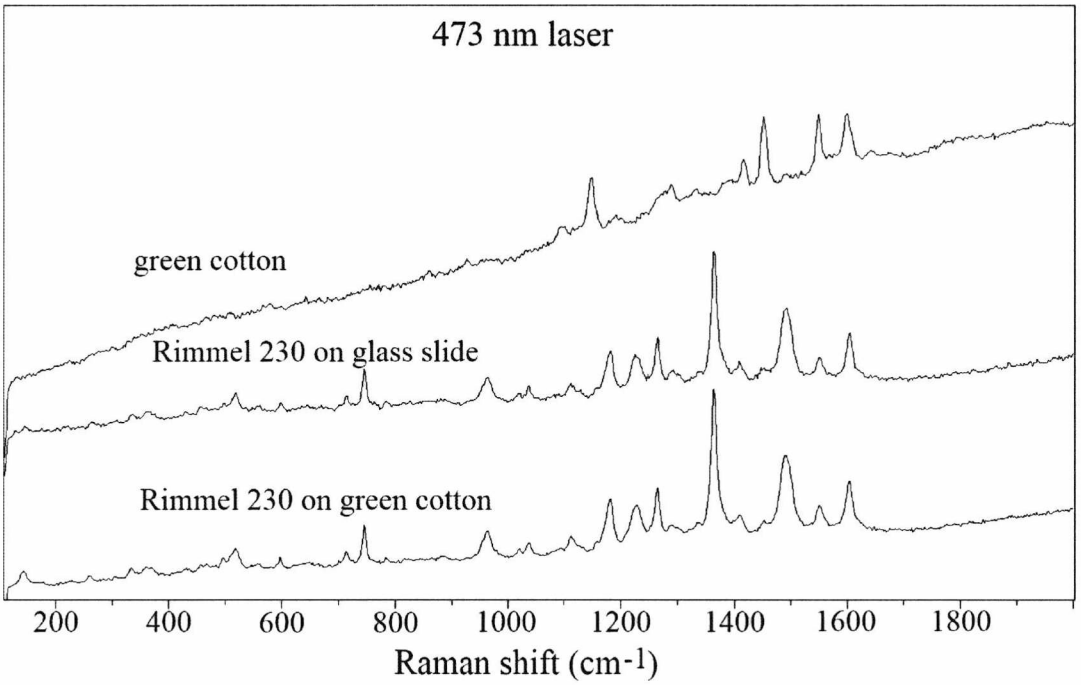

Figure A4.23. Figure comparing the spectra of green cotton, Rimmel 230 on a glass slide and on green cotton, analysed using the blue laser.

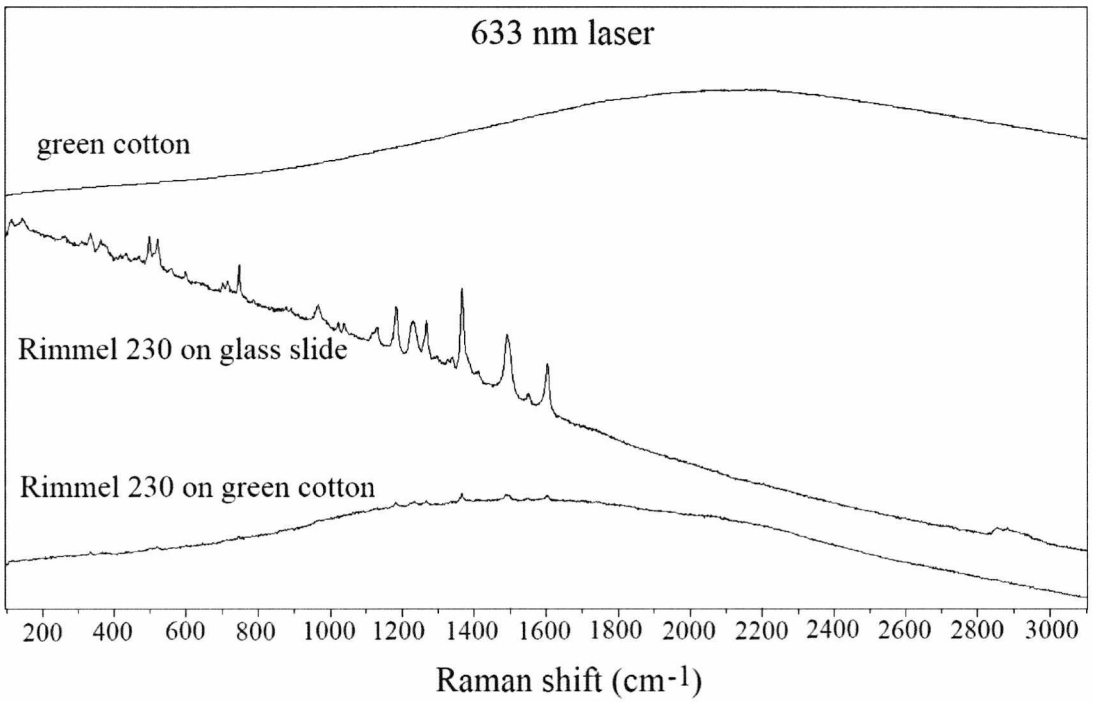

Figure A4.24. Figure comparing the spectra of green cotton, Rimmel 230 on a glass slide and on green cotton, analysed using the red laser.

Rimmel 230 on pink linen

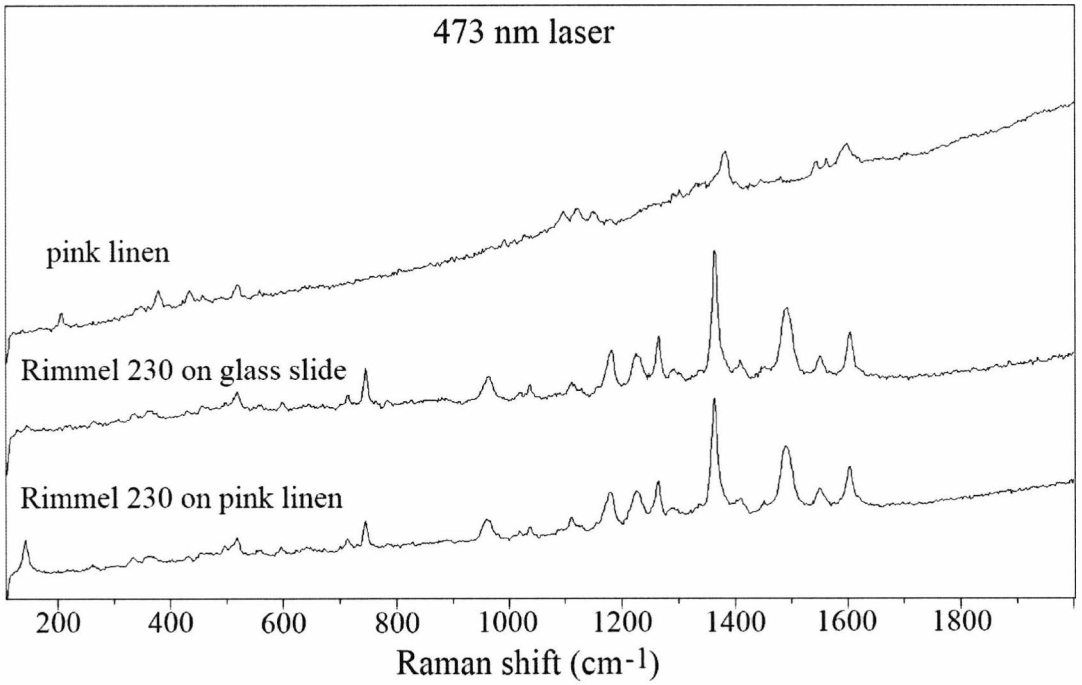

Figure A4.25. Figure comparing the spectra of pink linen, Rimmel 230 on a glass slide and on pink linen, analysed using the blue laser.

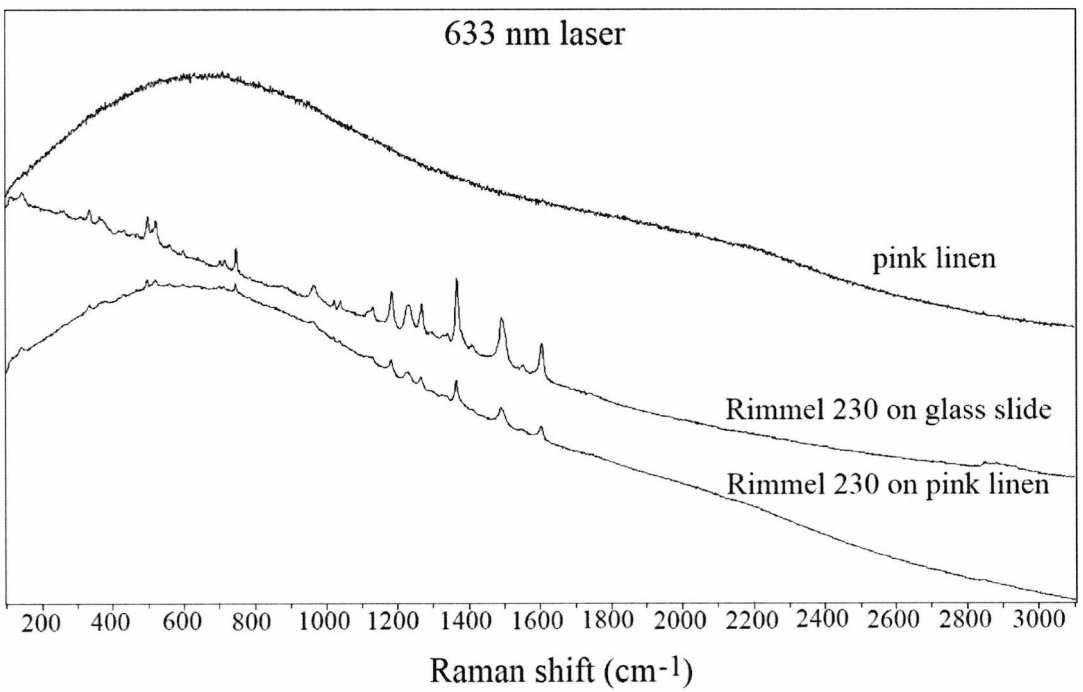

Figure A4.26. Figure comparing the spectra of pink linen, Rimmel 230 on a glass slide and on pink linen, analysed using the red laser.

Rimmel 230 on orange linen

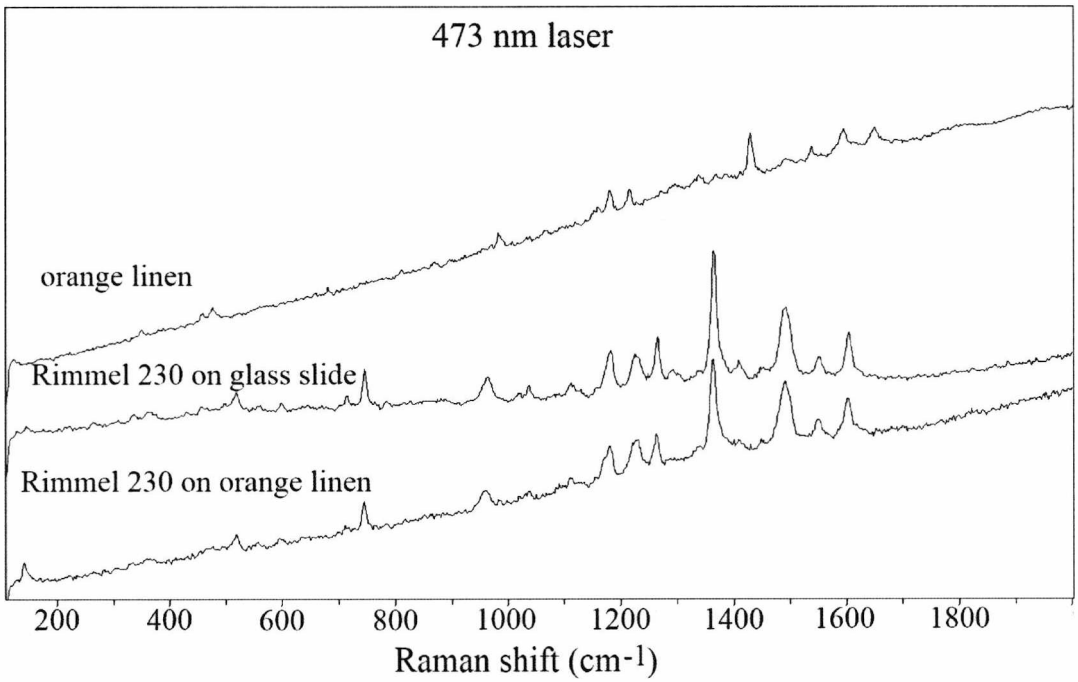

Figure A4.27. Figure comparing the spectra of orange linen, Rimmel 230 on a glass slide and on orange linen, analysed using the blue laser.

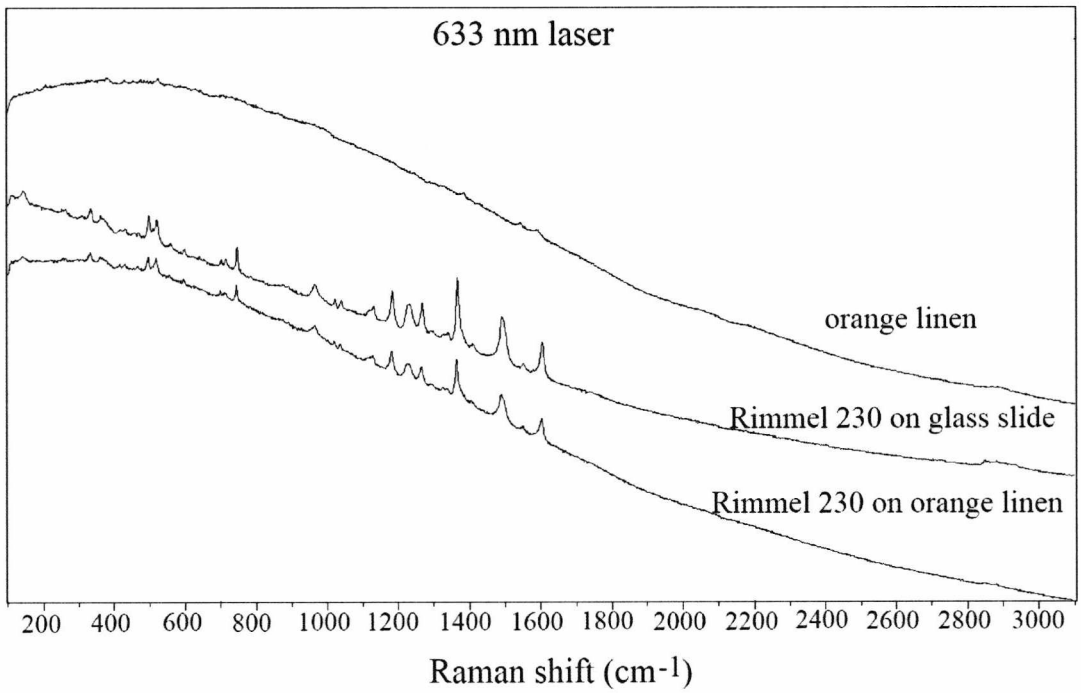

Figure A4.28. Figure comparing the spectra of orange linen, Rimmel 230 on a glass slide and on orange linen, analysed using the red laser.

Barry M 101 on yellow wool

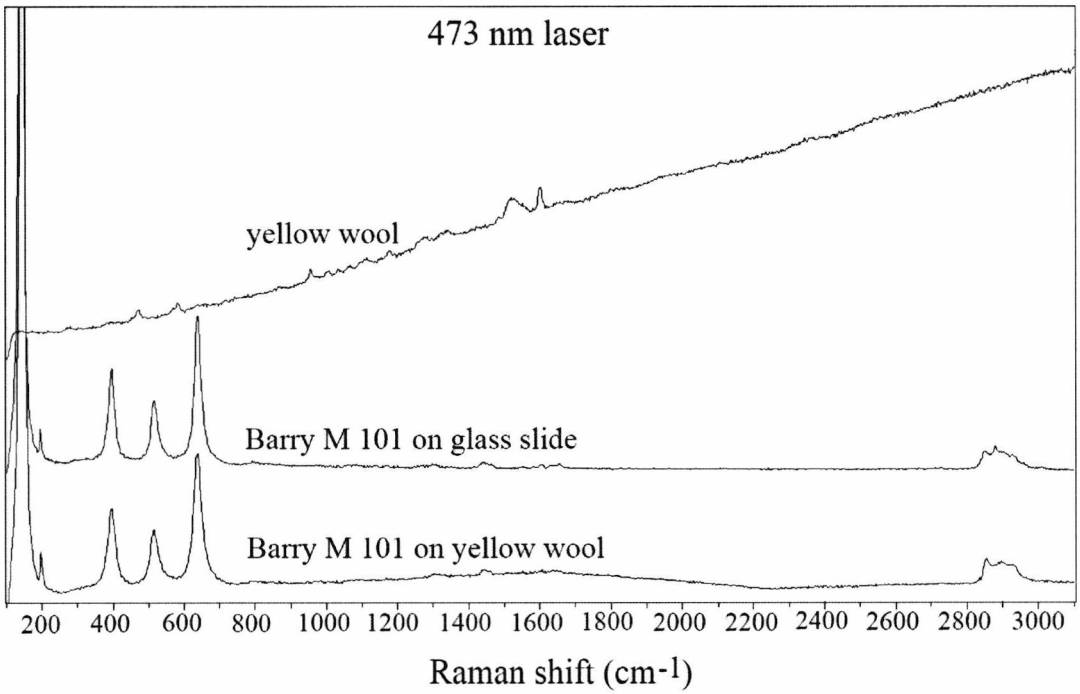

Figure A4.29. Figure comparing the spectra of yellow wool, Barry M 101 on a glass slide and on yellow wool, analysed using the blue laser.

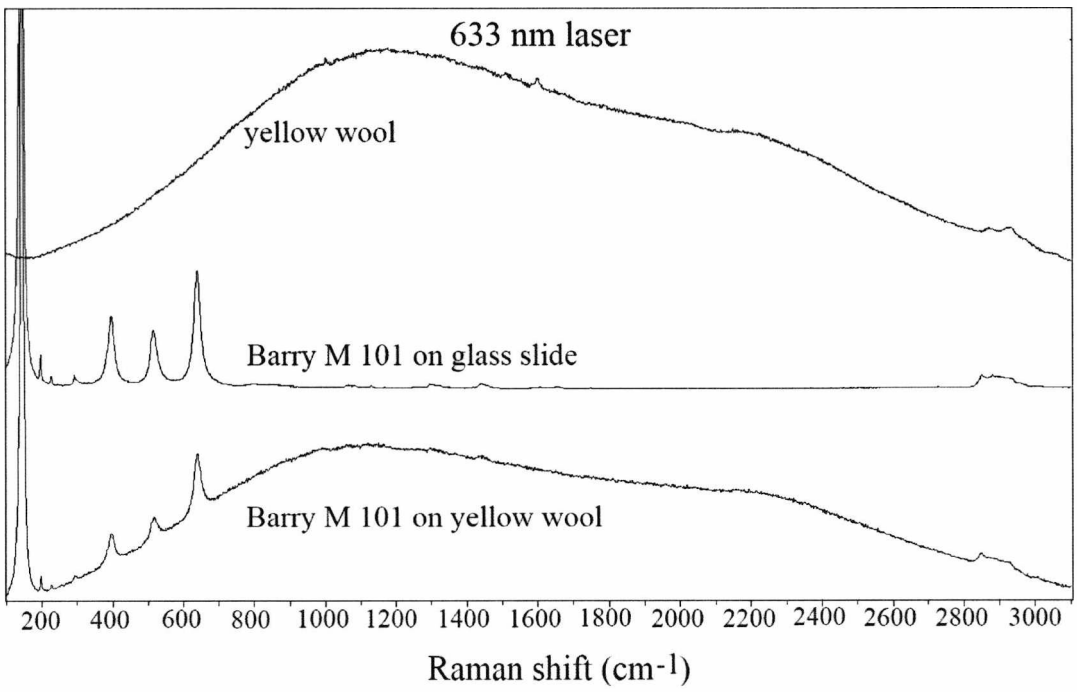

Figure A4.30. Figure comparing the spectra of yellow wool, Barry M 101 on a glass slide and on yellow wool, analysed using the red laser.

Barry M 101 on (light) blue wool

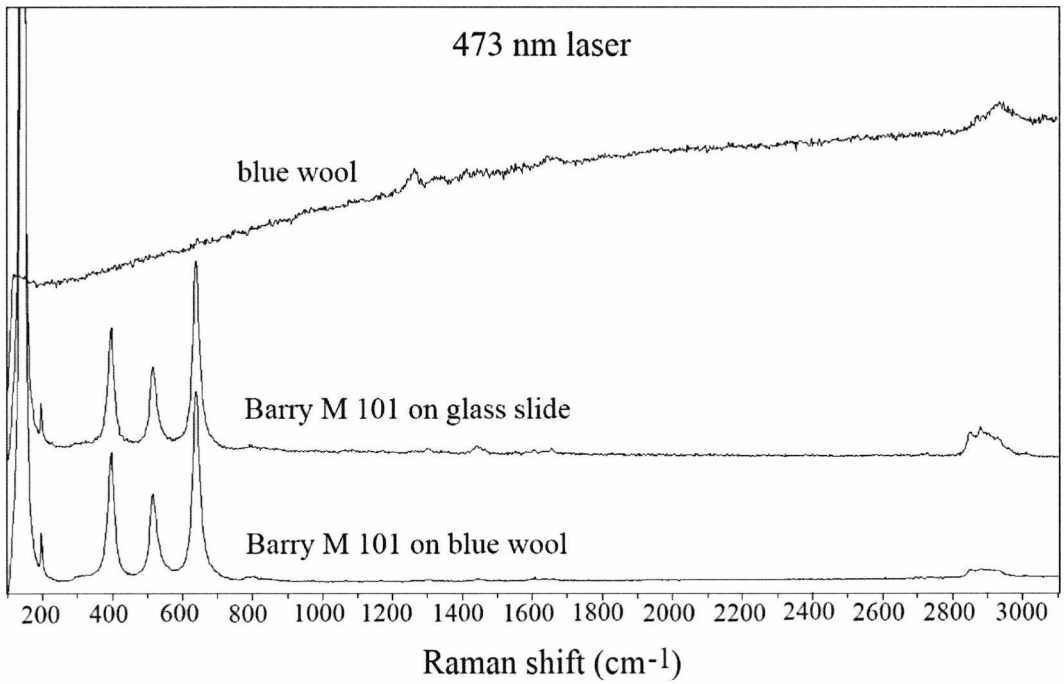

Figure A4.31. Figure comparing the spectra of blue wool, Barry M 101 on a glass slide and on blue wool, analysed using the blue laser.

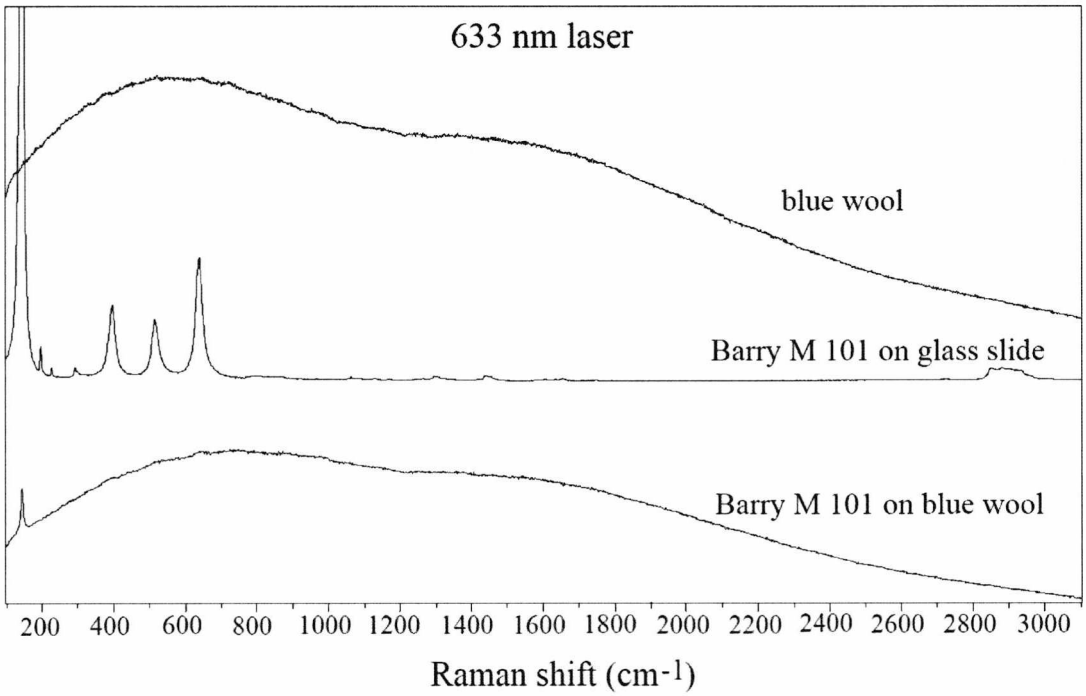

Figure A4.32. Figure comparing the spectra of blue wool, Barry M 101 on a glass slide and on blue wool, analysed using the red laser.

Barry M 101 on dark navy wool

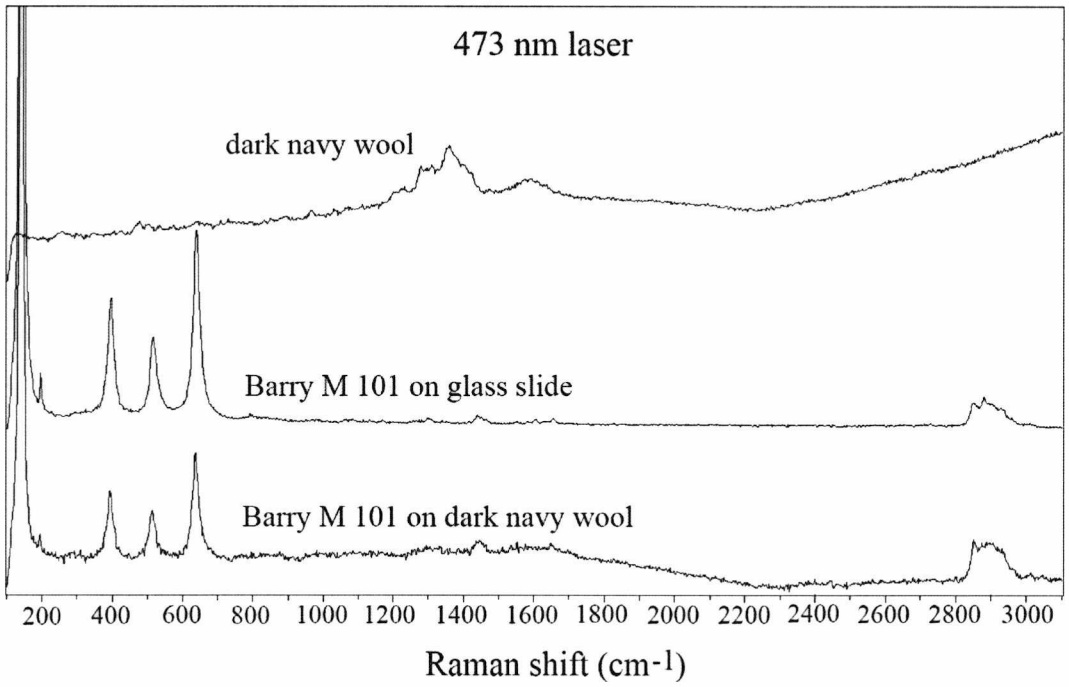

Figure A4.33. Figure comparing the spectra of dark navy wool, Barry M 101 on a glass slide and on dark navy wool, analysed using the blue laser.

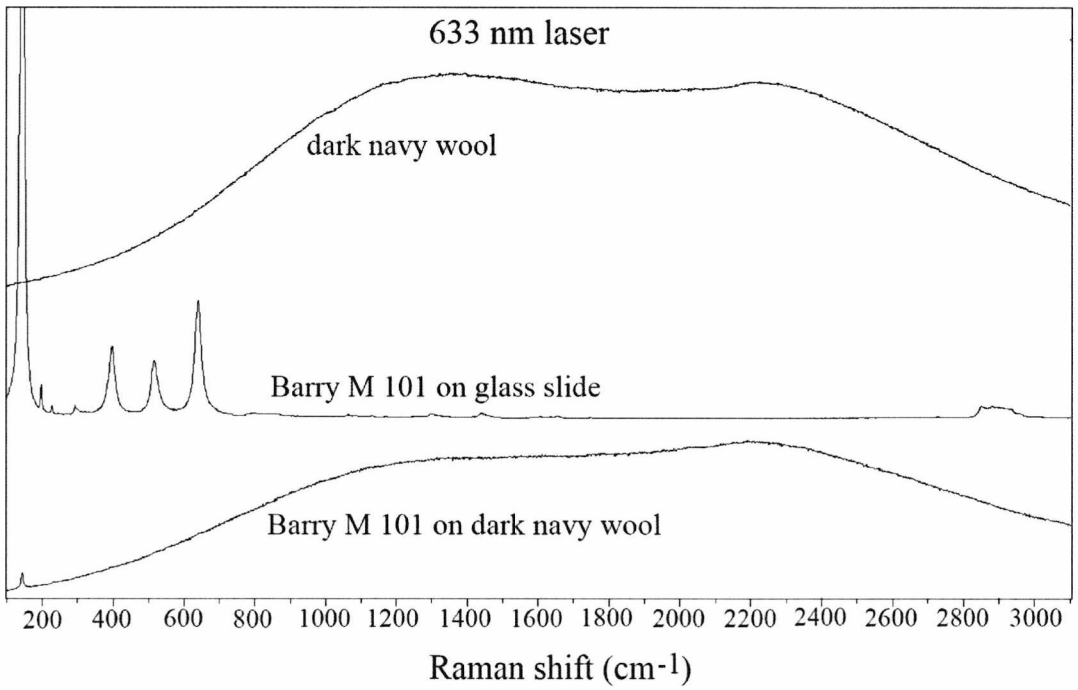

Figure A4.34. Figure comparing the spectra of dark navy wool, Barry M 101 on a glass slide and on dark navy wool, analysed using the red laser.

Barry M 101 on yellow cotton

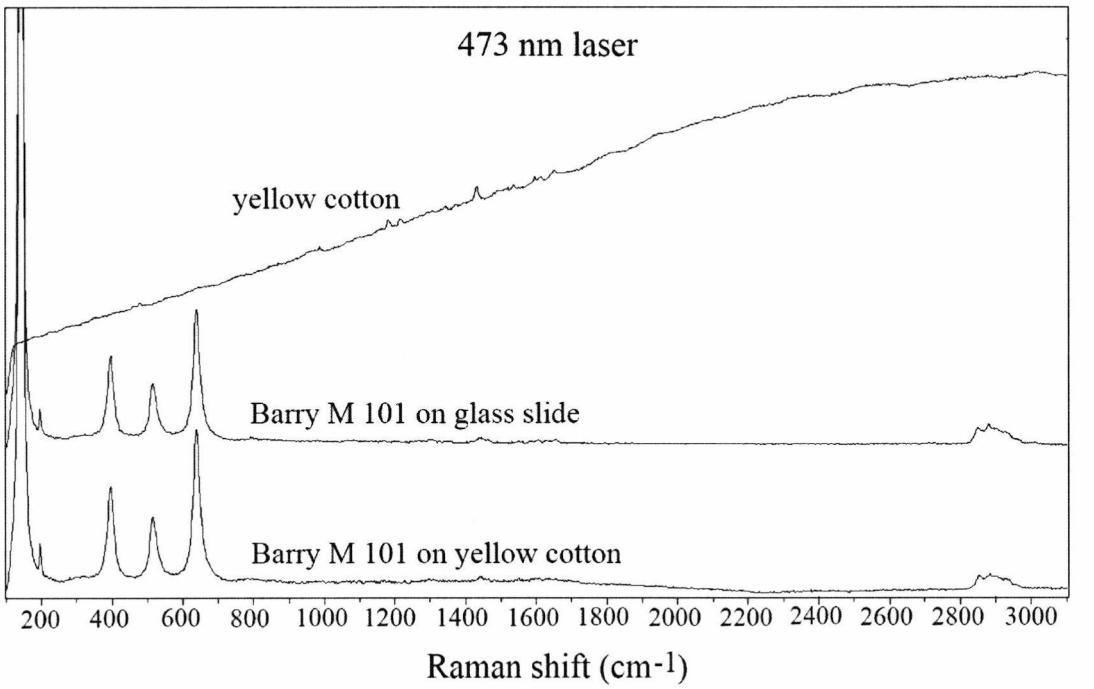

Figure A4.35. Figure comparing the spectra of yellow cotton, Barry M 101 on a glass slide and on yellow cotton, analysed using the blue laser.

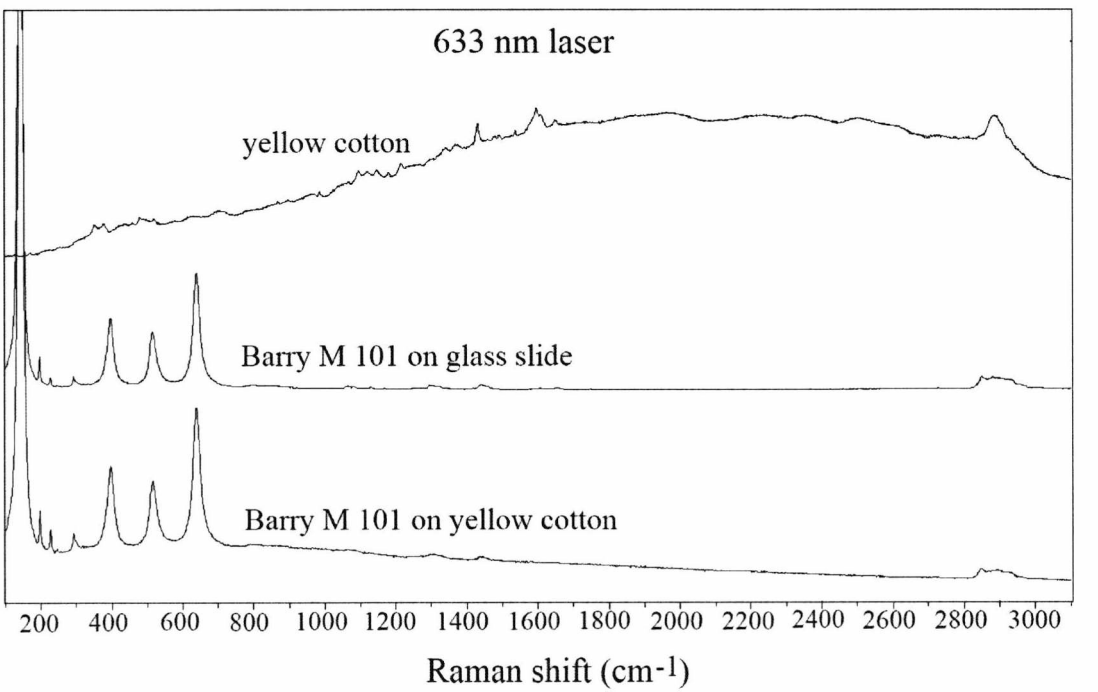

Figure A4.36. Figure comparing the spectra of yellow cotton, Barry M 101 on a glass slide and on yellow cotton, analysed using the red laser.

Barry M 101 on green cotton

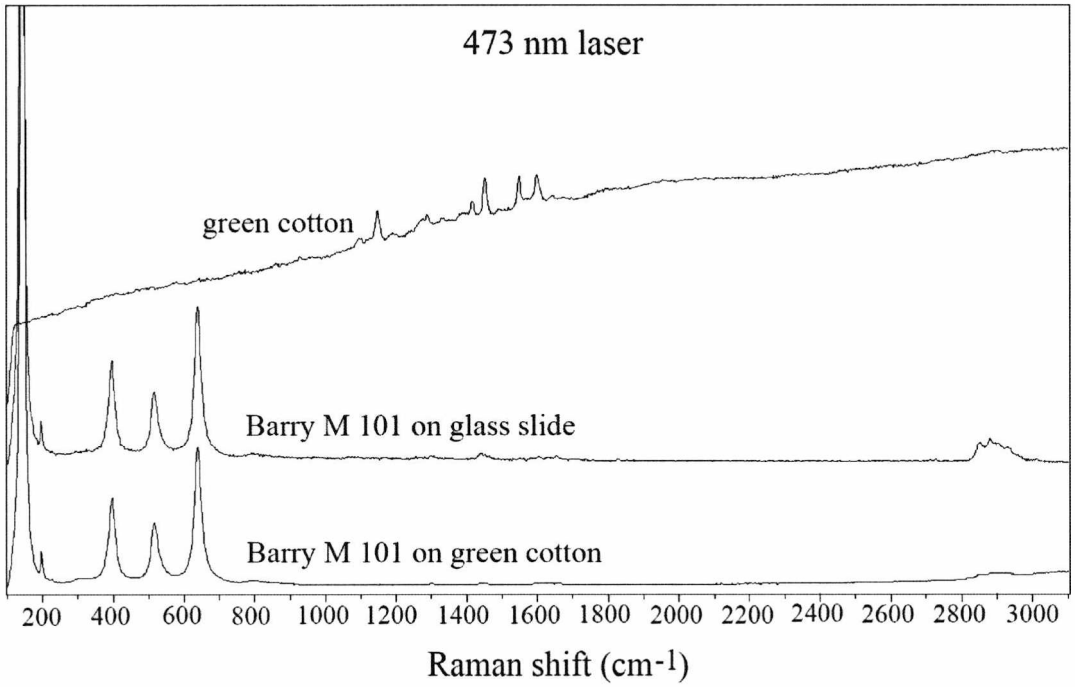

Figure A4.37. Figure comparing the spectra of green cotton, Barry M 101 on a glass slide and on green cotton, analysed using the blue laser.

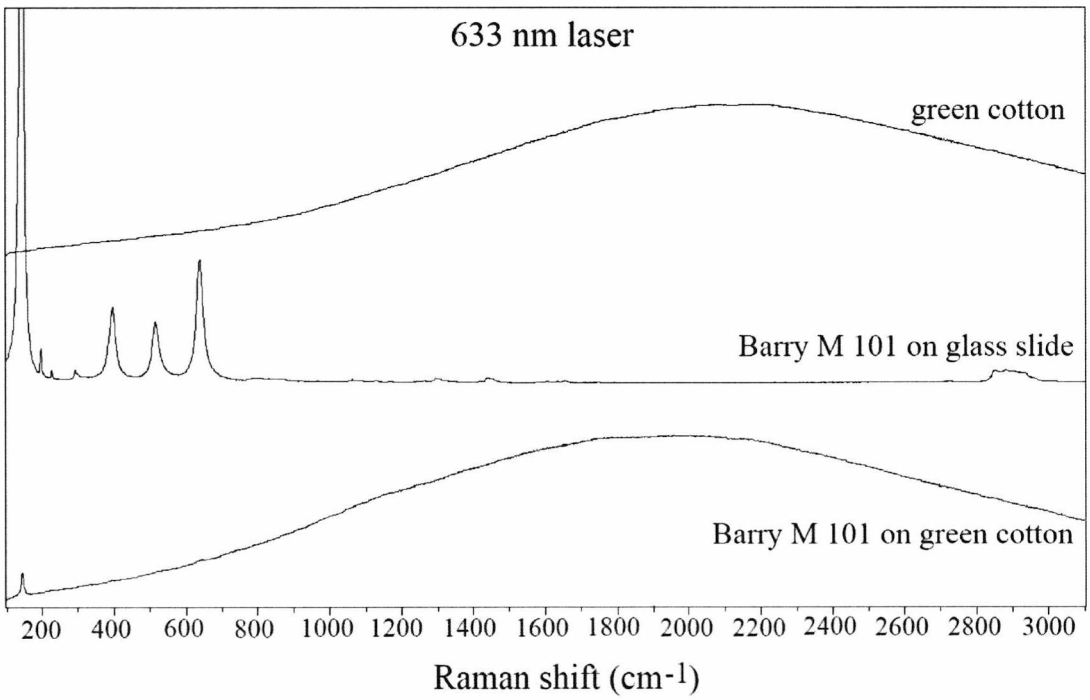

Figure A4.38. Figure comparing the spectra of green cotton, Barry M 101 on a glass slide and on green cotton, analysed using the red laser.

Barry M 101 on pink linen

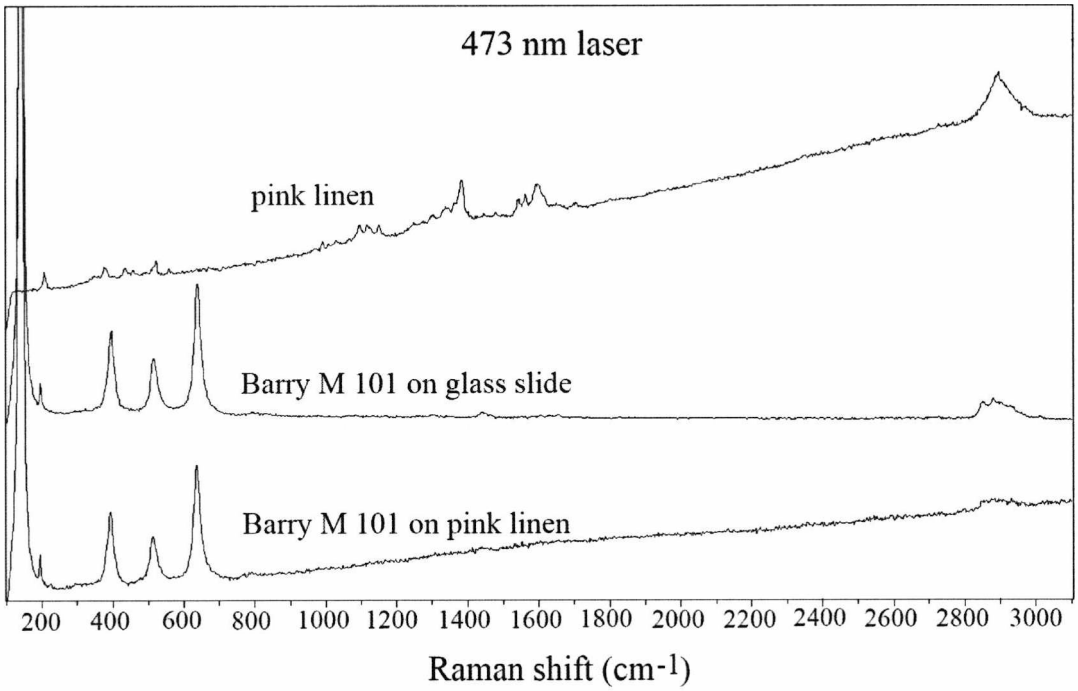

Figure A4.39. Figure comparing the spectra of pink linen, Barry M 101 on a glass slide and on pink linen, analysed using the blue laser.

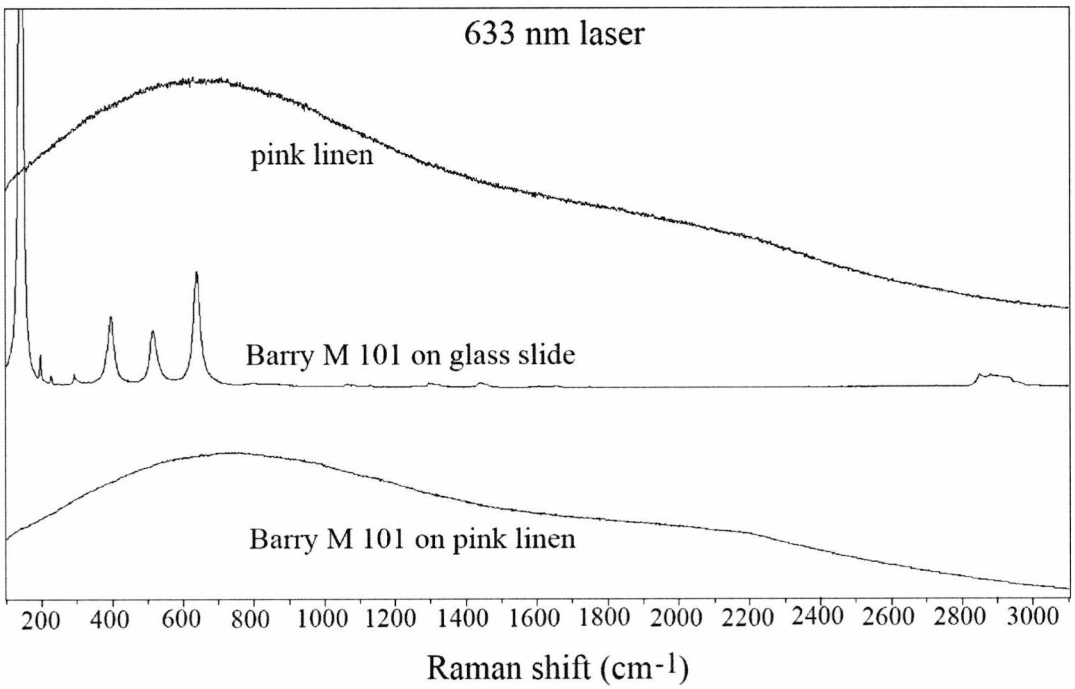

Figure A4.40. Figure comparing the spectra of pink linen, Barry M 101 on a glass slide and on pink linen, analysed using the red laser.

Barry M 101 on orange linen

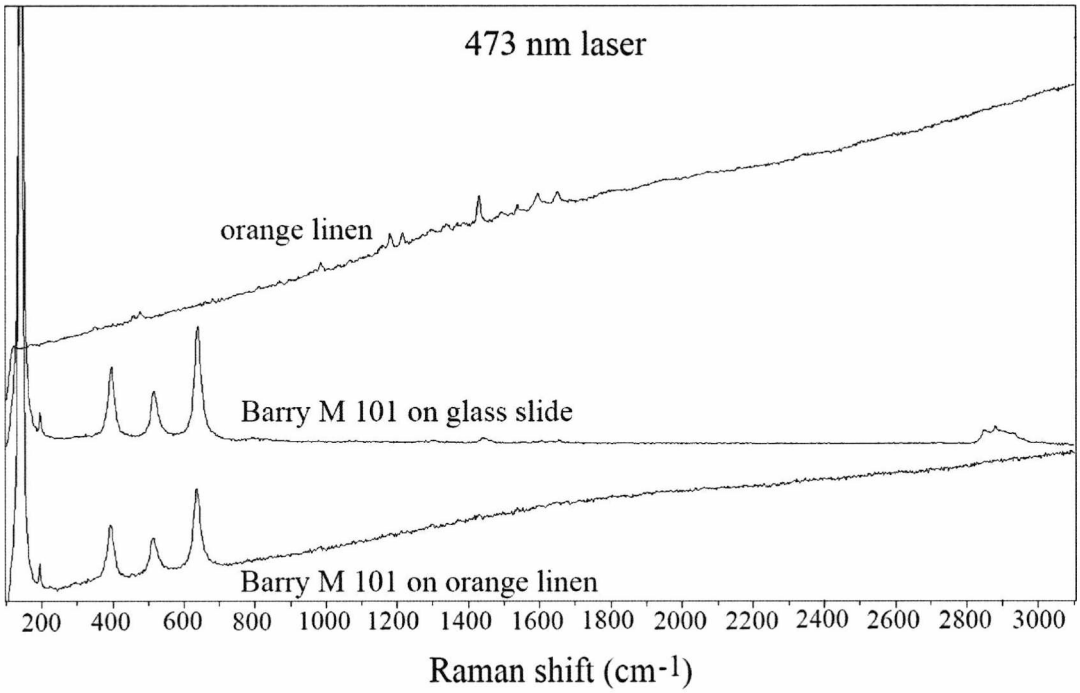

Figure A4.41. Figure comparing the spectra of orange linen, Barry M 101 on a glass slide and on orange linen, analysed using the blue laser.

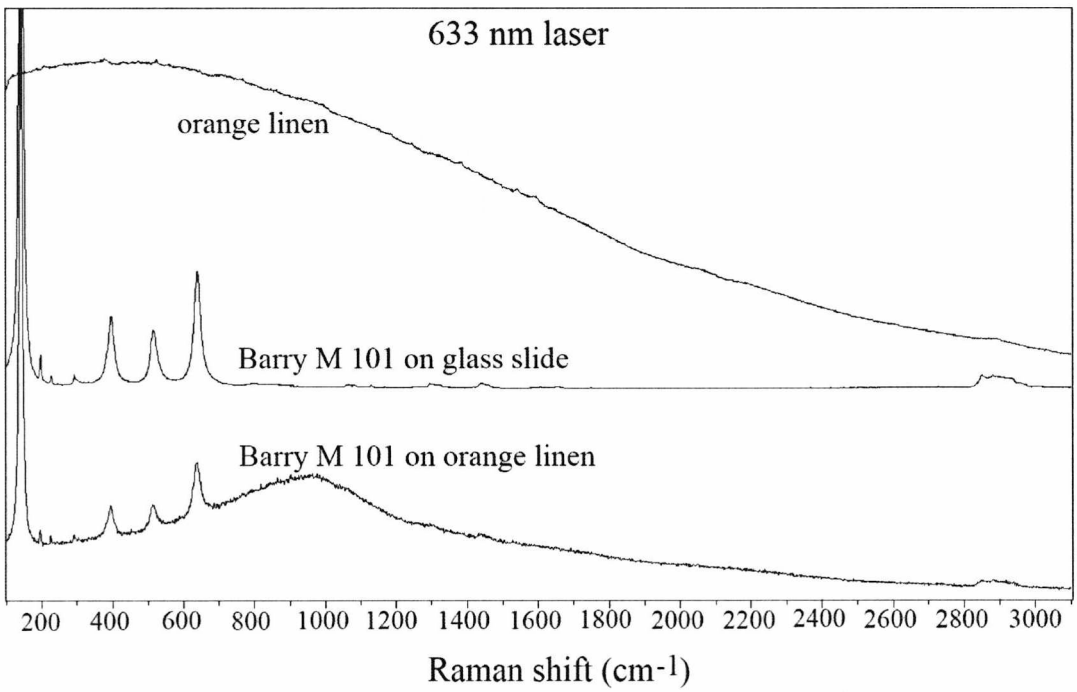

Figure A4.42. Figure comparing the spectra of orange linen, Barry M 101 on a glass slide and on orange linen, analysed using the red laser.

Revlon 07 on yellow wool

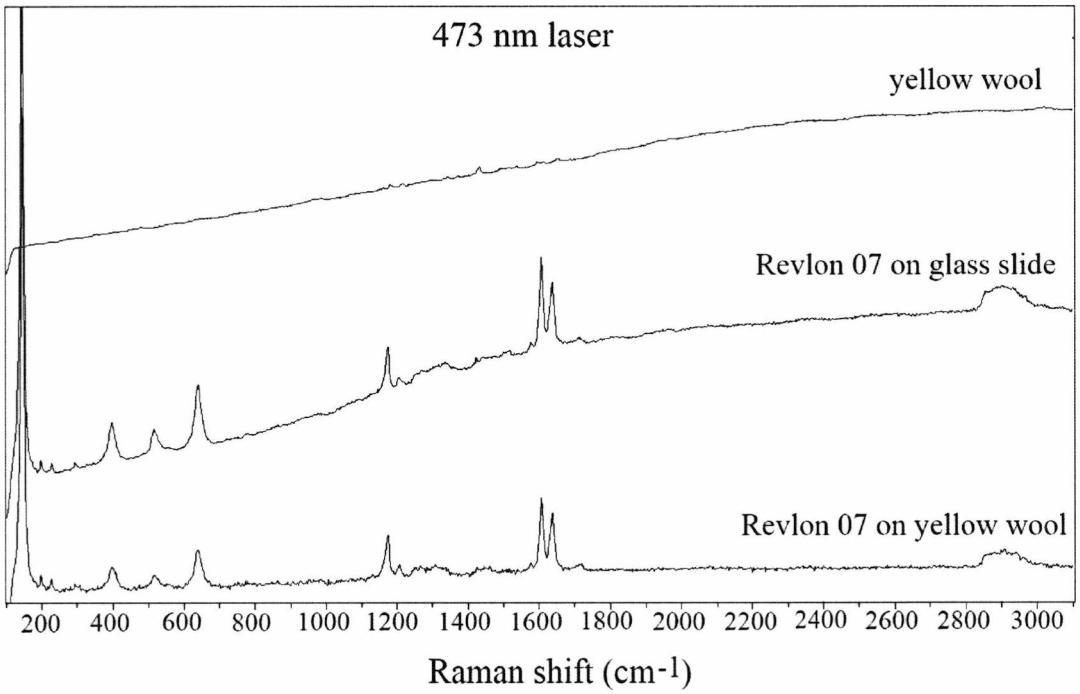

Figure A4.43. Figure comparing the spectra of yellow wool, Revlon 07 on a glass slide and on yellow wool, analysed using the blue laser.

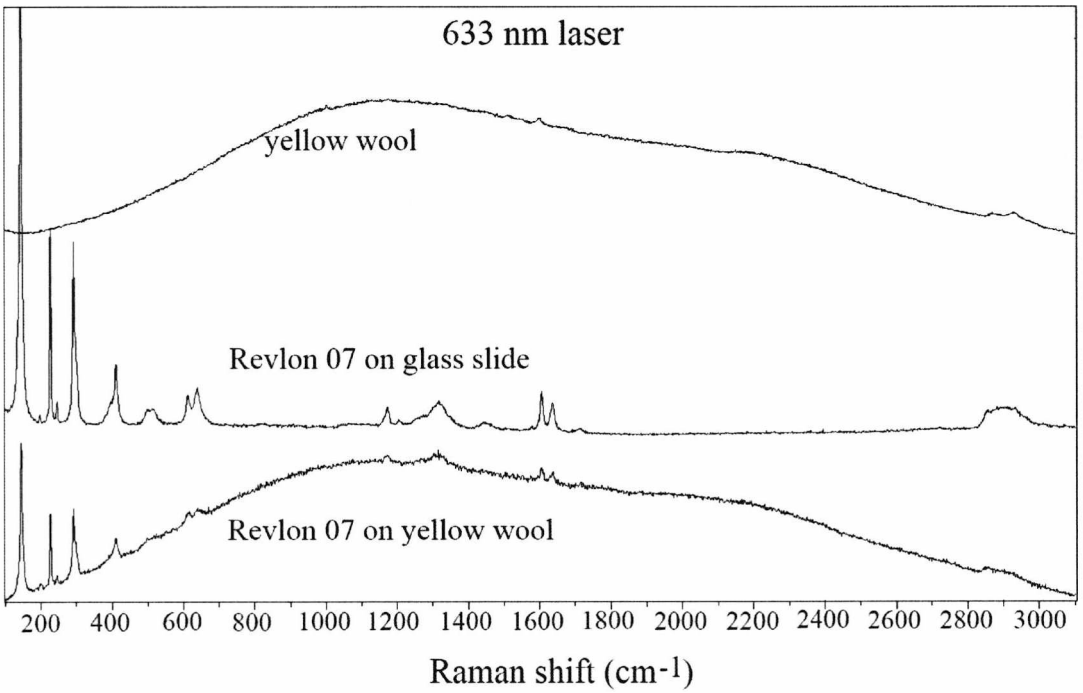

Figure A4.44. Figure comparing the spectra of yellow wool, Revlon 07 on a glass slide and on yellow wool, analysed using the red laser.

Revlon 07 on (light) blue wool

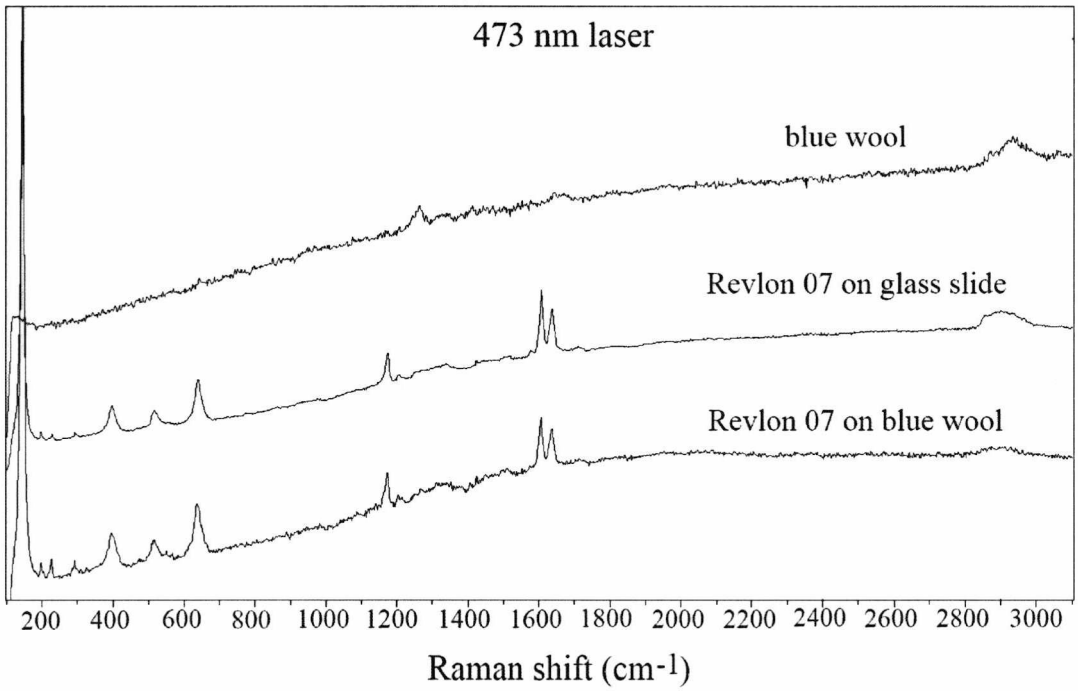

Figure A4.45. Figure comparing the spectra of blue wool, Revlon 07 on a glass slide and on blue wool, analysed using the blue laser.

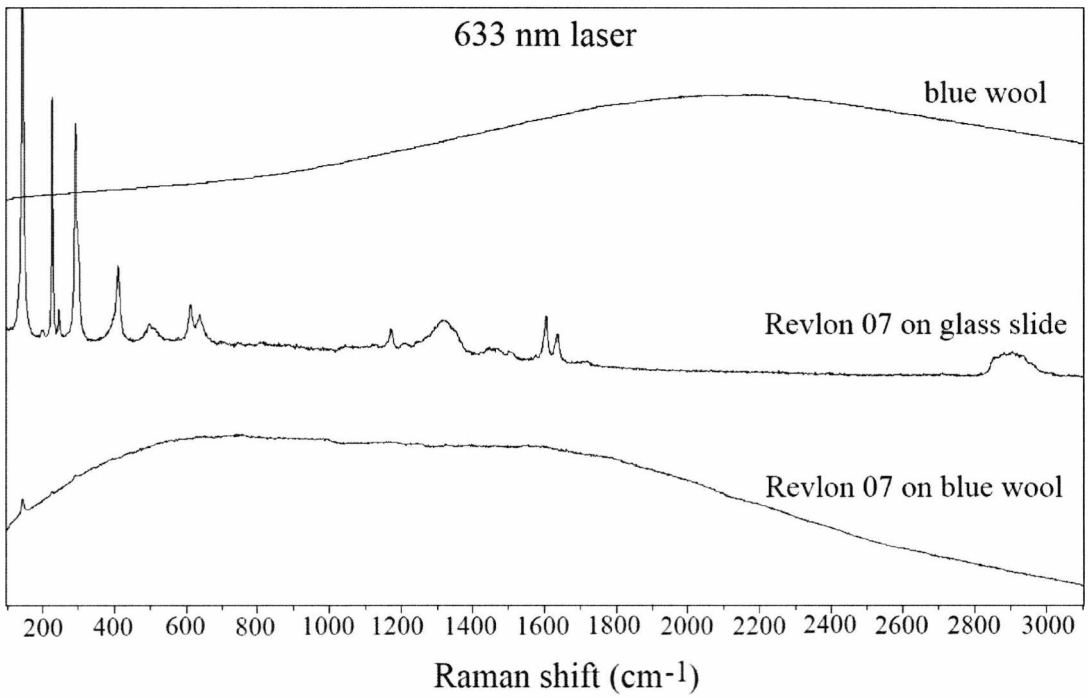

Figure A4.46. Figure comparing the spectra of blue wool, Revlon 07 on a glass slide and on blue wool, analysed using the red laser.

Revlon 07 on dark navy wool

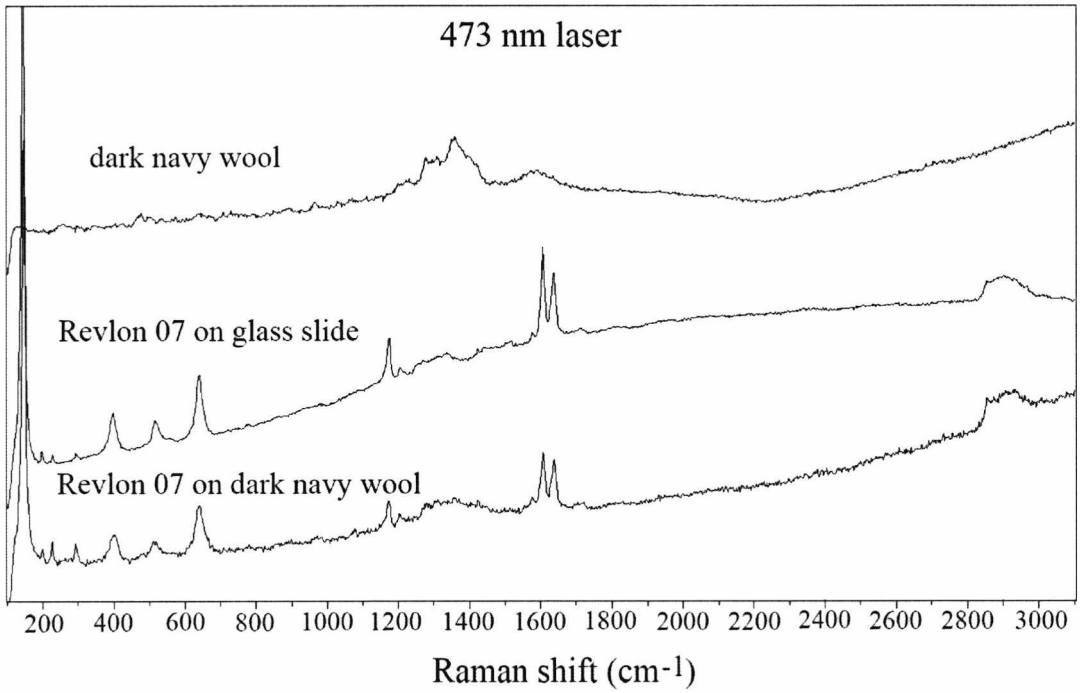

Figure A4.47. Figure comparing the spectra of dark navy wool, Revlon 07 on a glass slide and on dark navy wool, analysed using the blue laser.

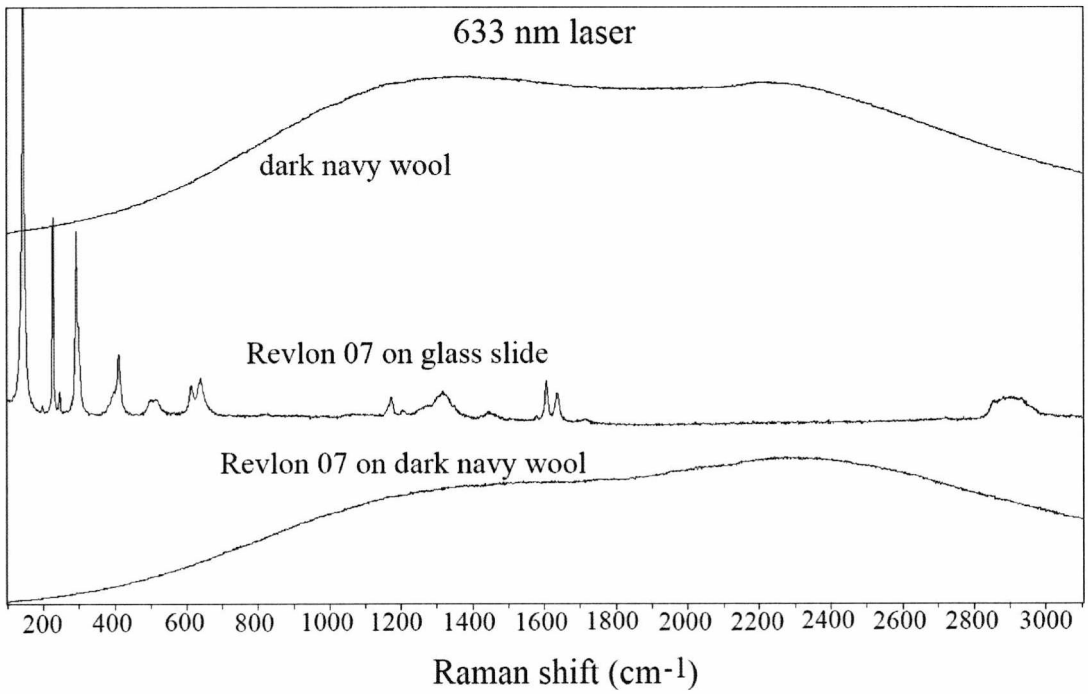

Figure A4.48. Figure comparing the spectra of dark navy wool, Revlon 07 on a glass slide and on dark navy wool, analysed using the red laser.

Revlon 07 on yellow cotton

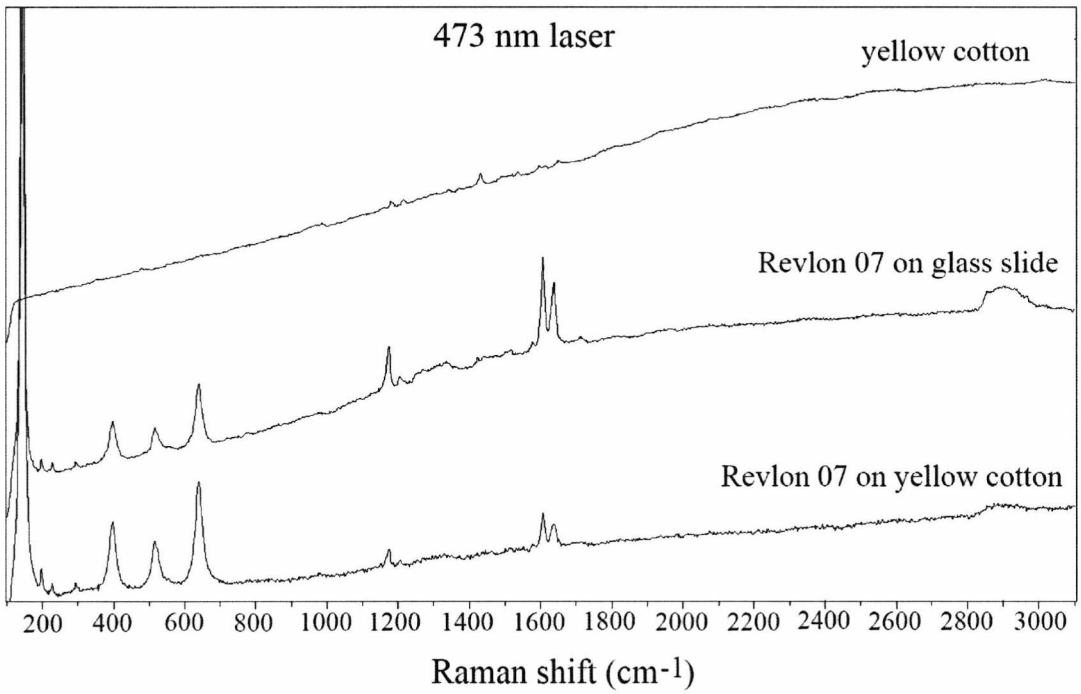

Figure A4.49. Figure comparing the spectra of yellow cotton, Revlon 07 on a glass slide and on yellow cotton, analysed using the blue laser.

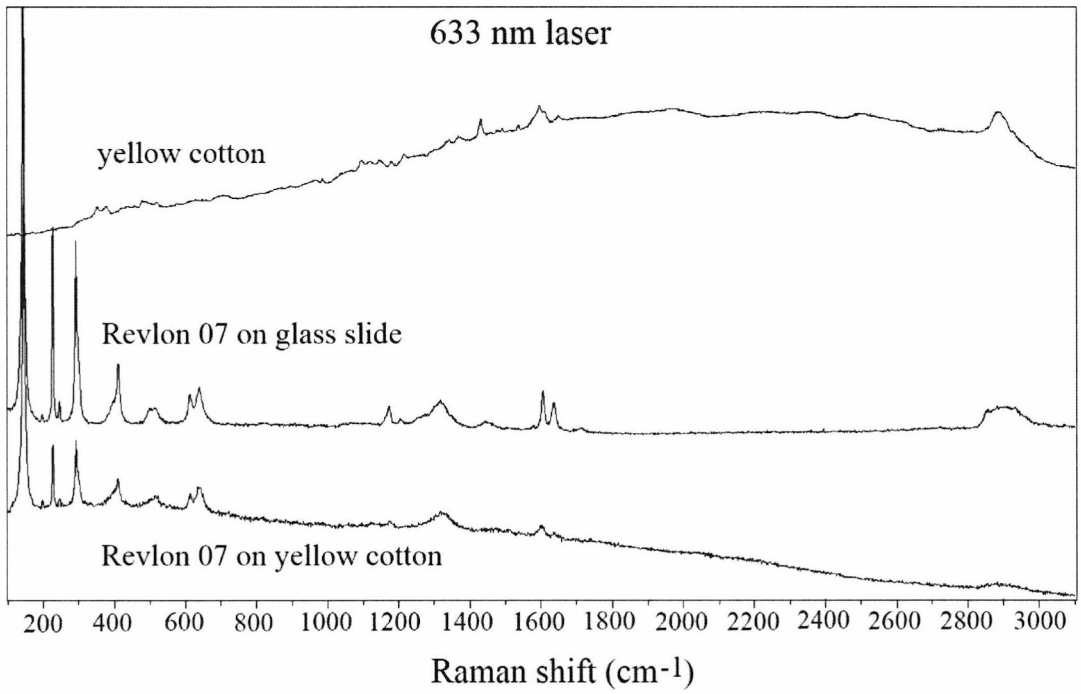

Figure A4.50. Figure comparing the spectra of yellow cotton, Revlon 07 on a glass slide and on yellow cotton, analysed using the red laser.

Revlon 07 on green cotton

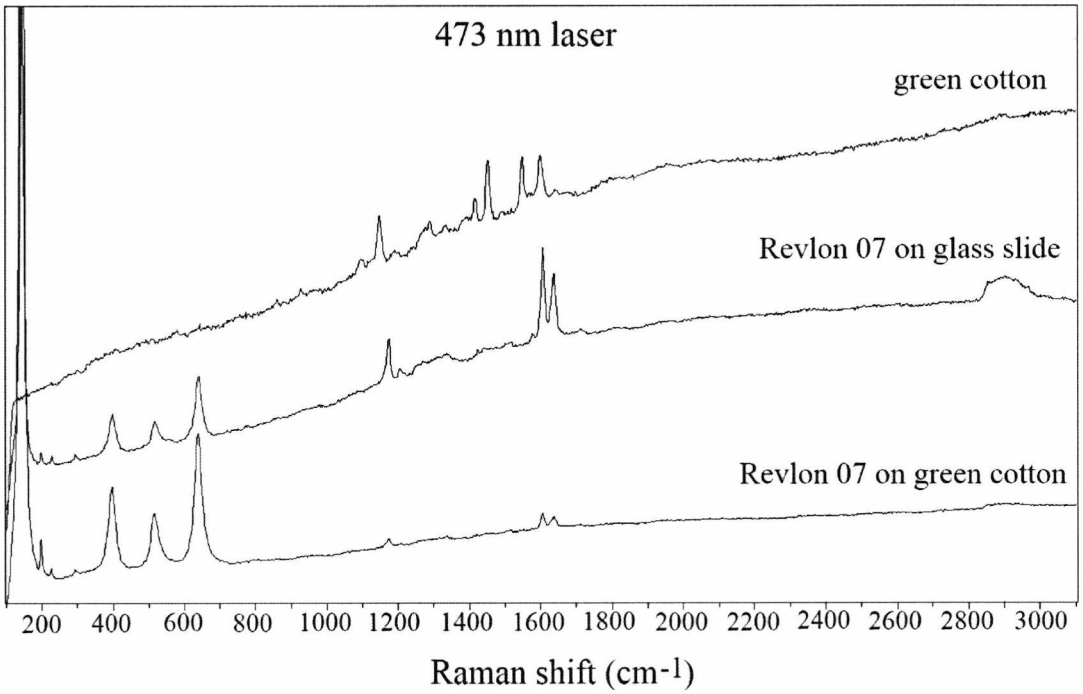

Figure A4.51. Figure comparing the spectra of green cotton, Revlon 07 on a glass slide and on green cotton, analysed using the blue laser.

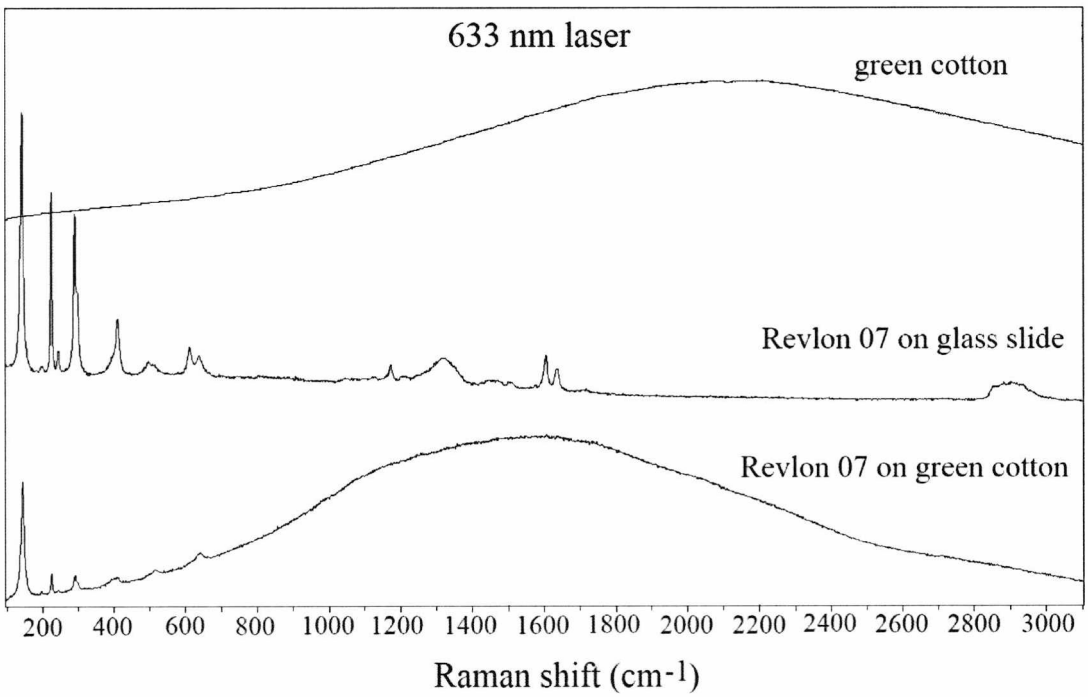

Figure A4.52. Figure comparing the spectra of green cotton, Revlon 07 on a glass slide and on green cotton, analysed using the red laser.

Revlon 07 on pink linen

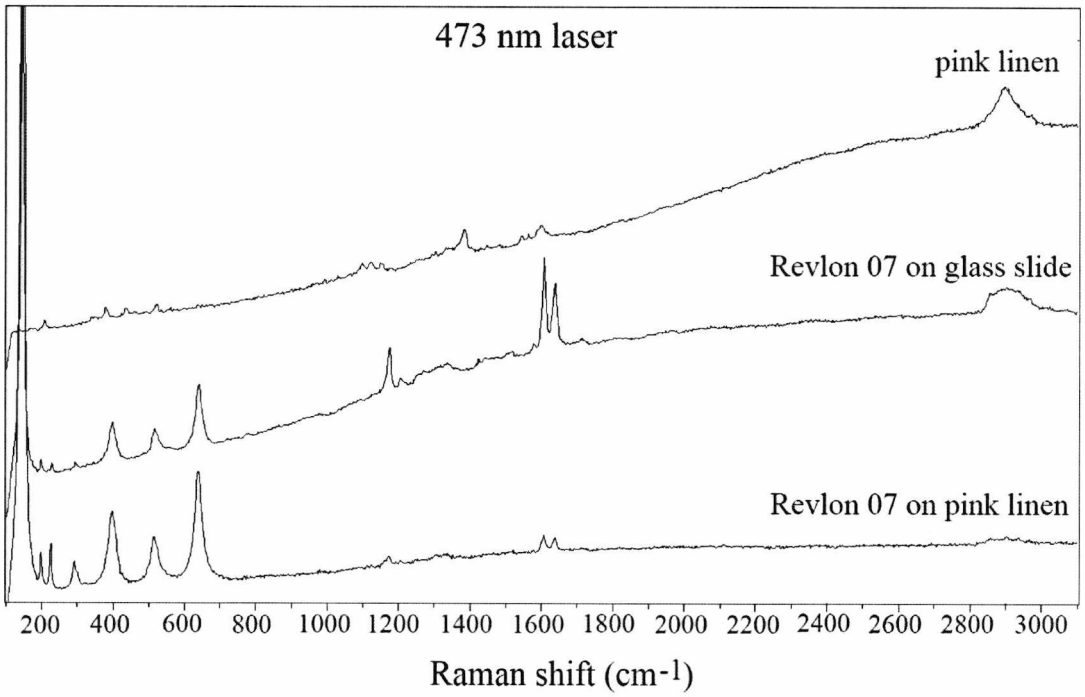

Figure A4.53. Figure comparing the spectra of pink linen, Revlon 07 on a glass slide and on pink linen, analysed using the blue laser.

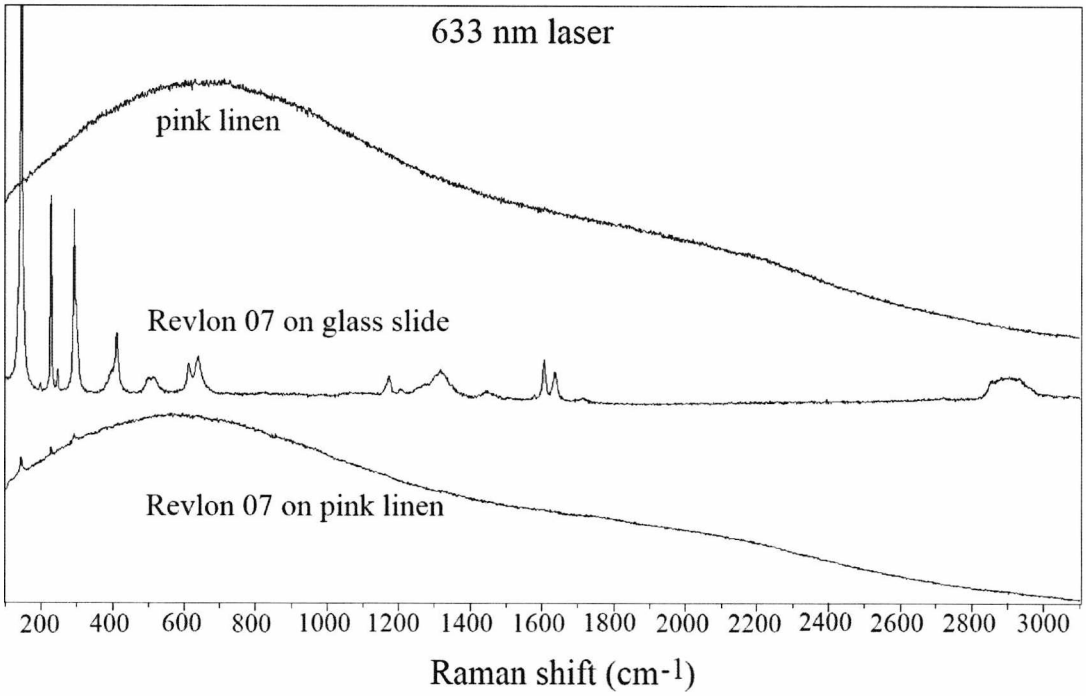

Figure A4.54. Figure comparing the spectra of pink linen, Revlon 07 on a glass slide and on pink linen, analysed using the red laser.

Revlon 07 on orange linen

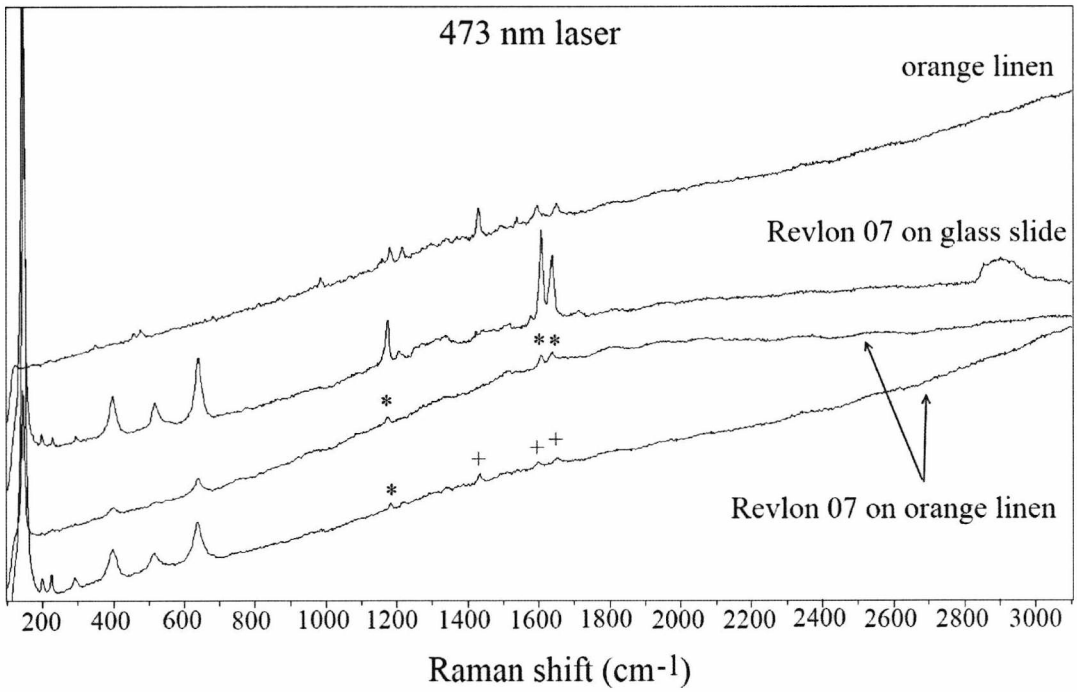

Figure A4.55. Figure comparing the spectra of orange linen, Revlon 07 on a glass slide and on orange linen, analysed using the blue laser. A '*' denotes the peaks that arise from the lipstick, and a '+' indicates those that arise from the orange linen.

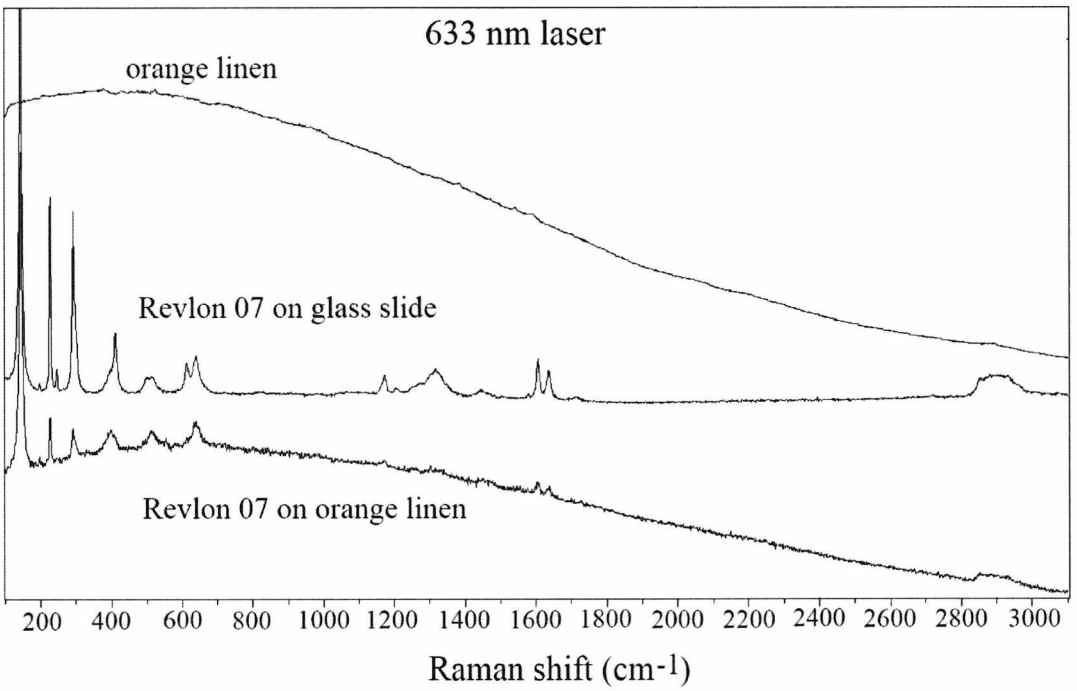

Figure A4.56. Figure comparing the spectra of orange linen, Revlon 07 on a glass slide and on orange linen, analysed using the red laser.